

**A study of the anatomy and physiology of sleep in
African rodents with unusual phenotypes and life
histories**

Jean-Leigh Krüger

PhD Thesis

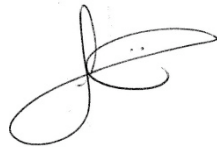
Supervisor: Prof. P.R. Manger

A thesis submitted to the Faculty of Health Sciences, University of the Witwatersrand, in
fulfillment of the requirements for the degree of Doctor of Philosophy.

Johannesburg, 2015

DECLARATION

I declare that this thesis is my own unaided work. It is being submitted for the degree of Doctor of Philosophy in the University of the Witwatersrand, Johannesburg. It has not been submitted before for any degree or examination in any other University.

A handwritten signature in black ink, consisting of a large, stylized 'J' followed by a horizontal line and a small flourish.

Jean-Leigh Krüger

18 May, 2015.

To my parents, Jean and Jerry Bernardo and Rudi Krüger.
Thank you for your love and support and for always believing in me.

Publications arising from this thesis:

- Kruger, J.L., Patzke, N., Fuxe, K., Bennett, N.C., Manger, P.R., 2012. Nuclear organization of cholinergic, putative catecholaminergic, serotonergic and orexinergic systems in the brain of the African pygmy mouse (*Mus minutoides*): organizational complexity is preserved in small brains. *J. Chem. Neuroanat.* 44, 45-56

Presentations arising from this thesis:

- Kruger, J.L., Patzke, N., Fuxe, K., Bennett, N.C., Manger, P.R., 2012. Nuclear organization of cholinergic, putative catecholaminergic, serotonergic and orexinergic systems in the brain of the African pygmy mouse (*Mus minutoides*): organizational complexity is preserved in small brains. *J. Chem. Neuroanat.* 44, 45-56
- The above paper was presented as a poster at:
 - ❖ Biennial SONA Congress held in Rabat, Morocco, June 2013

Abstract:

Studies of sleep in rodents have mainly focussed on the laboratory rat and mouse, and while all these studies are important they do not allow for inferences or predictions to be made regarding sleep phenomenology when changes in body size, brain size, phylogeny or natural history occur within a mammalian order. This thesis investigated the anatomical and physiological aspects of sleep in five unusual rodent species – the African pygmy mouse (*Mus minutoides*), the agouti (*Dasyprocta agouti*), the greater cane rat (*Thryonomys swinderianus*), the East African root rat (*Tachyoryctes splendens*) and the Cape mole rat (*Georychus capensis*). Upon investigation of the cholinergic, catecholaminergic, serotonergic and orexinergic systems in all five species I found that there was no discernible difference in the complement and number of nuclei in these systems despite very large differences in brain size, other phenotypes and natural history. The only real difference seen was in the pygmy mouse, where cortical cholinergic neurons were present and the A6 locus coeruleus had a different appearance to that seen in non-Murid rodents. These sleep-associated nuclei, which are responsible for the generation and regulation of both wake and sleep states appear to show strong similarities in the neurophysiological expression of wake and sleep across mammals. Furthermore I investigated the calcium-binding proteins parvalbumin, calbindin and calretinin as a means to investigate the GABAergic system associated with the above mentioned sleep-related nuclei. There was a global consistency in this system across species and thus it does not appear that the GABAergic neurons play a substantial role in the amount of time spent in a particular state, and appear to be more involved in the production and maintenance of a state than global amounts of time spent in a state. I investigated sleep physiology in two of the five species – the Cape mole rat and the East

African root rat. I found that the Cape mole rat compared most favourably with the giant
Zambian mole rat previously studied. While on average over a 24-hour period, the East African
root rat spent only 2.2 h in sleep (both non-REM and REM), this being the least amount of sleep
recorded in any rodent, or indeed any mammal, studied with electrophysiological methods to
date. This thesis has therefore shed light on the role played by the sleep-related nuclei in the
global picture of sleep, but with the discovery of the root rat as the shortest sleeper there are
many new questions to ask.

Acknowledgements

The following individuals and organizations were crucial in the completion of this PhD thesis:

- Professor Paul Manger: You are an amazing supervisor and I could never have hoped to achieve my PhD without all your guidance and support. You are a science rock star.
- Doctor Nadine Gravett: Thank you for all your help with the sleep studies. Your help was invaluable.
- Doctor Nina Patzke and Doctor Adhil Bhagwandin: Two postdoctoral fellows whose help with the immunohistochemistry was greatly appreciated. Nina, thank you for your friendship.
- Staff of the CAS: Thank you for all your assistance with the care and surgeries for my experimental animals.
- Yolande Swanepoel, Monique Nortje and Alexis Chaumeton: Without all your love and support I'm not sure I would have made it. Thank you.
- Ayanda Ngwenya and Leigh-Anne Dell: We have walked a long road together – thank you for all the adventures, commiserations and laughter. We did it!
- NRF: A grant-holder linked bursary from 2010 - 2014

Table of Contents

	Page
Title page	i
Declaration	ii
Dedication	iii
Publications arising from this thesis	iv
Presentations arising from this thesis	iv
Abstract	v
Acknowledgments	vii
Table of Contents	viii
List of Tables	xiii
List of Figures	xiii
CHAPTER ONE: Introduction and chapter outline	1
1.1. Introduction	1
1.2. Specific questions and hypotheses	2
1.3. Chapter outline	3
CHAPTER TWO: Literature Review	8
2.1. Sleep and sleep evolution	8
2.2. Sleep in rodents	10
2.3. Rodent species examined	12
2.3.1. The African pygmy mouse, <i>Mus minutoides</i>	12
2.3.2. The East African root rat, <i>Tachyoryctes splendens</i>	13
2.3.3. The Cape mole rat, <i>Georhynchus capensis</i>	14
2.3.4. The greater cane rat, <i>Thryonomys swinderianus</i>	15

2.3.5. The golden-rumped agouti, <i>Dasyprocta agouti</i>	15
2.4 Sleep and phenotypic, phylogenetic and natural history variances	16
CHAPTER THREE: Nuclear organisation of cholinergic, putative catecholaminergic, serotonergic and orexinergic systems in the brain of the African pygmy mouse (<i>Mus minutoides</i>): organizational complexity is preserved in small brains	18
3.1. Introduction	18
3.2. Materials and Methods	20
3.3. Results	28
3.3.1. Cholinergic nuclei	29
3.3.1.1. Cortical cholinergic neurons	29
3.3.1.2. Striatal cholinergic interneurons	30
3.3.1.3. Cholinergic nuclei of the basal forebrain	30
3.3.1.4. Diencephalic cholinergic nuclei	31
3.3.1.5. Pontomesencephalic cholinergic nuclei	31
3.3.1.6. Cholinergic cranial nerve motor nuclei	32
3.3.2. Putative catecholaminergic nuclei	32
3.3.2.1. Olfactory bulb (A16)	33
3.3.2.2. Diencephalic nuclei (A15 – A11)	33
3.3.2.3. Midbrain nuclei (A10 – A8)	34
3.3.2.4. Rostral rhombencephalon – the locus coeruleus complex, A7 – A4	35
3.3.2.5. Medullary nuclei (C1, C2, C3, A1, A2, Area postrema)	36
3.3.3. Serotonergic nuclei	37
3.3.3.1. Rostral cluster	37
3.3.3.2. Caudal cluster	39
3.3.4. Orexinergic (hypocretinergic) nuclei	40
3.4. Discussion	56

3.4.1. Cortical cholinergic neurons	57
3.4.2. The appearance of the locus coeruleus (A6) across rodent species	58
3.4.3. Systems level brain evolution	59
CHAPTER FOUR: Sleep in the Cape mole rat, <i>Georchus capensis</i> – sleeping underground	62
4.1. Introduction	62
4.2. Materials and Methods	63
4.2.1. Experimental animals	63
4.2.2. Surgical procedure	64
4.2.3. Sleep recording	66
4.2.4. Data analysis	67
4.3. Results	68
4.3.1. State definitions	69
4.3.2. Time spent in wake, non-REM and REM states	69
4.3.3. Number and duration of episodes of Wake, non-REM and REM	70
4.3.4. REM periodicity and state transitions	70
4.4. Discussion	84
4.4.1. Comparison to sleep in other mole rats	84
4.4.2. Comparison to sleep in other rodents	86
4.4.3. Why do the Bathyergid mole rats sleep differently to other rodents?	86
CHAPTER FIVE: Sleep in the East African root rat, <i>Tachyoryctes splendens</i> – a short sleeper for a mammal	89
5.1. Introduction	89
5.2. Materials and Methods	91
5.2.1. Experimental animals	91
5.2.2. Surgical procedures	92

5.2.3. Sleep recording	93
5.2.4. Data analysis	94
5.3. Results	95
5.3.1. State definitions	96
5.3.2. Time spent in Wake, non-REM and REM states	97
5.3.3. Number and duration of wake and sleep episodes	97
5.3.4. REM periodicity and state transitions	98
5.4. Discussion	116
5.4.1. Are East African root rats diurnal or nocturnal?	116
5.4.2. Is the East African root rat the shortest sleeping mammal?	118
5.4.3. What is the cause of reduced sleep time in East African root rats?	120
5.4.4. What can a short sleeper reveal about sleep and the function of sleep?	121
CHAPTER SIX: Organization of sleep related nuclei and inhibitory neurons/terminal networks in five species of phenotypically and phylogenetically varied rodents	123
6.1. Introduction	123
6.2. Materials and Methods	125
6.3. Results	129
6.3.1. Cholinergic nuclei of the basal forebrain and pons	129
6.3.2. Catecholaminergic nuclei of the locus coeruleus complex	131
6.3.3. Serotonergic nuclei of the dorsal raphe nuclear complex	132
6.3.4. Orexinergic neuronal clusters of the hypothalamus	133
6.3.5. Neurons and terminal networks containing calcium binding proteins	134
6.3.5.1. Neurons and terminal networks containing calcium binding proteins in the cholinergic nuclei of the basal forebrain and pons	134
6.3.5.2. Neurons and terminal networks containing calcium binding proteins in the locus coeruleus complex	137

6.3.5.3. Neurons and terminal networks containing calcium binding proteins in the serotonergic dorsal raphe nuclei	138
6.3.5.4. Neurons and terminal networks containing calcium binding proteins in the hypothalamic orexinergic nuclei	140
6.3.5.5. Neurons and terminal networks containing calcium binding proteins in thalamic reticular nucleus	141
6.4. Discussion	158
6.4.1. Similarities in the cholinergic, catecholaminergic, serotonergic and orexinergic sleep-related nuclei across the five rodent species	158
6.4.2. Similarities and variances in the locations of neurons and terminal networks containing the calcium binding proteins associated with inhibitory neurons	160
6.4.3. So what controls the variation in sleep times across mammals?	162
CHAPTER SEVEN: General Discussion	164
7.1. Hypothesis 1	164
7.2. Hypothesis 2	165
7.3. Hypothesis 3	167
7.4. Can the neuroanatomy lead to any predictability of sleep parameters within the rodent order?	167
7.5. Future studies	168
REFERENCES	171
Appendices	195

List of Tables

	Page
Table 5.1. Individual data for sleep in <i>Tachyoryctes splendens</i>	100
Table 5.2. Daily sleep data for the <i>Tachyoryctes splendens</i>	101
Table 6.1. Parvalbumin immunopositive structures in sleep related nuclei	143
Table 6.2. Calbindin immunopositive structures in sleep related nuclei	144
Table 6.3. Calretinin immunopositive structures in sleep related nuclei	145

List of Figures

	Page
Figure 3.1. Drawings of African pygmy mouse brain	42
Figure 3.2. Cholinergic neurons African pygmy mouse brain	48
Figure 3.3. Catecholaminergic neurons African pygmy mouse brain	50
Figure 3.4. Serotonergic neurons African pygmy mouse brain	52
Figure 3.5. Orexinergic neurons African pygmy mouse brain	54
Figure 4.1. Polygraphic traces of sleep in <i>Georhychus capensis</i>	72
Figure 4.2. Polygraphic traces of sleep in <i>Georhychus capensis</i>	74
Figure 4.3. Graphs of spectral power ranges in wake and sleep	76
Figure 4.4. Graphs of physiological data for a 24-hour cycle	78
Figure 4.5. Graph of REM periodicity for <i>Georhychus capensis</i>	80
Figure 4.6. State transitions in <i>Georhychus capensis</i>	82

Figure 5.1. Polygraphic traces of sleep in <i>Tachyoryctes splendens</i>	102
Figure 5.2. Polygraphic traces of sleep in <i>Tachyoryctes splendens</i>	104
Figure 5.3. Polygraphic traces of sleep in <i>Tachyoryctes splendens</i>	106
Figure 5.4. Graph of spectral power ranges in wake and sleep	108
Figure 5.5. Graphs of physiological data for a 24-hour cycle	110
Figure 5.6. Graph of REM periodicity for <i>Tachyoryctes splendens</i>	112
Figure 5.7. State transitions in <i>Tachyoryctes splendens</i>	114
Figure 6.1. Cholinergic nuclei in rodent basal forebrain	146
Figure 6.2. Cholinergic nuclei in rodent pons	148
Figure 6.3. Locus coeruleus in rodent pons	150
Figure 6.4. Dorsal raphe complex in rodent midbrain and pons	152
Figure 6.5. Orexinergic neurons in rodent hypothalamus	154
Figure 6.6. Thalamic reticular nucleus in various rodents	156

CHAPTER ONE: Introduction and chapter outline

1.1 Introduction

Studies of sleep in rodents have mainly focussed on the laboratory rat and mouse, and while this has provided important information it is necessary to investigate more species within the order if we are to gain a better understanding of what sleep in rodents actually entails (Clancy et al., 1978; Rosenberg et al., 1976; Timo-Iaria et al., 1970; Richardson et al., 1985; Tang and Sanford, 2002). Often when mammalian sleep evolution is studied, analyses are conducted across orders and with mammals of varying sizes, or on unusual forms of sleep (Nicolau et al., 2000; Kavanau, 2002; Cappellini et al., 2008; Lesku et al., 2006, 2008). One unusual form of sleep, unihemispheric slow wave sleep is found in Cetaceans, eared seals and manatees (reviewed in Lyamin et al., 2008). Although all these studies are important, they do not allow for inferences or predictions to be made regarding sleep phenomenology when changes in body size, brain size, phylogeny or natural history occur within a mammalian order. This thesis investigates the anatomical and physiological aspects of sleep in five unusual rodent species – the African pygmy mouse (*Mus minutoides*), the agouti (*Dasyprocta agouti*), the greater cane rat (*Thryonomys swinderianus*), the East African root rat (*Tachyoryctes splendens*) and the Cape mole rat (*Georychus capensis*). The African pygmy mouse is one of the smallest rodents with an average body mass of only 8 g (Downs and Perrin, 1996; Monadjem, 1999). In contrast the greater cane rat and the agouti can weigh as much as 5 kg (Jori et al., 1995; Dubost, 1988; Silviu and Fragoso, 2003). The East African root rat and the Cape mole rat fall between these two extremes at approximately 230 g body mass (Du Toit et al., 1985). Of the five species studied in this thesis, all are nocturnal except for the agouti which is diurnal. These species inhabit a wide variety of ecosystems from fairly arid areas (pygmy mouse), grasslands and forest (cane rat, root rat and mole rat) to the South

American rainforest (agouti). The root rat and mole rat are far more aggressive than the other species and they both have a subterranean lifestyle. These five species provide a unique opportunity to investigate sleep within an order as they are all rodents but these species vary greatly in body size, other phenotypes and natural history. A number of studies have found that there is predictability in the anatomy of the neural systems involved in sleep and that changes in the complexity of these systems does not readily occur within an order but rather between orders (Manger, 2005; Maseko et al., 2007; Dell et al., 2010; Calvey et al., 2013). These findings were all based upon the cholinergic, catecholaminergic and serotonergic systems, which were investigated in this study, as well as the GABAergic and orexinergic systems, which are all involved in sleep. Furthermore I investigated sleep phenomenology using polygraphic techniques (electroencephalograph and electromyography) in the East African root rat and the Cape mole rat to determine the architecture and patterns of sleep in these two species.

1.2. Specific questions and hypotheses

- The pygmy mouse, cane rat, agouti, root rat and mole rat will share the same complement of nuclear subdivisions within the hypnogenic system regardless of differences in brain size, phenotype or lifestyle.
- The sleep physiology should remain constant despite interspecies differences.
- The EEG and EMG recordings should show rodent specific features which correlate to brain and body size and which remain consistent between species of the same order.
- Can the neuroanatomy lead to any predictability of sleep parameters within the rodent order?

1.3. Chapter outline

Chapter Two – Literature review

In this literature review I exam whether all animals sleep and the answer was rather surprising. I also take a deeper look into mammalian sleep including unusual forms of sleep such as unihemispheric sleep and the lack of variance in sleep across mammals. There have been many studies conducted on laboratory rodents of which the findings are summarised in the review. There have also been studies conducted on a few non-laboratory rodent species such as the degu, vole, beaver and the Zambian mole rat. Finally, I describe each of the species used in the present study and summarised what is known, if anything, about their sleep anatomy or physiology and their circadian rhythms.

Chapter Three - Nuclear organisation of cholinergic, putative catecholaminergic, serotonergic and orexinergic systems in the brain of the African pygmy mouse (*Mus minutoides*): organizational complexity is preserved in small brains

This study investigated the nuclear organization of four immunohistochemically identifiable neural systems (cholinergic, catecholaminergic, serotonergic and orexinergic) within the brain of the African pygmy mouse (*Mus minutoides*). The African pygmy mice studied had a brain mass of around 275 mg, making these the smallest rodent brains to date in which these neural systems have been investigated. In contrast to the assumption that in this small brain there would be fewer subdivisions of these neural systems, we found that all nuclei generally observed for these systems in other rodent brains were also present in the brain of the African pygmy mouse. As with other rodents previously studied in the subfamily

Murinae, I observed the presence of cortical cholinergic neurons and a compactly organized locus coeruleus. These two features of these systems have not been observed in the non-Murinae rodents studied to date. Thus, the African pygmy mouse displays what might be considered a typical Murinae brain organization, and despite its small size, the brain does not appear to be any less complexly organized than other rodent brains, even those that are over 100 times larger such as the Cape porcupine brain. The results are consistent with the notion that changes in brain size do not affect the evolution of nuclear organization of complex neural systems. Thus, species belonging to the same order generally have the same number and complement of the subdivisions, or nuclei, of specific neural systems despite differences in brain size, phenotype or time since evolutionary divergence.

Chapter Four - Sleep in the Cape mole rat, *Georchus capensis* – sleeping underground

The Cape dune mole rat is a solitary subterranean rodent found in the Western Cape of South Africa. This approximately 200 g rodent shows a nocturnal circadian rhythm, but sleep in this species is yet to be investigated. Using telemetric recordings of EEG and EMG in conjunction with video recordings, I was able to show that the Cape mole rat, like all other rodents has sleep periods composed of both slow wave (non-REM) and rapid eye movement (REM) sleep. These mole rats spent on average 15.4 h awake, 7.1 h in non-REM sleep and 1.5 h in REM sleep each day. Thus, they sleep somewhat less than other rodents, but have a similar percentage of REM sleep with regard to total sleep time. In addition, the duration of both non-REM and REM episodes were markedly shorter in the Cape dune mole rat than observed in other rodents. Interestingly, these features (total sleep time and episode duration) are similar to that observed in another Bathyergid mole rat, *Fukomys mechowii*, studied

previously. Thus, there appears to be a Bathyergid type of sleep amongst the rodents that may be related to their environment and the effect of this on their circadian rhythm. Investigating further species of Bathyergid mole rats may fully define the emerging picture of sleep in these subterranean African rodents.

Chapter Five - Sleep in the East African root rat, *Tachyoryctes splendens* – a short sleeper for a mammal

The present study reports the results of an electrophysiological analysis of sleep in the East African root rat, a member of the *Tachyoryctes* genus belonging to the subfamily *Spalacinae*. Telemetric EEG and EMG recordings, along with video recording, on three root rats over a continuous 72 hour period (12 h light/12 h dark cycle) were undertaken and scored. The analysis revealed that the East African root rat is likely to be the shortest sleeping mammal studied to date, having a total sleep time of only 2.2 h per day. Despite this short total sleep time, non-REM and REM states, showing similar physiology to that observed in other rodents, were observed in the root rats, and no unusual sleep states were observed. Moreover, REM sleep occupied 21.2% total sleep time, which is well within the range observed in other rodents previously studied. The root rats were extremely active during the dark period, and appeared to spend much of the light period in quiet wake while maintaining vigilance (as determined from both EEG recordings and behavioural observation). Despite some methodological concerns, it appears that the East African root rat is indeed the shortest sleeping mammal studied to date. Thus, the East African root rat may provide a novel model animal in which to study the regulation of total sleep time and may lead to clues allowing the understanding of the elusive ultimate function of sleep.

Chapter Six - Organization of sleep related nuclei and inhibitory neurons/terminal networks in five species of phenotypically and phylogenetically varied rodents

The current study outlines the results of immunohistochemical staining identifying the sleep related nuclei and GABAergic innervation of these nuclei in five species of rodent. The rodents studied represent a range of body and brain sizes, life histories, morphological specializations and environmental niches. The species include the African pygmy mouse (*Mus minutoides*), the East African root rat (*Tachyoryctes splendens*), the Cape mole rat (*Georhynchus capensis*), the greater cane rat (*Thryonomys swinderianus*) and the agouti (*Dasyprocta agouti*). Across the five species the sleep-associated cholinergic nuclei of the basal forebrain and pons, locus coeruleus, dorsal raphe and orexinergic neurons of the hypothalamus showed a very similar nuclear organization and neuronal morphology. Moreover, the GABAergic neurons and terminal networks associated with these nuclei, even when broken down into three subtypes identified by immunostaining for the calcium-binding proteins, showed a global similarity across species. The variations in GABAergic innervation were minor and showed no consistency across species. We conclude that the neural systems involved in the generation of the specific neurophysiology associated with the differing sleep and wake states is very similar across rodent species. This similarity supports the concept that sleep across these species, and indeed across many mammals, in terms of the physiological appearance of the different sleep states, is based on very similar neuroanatomy and neurochemistry with very similar neurophysiological outcomes.

Chapter Seven: General Discussion

This chapter summarizes the implications and significance of the results obtained in the studies comprising this thesis and highlights future directions for sleep research in rodents and other mammalian species.

CHAPTER 2: Literature review

2.1. Sleep and sleep evolution

Sleep is a biological state characterised behaviourally by immobility and a substantial decrease in responsiveness to external sensory inputs, but it is distinct from a coma state in that it is rapidly reversible (Siegel, 2008). Furthermore, sleep deprivation or interruption must lead to an increased need to sleep (Siegel, 2008). Using this definition, is it possible to say that all animals sleep? Campbell and Tobler (1984), Lesku et al. (2006, 2008) and Siegel (2008) have all attempted to answer this question in their extensive reviews and it would appear that not all animals do sleep and certainly not all animals have a sleep state that exhibits all the same neurophysiological features.

Within the invertebrates, *Drosophila* has a phase of inactivity that appears to closely resemble mammalian sleep, while the locust, honey bee, butterfly, mosquito, scorpion and cockroach all exhibit a sleep-like state (Campbell and Tobler, 1984; Lesku et al., 2006, 2008; Siegel, 2008). When we consider sleep in fish, the definition of sleep becomes unclear. The aquatic habitat of fish has made it difficult to conduct electrophysiological studies, although the catfish and tench have been studied. The catfish exhibited slow wave electroencephalographic (EEG) activity during inactivity, while the tench only exhibited a decrease in muscle tone and respiratory rate (Lesku et al., 2006, 2008). Zebrafish also exhibit a sleep-like state, and it is well documented that parrot fish build a mucous cocoon at night in which they rest (Campbell and Tobler, 1984; Siegel, 2008). It would appear that fish probably do have a sleep-like state, but that this state is markedly different to mammalian sleep. As with fish, it would seem that there is no clear cut answer regarding sleep in amphibians. To date it would appear that captive bullfrogs do not sleep, whilst several species of tree frog do exhibit behavioural sleep (Lesku et al., 2006, 2008; Siegel 2008). Of particular

interest is that none of the amphibians studied showed any signs of rapid eye movement (REM) sleep as defined in mammals (Lesku et al., 2006, 2008; Siegel, 2008). So while salamanders, frogs and toads do undergo periods of inactivity, it would appear that only certain species exhibit actual behavioural sleep (Campbell and Tobler, 1984). Reptiles most certainly sleep, but under electrophysiological examination these sleep states vary both within and between species studied, and do not readily resemble either avian or mammalian sleep states (Campbell and Tobler, 1984; Lesku et al., 2006, 2008; Siegel, 2008). Birds sleep and in very much the same way that mammals do, both behaviourally and physiologically (Campbell and Tobler, 1984; Lesku et al., 2006, 2008; Siegel, 2008); however, whilst birds exhibit both non-rapid eye movement (NREM) and REM sleep, REM sleep tends to last for only a few seconds. Furthermore, a study of the white-crowned sparrow showed that these birds reduce the time spent sleeping by up to 60% during migration and although this reduction was not followed by a need to catch up on this lost sleep, there was a marked increase in the duration of REM sleep after the migration (Lesku et al., 2006, 2008; Siegel, 2008). It is important to note that investigating sleep in fish, amphibians, reptiles and birds is generally complicated by the comparison to mammalian sleep. There are thousands of species still to be studied and over time further studies may lead to a better understanding and definition of sleep as it relates to each of these animal groups.

Mammalian sleep is by far the most widely studied (Campbell and Tobler, 1984) and whilst the parameters for sleep are well established, there have been some very interesting findings. Mammalian sleep follows the standard definition as outlined above. The electrophysiological characteristics include slow wave sleep (SWS), which is seen as high amplitude, low frequency oscillations on an EEG recording. This type of sleep is also known as NREM sleep. REM sleep is characterised by low amplitude, mixed frequency waves and closely resembles the EEG pattern seen during wakefulness. REM sleep is also accompanied

by muscle atonia and rapid eye movements (Capellini et al., 2008; Lesku et al., 2006, 2008; Nicolau, 2000; Tobler, 1995). Whilst all mammals sleep, there is much variation between different species in terms of total sleep time and time spent in SWS sleep and REM sleep (Lesku et al., 2006, 2008). Large herbivorous terrestrial mammals such as elephants and giraffes sleep the least of all land mammals averaging around 3 h of sleep per day, whereas some of the smallest rodents and bats can sleep for up to 20 h each day (Lesku et al., 2006, 2008; Siegel, 2005). Furthermore, most mammals tend to have numerous sleep episodes throughout the day, known as polyphasic sleep, with primates being the only mammals that sleep in a single consolidated block (monophasic sleep) (Phillips et al., 2010). Some of the most interesting findings to date involve sleep in cetaceans (whales and dolphins) and manatees, which exhibit unihemispheric slow wave sleep (Lyamin et al., 2008). Whereas other mammals will show a pattern of slow wave sleep in both brain hemispheres during sleep, cetaceans only exhibit slow waves in one hemisphere, whilst the other hemisphere remains awake (Lyamin et al., 2008). Furthermore the cetaceans do not appear to have REM sleep (Lyamin et al., 2008). Fur seals, like cetaceans, also exhibit unihemispheric slow wave sleep (USWS) and very low amounts of REM sleep, but this only occurs when the seals are in the water (Siegel, 2005). More striking though is that as soon as the fur seal moves back onto land it reverts back to the standard mammalian pattern of bihemispheric sleep and expected levels of REM sleep (Siegel, 2005).

2.2. Sleep in rodents

Of all non-human mammals studied to date, rodents have been scrutinized in the most detail, but these studies are mostly focussed on laboratory rats, mice and hamsters. Numerous studies have been conducted to define the phases and states of sleep in the laboratory rat

(Clancy et al., 1978; Rosenberg et al., 1976; Timo-Iaria et al., 1970), as well as in the laboratory mouse (Richardson et al., 1985; Tang and Sanford, 2002). van Twyver (1969) studied the sleep patterns of 5 rodent species: hamster, mouse, rat, ground squirrel and chinchilla. Of these only the squirrels had been caught from the wild but had lived in the laboratory for one year prior to the study. All 5 species studied showed the typical rodent EEG sleep pattern of waking, SWS and REM sleep, with each stage accompanied by the expected behavioural and physiological responses. The greatest variation seen between the species was in the percentage of REM sleep, with the mouse spending only 10% of total sleep time (TST) in REM sleep, while the squirrel spent as much as 24% of TST in REM sleep. Other studies have examined the effects of aging on sleep in mice, rats and hamsters (Naylor et al., 1998; Rosenberg et al., 1979; Welsh et al., 1986) or attempts to modify sleep patterns (Webb and Friedman, 1970). The greatest percentage of sleep studies involving rodents are those which use a rodent model to investigate sleep disorders. Several studies have been conducted that investigate the neuroanatomical basis of sleep, as well as communication between different parts of the rodent brain during sleep (Sirota et al., 2003; Gerashchenko et al., 2008; Liu et al., 2010).

It can thus be seen that rodent sleep is very well studied in terms of standard laboratory rodents, and while this information is important, to fully characterize sleep in rodents it is necessary to study more wild-caught species. Dijk and Daan (1989) used polysomnography to study sleep in the Siberian chipmunk, an unusual rodent species in that it is diurnal. Their findings were similar to those for the rat, with TST at 12 h per day and REM sleep accounting for approximately 16% of the TST. Bhagwandin et al. (2011) studied the giant Zambian mole rat, which is a microphthalmic subterranean rodent. TST for this mole rat was found to be shorter than other rodents (~30%, or 7.2 h), although REM sleep time was found to be in the upper ranges when compared to other rodents (16% of TST).

There is a lack of information regarding both the neuroanatomy and physiology of sleep in non-laboratory rodent species and therefore inferences or predictions cannot be made regarding sleep phenomenology when changes in body size, brain size, phylogeny or lifestyle occur within this mammalian order. In order to begin to fill this gap in our knowledge base, the current thesis has examined aspects of both the neuroanatomy and neurophysiology of sleep in five species of wild-caught rodents.

2.3. Rodent species examined

2.3.1. The African pygmy mouse, *Mus minutoides*

The African pygmy mouse (*Mus minutoides*), a member of the family Muridae, is one of the smallest extant rodents, with an average body mass of 8 g (Kerley, 1991; Downs and Perrin, 1996; Monadjem, 1999; Wilson and Reeder, 2005). It is important to note that there have been no studies to date on the circadian rhythms of this species, although it is believed to be nocturnal from field observations (Monadjem, 1999). In captivity, it is seen to be crepuscular, being active in the early morning and early evening, and there is no discernible difference in body mass between males and females (Monadjem, 1999). This tiny rodent is commonly found in the grasslands of southern Africa, although its habitat can range from riverine forest to savannah, where it lives in burrows (Kerley, 1991; Downs and Perrin, 1996; Monadjem, 1999). The pygmy mouse is omnivorous although plant matter makes up the largest percentage of its diet (Kerley, 1991). Pygmy mice live in pairs or colonies and reach sexual maturity at 6 weeks of age. In captivity, pygmy mice breed throughout the year with an average gestation of 20 days. The young are born naked, blind and helpless and begin to leave the nest to explore after 7 days (Heritage Pets, 2013). This species also exhibits an unusual form of sex determination, with a large number (~75%) of fertile females found with

the XY chromosome pairing, which would typically be associated with a male genotype (Veyrunes et al., 2010). There have been no studies to date investigating the sleep related neural systems in this species.

2.3.2. The East African root rat, *Tachyoryctes splendens*

Tachyoryctes splendens, the East African root rat, also belongs to the family Muridae, although some taxonomists assign it to the family Rhizomyidae (Baskevich et al., 1993). The root rat is an aggressive subterranean species found in the highlands of North-East Africa at elevations between 1200 m and 4000 m above sea level (Jarvis, 1973; Baskevich et al., 1993). This rodent has a brownish-grey coat with small eyes and ears and has an average body mass of 230 g (Jarvis and Sale, 1971). There is sexual dimorphism with the males being slightly larger than the females (Jarvis and Sale, 1971). Root rats are solitary, living in burrows that stretch up to 44 m in length. These burrows contain nests, which are filled with pieces of shredded vegetation and faecal matter (Hickman, 1983, 1993). The root rat excavates these burrows using its very long incisors and then pushing the soil out behind with its feet. They are herbivorous, feeding on the roots, stems and leaves of plants, although they will occasionally pull plants in from above the ground down into the burrow (Jarvis and Sale, 1971; Jarvis, 1973). Females reach sexual maturity at 3 months of age and gestation lasts on average 38.5 days, whereafter they give birth to 1 or 2 pups (Jarvis, 1973). In the laboratory setting, the root rat was found to have a nocturnal circadian rhythm being most active between 6 pm and 6 am (Katandukila et al., 2013); however, this contradicts the field study conducted by Jarvis (1973), which found this species to be diurnal. There have been no studies conducted to date on the sleep related neural systems or sleep physiology in this species.

2.3.3. The Cape mole rat, *Georchus capensis*

The Cape mole rat (*Georchus capensis*) is a member of the family Bathyergidae, which is distantly related to the Murid rodents within the order Rodentia. The Cape mole rat is a common species within the Western Cape of South Africa (Du Toit et al., 1985). Similar to the root rat described above, the cape mole rat is solitary and lives in extensive underground burrow systems (Du Toit et al., 1985). The cape mole rat has a greyish-brown coat with white patches on the head and under the belly. It is similar in size to the root rat with an average body mass of 200 g. It is microphthalmic with no external ears and very long incisors, which are used for excavating the burrows (Du Toit et al., 1985). It eats the roots and tubers of the fynbos where it occurs (Du Toit et al., 1985). Cape mole rats are seasonal breeders producing up to 2 litters between August to December (Bennett and Jarvis, 1987). The gestation period is about 44 days and the young leave to build a new burrow at around 60 days of age (Bennett and Jarvis, 1987). The Cape mole rat has been found to be nocturnal being most active between 6 pm and 6 am (Lovegrove and Papenfus, 1995; Oosthuizen et al., 2003). Sleep has previously been investigated in two other species of mole rat using polysomnography: the blind mole rat (Tobler and Deboer, 2001) and the giant Zambian mole rat (Bhagwandin et al., 2011). Furthermore the sleep related nuclei were also studied in the Zambian mole rat (Bhagwandin et al., 2013). The inclusion of the Cape mole rat in the present study is of importance as it is a microphthalmic species that can see, as opposed to the blind mole rat. Furthermore, the Zambian mole rat was found to have two chronotypes: rhythmic and arrhythmic (Bhagwandin et al. 2011), whereas the Cape mole rat has a distinctly nocturnal circadian rhythm as mentioned above.

2.3.4. The greater cane rat, *Thryonomys swinderianus*

The greater cane rat belongs to the family Thryonomyidae and is distantly related to the Muridae, but more closely to the Bathyergidae (Meester et al., 1986). The greater cane rat is one of the largest African rodents, with only the Cape porcupine being larger (Jori et al., 1995). This herbivorous group-living rodent is commonly found throughout southern, central and west Africa where it is hunted or farmed for bush meat (Ewer, 1968; Jori et al., 1995). Male greater cane rats can weigh up to 6 kg in body mass, with females being somewhat smaller, attaining a body mass of approximately 4 kg (Jori et al., 1995). Cane rats have a brownish coat, a long thick tail (25 cm) and 4 large incisors that grow continuously throughout life (Jori et al., 1995). It is interesting to note that while most rodents make a chattering or gnashing sound with their teeth as a warning, the cane rat growls (Ewer, 1968). Cane rats are nocturnal although they do display some crepuscular behaviour in the early evening (Skinner and Chimimba, 2006). To date no studies have been conducted on sleep phenomenology or the sleep related neural systems in this species.

2.3.5. The golden-rumped agouti, *Dasyprocta aguti*

Agoutis (Family Dasyproctidae) are large diurnal South American rodents, of similar size to cane rats (~5 kg), found throughout the South American rain forests (Dubost, 1988; Silvius and Fragoso, 2003). Agoutis feed mainly on fruits and grains, although they may supplement their diet with leaves and insects, and are known to store seeds to be consumed during leaner months (Dubost, 1988; Silvius and Fragoso, 2003). Agoutis have sleep sites in or close to trees (Dubost, 1988). To date no studies have been conducted on the sleep physiology or sleep neuroanatomy in any of the agouti species.

2.4. Sleep and phenotypic, phylogenetic and natural history variances

When we consider mammalian sleep from a phenotypic viewpoint, it can be seen that where there are certain phenotypic changes, there may be changes in sleep patterns. For example, as body mass increases TST decreases (elephants ~ 3 h TST, bats ~ 20 h TST) (Campbell and Tobler, 1984; Lesku et al., 2008); however, if there is a reduction in the visual system, as in the blind mole rat, there does not seem to be any change in the sleep patterns, as this species falls within the expected range for rodents at 12.4 h TST (Tobler and Deboer, 2001).

Sleep patterns vary greatly across the major mammalian groups. Drowsiness, a stage between wake and sleep, although likely to be present in all mammalian groups, is a very distinct stage in carnivores, ungulates and insectivores (Lesku et al., 2006, 2008). Monotremes exhibit some very unusual sleep patterns with the platypus having the most REM sleep of any animal studied to date (Siegel et al., 1998). Cetaceans exhibit unihemispheric slow wave sleep (Lyamin et al, 2008).

Sleep patterns in rodents vary in terms of TST, time spent in NREM and REM. For example, the diurnal Siberian chipmunk spends approximately 12 h asleep every day, which is similar to the arrhythmic blind mole rat (Dijk and Daan, 1989; Tobler and Deboer, 2001); however, the nocturnal giant Zambian mole rat sleeps for only 4.3 h per day and it is subterranean like the blind mole rat, and certain individuals show arrhythmicity (Bhagwandin et al., 2011). There are no studies to date that investigate differences between rodent sleep patterns in terms of natural history changes. It is unclear presently whether any changes in the sleep patterns within rodents are correlated with phenotypic, phylogenetic or natural history

changes or even if there are neuroanatomical correlates to these differences. It is this gap in the literature that the current series of studies hopes to at least partially fill.

Chapter Three: Nuclear organisation of cholinergic, putative catecholaminergic, serotonergic and orexinergic systems in the brain of the African pygmy mouse (*Mus minutoides*): organizational complexity is preserved in small brains

3.1. Introduction

The order Rodentia is comprised of over 2300 species in 34 families (Jansa and Weksler, 2004; Wilson and Reeder, 2005). Within the family *Muridae* are the true rats and mice, including the African pygmy mouse (*Mus minutoides*) (Wilson and Reeder, 2005). This omnivorous nocturnal mouse is one of the smallest extant African rodents with an average body mass of only 8g and inhabits both arid areas and riverine forest (Kerley, 1991; Downs and Perrin, 1996; Monadjem, 1999). *M. minutoides* is an interesting species, not only because of its diminutive size, but also because this species exhibits an unusual form of sex determination. A large number (~75%) of fertile females of this species have been found with the XY chromosome pairing, which would typically be associated with a male genotype (Veyrunes et al., 2010).

The current study investigates several systems within in the brain of *M. minutoides*, using immunohistochemical techniques to reveal the cholinergic, putative catecholaminergic, serotonergic and orexinergic systems. The cholinergic system, which is found from the olfactory bulbs to the spinal cord, is involved in certain sleep stages and wakefulness (Jones and Cuello, 1989; Siegel, 2006), learning and memory (Reiner and Fibiger, 1995; Ferreira et al., 2001), the determination of EEG patterns such as during REM sleep (Siegel, 2006) and even in the generation of the conscious experience (Woolf and Hammeroff, 2001). The

catecholaminergic system is also widely distributed throughout the brain and has a variety of functions including cognitive (memory, abstract thinking and motor planning) (Previc, 1999; Agnati et al., 2003), neuroendocrine (including stress and growth functions) (Fuxe, 1964; Fuxe et al., 1970; Tillet and Kitahama, 1998; Leshin et al., 1995) and cardiorespiratory functions (Feldman and Ellenberger, 1988; Fuxe et al., 1987). The serotonergic system plays a role in mood, sleep and pain regulation (Törk, 1990; Jacobs and Azmitia, 1992), and orexin (hypocretin) is a hypothalamic neuromodulatory peptide produced by neurons in the perifornical and lateral hypothalamus that has been shown to have a role in the control of feeding and arousal (Mintz et al., 2001; Ferguson and Samson, 2003; Zeitzer et al., 2003; Kirouac et al., 2005; Takakusaki et al., 2005).

If we consider the pygmy mouse's natural history, phenotype, sex determination, body size and most importantly its tiny absolute brain mass (~275mg), this species is uniquely placed to shed further light on rodent brain evolution and more generally on patterns of brain evolution across mammals. Studies of the cholinergic, catecholaminergic, serotonergic and orexinergic systems in a range of rodent species including the greater canerat (Dwarika et al., 2008), the highveld gerbil (Moon et al., 2007), the African molerats (Da Silva et al., 2006; Bhagwandin et al., 2006, 2008, 2011), the Cape porcupine (Limacher et al., 2008), the Syrian hamster (McGranaghan and Piggins, 2001; Mintz et al., 2001), the Siberian hamster (McGranaghan and Piggins, 2001) and the unstriped Nile grass rat (Novak and Albers, 2002) complement the wealth of published information on typical laboratory rodents (Dahlström and Fuxe, 1964; Fuxe, 1964; Fuxe et al., 1969, 1970; Hökfelt et al., 1976; 1984; Steinbusch, 1981; Skagerberg et al., 1988; Jones and Cuello, 1989, Peyron et al., 1998; Chen et al., 1999; Cutler et al., 1999; Wagner et al., 2000; Baldo et al., 2003; Espana et al., 2005; Khorooshi and Klingenspor, 2005; Kirouac et al., 2005; Vidal et al., 2005; Nixon and Smale, 2007). Thus, to date, a range of rodent species with varying life histories (schedule

and duration of key life events), phenotypes (including a range of brain and body sizes) and from a range of rodent families have been investigated; however, a rodent species with a very small brain has yet to be examined. Apart from the demonstration of the variation found in the species belonging to the family Muridae (Dahlström and Fuxe, 1964; Björklund and Lindvall, 1984; Limacher et al., 2008 – locus coeruleus proper different in Murids compared to other rodents; Bhagwandin et al., 2006 – cortical cholinergic neurons only found in Murid rodents, but not other species) all species within this order have the same nuclear organisation of these systems regardless of the variation in phenotype, natural history, or evolutionary temporal distance (Manger, 2005). Thus, the present study poses the question of whether, in a very small brain, the nuclear organization of the systems under investigation are less complexly organized, as might be proposed from theories and observations across mammalian orders (Ebbeson, 1980; Stephan et al., 1981), or whether, despite the small brain, does *M. minutoides* display a typically rodent-like organization of these system (Manger, 2005).

3.2. Materials and Methods

The brains from three adult male African pygmy mice were used in this study (average body mass = 8.8 g; average brain mass = 275 mg). All the mice were captured from a wild population in the Eastern Cape of South Africa and were treated and used according to the guidelines of the University of the Witwatersrand Animal Ethics Committee. The animals were euthanized (Euthanase, 200 mg sodium pentobarbital/kg, i.p.) and, upon cessation of respiration, perfused intracardially with an initial rinse of 0.9% saline solution at 4°C (10 ml), which was followed by a solution of 4% paraformaldehyde in 0.1M phosphate buffer (PB) (10 ml). After removal from the skull, each brain was post-fixed overnight in the

paraformaldehyde solution and subsequently stored in anti-freeze at -20°C. Before sectioning, the brains were allowed to equilibrate in 30% sucrose in 0.1 M PB at 4°C. Each brain was then frozen and sectioned into 50 µm thick serial coronal sections. A one in six series of sections was used for Nissl, myelin, choline-acetyltransferase (ChAT), tyrosine hydroxylase (TH), serotonin (5HT) and orexin (hypocretin/OxA). Sections for Nissl staining were first mounted on 0.5% gelatine coated slides, cleared in a solution of 1:1 absolute alcohol and chloroform and then stained with 1% cresyl violet. The myelin series sections were refrigerated for two weeks in 5% formalin then mounted on 1% gelatine coated slides and stained with a modified silver stain (Gallyas, 1979).

The sections for immunohistochemical staining were treated for 30 min in an endogenous peroxidase inhibitor (49.2% methanol: 49.2% 0.1M PB: 1.6% of 30% hydrogen peroxide) followed by three 10 min rinses in 0.1M PB. Sections were then preincubated for 2 h, at room temperature, in blocking buffer (3% normal goat serum, NGS, for TH, serotonin and orexin sections; 3% normal rabbit serum, NRS, for ChAT sections, 2% bovine serum albumin for all sections and 0.25% Triton-X in 0.1M PB for all sections). Thereafter sections were incubated in the primary antibody solution in blocking buffer for 48h at 4°C. Anti-cholineacetyltransferase (AB144P, Millipore, raised in goat) at a dilution of 1:3000 was used to reveal cholinergic neurons. Anti-tyrosine hydroxylase (AB151, Millipore, raised in rabbit) at a dilution of 1:7500 revealed the putative catecholaminergic neurons. Serotonergic neurons were revealed using anti-serotonin (AB938, Millipore, raised in rabbit) at a dilution of 1:10000. Orexinergic neurons were revealed using anti-OrexinA (AB3704, Millipore, raised in rabbit) at a dilution of 1:3000. This incubation was followed by three 10 min rinses in 0.1M PB and the sections were then incubated in a secondary antibody solution (1:1000 dilution of biotinylated anti-rabbit IgG for TH, serotonin and orexin sections, or a 1:1000 dilution of biotinylated anti-goat IgG for ChAT sections, in a blocking buffer containing 3%

NGS/NRS and 2% BSA in 0.1M PB) for 2h at room temperature. This was followed by three 10 min rinses in 0.1M PB, after which sections were incubated for 1h in Avidin-Biotin solution (Vector Labs), followed by three 10 min rinses in 0.1M PB. Sections were then placed in a 0.05% diaminobenzidine (DAB) in 0.1M PB solution for 5 min, followed by the addition of 3 μ l of 3% hydrogen peroxide to each 1 ml of solution in which each section was immersed. Chromatic precipitation was visually monitored and verified under a low power stereomicroscope. Staining continued until such time as the background stain was at a level that would assist reconstruction without obscuring the immunopositive neurons. Precipitation was arrested by placing sections in 0.1M PB, followed by two more rinses in this solution. Sections were then mounted on 0.5% gelatine coated glass slides, dried overnight, dehydrated in a graded series of alcohols, cleared in xylene and coverslipped with Depex. The controls employed in this experiment included the omission of the primary antibody and the omission of the secondary antibody in selected sections for which no staining was evident.

Sections were examined under a low power stereomicroscope and using a camera lucida, the architectonic borders of the sections were traced following the Nissl and myelin stained sections. Sections containing the immunopositive neurons were matched to the drawings and the neurons were marked. All drawings were then scanned and redrawn using the Canvas 8 drawing program. All architectonic nomenclature was taken from the atlas of a rodent brain (Paxinos and Watson, 2009). The nomenclature used for the cholinergic system was adopted from Woolf (1991), Limacher et al. (2008) and Bhagwandin et al. (2008), the catecholaminergic from Hökfelt et al. (1984), Smeets and Gonzalez (2000), Limacher et al. (2008) and Bhagwandin et al. (2008), the serotonergic from Törk (1990), Limacher et al. (2008) and Bhagwandin et al. (2008) and the orexinergic from Kruger et al. (2010a), Bhagwandin et al. (2011) and Gravett et al (2011). While we use the standard nomenclature for the catecholaminergic system in this paper, we realise that the neuronal groups we

revealed with tyrosine hydroxylase immunohistochemistry may not directly correspond with these nuclei as has been described in previous studies by Dahlström and Fuxe (1964), Hökfelt et al. (1976), Meister et al. (1988), Kitahama et al. (1990, 1996), and Ruggiero et al. (1992). However, given the striking similarity of the results of the tyrosine hydroxylase immunohistochemistry to that seen in other mammals, we feel this terminology is appropriate. Clearly further studies in the pygmy mouse used with a wider range of antibodies, such as those to phenylethanolamine-N-methyltransferase (PNMT), dopamine- β -hydroxylase (DBH) and aromatic L-amino acid decarboxylase (AADC) would be required to fully determine the implied homologies ascribed in this study (e.g. Weihe et al., 2006). We address this potential problem with the caveat of putative catecholaminergic neurons where appropriate in the text.

Abbreviations used for Anatomical Structures:

III – oculomotor nucleus

IV – trochlear nucleus

Vmot – motor division of trigeminal nerve nucleus

Vsens – sensory division of trigeminal nerve nucleus

VI – abducens nucleus

VII_d – dorsal division of facial nerve nucleus

VII_v – ventral division of facial nerve nucleus

X – dorsal motor vagus nucleus

XII – hypoglossal nucleus

3V – third ventricle

4V – fourth ventricle

7n – facial nerve

A1 – caudal ventrolateral medullary tegmental nucleus

A2 – caudal dorsomedial medullary nucleus

A4 – dorsolateral division of locus coeruleus

A5 – fifth arcuate nucleus

A6c – compact portion of locus coeruleus

A7d – nucleus subcoeruleus, diffuse portion

A7sc – nucleus subcoeruleus, compact portion

A8 – retrorubral nucleus

A9l – substantia nigra, lateral

A9m – substantia nigra, medial

A9pc – substantia nigra, pars compacta

A9v – substantia nigra, ventral, pars reticulata

A10 – ventral tegmental area

A10c – ventral tegmental area, central

A10d – ventral tegmental area, dorsal

A10dc – ventral tegmental area, dorsal caudal

A11 – caudal diencephalic group

A12 – tuberal cell group

A13 – zona incerta cell group

A14 – rostral periventricular nucleus

A15d – anterior hypothalamic group, dorsal division

A15v – anterior hypothalamic group, ventral division

A16 – catecholaminergic neurosn of the olfactory bulb

ac – anterior commissure

Amyg – amygdala

AP – area postrema

ARC – arcuate nucleus of the hypothalamus

B9 – suprallemniscal serotonergic nucleus

C1 – rostral ventrolateral medullary tegmental group

C2 – rostral dorsomedial medullary nucleus

C3 – rostral dorsal midline medullary nucleus

C – caudate nucleus

ca – cerebral aqueduct

cc – corpus callosum

Cer - cerebellum

CLi – caudal linear nucleus

CN – deep cerebellar nucleus

CVL – caudal ventrolateral serotonergic group

Diag.B – diagonal band of Broca

DRc – dorsal raphe, caudal division

DRd – dorsal raphe, dorsal division

DRif – dorsal raphe, interfascicular division

DRl – dorsal raphe, lateral division

DRp – dorsal raphe, peripheral division

DRv – dorsal raphe, ventral division

DT – dorsal thalamus

EW – Edinger-Westphal nucleus

f – fornix

fr – fasciculus retroflexus

GC – central grey matter

GCL – granular cell layer of olfactory bulb

GP – globus pallidus

Hbl – lateral habenular nucleus

Hbm – medial habenular nucleus

HIP - hippocampus

Hyp – hypothalamus

Hyp.d – dorsal hypothalamic cholinergic nucleus

Hyp.l – lateral hypothalamic cholinergic nucleus

Hyp.v – ventral hypothalamic cholinergic nucleus

IC – inferior colliculus

ic – internal capsule

io – inferior olive

IP – interpeduncular nucleus

Is.Call/TOL – islands of Calleja/olfactory tubercle

LDT – laterodorsal tegmental nucleus

LGv – ventral lateral geniculate nucleus

LOT – lateral olfactory tract

LV – lateral ventricle

Mc – orexinergic main cluster

mcp – middle cerebellar peduncle

MnR – median raphe nucleus

mtf – medullary tegmental field

N.Acc – nucleus accumbens

N.Amb – nucleus ambiguus

N.Bas – nucleus basalis

Neo – neocortex

OB – olfactory bulb

OC – optic chiasm

OT – optic tract

Otc – orexinergic optic tract cluster

P – putamen nucleus

PB – parabrachial nucleus

PBg – parabigeminal nucleus

PC – cerebral peduncle

PIR – piriform cortex

PPT – pedunculopontine nucleus

Pta – pretectal area

py – pyramidal tract

pVII – preganglionic motor neurons of the superior salivatory nucleus or facial nerve

pIX – preganglionic motor neurons of the inferior salivatory nucleus

R – reticular nucleus of the thalamus

RMg – raphe magnus nucleus

ROb – raphe obscurus nucleus

RPa – raphe pallidus nucleus

RVL – rostral ventrolateral serotonergic group

S – septal nuclear complex

SC – superior colliculus

scp – superior cerebellar peduncle

Sep.M – medial septal nucleus

SON – superior olivary nucleus

sp5 – spinal trigeminal tract

VCO – ventral cochlear nucleus

VPO – ventral pontine nucleus

xpy – decussation of the pyramidal tract

xscp – decussation of the superior cerebellar peduncle

zi – zona incerta

Zic – orexinergic zona incerta cluster

3.3. Results

The current study delineates the nuclear organization of the cholinergic, putative catecholaminergic, serotonergic and orexinergic neural systems of the African pygmy mouse (Fig. 3.1). The three pygmy mice used in this study had an average body mass of 8.8 g and an average brain mass of 275 mg, making the African pygmy mouse brain the smallest of any rodent species studied to date; however, this diminutively sized brain (in comparison to the

mass of previously studied rodent brains) has not led to any reduction in the number or complement of nuclei present. In fact, the overall complexity of neural systems investigated within the pygmy mouse brain showed all the typical subdivisions across all of the regions that would be expected in a rodent brain (e.g. Bhagwandin et al., 2008, 2011; Limacher et al., 2008).

3.3.1. Cholinergic nuclei

The cholinergic system can be subdivided into the cortical interneurons, the striatal, basal forebrain, diencephalic, pontomesencephalic and the cranial motor nerve nuclei (Woolf, 1991), each subdivision containing a cluster of distinct nuclei (Figs. 3.1, 3.2).

Cholineacetyltransferase immunoreactive neurons (ChAT+) were identified in all these subdivisions, including the cortical cholinergic interneurons, which have a variable occurrence across rodent species studied to date (e.g. Bhagwandin et al., 2006).

3.3.1.1 Cortical cholinergic neurons

In a previous study (Bhagwandin et al., 2006) it was demonstrated that the appearance of cholinergic interneurons within the cerebral cortex of rodents appears to be limited to the members of the Murid family. The African pygmy mouse (*Mus minutoides*) is a member of this family, and in the current study we observed cortical neurons immunoreactive to the ChAT antibody through all regions of the cortex (Fig. 3.2B). The majority of these neurons were found in the supragranular cortical layers, but were observed to occur in all cortical layers except layer one. The ChAT+ neurons were bipolar in nature with the majority being vertically oriented within the cortical mantle.

3.3.1.2. Striatal cholinergic interneurons

ChAT+ neurons were found in the caudate/putamen complex, the globus pallidus, the nucleus accumbens, the Islands of Calleja and the olfactory tubercle (Fig. 3.1C – 3.1H). A moderate density of ChAT+ neurons were found within the caudate/putamen and throughout the globus pallidus, but most densely at its borders with the putamen and nucleus basalis (Fig. 3.2A, 3.2C). Through the nucleus accumbens a moderate density of ChAT+ neurons was observed, and at the ventral border of this nucleus, they appear to intermingle with the most dorsal cholinergic neurons of the olfactory tubercle (Fig. 3.2A). The ChAT+ neurons within the olfactory tubercle and Islands of Calleja were found in the most ventral portion of the anterior telencephalon (Fig. 3.2A). Throughout the olfactory tubercle a moderate density of ChAT+ neurons were observed, and within the most ventral portion of this region clusters of ChAT+ neurons were observed to form the Islands of Calleja.

3.3.1.3. Cholinergic nuclei of the basal forebrain

Cholinergic nuclei that could be identified within the basal forebrain of the African pygmy mouse included the medial septal nucleus, the Diagonal band of Broca and the nucleus basalis (Fig. 3.1D – 3.1G). The medial septal nucleus exhibited a moderate to high density of ChAT+ neurons and was located within the rostral half of the medial wall of the septal nuclear complex immediately below the rostrum of the corpus callosum. The ChAT + neurons forming the diagonal band of Broca were evidenced as a high density of neurons located in the ventromedial corner of the cerebral hemisphere anterior to the hypothalamus (Fig. 3.2A). It was possible to divide this nucleus into both horizontal and vertical limbs, but

this was not deemed necessary since it would not add any value to the description. A cluster of moderate to high-density ChAT⁺ neurons located anterior and ventral to the globus pallidus and caudal to the olfactory tubercle were assigned to the nucleus basalis (Fig. 3.2C). At the posterior portion of this nucleus, the neurons appear to be continuous with those of the globus pallidus.

3.3.1.4. Diencephalic cholinergic nuclei

ChAT⁺ neurons were found in the medial habenular nucleus, as well as the dorsal, lateral and ventral hypothalamic clusters (Fig. 3.1F – 3.1I). The medial habenular nucleus was located in the dorsomedial aspect of the diencephalon adjacent to the third ventricle. The ChAT⁺ neurons within this nucleus were very densely packed (Fig. 3.2D). The three clusters of ChAT⁺ neurons within the hypothalamus all showed moderate to weak immunoreactivity, but were clearly observed. The dorsal cluster was found in the dorsomedial aspect of the hypothalamus between the third ventricle and fornix (Fig. 3.2C), the lateral cluster was found in the dorsolateral aspect of the hypothalamus, lateral to the fornix, while the ventral cluster was located in the ventral medial portion of the hypothalamus adjacent to the neurons of the A12 nucleus (see below).

3.3.1.5. Pontomesencephalic cholinergic nuclei

ChAT⁺ immunoreactive neurons were used to delineate the parabigeminal nucleus, as well as the pedunculopontine (PPT) and the laterodorsal (LDT) nuclei (Fig. 3.1K – 3.1M). The parabigeminal nucleus was located at the very lateral margin of the pontine tegementum in a location ventral to the inferior colliculus. Within this nucleus the ChAT⁺ neurons were

moderately densely packed (Fig. 3.1E). The ChAT⁺ neurons forming the PPT were located within the dorsal aspect of the pontine tegmentum surrounding the superior cerebellar peduncle. A moderate to high density of ChAT⁺ neurons were observed in this region (Fig. 3.2E, 3.2F). Within the periventricular grey matter, caudal to the oculomotor nucleus, a moderate to high density of ChAT⁺ neurons were designated as those forming the LDT nucleus (Fig. 3.2F). The ventrolateral border of the LDT neurons was contiguous with the dorsomedial border of the PPT nucleus, the only reason to separate these two nuclei being the transition from the periventricular grey matter to the pontine tegmentum.

3.3.1.6. Cholinergic cranial nerve motor nuclei

These nuclei were found in positions typical of all mammals (Woolf, 1991; Manger et al., 2002a; Maseko et al., 2007). The ChAT⁺ nuclei identified in the African pygmy mouse include: the oculomotor (III), trochlear (IV), motor division of the trigeminal (Vmot), abducens (VI), dorsal and ventral subdivisions of the facial (VII_d and VII_v), nucleus ambiguus, dorsal motor vagus (X), hypoglossal (XII), Edinger–Westphal (EW), medullary tegmental field (mtf) and the preganglionic motor neurons of the salivatory (pVII) and the glossopharyngeal (pIX) nerves (Fig. 3.1J – 3.1R).

3.3.2. Putative catecholaminergic nuclei

Tyrosine hydroxylase (TH) immunoreactivity was used to reveal the putatively catecholaminergic neurons (see above) in the African pygmy mouse brain. The nuclei formed by these neurons were arranged in a number of identifiable nuclear complexes that extended from the olfactory bulb through to the spinomedullary junction (Fig. 3.1). These complexes correspond to that seen in other rodents and could be divided into the olfactory bulb,

diencephalic, midbrain, pontine and medullary nuclear clusters. For simplicity, in the current description, the nuclei are referred to using the nomenclature of Dahlström and Fuxe (1964) and Hökfelt et al. (1984). No putatively catecholaminergic nuclei outside the classically defined nuclei (e.g. Smeets and Gonzalez, 2000) were observed.

3.3.2.1. Olfactory bulb (A16)

A high density of TH⁺ neurons was found in and around the stratum granulosum of the olfactory bulb. These neurons probably represent the periglomerular dopaminergic interneurons, were small in size, and were found in equal density surrounding the entire glomeruli (Fig. 3.1A, 3.1B).

3.3.2.2. Diencephalic nuclei (A15 – A11)

Six clusters of TH⁺ neurons, forming distinct nuclei, were observed within the hypothalamus, these being: the anterior hypothalamic group, dorsal division (A15d); the anterior hypothalamic group, ventral division (A15v); the rostral periventricular cell group (A14); the zona incerta (A13); the tuberal cell group (A12); and the caudal diencephalic group (A11) (Fig. 1E-J). Within the dorsal anterior portion of the hypothalamus, between the third ventricle and the fornix, a moderate density of TH⁺ neurons was designated as the A15d nucleus (Fig. 3.3A). The TH⁺ neurons forming the A15v nucleus were located in the ventrolateral portion of the hypothalamus in a moderate density close to the floor of the brain. A low to moderate density of TH⁺ neurons within the hypothalamus and preoptic area, forming two columns adjacent to the lateral walls of the third ventricle, were assigned as the A14 nucleus (Fig. 3.3A, 3.3B). Within the dorsolateral aspect of the hypothalamus, lateral to

the fornix and intermingling with the neurons forming the zona incerta of the ventral thalamus, was a low to moderate density of TH⁺ neurons belonging to the A13 nucleus (Fig. 3.3B). TH⁺ neurons assigned to the A12 nucleus were located in the ventromedial portion of the hypothalamus, surrounding and below the floor of the third ventricle in the arcuate nucleus and the immediate vicinity (Fig. 3.3B). Lastly, within the hypothalamic grey matter adjacent to the posterior pole of the third ventricle, a moderate density of TH⁺ neurons formed the A11 nucleus.

3.3.2.3. Midbrain nuclei (A10 – A8)

Within the midbrain, the TH⁺ neurons were found within the ventral tegmental area (the A10 complex, including the A10, A10c, A10d, A10dc nuclei), the substantia nigra (the A9 complex, including the A9pc, A9l, A9v, A9m nuclei) and the retrorubral nucleus (A8) within the midbrain tegmentum (Fig. 3.1J, 3.1K). The nuclei of the A10 complex extended from within the periaqueductal grey matter around the base of the aqueduct, into the tegmentum below the periaqueductal grey matter around the midline, through to and around the interpeduncular nucleus. A high density of TH⁺ neurons, found dorsal and dorsolateral to the interpeduncular nucleus, between this nucleus and the root of the oculomotor nerve (III_n), was assigned to the A10 nucleus. Immediately dorsal to the interpeduncular nucleus, in a location just anterior to the decussation of the superior cerebellar peduncle, was a dense cluster of TH⁺ neurons forming the A10c nucleus. Immediately dorsal to A10c, between it and the oculomotor nucleus, was a dense bilateral parasagittal cluster of TH⁺ neurons that formed the A10d nucleus (Fig. 3.3C). The TH⁺ neurons assigned to the A10dc nuclear complex were found within the periaqueductal grey matter adjacent to and surrounding the ventral half of the cerebral aqueduct.

The substantia nigra nuclear complex was located in the ventral and lateral portions of

the midbrain tegmentum, lying just dorsal to the cerebral peduncles. Evidence for four distinct nuclei namely, the substantia nigra, pars compacta (A9pc), substantia nigra, ventral or pars reticulata (A9v), substantia nigra, pars lateralis (A9l) and substantia nigra, pars medialis (A9m), were found within the A9 complex. A9pc was seen to be a dense band of TH+ neurons that ran from medial to lateral immediately ventral to the medial lemniscus. Throughout the grey matter (pars reticulata of the substantia nigra) ventral to A9pc, several scattered TH+ neurons were assigned to the A9v nucleus (Fig. 3.3C). At the lateral edge of A9pc, a moderate density and loose aggregation of TH+ neurons formed the A9l nucleus. Medial to A9pc and lateral to the root of the oculomotor nerve (III_n), a dense cluster of TH+ neurons formed the A9m nucleus. Scattered throughout the midbrain tegmentum, in a position caudal to the magnocellular division of the red nucleus and dorsal to the A9 complex, was a sparsely packed but relatively numerous, cluster of TH+ neurons that formed the A8 nucleus (Fig. 3.3C).

3.3.2.4. Rostral rhombencephalon – the locus coeruleus complex, A7 – A4

Within the pontine region a large number of TH+ neurons forming the locus coeruleus complex were readily observed (Fig. 3.1M – 3.1O). The locus coeruleus complex could be readily subdivided into five nuclei, these being: the subcoeruleus compact portion (A7sc), subcoeruleus diffuse portion (A7d), locus coeruleus compact portion (A6c), fifth arcuate nucleus (A5), and the dorsolateral division of locus coeruleus (A4). Within the dorsal portion of the pontine tegmentum adjacent to the ventrolateral region of the periaqueductal grey matter, a tightly packed cluster of TH+ neurons represented the A7 compact portion of the LC. This division is the same as what was previously described as the subcoeruleus (Dahlström and Fuxe, 1964; Olson and Fuxe, 1972). Ventral and lateral to the A7sc, a diffusely organised aggregation of TH+ neurons formed the A7d nuclear complex. These

neurons are located both medially and laterally around the trigeminal motor nucleus (Vmot). Within the lateral portion of the periventricular grey matter a tightly packed, moderate to high density of TH⁺ neurons were assigned to the A6c nucleus (Fig. 3.3D). The neurons of this group were found adjacent to the wall of the fourth ventricle, stretching across the periventricular grey matter to its lateral edge as seen in the laboratory rat (Dahlström and Fuxe, 1964), and were not seen as a loosely packed cluster of neurons located in the ventrolateral half of the periventricular grey matter as seen in other non-Murid rodent species (Moon et al., 2007; Dwarika et al., 2008; Bhagwandin et al., 2008; Limacher et al., 2008). In the ventrolateral pontine tegmentum lateral to the superior olivary nucleus and lateral to Vmot and A7d, a small cluster of TH⁺ neurons formed the A5 nucleus. These neurons formed a rough meshlike dendritic network around the ascending fascicles located within the ventrolateral pontine tegmentum. Immediately adjacent to the wall of the fourth ventricle, in the dorsolateral portion of the periaqueductal grey matter, a very dense, but small cluster of TH⁺ neurons represent the A4 nucleus.

3.3.2.5. Medullary nuclei (C1, C2, C3, A1, A2, Area postrema)

Within the medulla of the African pygmy mouse we found evidence for six putative catecholaminergic nuclei these being: rostral ventrolateral tegmental group (C1), rostral dorsomedial group (C2), rostral dorsal midline group (C3), caudal ventrolateral tegmental group (A1), caudal dorsomedial group (A2) and area postrema (AP) (Fig. 3.1N – 3.1R). A low density of TH⁺ neurons forming the C1 nucleus were found in the ventrolateral medulla from the level of the facial nerve nucleus to the mid-level of nucleus ambiguus. Continuing in the ventrolateral medulla, a column of TH⁺ neurons located laterally to the posterior most part of the C1 nucleus and extending to the spinomedullary junction was designated as the A1 nucleus. The A1 column was distinguished from the ventrolateral C1 column by occupying a

position lateral to the lateral reticular nucleus and nucleus ambiguus, whereas C1 was located medial to these structures. In the dorsal part of the medulla, in the region of the anterior part of the dorsal and medial border of the nucleus tractus solitarius, a distinct cluster of numerous TH⁺ neurons was designated as the C2 nucleus. Within this nucleus there was a clear region close to the floor of the fourth ventricle termed the dorsal strip and a continuation of this cluster into the region of the tractus solitarius termed the rostral subdivision of the C2 nucleus. Within the dorsal medial medullary tegmentum at the midline, dorsal to the raphe obscurus and close to the floor of the fourth ventricle, a very few TH⁺ neurons representing the C3 nucleus were found. Between the caudal portions of the dorsal motor vagus and hypoglossal cranial nerve nuclei, a small number of TH⁺ neurons represented the A2 nucleus. Some of these A2 neurons were located a small distance into the dorsal caudal medullary tegmentum. Straddling the midline, dorsal to the central canal and the dorsal motor vagus nucleus, and between the most caudal region of the bilateral C2 nucleus, was a single large, densely packed, cluster of intensely stained TH⁺ neurons, the area postrema.

3.3.3. Serotonergic nuclei

The serotonergic (5HT⁺) nuclei identified in the African pygmy mouse were the same as those previously identified in all rodents and other eutherian mammals studied to date (Steinbusch, 1981; Maseko et al., 2007; Dell et al., 2010). The serotonergic nuclei were all located within the brainstem and can be divided into a rostral and a caudal cluster. Both of these clusters contained a number of distinct nuclei that are found throughout the brainstem from the level of the decussation of the superior cerebellar peduncle through to the spinomedullary junction (Fig. 3.1K – 3.1R).

3.3.3.1. Rostral cluster

Within the rostral cluster we found evidence for the caudal linear nucleus (CLi), the suprallemniscal nucleus (B9), the median raphe nucleus (MnR) and the dorsal raphe complex formed of six distinct nuclei (Fig. 3.1K – 3.1M). The CLi nucleus was the most rostral of the serotonergic nuclei found and the 5HT⁺ neurons formed a moderate density cluster around the midline immediately dorsal to the interpeduncular nucleus in a location just anterior to the decussation of the superior cerebellar peduncle (Fig. 3.4A). The neurons forming the B9 nucleus appeared to be a lateral extension of the neuronal cluster comprising the most ventral portion of CLi. The 5HT⁺ B9 neurons were found in a low to moderate density immediately caudal to the A9pc (see above) within and above the medial lemniscus and extended as an arc of neurons into the lateral and ventrolateral portion of the midbrain tegmentum (Fig. 3.4A). The median raphe nucleus (MnR) was characterised by two distinct, densely packed 5HT⁺ neuronal columns on either side of the midline in a para-raphé position (Fig. 3.4B, 3.4C). The rostral border of this nucleus was coincident with the level of the decussation of the superior cerebellar peduncle and the caudal border of this nucleus was found at the level of the trigeminal motor nucleus.

Within the 5HT⁺ neuronal region designated as the dorsal raphe nuclear complex there were six distinct nuclei, these being: the dorsal raphe interfascicular (DRif) nucleus, dorsal raphe ventral (DRv) nucleus, dorsal raphe dorsal (DRd) nucleus, dorsal raphe lateral (DRI) nucleus, dorsal raphe peripheral (DRp) nucleus and the dorsal raphe caudal (DRc) nucleus (Figs. 3.1K – 3.1M, 3.4B, 3.4C). These six nuclei were found, for the most part, within the periaqueductal and periventricular grey matter from the level of the oculomotor nucleus to the trigeminal motor nucleus. The DRif was located between the two medial longitudinal fasciculi and exhibited a high density of 5HT⁺ neurons. The DRv was found immediately dorsal to the DRif between and just caudal to the oculomotor nuclei. The DRv exhibited a high density of 5HT⁺ neurons. Immediately dorsal to DRv and ventral to the

inferior border of the cerebral aqueduct a high-density cluster of 5HT+ neurons was designated as the DRd nucleus. A moderate density of 5HT+ neurons representing the DRp, were located in the ventrolateral portion of the periaqueductal grey matter lateral to the DRd and DRv. Some neurons of the DRp were found in the adjacent tegmentum and are the only ones found outside the periaqueductal grey matter. The 5HT+ neurons of the DRI were located dorsolateral to the DRd and adjacent to the ventrolateral edges of the cerebral aqueduct in a low to moderate density. The neurons of this nucleus were readily distinguishable from the remainder of the dorsal raphe nuclei since they were substantially larger. As we followed the DRI caudally, where the cerebral aqueduct opened into the fourth ventricle and the DRd, DRv and DRif disappeared, the neurons of the DRI formed an arc across the midline of the dorsal portion of the periventricular grey matter. This caudal arc of the DRI was classified as the DRc nucleus. We classified this as an independent nucleus due to the lack of 5HT+ neurons in this region in the brain of monotremes (Manger et al., 2002c; Maseko et al., 2007; Dell et al., 2010).

3.3.3.2. Caudal cluster

Within the caudal cluster we found evidence for the raphe magnus (RMg), rostral and caudal ventrolateral (RVL and CVL), raphe pallidus (RPa) and raphe obscurus (ROb) nuclei (Figs. 3.1M – 3.1R, 3.4D). This RMg was seen to be two columns of loosely aggregated moderate to large 5HT+ neurons located on either side of the midline from the level of the caudal pole of the trigeminal motor nucleus to the anterior pole of nucleus ambiguus. Within the left and right ventrolateral medullary tegmentum a distinct anteroposterior column of 5HT+ neurons extending from the level of the facial nucleus to the spinomedullary junction were observed. These have previously been termed the rostral and caudal ventrolateral serotonergic columns (e.g. Maseko et al., 2007; Moon et al., 2007; Dwarika et al., 2008). The

RVL began as a lateroventral continuation of 5HT+ neurons from the lower portion of the RMg extending over the pyramidal tracts and consolidating as a distinct column lateral to the inferior olives. The inferior olive topologically distinguishes left and right RVL, and at the level of nucleus ambiguus the RVL becomes the CVL. The CVL continues in the caudal ventrolateral medullary tegmentum until the spinomedullary junction is reached. The number of neurons within this RVL/CVL column steadily decreases from rostral to caudal. Although the RVL and CVL are continuous in the African pygmy mice studied, and indeed several other eutherian mammals previously studied (e.g. Maseko et al., 2007; Moon et al., 2007; Dwarika et al., 2008), we make the distinction of two components of these ventrolateral columns, as the caudal portions have not been reported in the opossum or the monotremes (Crutcher and Humbertson, 1978; Manger et al., 2002c). The 5HT+ neurons forming the RPa nucleus were found in the ventral midline of the medulla associated with the pyramidal tracts. These neurons were for the most part located between the two pyramidal tracts, but some neurons belonging to this nucleus (based on neuronal morphology) were identified dorsal to the pyramidal tract, between it and the inferior olive. Two loosely arranged bilateral columns of 5HT+ neurons located either side of the midline from the level of nucleus ambiguus to the spinomedullary junction were classified as the ROb. Occasional 5HT+ neurons associated with this nucleus were identified within a short distance (less than 200 μ m) lateral to the central columns.

3.3.4. Orexinergic (hypocretinerbic) nuclei

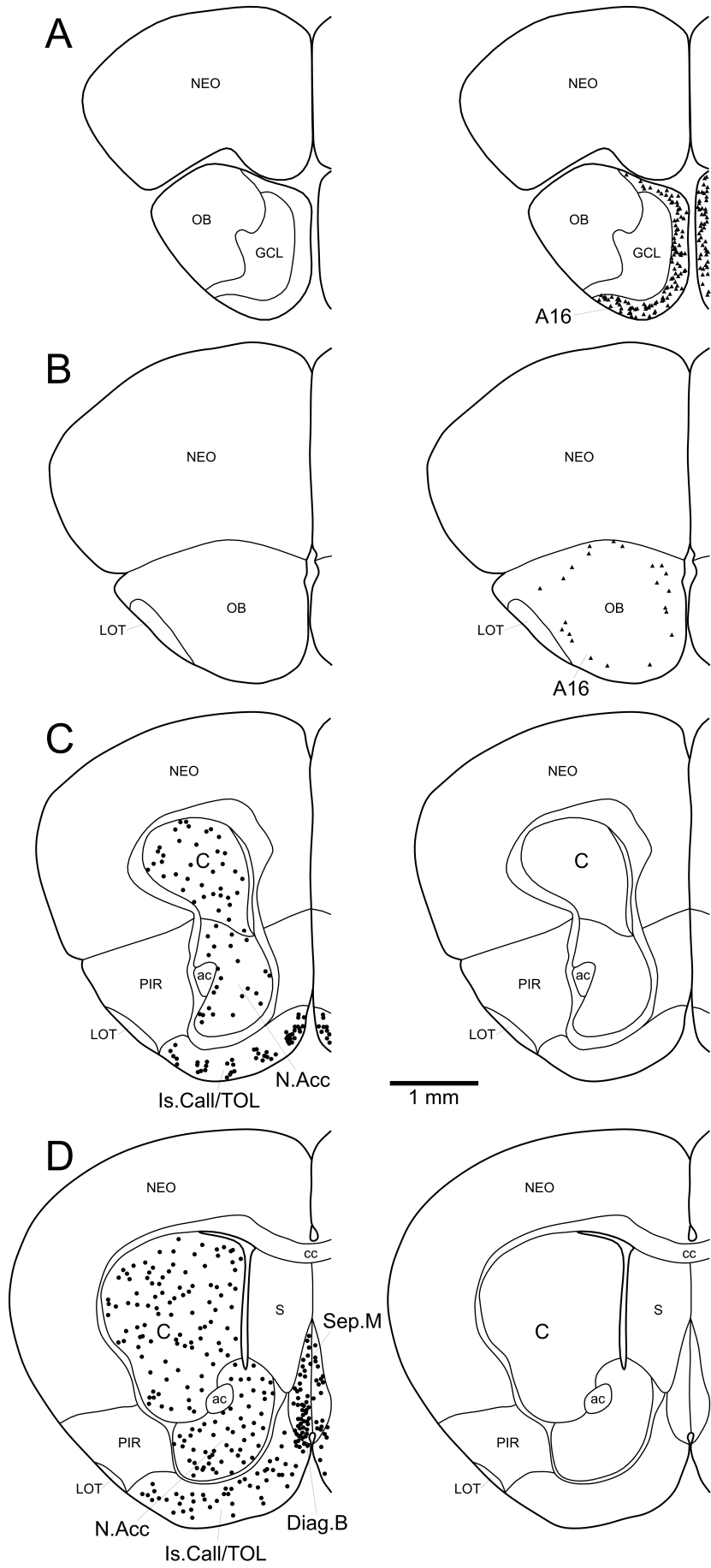
The vast majority of orexin-A immunopositive neurons (OrX+) identified in the brain of the African pygmy mouse were localised in the hypothalamus (Fig. 3.1F – 3.1I). Within this aggregation of OrX+ cells we could identify three distinct clusters – a main cluster (Mc), a zona incerta cluster (Zic) and an optic tract cluster (Otc) (Fig. 3.5). The main cluster (Mc)

was identified as a large group of densely packed OrX⁺ neuronal cell bodies located lateral to the third ventricle in the perifornical region, with a moderate number of neuronal cell bodies extending medially from this area into the dorsomedial hypothalamus and a larger number extending into the lateral hypothalamic areas. From the main cluster a group of OrX⁺ neuronal cell bodies extended laterally into the region of the zona incerta (Zic). This cluster had a very low density of OrX⁺ neurons that were mixed with neurons of the lateral hypothalamic cholinergic nucleus and the A13 nucleus of the catecholaminergic system (see above). The third cluster, the optic tract cluster (Otc) extended ventrolaterally from the main cluster to the ventrolateral region of the hypothalamus adjacent to the optic tract. This cluster exhibited a moderate density of OrX⁺ neuronal cell bodies.

Figure 3.1: Serial drawings of coronal sections through one half of the African pygmy mouse brain from the olfactory bulb through to the spinomedullary junction. **A** is the most rostral section, **R** the most caudal. The outlines of the architectonic regions were drawn using Nissl and myelin stains and immunoreactive cells marked on the drawings. Solid black circles depict cholinergic neurons, solid triangles depict catecholaminergic neurons (those immunoreactive for tyrosine hydroxylase), open squares depict serotonergic neurons and closed stars represent orexinergic neurons. Each circle, triangle, square or star represents an individual neuron. The figures are approximately 600 μm apart. See list for abbreviations.

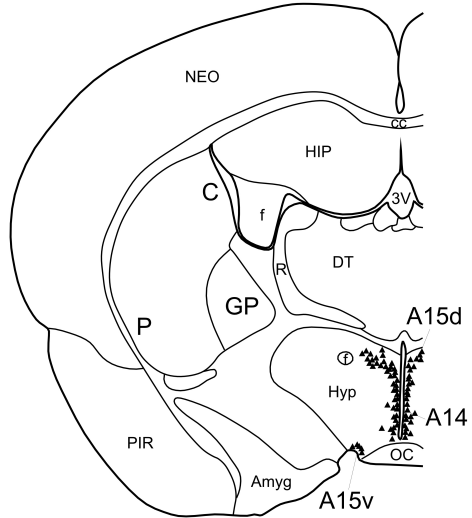
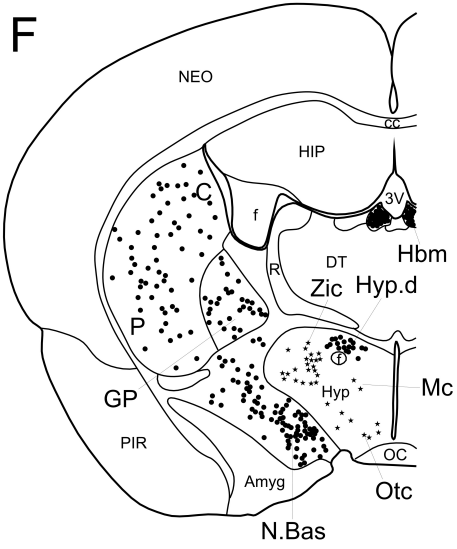
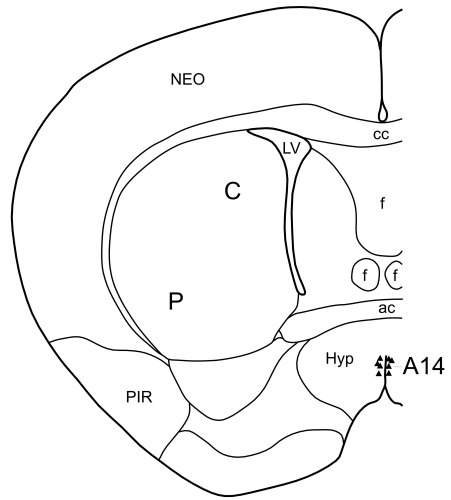
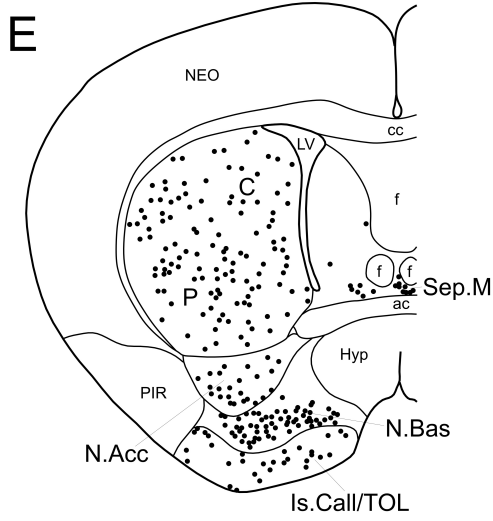
Cholinergic and Orexinergic

Catecholaminergic and Serotonergic

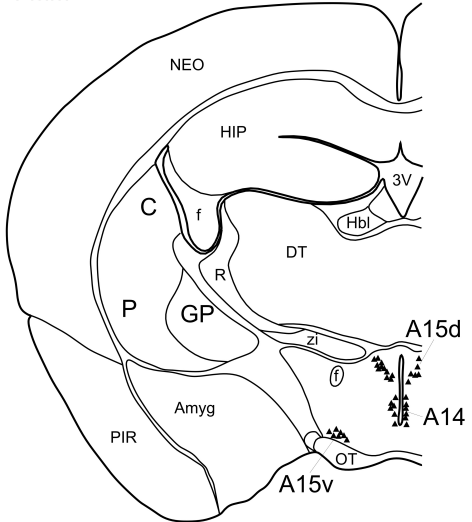
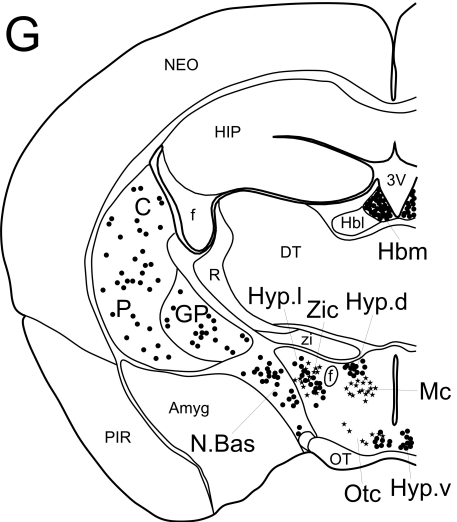


Cholinergic and Orexinergic

Catecholaminergic and Serotonergic

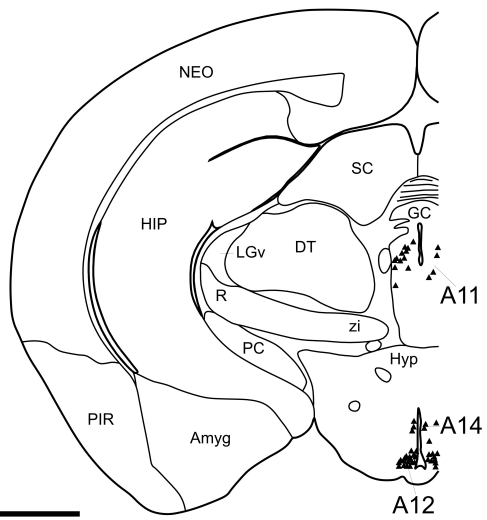
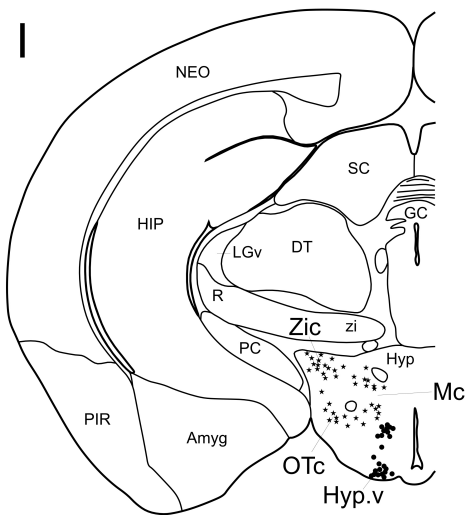
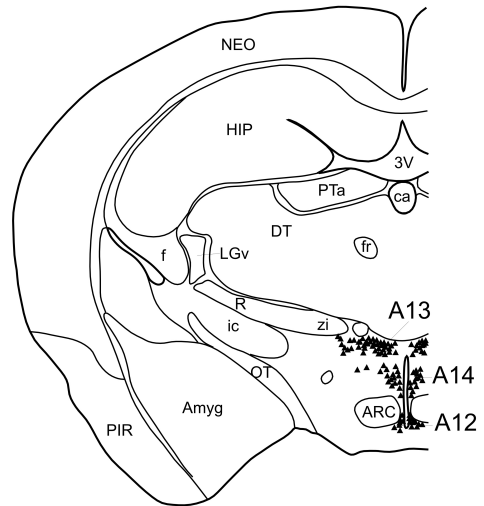
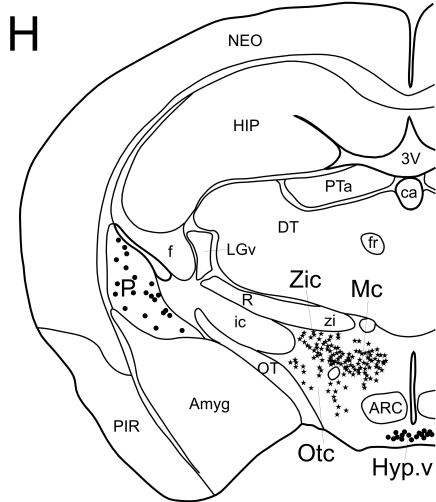


1 mm

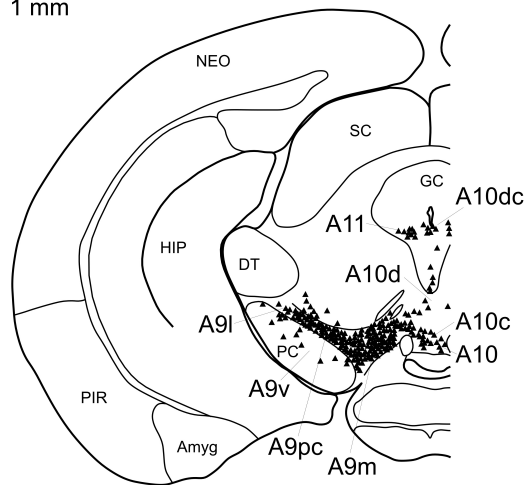
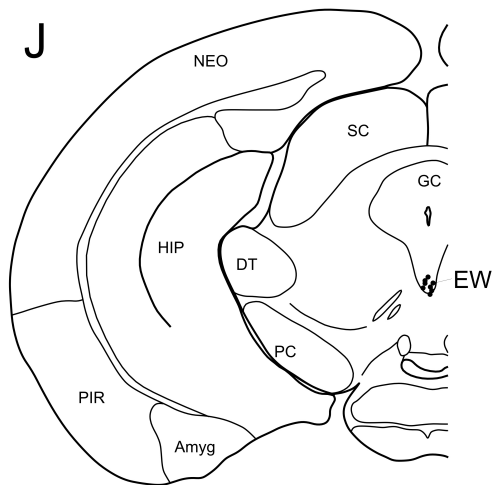


Cholinergic and Orexinergic

Catecholaminergic and Serotonergic

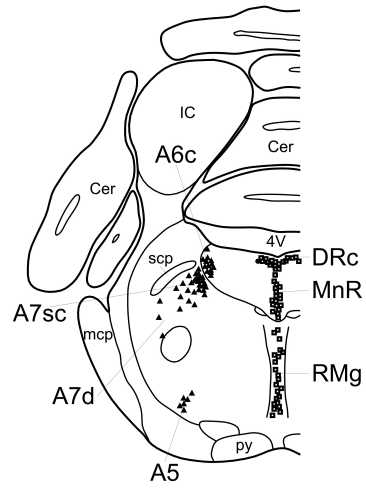
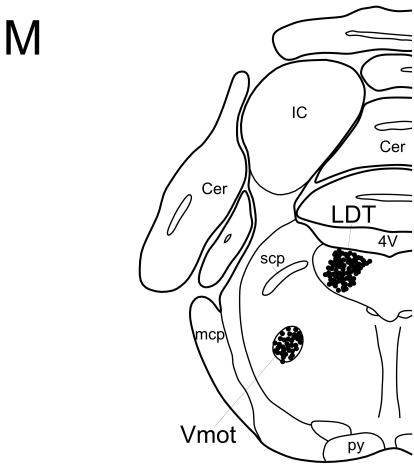
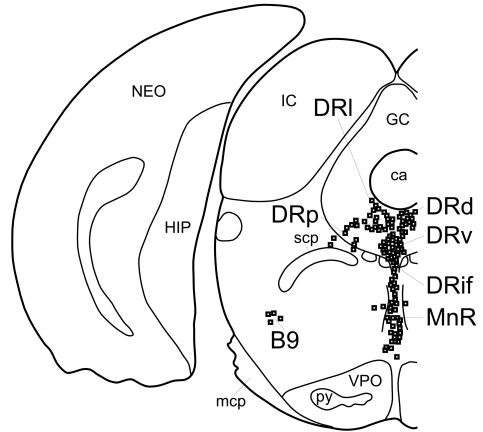
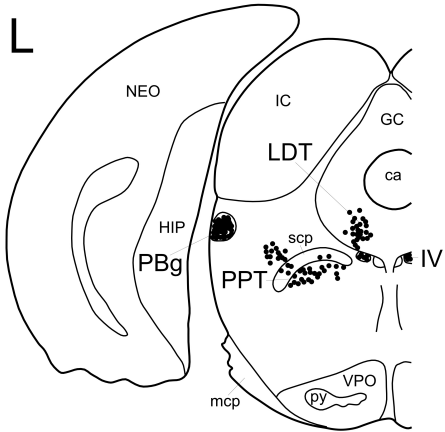
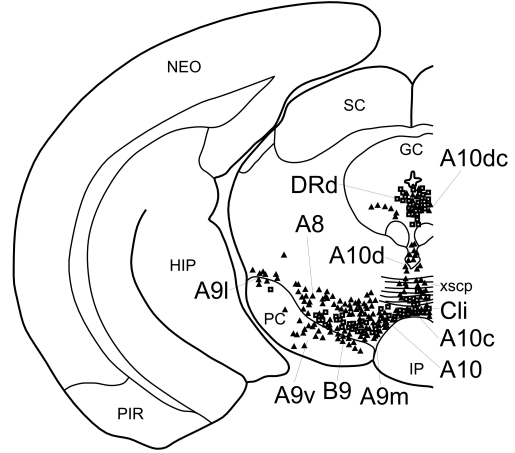
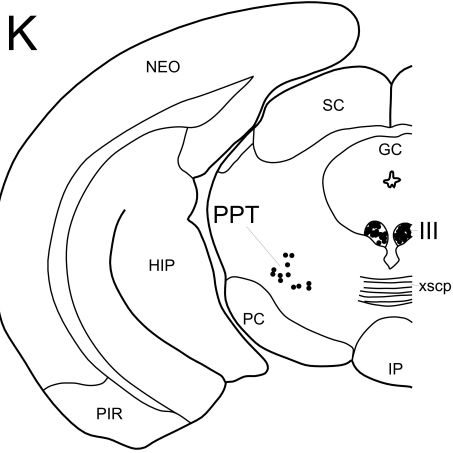


1 mm

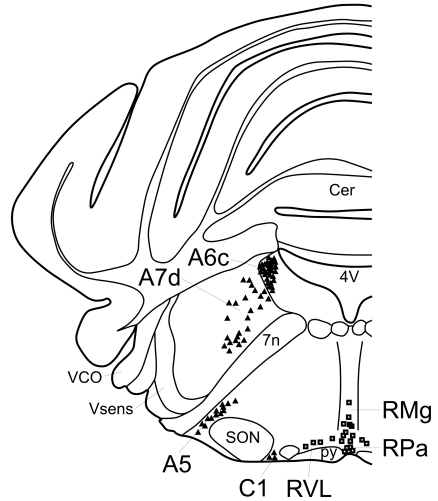
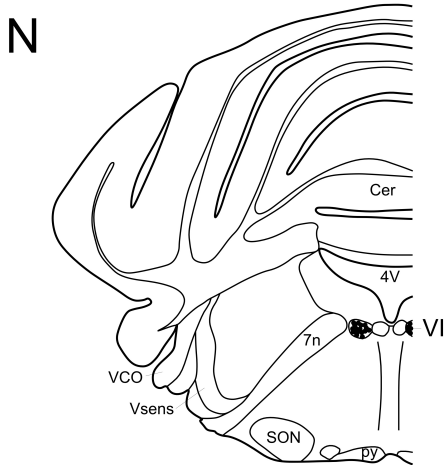


Cholinergic and Orexinergic

Catecholaminergic and Serotonergic



1 mm



Cholinergic and Orexinergic

Catecholaminergic and Serotonergic

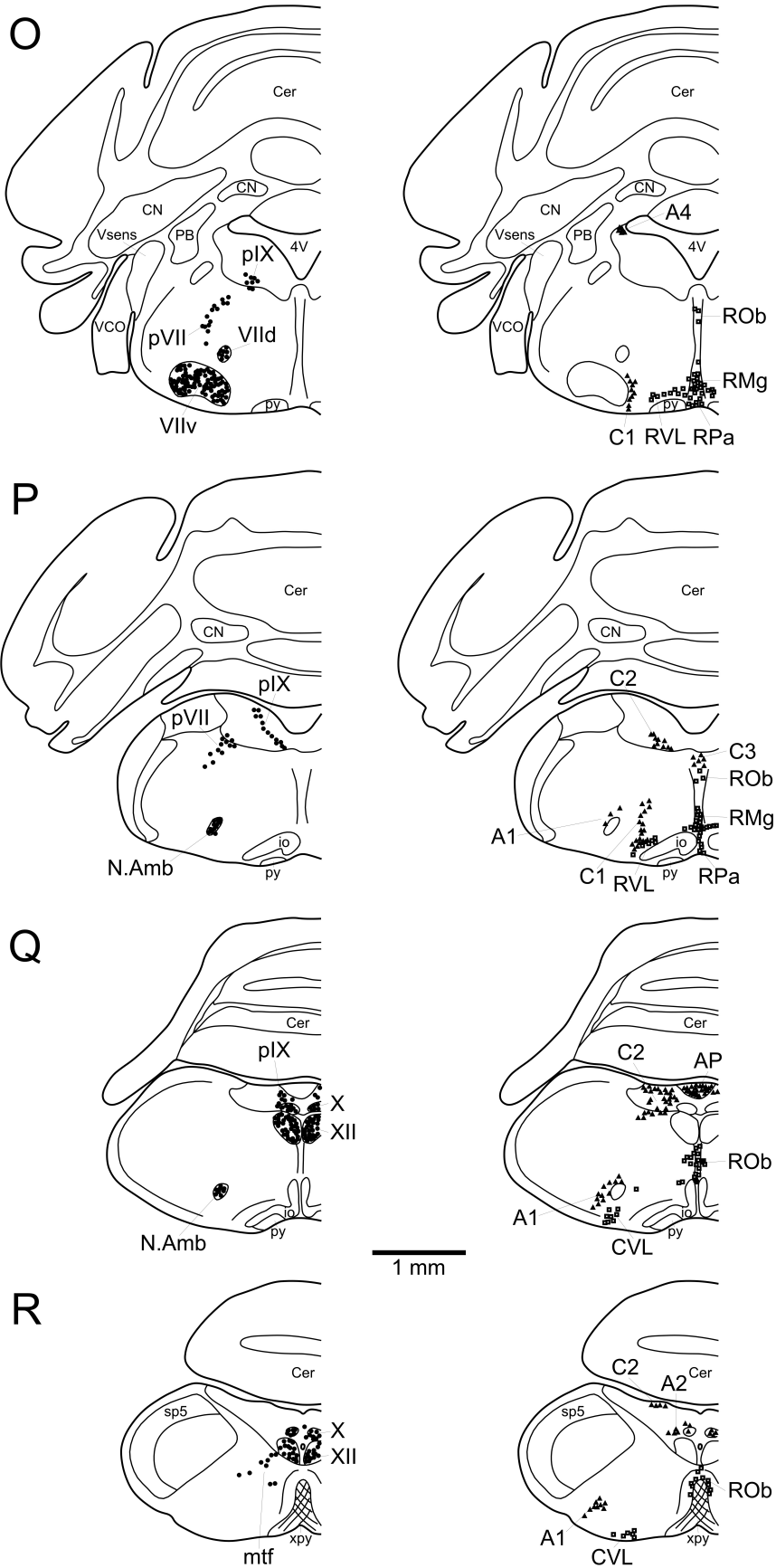


Figure 3.2: Photomicrographs showing neuronal groups immunoreactive for choline acetyltransferase in the brain of the African pygmy mouse. **A**. Basal forebrain region showing the diagonal band of Broca (**Diag.B**), the caudate nucleus (**C**), nucleus accumbens (**N.Acc**) and the olfactory tubercle (**TOL**). Scale bar in **A** = 1 mm. ac – anterior commissure; LOT – lateral olfactory tract. **B**. Cerebral cortex showing the widespread distribution of cortical cholinergic neurons. **Inset**: high power photomicrograph of the cell bodies of cortical cholinergic neurons. Scale bar of **Inset** = 50 μ m. **C**. The dorsal hypothalamic cholinergic nucleus (**Hyp.d**) lying between and just dorsal to the third ventricle (**3V**) and the fornix (**f**). **GP** – globus pallidus; **N.Bas** – nucleus basalis. **D**. The medial habenular nucleus (**Hbm**) and fasciculus retroflexus (**fr**). **E**. The pedunculopontine (**PPT**) and parabigeminal (**PBg**) nuclei found in the pontine region. **F**. The laterodorsal tegmental nucleus (**LDT**) and the pedunculopontine nucleus (**PPT**) lying immediately beneath the superior cerebellar peduncle (**scp**). In all images, except **D** which is at the midline, medial is to the left, and dorsal to the top. Scale bar in **F** = 500 μ m, and applies to **B-F**, except for the **Inset** in **B**.

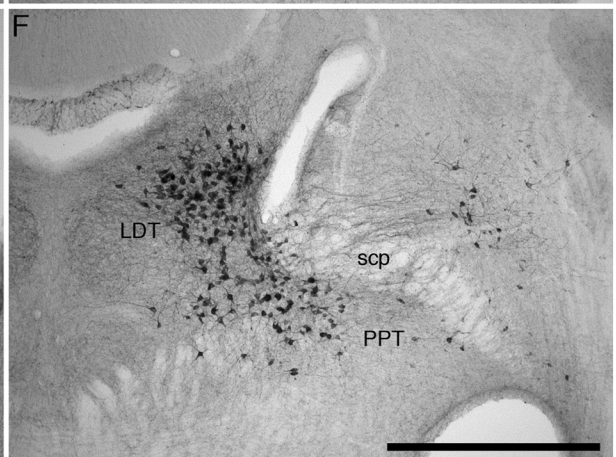
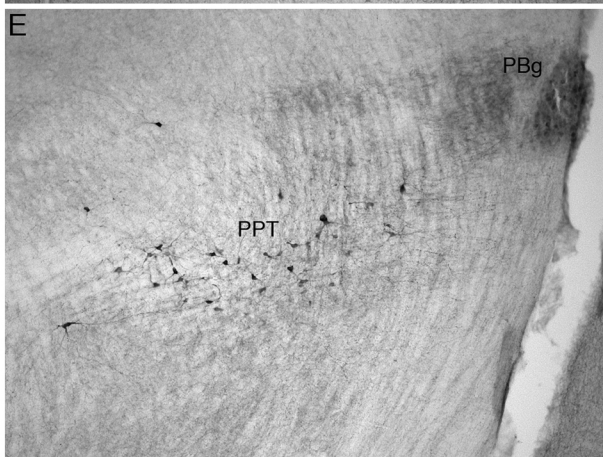
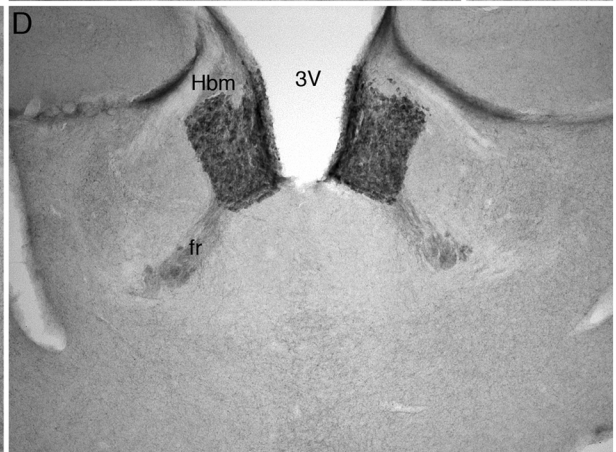
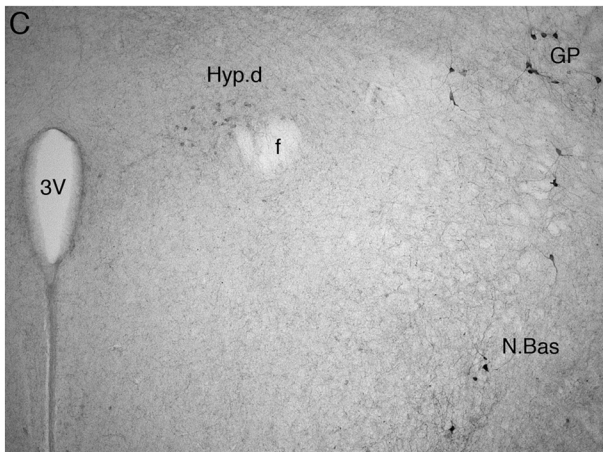
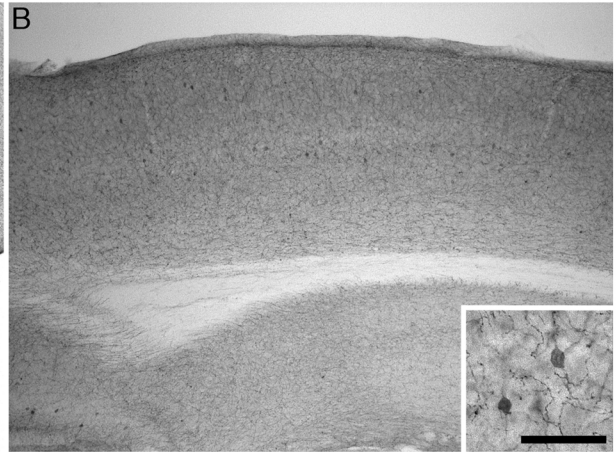
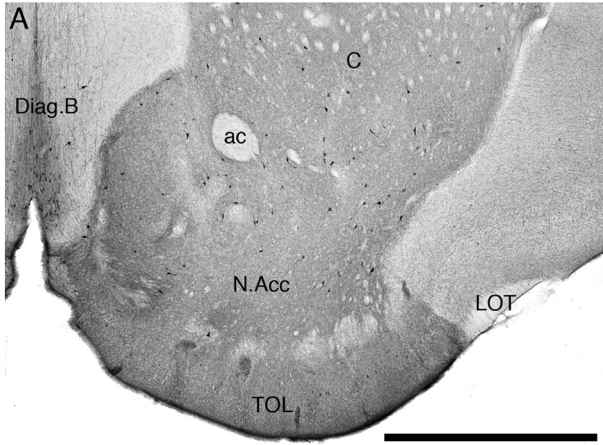


Figure 3.3: Photomicrographs showing neuronal groups that are immunopositive for tyrosine hydroxylase in the brain of the African pygmy mouse. **A**. In the rostral hypothalamus the dorsal division of the anterior hypothalamic group (**A15d**) and the rostral periventricular nucleus (**A14**) were observed. **B**. In the caudal hypothalamus, the rostral periventricular nucleus (**A14**), zona incerta cell group (**A13**) and the tuberal cell group (**A12**) were observed. **OT** – optic tract. **C**. In the ventral midbrain, the dorsal division of the ventral tegmental area (**A10d**), the retrorubral nucleus (**A8**) and the pars reticulata of the substantia nigra (**A9v**) nuclei were seen. **IP** – interpeduncular nucleus. **D**. The compact nature of the locus coeruleus (**A6c**) in the African pygmy mouse is typical of Murid rodents. **4V** – fourth ventricle; **scp** – superior cerebellar peduncle. In all images, except **A** which is at the midline, medial is to the left, and dorsal to the top. Scale bar in **D** = 500 μm , and applies to all.

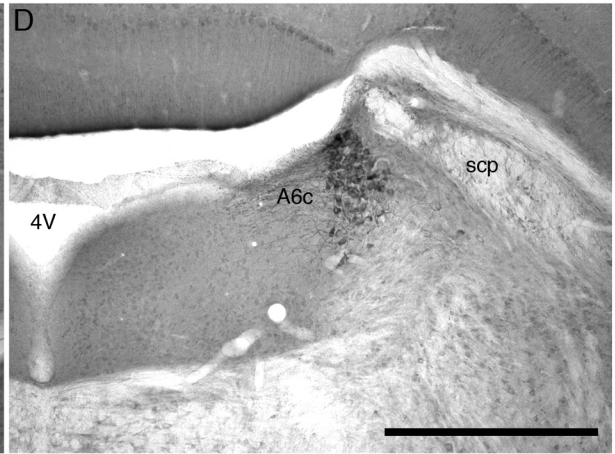
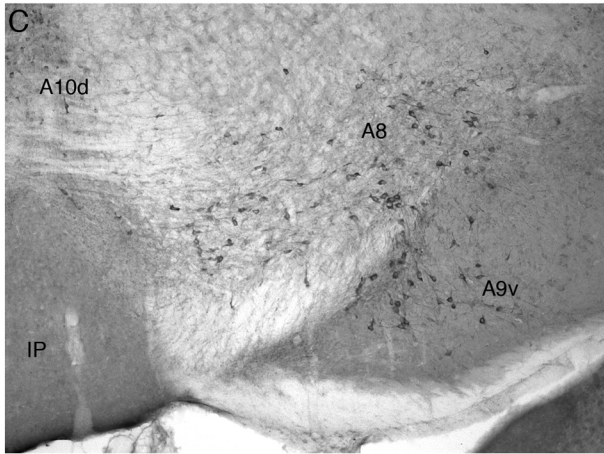
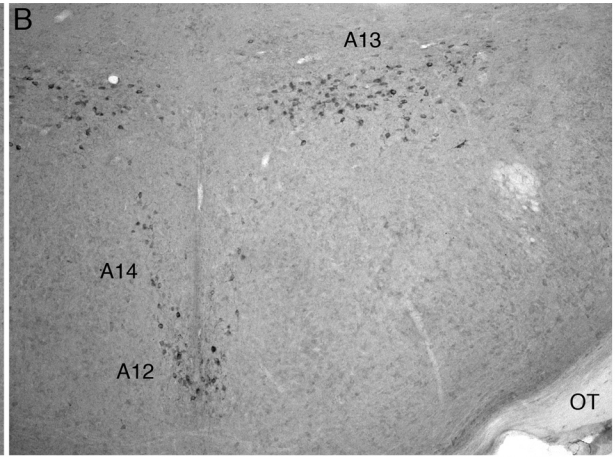
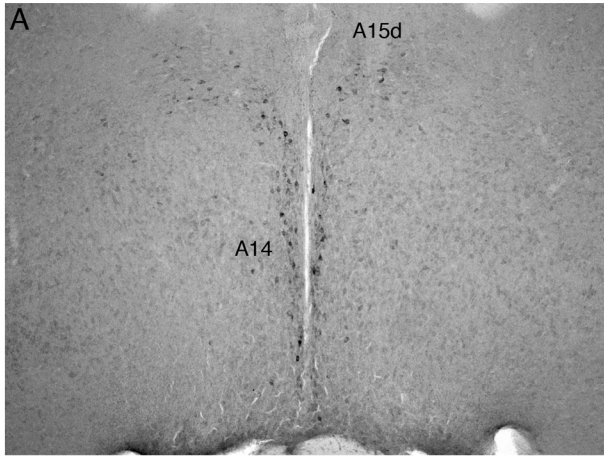


Figure 3.4: Photomicrographs showing neuronal groups that are immunopositive for serotonin in the brain of the African pygmy mouse. **A**. In the ventral portion of the rostral midbrain, the most rostral serotonergic nuclei, the caudal linear nucleus (**CLi**) and the suprallemniscal serotonergic nucleus (**B9**) were observed dorsal and lateral to the interpeduncular nucleus (**IP**), respectively. **VPO** – ventral pontine nucleus. **B**. In the central grey matter of the midbrain the dorsal (**DRd**), ventral (**DRv**), interfascicular (**DRif**) and peripherhal (**DRp**) subdivisions of the dorsal raphe were observed. **ca** – cerebral aqueduct. **C**. In the caudal most portion of the dorsal midbrain where the cerebral aqueduct opens in the fourth ventricle (**4V**) the caudal division of the dorsal raphe (**DRc**) and the median raphe nucleus (**MnR**) were observed. **D**. In the ventral portions of the rostral medulla, the raphe magnus (**RMg**), raphe pallidus (**RPa**) and rostral ventrolateral serotonergic group (**RVL**) were observed close to the pyramidal tract (**py**). In all images, except **C** which is at the midline, medial is to the left, and dorsal to the top. Scale bar in **D** = 500 μm , and applies to all.

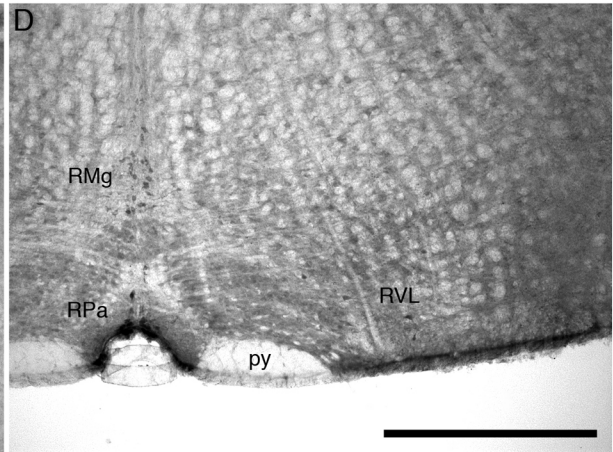
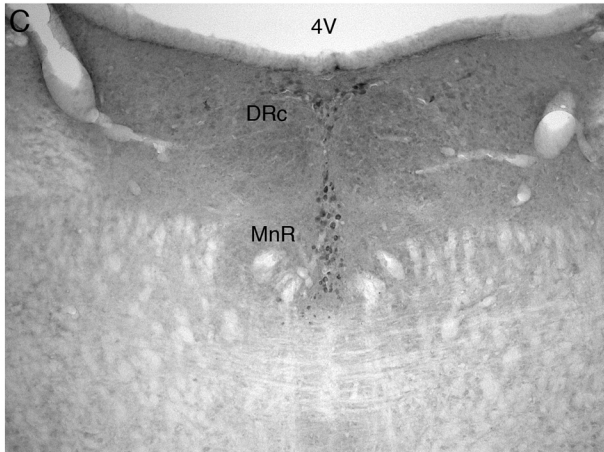
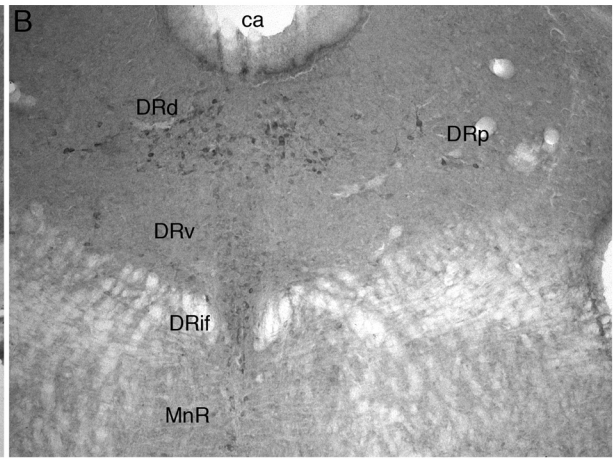
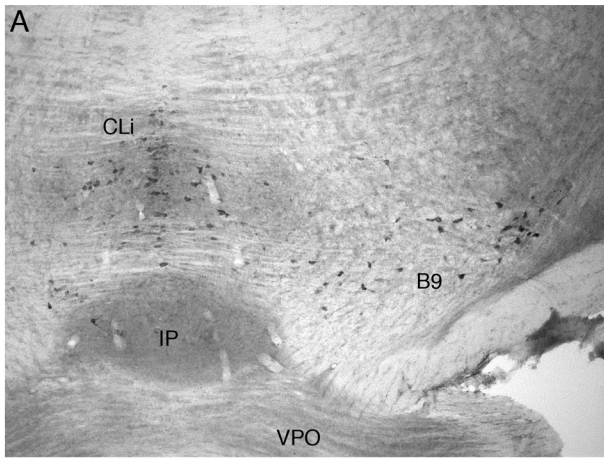
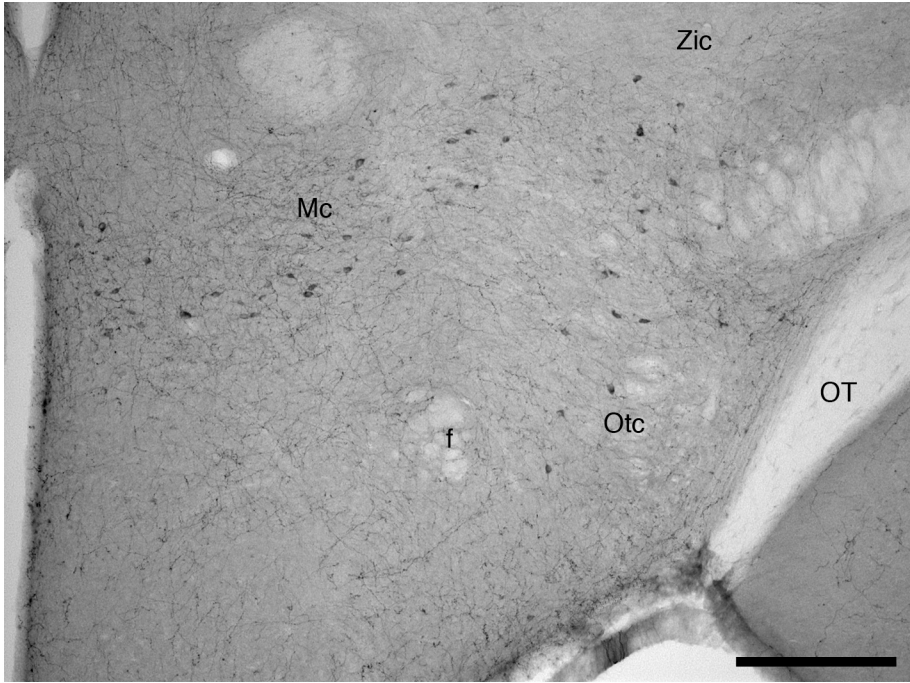


Figure 3.5: Photomicrograph showing hypothalamic neuronal groups that are immunoreactive for orexin-A in the brain of the African pygmy mouse. **f** – fornix; **Mc** – main orexinergic cluster; **OT** – optic tract; **Otc** – optic tract orexinergic cluster; **Zic** – zona incerta orexinergic cluster. Dorsal is to the top and the midline is to the left. Scale bar = 250 μ m.



3.4. Discussion

The African pygmy mouse, with its diminutive body mass (~8 g) and more importantly its small absolute brain mass (~275 mg), can shed much light on the suggestion that changes in brain size leads to increased or decreased differentiation within neural systems (Ebbesson, 1980; Stephan et al., 1981). The current study highlights that within the cholinergic, catecholaminergic, and serotonergic systems there is no difference in the number and complement of nuclei when compared with previous findings for the Cape porcupine (Limacher et al., 2008), which has a brain mass of approximately 37 g, or around 135 times larger than that of the pygmy mouse. Furthermore, the current findings underscore that even following major changes in phenotype, such as that observed in the microphthalmic African mole rats (Bhagwandin et al., 2008, 2011), or in the current study the small body mass of the African pygmy mouse, no changes in the complement or number of nuclei are apparent as long as the comparison is limited to rodent species. Thirdly, the range of rodent species in which these systems have now been investigated (e.g. Dahlström and Fuxe, 1964; Hökfelt et al., 1976; Steinbusch, 1981; Jones and Cuello, 1989; Peyron et al., 1998; Chen et al., 1999; Wagner et al., 2000; McGranaghan and Piggins, 2001; Mintz et al., 2001; Novak and Albers, 2002; Da Silva et al., 2006; Bhagwandin et al., 2006, 2008, 2011; Nixon and Smale, 2007; Moon et al., 2007; Dwarika et al., 2008; Limacher et al., 2008) also indicates that, for the most part, it does not appear to matter how long a species has been separated from another of the same order (the time since they last shared a common ancestor), they will in all likelihood show the same complement and number of any given neural system (Manger, 2005). This finding appears not only to be relevant to the rodents,

but also to be more generally relevant to all mammalian orders (e.g. Maseko et al., 2007; Dell et al., 2010) and perhaps even to other vertebrate classes (Rodrigues et al., 2008). Despite this general applicability of the conserved nature of systems level brain evolution, the current study highlighted two features of interest in the brain of the African pygmy mouse regarding intraordinal brain evolution and phylogeny, these being: (1) The presence of cortical cholinergic neurons; and (2) the anatomical appearance of the locus coeruleus (A6c); both features appearing to be found only within the subfamily Murinae from the range of rodent species studied to date.

3.4.1. Cortical cholinergic neurons

Cholinergic, or ChAT immunoreactive neurons have been observed in the brains of all species of the subfamily Murinae that have been examined (including *Mus minutoides* – this study, *Rhabdomys pumilio*, *Rattus norvegicus* and *Mus musculus* – Bhagwandin et al., 2006); but have not been observed within the cerebral cortex of all other rodent species that have been examined with the AB144P Chemicon/Millipore antibody to choline acetyltransferase (including *Tatera brantsii*, *Cryptomys hottentotus natalensis*, *Thryonomys swinderianus* – Bhagwandin et al., 2006; *Hystrix africaeaustralis* – Limacher et al., 2008; *Bathyergus suillus*, *Cryptomys hottentotus pretoriae*, Bhagwandin et al., 2008). In studies on the occurrence of cholinergic neurons in the cerebral cortex of *R. norvegicus*, it was observed that up to 80% of these cortical cholinergic neurons were also immunoreactive for vasoactive intestinal polypeptide (VIP) (Eckenstien and Baughman, 1984), and that virtually all of these VIP neurons co-

contain gamma-aminobutyric acid (GABA), with 88% of cortical cholinergic neurons co-containing GABA (Bayraktart et al., 1997). Interestingly, no cortical cholinergic neurons were immunoreactive for vesicular acetylcholine transporter (VChAT) (Bhagwandin et al., 2006), indicating that they do not form part of the traditionally defined cholinergic system (Woolf, 1991). The production of acetylcholine by cortical inhibitory interneurons appears to be limited to the rodent subfamily Murinae, and this may be related to increased functional demands on these cortical neurons allowing them to play a modulatory role in cortical microcirculation (Bhagwandin et al., 2006). As to exactly why this would appear only within the subfamily Murinae (cortical cholinergic neurons are not found in the closely related gerbil *Tatera brantsii*) is unclear at present; however, what is clear is that the Murinae are perhaps the most diverse and speciose (over 500 species) of the rodent subfamilies (Jansa and Weksler, 2004), indicating that either potentially some survival advantage is provided by this feature, or that this feature is evolutionarily neutral in terms of survival.

3.4.2. The appearance of the locus coeruleus (A6) across rodent species

The second feature observed in the current study that seems to be limited in its phylogenetic occurrence to the subfamily Murinae, is the appearance of the locus coeruleus, or A6, cluster of noradrenergic neurons. This cluster of neurons, first described by Dahlström and Fuxe (1964) in *R. norvegicus*, was described as a tightly packed cluster of neurons stretching the majority of the way across the periventricular grey matter from the pontine tegmental border to the floor of the fourth ventricle (Dahlström and Fuxe,

1964; Hökfelt et al., 1976, 1984; Björklund and Lindvall, 1984). Similar descriptions have been furnished for *M. musculus* (Ginovart et al., 1996; von Coelln et al., 2004) and in the current study for *M. minutoides*. Interestingly, this compact appearance of the neurons forming the locus coeruleus does not occur in the closely related *T. brantsii* (Moon et al., 2007), or the more distantly related *T. swinderianus* (Dwarika et al., 2008), *H. africae australis* (Limacher et al., 2008) or *B. suillus* and *C. hottentotus* (Bhagwandin et al., 2008). In these other rodent species a far less compact packing of the noradrenergic neurons forming the locus coeruleus is observed, and in general they do not approach the floor of the fourth ventricle as closely as they do in the Murinae. Again, it is unclear whether any advantage is to be gained by such a change to the structure of the locus coeruleus in the Murinae rodents, but as indicated above, the speciose nature of this subfamily does indicate that if anything, the genetic changes associated with this different adult phenotype are certainly not disadvantageous.

3.4.3 Systems level brain evolution

Manger (2005) proposed that all species within an order will have the same organisation of nuclear systems regardless of natural history, adult phenotypic variation (including variance in brain size) and time since evolutionary divergence. This concept is supported by the current findings for the African pygmy mouse, which, despite its very small absolute brain mass (~275 mg), shares the same number and complement of nuclei in the cholinergic, catecholaminergic, serotonergic and orexinergic systems as all other rodent species in which these systems have been studied to date. We can therefore

conclude that decreases in absolute brain mass do not necessarily lead to a decrease in the nuclear differentiation of the systems investigated in species belonging to the same order, a finding that has been confirmed across several mammalian orders (Kruger et al., 2010b; Dell et al., 2010). Thus, in the Rodentia, species covering a range of brain masses, phylogenetic relatedness and phenotypes have been examined. The only potential variance regarding brain evolution that has yet to be explored is to examine rodents with a relatively large brain. Two closely related families of rodents, the scaly-tailed squirrels (Anomaluridae) and Springhares (Pedetidae) (Blanga-Kanfi et al., 2009), have relatively large brain sizes and thus would be of interest to examine to evaluate whether organizational complexity is altered with an increase in relative brain size. If, as seems likely, there is no change in organizational complexity at the systems level, these series of studies will have important ramifications for our understanding of systems level brain evolution.

Despite this well-supported generality regarding systems level complexity and evolution in mammalian brains, there are two specific examples that appear to not be entirely consistent with this generality. As outlined above, the Murinae rodents appears to have two features that distinguish them from the remainder of the Rodentia, the second example being that two species of microchiropterans (*Cardioderma cor* and *Coleura afra*) have three features (presence of a parabigeminal nucleus and the dorsal caudal nucleus of the ventral tegmental area, A10dc, and the poor expression of the ventral division of the hypothalamic group, A15v) that distinguish them from the remainder of microchiropterans that have been studied (Kruger et al., 2010b). The microchiroptera and the Rodentia, especially the Muroidea, are two extremely speciose mammalian

groupings with long evolutionary histories. Due to this, and the diversity of the species within these groupings, it is perhaps not surprising that some lineages within these groups have evolved specific apomorphies (derived features of the group) not represented in the remaining species of the order to which they belong (are they on an evolutionary trajectory that may lead to the establishment of a new mammalian order?). As noted above, the genetic alterations related to the appearance of these specific traits may be neutral in nature (unlike in experimentally manipulated mice, von Coelln et al., 2004), or they may indeed have some role that proves to be advantageous to the lineage in which they have appeared; however, the fact that these apomorphies do appear is of great interest. The laboratory rat and mouse (*R. norvegicus* and *M. musculus*) are known to be the two species most widely used in the neurosciences (Manger et al., 2008) and both have the Murinae apomorphies. Based on the range of rodents studied to date, this independent evolution of the cortical cholinergic neurons and the compact appearing locus coeruleus in the Murinae is cause for some concern, as it is highly likely that observations regarding these portions of the cholinergic and catecholaminergic systems will be difficult to translate to other species, especially humans that may have independently evolved similar apomorphies. It might also be true that these apomorphies in the different lineages (Murinae and Homo) are analogous, which would also be of great interest. Clearly, further comparative observational and functional assessments are required to determine whether any potential advantages or disadvantages to the extensive use of rats and mice as experimental animal models are apparent.

Chapter Four - Sleep in the Cape mole rat, *Georchus capensis* – sleeping underground

4.1. Introduction

Sleep is characterised as a homeostatically controlled, rapidly reversible state of reduced motor activity, lack of responsiveness to external stimuli and increased arousal threshold (Siegel, 2008). Behavioural sleep has been identified in both invertebrates and vertebrates (Campbell and Tobler, 1984; Lesku et al., 2006; Siegel, 2008), but studies of mammalian sleep have been conducted on over 127 species (McNamara et al., 2008). In general mammals show both non-REM and REM sleep, but there are exceptions (e.g. Siegel et al., 1998; Lyamin et al., 2008).

Within mammals, species from the order Rodentia are the most well studied. While most electrophysiological and behavioural studies on sleep in rodents have been undertaken on the typical laboratory species such as the rat, a range of other species have been examined (reviewed in Lesku et al., 2006). All rodents studied to date show the stages of wake, non-REM and REM sleep, but there is great variation in the total sleep time (TST) and time spent in REM (Campbell and Tobler, 1984; Lesku et al., 2008). TST can vary from approximately 4 hours in the giant Zambian mole rat (*Cryptomys mehowi*) to as much as 20 hours in the pocket mouse (*Perognathus longimembris*) (Lesku et al., 2008; Bhagwandin et al., 2011). REM ranges from as little as 9% of TST up to 25% of TST in rodent species studied to date (van Twyver, 1969; Meddis, 1983). Across the 15 rodent species where sleep has been studied electrophysiologically (reviewed in Lesku et al., 2006, but not including the giant Zambian mole rat), the

average TST was 13.58 h/day (SD 2.6 h, range 8.64 – 20.06 h), with REM sleep occupying an average of 17.41% of TST (SD 4.45%, range 9.58 – 24.71%). Despite both the similarity in observable wake and sleep states, and the observed variation in the times dedicated to these states, no real explanation of this variation has been forthcoming.

The Cape mole rat is a species of the exclusively subterranean rodent family Bathyergidae, is a common species within the Western Cape of South Africa and lives a solitary lifestyle in extensive underground burrow systems (Du Toit et al., 1985). Cape mole rats are microphthalmic with no external ears and very long incisors, which are used for excavating the burrows and obtaining the tubers of the fynbos on which they feed (Du Toit et al., 1985). It is notable that despite these animals having a greatly regressed visual system they are still able to perceive light and have been shown to have a nocturnal circadian rhythm (Oosthuizen et al., 2003). This particular species is an excellent model to investigate whether changes in phenotype, such as the regressed visual system, and changes in lifestyle, such as living in a subterranean environment, lead to any discernible changes in the sleep states and times previously reported for other rodent species.

4.2. Materials and methods

4.2.1. Experimental animals

Two physiological measures of sleep (EEG and EMG) and the accompanying behaviour were recorded from two adult female Cape mole rats (body masses of 205 g and 200 g). The animals used in the current study were caught from wild populations and subsequently housed at the Central Animal Facility at the University of the

Witwatersrand, South Africa. Ethical clearance for the study (clearance number: 2012/51/05) was obtained from the University of the Witwatersrand Animal Ethics Committee, and all animals were treated according to the guidelines of this committee which parallel those of the NIH for the care and use of animals in scientific experimentation. All animals were acclimatised to the laboratory environment for approximately one month prior to experimentation. Animals were housed individually in a large plastic enclosure (60 cm x 50 cm) with wood shavings lining the floor (to a depth of 3 cm) and a transparent Perspex tube (20 cm long with a diameter of 6.5 cm) that was secured to the floor of the enclosure. The animal enclosures were placed in an isolated room that was controlled for temperature (25° C), sound attenuated and with a 12 h light/dark cycle. The animals were fed once a day (16h00) on a diet of carrots, sweet potatoes and apples and it took approximately 2 min to feed both animals. Following the acclimatisation period a telemetric recording device (see below) was implanted subcutaneously in each animal and once fully recovered from the surgical procedure, sleep was recorded continuously for 72 h. In addition, a low light CCD camera was mounted above the enclosure for visual recordings of the animal's behaviour.

4.2.2. Surgical procedure

The animals were anaesthetised using Isoflurane (1 - 2.5% in an oxygen/70% nitrous oxide mixture, Safe Line Pharmaceuticals) administered *via* a mask placed over the nostrils. Throughout the surgical procedure the animal's heart rate, O₂ saturation levels and body temperature were monitored, all of which were consistent. The scalp and

left abdominal region were shaved and cleaned with disinfectant (0.5% chlorhexidine in 75% alcohol, Kyron Laboratories). A mid-sagittal incision was made over the skull and the skin and left temporalis muscle were reflected to expose the dorsal aspect of the cranium. Two small holes were drilled with the aid of a dental drill in the region overlying the presumptive left motor cortex. These holes were drilled approximately 8 mm apart, 5 mm lateral to the sagittal suture, and care was taken to ensure that the underlying dura mater and cortex was not pierced. One stranded stainless steel electrode was carefully placed in each hole, again ensuring that the electrodes rested firmly on the surface of the dura mater, but did not pierce it, and were secured in place and to the surface of the skull with dental cement (Ketacem, 3M). These electrodes served as the EEG (electroencephalogram) recording electrodes. In addition two stranded stainless steel electrodes were sutured into the dorsal nuchal muscles and served as the EMG (electromyogram) recording electrodes. These electrodes were placed approximately 1 cm apart, ensuring that the tips did not come into contact with one another. The EEG and EMG electrodes were all connected to a transmitter (see below) which was implanted in a subcutaneous pocket (2 cm x 2 cm) created over the left abdominal region. The surgery lasted less than 1.5 hours. Both incision sites were sutured following electrode and implant placement, Isoflurane was stopped and 100% oxygen was administered until the animal recovered from anaesthesia. The animal was returned to its enclosure where it was closely monitored until it began to move freely. The animals received 1 cm x 1 cm jelly containing the analgesic Meloxicam (1 g per 1 cm x 1 cm cube of jelly; Ingelheim Pharmaceuticals) twice per day, from the afternoon preceding the surgery for two full

days. The animals were allowed to recuperate for seven days prior to recording to allow for recovery and any remnant of the drugs to wear off.

4.2.3. Sleep recording

The telemetric system used in the current study was from Data Sciences International (<http://www.datasci.com>, PhysioTel Telemeric Systems) and consisted of a transmitter (TL11 M2 F40-EET implant, the leads of which were made out of stainless steel, had an outer diameter of 0.3 mm and a lead diameter of 0.2 mm; weight: 7 g; volume: 4.5 cc; length: 13.8 mm) and a receiver (placed directly under the animal's enclosure) which transmitted to the DEM multiplex interface. The interface was in turn connected to the input amplifier of the Data Sciences computer system, which digitally recorded the signals received (in DSI format). After the recording was completed, data digitally saved in the DSI format was converted to text format and these files were in turn converted into the appropriate format needed for recognition and analysis by the Spike 2 computer program (version 5, Cambridge Electronic Design). The Spike files allowed for the visual scoring of the EEG and EMG data of the various physiological states. The EEG spectral power was also calculated. The EEG and EMG were recorded continuously for 72 h. In addition a low light CCD camera (connected to a DVD recorder) was mounted above the enclosure to allow for visual recordings of the animal's behaviour. These data were not scored but provided behavioural verification for the polygraphically assessed physiological states. The animals were only disturbed once a day at 16h00 for feeding and the disturbance lasted approximately 2 min.

4.2.4. Data analysis

Spike 2 version 5 (Cambridge Electronic Design) was used in all offline analyses of the EEG and EMG data. Data was scored in 5 s epochs as either: (1) Wake – characterised by a high-frequency, low-voltage EEG and a high-voltage EMG; (2) non-rapid eye movement sleep (non-REM) – characterised by a low-frequency, high-voltage EEG, and a low-voltage EMG; or (3) rapid eye movement sleep (REM) – characterised by an EEG that resembled wake but with an EMG that was low-voltage as seen in non-REM sleep or slightly lower. At least fifty percent of an epoch had to be occupied by a particular state for assignment of that state to the epoch. From the 5 s epoch data, the modal state per minute was determined and this per minute modal data was used in all subsequent analyses. The average number and duration of episodes of wake, non-REM and REM were calculated for a 24 h period, as well as for the light phase and dark phase. Total spectral power for each of the states was also calculated using the Spike 2 computer program (Hanning window, FFT number 512, sampling frequency 500 Hz, and segment length 1.024s). The difference in time between the onsets of consecutive REM episodes was used to calculate the length of a sleep cycle and waking periods of less than 5 minutes and greater than 10 minutes between REM episodes were excluded.

4.3. Results

In the present study EEG and EMG were continuously recorded in two Cape mole rats (*Georychus capensis*) over a period of 72 hours to determine the physiological states of Wake, non-REM sleep and REM sleep. It is important to note that during REM sleep the EMG muscle tone did not decrease any further than seen in non-REM sleep, but the EEG data in concert with the EMG data allowed for the correct assignation of sleep states. Video recording was conducted simultaneously to allow for behavioural verification of the physiologically defined states. During Wake the animals would move around the enclosure, eat, groom, shred the nesting material and crawl in and out of the perspex tube. During sleep the animals would either lie curled in a ball with the head tucked under the body, or inside the tube with the head resting on the floor. The same body posture was adopted during non-REM sleep and REM sleep, although the characteristic twitches of the head and neck were only seen during REM. The results from this study indicate that the Cape mole rats spent 8.6 hours asleep in a 24 hour period (35.8%) and that REM sleep comprised 17.3% of the total sleep time (TST). The mole rats spent more time awake during the dark phase (7.9 h) and slept more during the light phase (4.5 h), with REM showing a marked increase during the light phase (51 min in light phase vs 38 min in dark phase). In the Cape mole rats the major sleep bout always occurred during the light phase, in the middle to late afternoon, and lasted approximately 41 mins, with REM sleep accounting for 11.5 minutes of this major sleep bout. The results indicate that these animals are nocturnal, polyphasic sleepers.

4.3.1. State definitions

In the Cape mole rat the three states, Wake, non-REM and REM, typically observed in rodents, were observed in this species (Figs. 4.1, 4.2). Wake was characterised by high frequency, low amplitude EEG activity accompanied by high amplitude EMG activity. Non-REM presented as low frequency, high amplitude EEG activity with a low amplitude EMG. REM consisted of high frequency, low amplitude EEG activity, similar to waking, and a low amplitude EMG (as low or slightly lower than seen in non-REM sleep) with large, infrequent spikes (muscle twitches).

The spectral power was calculated separately for each state in each mole rat (Fig. 4.3). The frequency range for spectral power in Mole rat 1 was 0 - 7 Hz with the peak amplitude occurring at 3 Hz during Wake, non-REM and REM. The frequency range for spectral power in mole rat 2 was 0 – 7 Hz with the peak amplitude occurring at 4 Hz during Wake, non-REM and REM.

4.3.2. Time spent in wake, non-REM and REM states

Analysis of the 1 min epoch data revealed that the Cape mole rats spent, on average, 64.2 % (SER \pm 3%, 15.4 h) of a 24 h day awake, 29.6 % (SER \pm 2.1%, 7.1 h) in non-REM sleep and 6.2% (SER \pm 1%, 1.5 h) in REM sleep (Fig. 4.4A). During the light phase, the Cape mole rats were awake 62.9% (SER \pm 1.8%, 7.6 h), in non-REM 30% (SER \pm 1.4%, 3.6 h) and in REM sleep 7.1% (SER \pm 0.5%, 54 min) for the 12 h period (Fig. 4.4A). During the dark phase, Wake occupied 65.6% (SER \pm 1.4%, 7.9 h), non-REM occupied 29.3% (SER \pm 0.9%, 3.5 h) and REM occupied 5.3% (SER \pm 0.5%, 36

min) of the 12 h phase (Fig. 4.4A). Total sleep time for the Cape mole rats was calculated at 35.8% (SER \pm 3.1, 8.6 h) and the percentage REM of TST was 17.3% (SER \pm 1%, 1.5 h) during the 24 hour period.

4.3.3. Number and duration of episodes of Wake, non-REM and REM states

The average number of episodes in 24 h was: 185 (SER \pm 12.7) for waking, 189 (SER \pm 12.5) for non-REM and 56 (SER \pm 11.6) for REM sleep (Fig. 4.4B). The average number of episodes for wake was very similar between the light phase (92, SER \pm 7.5) and dark phase (94, SER \pm 6), and the number of episodes for non-REM was identical between the two phases (94 SER \pm 6). For REM there was an increase in the number of episodes in the light phase (31, SER \pm 6) compared to the dark phase (25, SER \pm 6).

The average duration of a wake episode was 5.1 min (SER \pm 0.5 min), 2.3 min for non-REM (SER \pm 0.1 min) and 1.7 min (SER \pm 0.2 min) for REM in a 24 h period (Fig. 4.4C). There was no difference between the dark phase and light phase for wake (5.2 min, SER \pm 0.5 min) and non-REM (2.3 min, SER \pm 0.1 min). During the light phase an episode of REM lasted 1.8 min (SER \pm 0.2 min) and during the dark phase it lasted for 1.6 min (SER \pm 0.2 min) (Fig. 4.4C).

4.3.4. REM periodicity and state transitions

To establish the REM periodicity, the time difference between the onset of consecutive bouts of REM sleep was calculated and waking periods of less than 5 min or

greater than 10 minutes were excluded. REM onset occurred with the highest frequency between 5 – 15 minutes and the peak cycle duration was 10 minutes (Fig. 4.5).

The transitions between the various states were calculated and it was found that Wake transitioned to non-REM sleep 100% of the time. Wake never transitioned to REM sleep, but non-REM sleep transitioned to Wake (74.41%) with a higher frequency than to REM sleep (25.59%). REM transitioned to Wake more frequently (84.69%) than to non-REM sleep (15.31%) (Fig. 4.6). In *C. mechowi* REM sleep never transitioned to non-REM sleep but in the Cape mole rat REM transitioned to non-REM 15.31% of the time (Bhagwandin et al., 2011).

Figure 4.1: Polygraphic traces illustrating the changes in the EEG

(electroencephalogram) and EMG (electromyogram) during the transition from non-REM sleep to REM (upper traces) and REM to Wake (lower traces) in the Cape mole rat. Wake

was characterized by low-amplitude, high-frequency EEG and high amplitude EMG.

non-REM sleep was characterized by high-amplitude, low frequency EEG and low

amplitude EMG, while REM sleep was characterized by low-amplitude, high frequency

EEG and very low amplitude EMG.

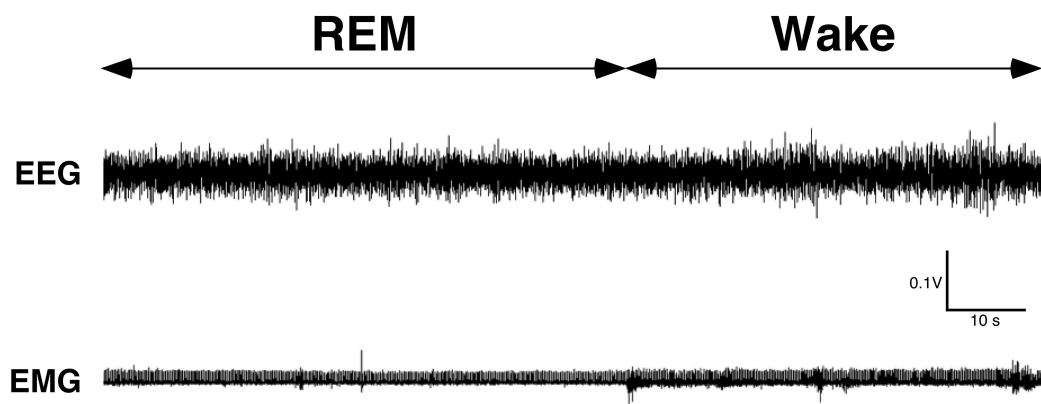
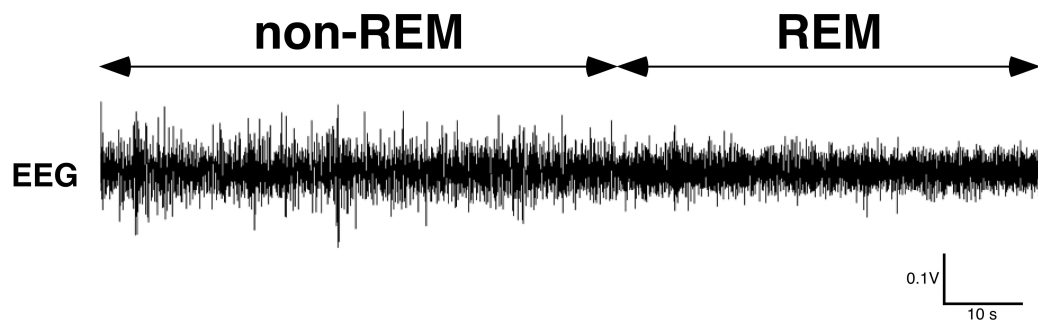
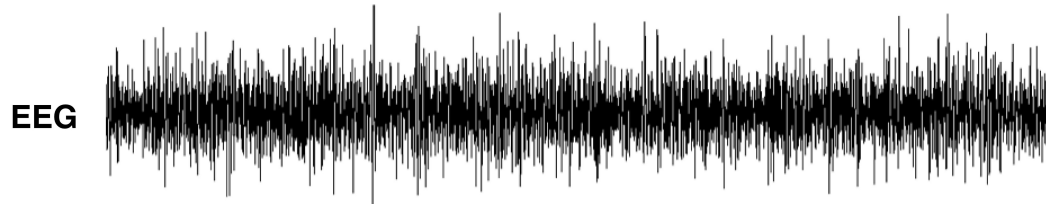


Figure 4.2: Polygraphic traces illustrating the EEG (electroencephalogram) and EMG (electromyogram) during non-REM sleep (upper traces) and REM sleep (lower traces) in the Cape mole rat. non-REM sleep was characterized by high-amplitude, low frequency EEG and low amplitude EMG, while REM sleep was characterized by low-amplitude, high-frequency EEG (similar to that seen in Wake) and very low-amplitude EMG.

non-REM



REM

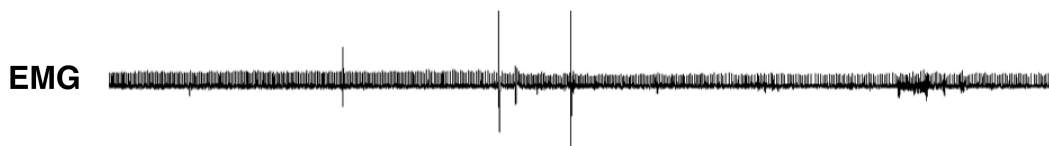


Figure 4.3: Graphs indicating the spectral power range during wake, non-REM and REM states for the Cape mole rats used in this study (upper graph for Mole rat 1, lower graph for Mole rat 2).

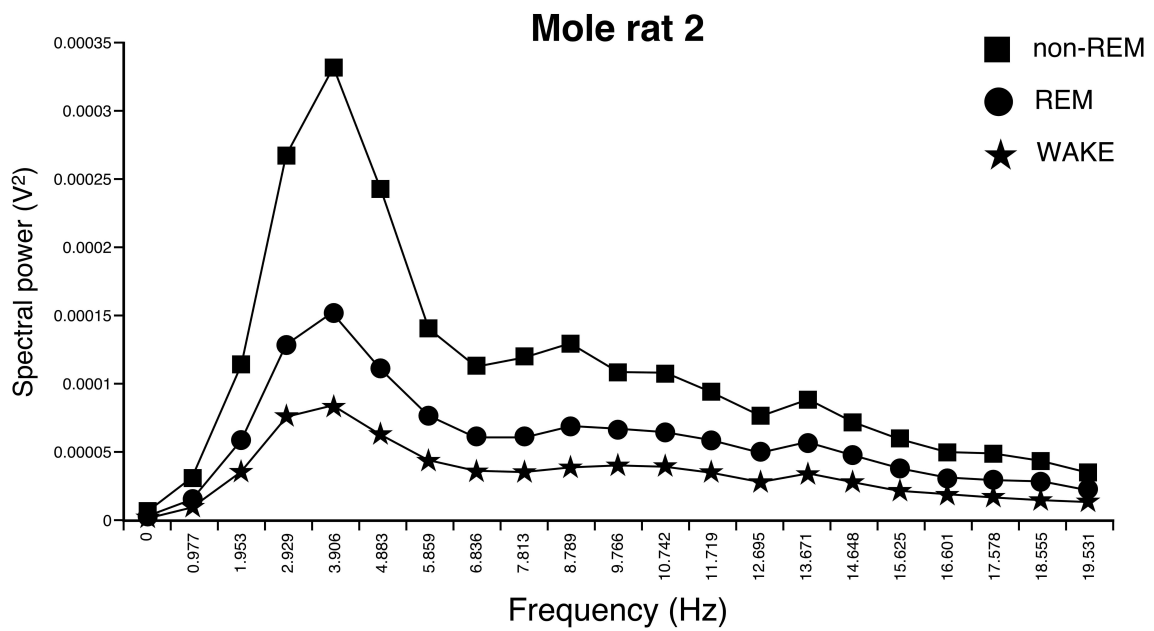
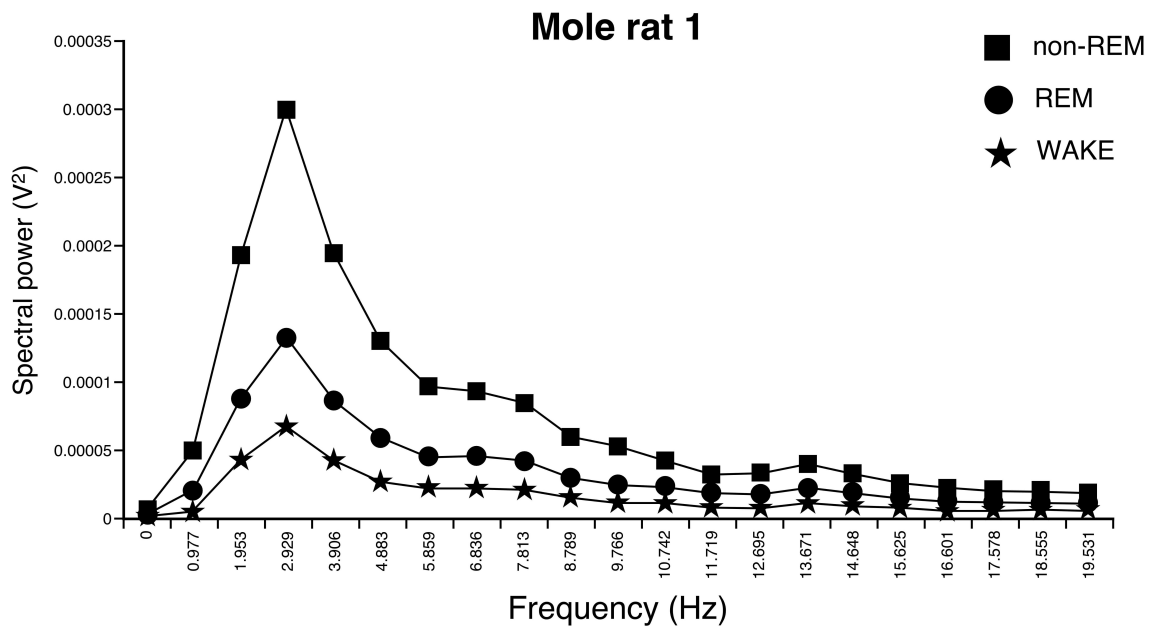


Figure 4.4: Graphs illustrating the physiological data for wake, non-REM and REM during a 24-hour cycle, the 12 h light period (Day) and 12 h dark period (Night) in the Cape mole rat. **(A)** The percentage of time spent in wake, non-REM and REM. **(B)** The number of 1 min episodes of wake, non-REM and REM. **(C)**, the average episode duration (in minutes) of wake, non-REM and REM.

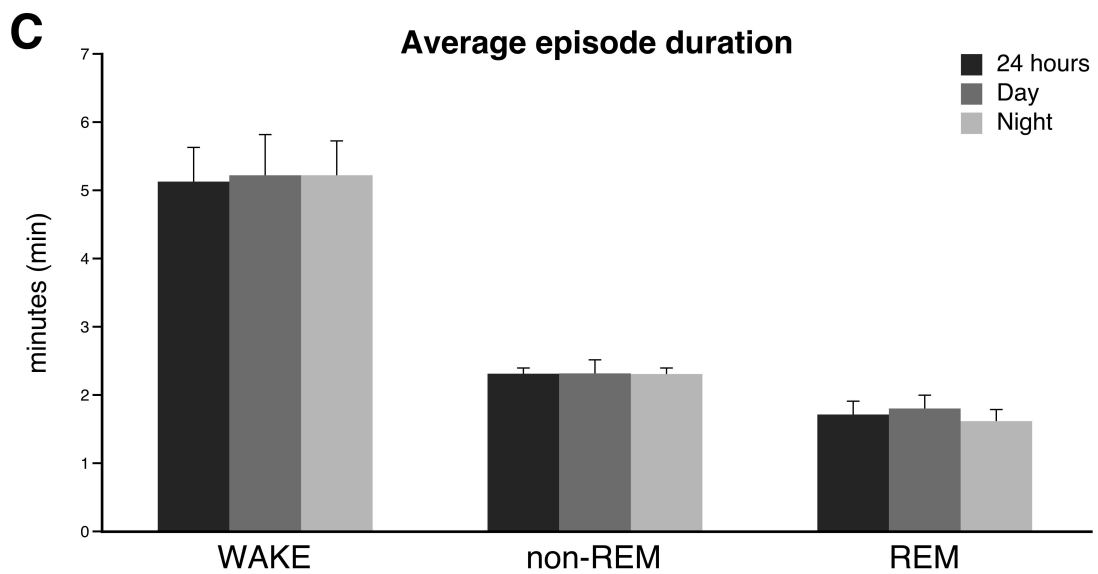
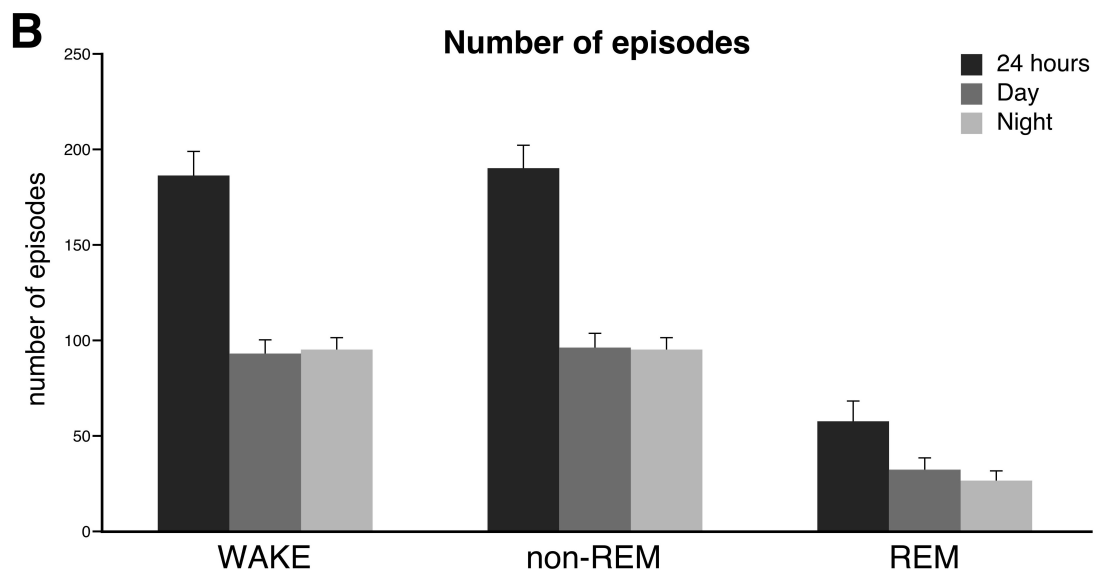
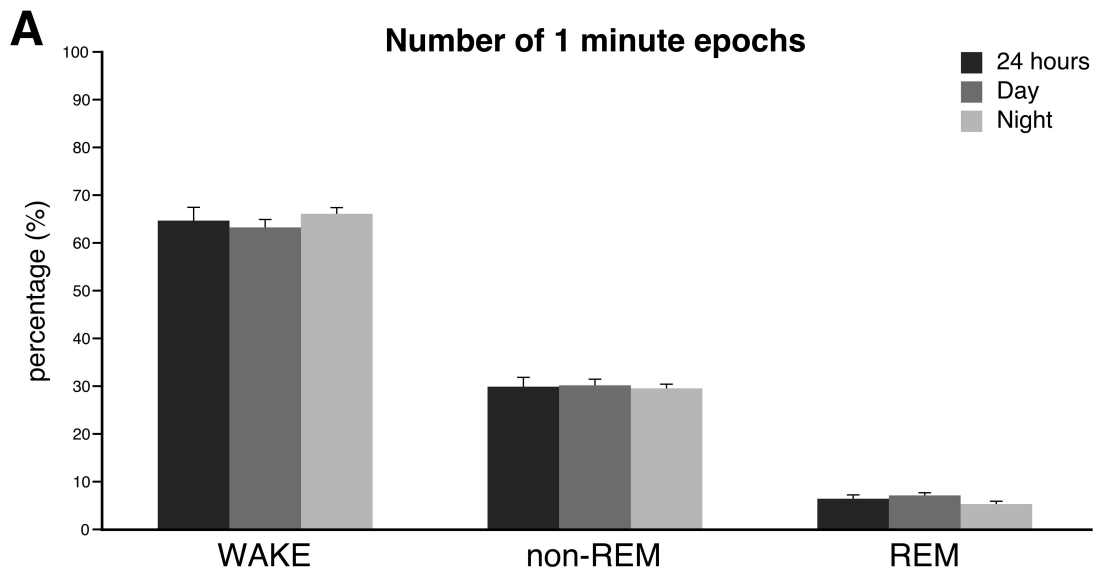


Figure 4.5: Graph representing the time lapse (5-min periods) between onsets of physiologically identified REM episodes (REM periodicity) for the Cape mole rats excluding episodes of waking greater than 10 min.

REM Periodicity

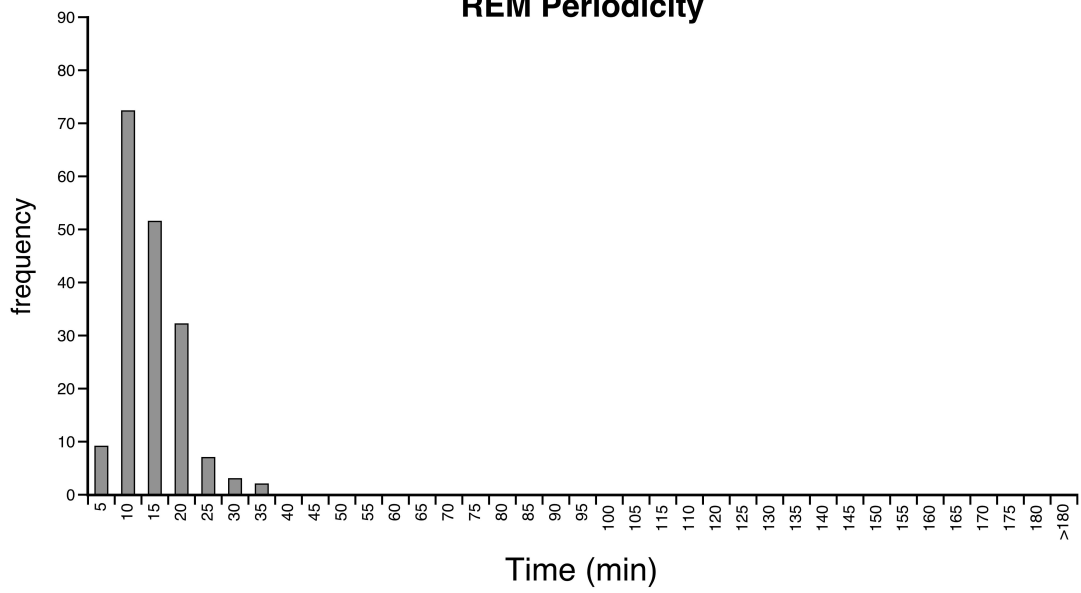
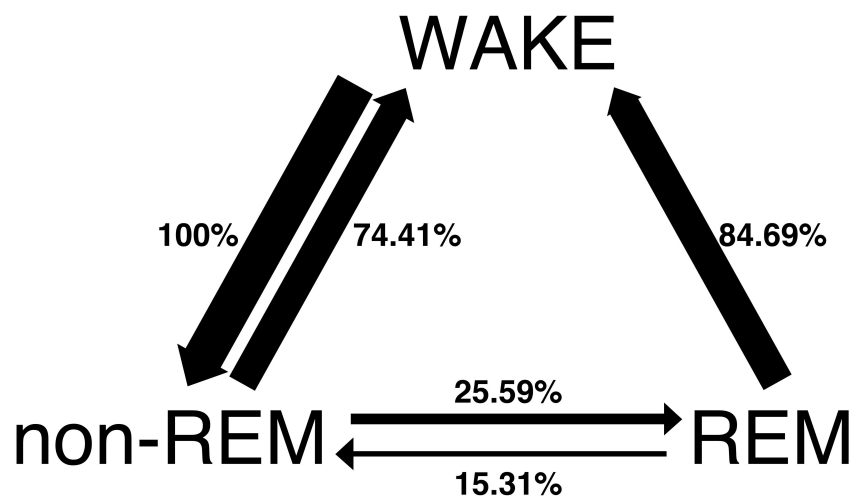


Figure 4.6: Flow diagram illustrating transitions (represented as a percentage) between wake, non-REM and REM in the Cape mole rat. Note that wake always transitions into non-REM sleep, and that both non-REM and REM transition to wake more often than to each other.



4.4. Discussion

The present study examined sleep in the Cape mole rat and showed that in a 24 h period, these rodents spent on average 15.4 h awake, 7.1 h in non-REM sleep and 1.5 h in REM sleep. There were no unusual sleep states observed and the polygraphic EEG and EMG features were typical of that seen in other rodents studied to date (Campbell and Tobler, 1984; Tobler, 1995; Tobler and Deboer, 2001; McNamara et al., 2008; Bhagwandin et al., 2011).

4.4.1. Comparison to sleep in other mole rats

To date two other species of mole rat have been studied using polygraphic methods to determine their sleep patterns – the giant Zambian mole rat and the blind mole rat. As with these other mole rat species investigated, and indeed all other rodents, the Cape mole rat showed both non-REM and REM sleep. This indicates that sleep across rodents, and indeed across most mammals, has a very similar physiological signature (Tobler, 1995). Tobler and Deboer (2001) investigated sleep in the blind mole rat (*Spalax ehrenbergi*), which had a TST of 12.5 h (52%) of which REM comprised 1.9 h (15%). Bhagwandin et al. (2011) found that rhythmic individuals of the giant Zambian mole rat species (*Cryptomys mechowii*) had a TST of 6.2 h (26%) of which REM comprised 1.2 h (19%); however, the arrhythmic individuals of this species had only 4.3 h TST (18%) and REM comprised 1 h of TST (23%). In the present study the Cape mole rat falls in the middle of that reported for other mole rats with a TST of 8.6 h (36%). 1.5 h of TST was devoted to REM (17%), which is comparable to the amount of REM sleep seen in the

giant Zambian and blind mole rat species. Non-REM episodes in the Cape mole rat lasted on average 2.3 min, which is similar to that for the giant Zambian mole rat (2.5 min); however, this average duration is markedly less than seen in the blind mole rat (9.7 min). The duration of REM episodes lasted 2.5 min for the giant Zambian mole rat and 3.3 min for the blind mole rat, whereas it was slightly lower in the Cape mole rat at 1.7 min per episode. It would therefore appear that the Cape mole rat and giant Zambian mole rat may be more indicative of the sleep patterns associated with mole rats, whilst the microphthalmia of *S. ehrenbergi* may result in the longer TST and non-REM episode duration seen in that species, but further mole rat species would need to be studied to ascertain this potential difference based on the extent of regression of the visual system. Furthermore the similarities seen in the REM percentage of TST across all three species would indicate that there is some baseline function for REM in the mole rats and that it is conserved across the species. As all three mole rat species that have been investigated to date are solitary, highly aggressive fossorial species, it would therefore be of interest to investigate sleep in, for example, the social *Cryptomys hottentotus* and the eusocial *Cryptomys damarensis* to determine if the changes in TST are related to the social environment of the mole rat species studied to date. Furthermore while TST changes between species, the REM composition remains stable, which could be genetically determined.

4.4.2. Comparison to sleep in other rodents

The Cape mole rat has a TST of 8.6 h per day, which falls just below the range of TST seen for other non-mole-rat rodents (average TST = 13.58 h/day, SD 2.6 h, range 8.64 – 20.06 h, Lesku et al., 2006). With REM occupying 17% of TST, the Cape mole rat falls in the middle of the range seen for other non-mole-rat rodents (average REM% of TST = 17.41%, SD 4.45%, range 9.58 – 24.71%, Lesku et al., 2006). The duration of non-REM episodes, which average 2.3 min in the Cape mole rat, are lower than that seen in other non-mole-rat rodents, which have average non-REM episode durations of around 5.15 min (SD 0.73 min) (van Twyver, 1969). In addition, the average REM episode duration of the Cape mole rat, at 1.7 min, is slightly lower than that observed in other non-mole-rat rodents which show an average duration of 2.89 min (SD 0.8 min) for each REM episode (van Twyver, 1969). Thus, the two Bathyergid mole rats studied, the Cape mole rat and Zambian mole rat, are quite similar, but both are different to the other rodent species studied in terms of episode duration of non-REM and REM. These difference may be attributable to their regressed visual system and their subterranean lifestyle as the circadian clock is influenced by light (Dijk and Franken, 2005), or may be the result of a specific phylogenetic difference in the Bathyergids compared to other rodents.

4.4.3. Why do the Bathyergid mole rats sleep differently to other rodents?

The current study and that of Bhagwandin et al. (2011) indicate that the Bathyergid mole rats sleep less than other rodents and have shorter episode durations of both non-REM and REM when asleep. Thus, despite showing an overall similarity in the

physiological signature of sleep with other rodents, the quantities are somewhat shorter. This begs the question as to why there are these differences. If the circadian clock is affected by the lack of light stimulus, due to the mostly subterranean existence of the mole rats, it may result in changes to the structure, duration and episode lengths of sleep as related to the circadian phase in which sleep occurs (Czeisler et al., 1980; Zulley et al., 1981). While the Bathyergid rodents do show strong and entrainable circadian rhythms in the laboratory setting (e.g. Oosthuizen et al., 2003), this entrainment may be less significant in the natural habitat of these animals and indeed may be more variable across individuals in the species within this family (e.g. Oosthuizen et al., 2003). Thus, one source of the observed differences in sleep between the Bathyergid mole rats and the other rodents may be related to the differences in the sensitivity of the circadian clock to light.

A second possibility is the founder effect (Wright, 1945), where the original Bathyergid rodents derived from a population of tunneling rodents that naturally had less sleep than other rodents. The similarities seen regarding sleep in the Cape mole rat and the giant *Zambian* mole rat indicate that further investigation into the quantitative trait loci associated with sleep would be beneficial in understanding the differences in sleep in these rodents compared to other rodents. Thus, there might be a genetically inherited basis for the differences in sleep currently observed. Despite this, it is more likely that a complex interplay between phylogenetic history (genetics), environmental pressures (past and present) and natural history will explain the observed differences. Given that only two species of Bathyergid mole rat have had their sleep studied electrophysiologically, it would be important to investigate other Bathyergid species to determine if the findings

reported herein are applicable to the Bathyergidae as a whole. The two species studied to date, *Georchys capensis* and *Fukomys mechowii*, are both solitary species and socially intolerant, whereas other Bathyergid mole rats show a range of sociality from small to large colonies through to eusociality (Faulkes and Bennett, 2013). The variations in sociality may also lead to variations in sleep times and sleep architecture that would be interesting to examine in this unusual rodent family. Thus, while it is not yet clear why the Bathyergidae sleep somewhat differently to other mammals, this family as a whole does represent a unique opportunity to answer specific questions regarding the expression and control of sleep in accessible model species.

Chapter Five - Sleep in the East African root rat, *Tachyoryctes*

splendens – a short sleeper for a mammal

5.1. Introduction

All mammals studied to date engage in sleep and although there is some variation in the type of sleep exhibited, there is more variation in the length, duration and quality of the various physiological sleep states (e.g. Campbell and Tobler, 1984; Tobler, 1995; Siegel et al., 1998; Lesku et al., 2006, 2008; Lyamin et al., 2008; Siegel, 2008; Gravett et al., 2012). Even within a mammalian order there is variation in the total sleep time (TST) and the amount of REM sleep, although the sleep states exhibited by species within an order appear to be consistent (Campbell and Tobler, 1984; Lesku et al., 2008). Within the order Rodentia, the little pocket mouse, *Perognathus longimembris*, has the greatest TST (approximately 20 h per day), while arrhythmic individuals of giant Zambian mole rat, *Fukomys mechowii*, have a TST of only 4.3 h per day (Lesku et al., 2008; Bhagwandin et al., 2011). Across the 15 rodent species where sleep has been studied electrophysiologically (reviewed in Lesku et al., 2006, but not including the giant Zambian mole rat), the average TST was 13.58 h/day (s.d. 2.6 h, range 8.64 – 20.06 h), with REM sleep occupying an average of 17.41% of TST (s.d. 4.45%, range 9.58 – 24.71%). There are also variations in the circadian rhythmicity between rodent species, and while many rodents are nocturnal, the Sciuridae (squirrels and chipmunks) and the degu, are reported to be diurnal (Elgar et al., 1988; Dijk and Daan, 1989). Thus, there is variation in the total daily amount of sleep and the amount of this sleep occupied by REM

in the various rodent species that have been studied, yet it is unclear what is the root of the variation – is it genetically or environmentally influenced?

In order to add data relevant to this question, sleep was physiologically recorded (and behaviourally verified) in *Tachyoryctes splendens* (the East African root rat). The East African root rat is a highly aggressive subterranean species of the Spalacidae family and is found in the highlands of North East Africa (Jarvis, 1973; Baskevich et al., 1993). These rodents have a brownish-grey coat with small eyes and ears and have an average body mass of 230 g (Jarvis and Sale, 1971). East African root rats are solitary and live in extensive underground burrows where they make nests of plant and faecal matter (Hickman, 1983). The East African root rats do not dig these burrows with their forepaws, but excavate using their very long incisors and push the soil out of the burrow behind them (Jarvis and Sale, 1971; Jarvis, 1973). Although the East African root rat is subterranean, it is not exclusively so, and in the field East African root rats have been observed above ground foraging and pulling plant matter down into their burrows (Jarvis, 1973). In the laboratory setting, the East African root rat was found to have a nocturnal circadian rhythm, being most active between 6 pm and 6 am (Katandukila et al. 2013); however, this contradicts the field observations of Jarvis (1973), which reported this species to be diurnal. The aim of the present study was to provide a quantitative analysis of sleep in the East African root rat to reveal whether changes in phenotype (regressed visual system) and/or natural history (subterranean, nocturnal) affect the amount of the day occupied by both non-REM and REM sleep in this Murid rodent.

5.2. Materials and methods

5.2.1. Experimental animals

Two physiological measures of sleep (EEG and EMG) and the accompanying behaviour were recorded for three adult East African root rats, two males (body masses of 235 g and 228 g) and one female (body mass of 210 g). The animals used in the current study were caught from wild populations and subsequently housed at the Central Animal Facility at the University of the Witwatersrand, South Africa. Ethical clearance for the study (clearance number: 2012/51/05) was obtained from the University of the Witwatersrand Animal Ethics Committee, and all animals were treated according to the guidelines of this committee which parallel those of the NIH for the care and use of animals in scientific experimentation. All animals were acclimatised to the laboratory environment for approximately one month prior to experimentation. Animals were housed individually in a large plastic enclosure (60 cm x 50 cm) with wood shavings lining the floor (to a depth of 3 cm). The animal enclosures were placed in an isolated room that was controlled for temperature (25° C), sound attenuated and with a 12 h light/dark cycle. The animals were fed once a day (4 pm) on a diet of carrots, sweet potatoes and apples and it took approximately 2 min to feed all three animals. Following the acclimatisation period a telemetric recording device (see below) was implanted subcutaneously in each animal and once fully recovered from the surgical procedure, sleep was recorded continuously for 72 h. In addition, a low light CCD camera was mounted above the enclosure for video recordings of the animal's behaviour.

5.2.2. Surgical procedure

Animals were anaesthetised using Isoflurane (1 - 2.5% in an oxygen/70% nitrous oxide mixture, Safe Line Pharmaceuticals) administered *via* a mask placed over the nostrils. Throughout the surgical procedure the animal's heart rate, O₂ saturation levels and body temperature were monitored - all of which were consistent. The scalp and left abdominal region were shaved and cleaned with disinfectant (0.5% chlorhexidine in 75% alcohol, Kyron Laboratories). A mid-sagittal incision was made over the skull and the skin and left temporalis muscle were reflected to expose the dorsal midline of the cranium. Two small holes were drilled with the aid of a dental drill in the region overlying the presumptive left motor cortex. These holes were drilled approximately 8 mm apart, lateral to the mid-sagittal suture, and care was taken to ensure that the underlying dura mater and cortex was not pierced. One stranded stainless steel electrode was carefully placed in each hole, again ensuring that the electrodes rested firmly on the surface of the dura mater, but did not pierce it, and were secured in place and to the surface of the skull with dental cement (Ketacem, 3M). These electrodes served as the EEG (electroencephalogram) recording electrodes. In addition two stranded stainless steel electrodes were sutured into the dorsal nuchal muscles and served as the EMG (electromyogram) recording electrodes. These electrodes were placed approximately 1 cm apart, ensuring that the tips did not come into contact with one another. The EEG and EMG electrodes were all connected to the transmitter (see below) which was implanted in a subcutaneous pocket (2 cm x 2 cm) created over the left abdominal region by a subcutaneous tunnel created between the cranial and abdominal openings. Both openings were sutured following electrode and implant placement, Isoflurane was stopped and

100% oxygen was administered until the animal recovered from anaesthesia. The animal was returned to its enclosure where it was closely monitored until it began to move freely. The animals received 1 cm x 1 cm jelly containing the analgesic Meloxicam (1 g per 1 cm x 1 cm cube of jelly; Ingelheim Pharmaceuticals) twice per day, from the afternoon preceding the surgery for two full days. The animals were allowed to recuperate for seven days prior to recording to allow for recovery and any remnants of the drugs to wear off.

5.2.3. Sleep recording

The telemetric system used in the current study was from Data Sciences International (<http://www.datasci.com>, PhysioTel Telemetric Systems) and consisted of a transmitter (TL11 M2 F40-EET implant, the leads of which were made out of stainless steel, had an outer diameter of 0.3 mm and a lead diameter of 0.2 mm; weight: 7 g; volume: 4.5 cc; length: 13.8 mm) and a receiver (placed directly under the animal's enclosure) which transmitted to the DEM multiplex interface. The interface was in turn connected to the input amplifier of the Data Sciences computer system, which digitally recorded the signals received (in DSI format). After the recording was completed, data digitally saved in the DSI format were converted to text format and these files were in turn converted into the appropriate format needed for recognition and analysis by the Spike 2 computer program (version 5, Cambridge Electronic Design). The Spike files allowed for the visual scoring of the EEG and EMG data of the various physiological states. The EEG spectral power was also calculated. The EEG and EMG were recorded

continuously for 72 h. In addition a low light CCD camera (connected to a DVD recorder) was mounted above the enclosure to allow for visual recordings of the animal's behaviour. The video recording was not scored, but provided behavioural verification for the polygraphically assessed physiological states as described above. The animals were only disturbed once a day at 4 pm for feeding and the disturbance lasted approximately 2 min.

5.2.4. Data analysis

Spike 2 version 5 (Cambridge Electronic Design) was used in all offline analyses of the EEG and EMG data. Data was scored in 5 s epochs as either: (1) wake – characterised by a high-frequency, low-voltage EEG and a high-voltage EMG (Wake); (2) non-rapid eye movement sleep (non-REM) – characterised by a low-frequency, high-voltage EEG, and a low-voltage EMG; or (3) rapid eye movement sleep (REM) – characterised by an EEG that resembled wake but with an EMG that was low-voltage as seen in non-REM sleep or slightly lower. At least fifty percent of an epoch had to be occupied by a particular state for assignation of that state to the epoch. From the 5 s epoch data, the modal state per minute was determined and this per minute modal data was used in all subsequent analyses. The average number and duration of episodes of wake, non-REM and REM were calculated for a 24 h period, as well as for the light phase and dark phase. Total spectral power for each of the states was also calculated using the Spike 2 computer program (Hanning window, FFT number 512, sampling frequency 500 Hz, and segment length 1.024s). The difference in time between the onsets

of consecutive REM episodes was used to calculate the length of a sleep cycle, but for this analysis waking periods of less than 5 minutes between REM episodes were excluded.

5.3. Results

In the present study EEG, EMG and behaviour were recorded in three adult East African root rats over a continuous period of 72 h. These recordings were used to determine wake, non-REM and REM stages. The results from the present study showed that the root rats spent the greatest proportion of time awake (90.8%) (SER+0.6) with a total sleep time (TST) of approximately 2.2 h per day. Non-REM and REM sleep were readily identified, with REM sleep accounting for 21.2% of TST. It is important to note that the EMG during REM did not show atonia in all instances, but in most cases the EMG remained similar or decreased slightly compared to the amplitude of the EMG of the preceding non-REM episode. All REM episodes were visually verified from the video recording. During the dark phase these animals were highly active (eating, grooming, moving around the enclosure, climbing up against the walls, digging/burrowing), but during the day they spend much of their time in quiet waking (lying in a ball but with constant small amplitude head and body movements and repositioning). The animals used in the study included two males and one female. There was no difference between the values for time spent in the different states if we excluded the female from the analysis (time awake = 89.8%, TST = 2.45 h, 19% REM of TST, avg duration non-REM = 2 min, avg duration REM = 1 min), thus we included the data for both males and the female in

all analyses. The major sleep bout in the East African root rat generally occurred between 05:00 - 06:00 am, although it varied and could appear at other times of the day. The major sleep bout usually lasted for 18 min and REM comprised 3 min of the sleep bout. There was only a slight difference between the amount of wake during the light phase (89.2%, SER \pm 0.6%) and the dark phase (92.5%, SER \pm 0.5%). Non-REM (8.3%, SER \pm 0.5%) and REM (2.5%, SER \pm 0.1%) were increased during the light phase compared to the dark phase (non-REM = 6.1%, SER \pm 0.3%; REM = 1.4%, SER \pm 0.2%). The East African root rat is a polyphasic sleeper with sleep occurring at any time during the 24 h period. No unusual sleep states differing from that recorded in rodents previously were identified.

5.3.1. State definitions

Wake was identified by high frequency, low amplitude EEG activity and high amplitude EMG activity (Figs. 5.1, 5.2). Waking behaviour included eating, grooming or moving/burrowing around the enclosure. Non-REM sleep was characterised by low-frequency, high-amplitude EEG activity with low-amplitude EMG activity (Figs. 5.1, 5.2, 5.3), with the animal lying still having the head tucked under the body. REM sleep was scored when there was high-frequency, low-amplitude EEG activity coupled with very low amplitude EMG activity associated with few large high-amplitude EMG spikes (muscle twitches) (Figs. 5.2, 5.3). During REM sleep the animal was either lying in the curled up position with the head tucked under the body or with the head resting on the floor of the enclosure. The frequency range for spectral power was 0 – 7 Hz but the peak

amplitude occurred at: 3 Hz for waking, 4.2 Hz for non-REM and 3.9 Hz for REM (Fig. 5.4).

5.3.2. Time spent in Wake, non-REM and REM states

The physiological data (summarized in Table 5.1) was scored in 1 min epochs and it was observed that the East African root rats spent on average in a 24 h cycle, 90.8% (SER \pm 0.6%, 21.8 h) in a state of Wake, 7.2% (SER \pm 0.6%, 1.7 h) in non-REM and 1.9% (SER \pm 0.2%, 0.46 h) in REM (Fig. 5.5A). The time spent in Wake was higher during the dark phase (11.1 h in dark vs 10.7 h in light), while the time spent in non-REM (1 h in light vs 44 min in dark) and REM sleep (18 min in light vs 10 min in dark) was higher during the light phase (Fig. 5A). Total sleep time (TST) was 9.1% (2.2 h) and the percentage of REM of TST was 21.2% (0.46 h) (Table 5.2).

5.3.3. Number and duration of wake and sleep episodes

The 1 min epoch data was analysed to determine the number of episodes of Wake, non-REM and REM sleep. The average number of episodes in 24 h was: 49 (SER \pm 2.7) for Wake, 54 (SER \pm 3.3) for non-REM and 21 (SER \pm 2.0) for REM (Fig. 5.5B). The average number of episodes during the light phase was higher than the dark phase: 29 in light vs 20 in dark for Wake, 31 in light vs 23 in dark for non-REM and 14 in light vs 7 in dark for REM (Fig. 5.5B). The average duration of an episode of Wake was 28 min (SER \pm 1.9 min), a non-REM episode was 2 min (SER \pm 0.1 min) and a REM episode was 1

min (SER \pm 0.1 min) (Fig. 5.5C). The average duration of a waking episode was markedly longer during the dark phase than the light phase (39 SER \pm 6.7 min vs 24 SER \pm 2.1 min), but there was no marked difference between the duration of an episode of either non-REM or REM sleep in the light or dark phases (non-REM = 2 mins, SER \pm 0.1min; REM = 1 min, SER \pm 0.1 min) (Fig. 5.5C).

5.3.4. REM periodicity and state transitions

The time lapse between the onsets of consecutive episodes of REM sleep was calculated to establish REM periodicity. The highest frequency of consecutive REM sleep onsets occurred between 5 – 10 min, followed by a smaller peak at 25 – 30 min and an additional peak at >180 min. The peak sleep cycle duration was observed to be between 5-15 min (Fig. 5.6). Waking episodes that occurred between REM episodes but lasted less than 5 minutes were removed from this analysis. While it is the generally accepted practice to remove waking episodes of longer than 10 min, when we did this for the East African root rat it resulted in very few data points across the 72 h of recording. Due to the very low amount of sleep in these animals, the extended periods of wake between sleep cycles and the inconclusivity of the major sleep bout, we decided to retain all waking episodes in the analysis except those less than 5 minutes. It may be that using the method of excluding waking episodes of more than 10 minutes is better suited for use in monophasic sleepers or animals with a more distinct set time for the major sleep bout.

The transitions between the physiologically identified states were counted to determine the frequency with which one state transitioned into another (Fig. 5.7). It was

found that Wake always transitioned to non-REM sleep and never to REM sleep. Non-REM sleep was observed to transition to Wake (69.08%) more often than to REM sleep (30.92%), while REM sleep transitioned to Wake more frequently (61.11%) than to non-REM sleep (38.89%).

Table 5.1: Data over the 72 hour recording period for the three East African root rats for the various parameters measured in the current study. **TWT (% 24 h)** – total waking time as a percentage of 24 hours; **TST (& 24 h)** – total sleep time as a percentage of 24 hours; **Tnon-REM (% 24 h)** – total non-REM sleep time as a percentage of 24 hours; **TREM (% 24 h)** – total REM sleep time as a percentage of 24 hours; **TWT-Light phase (% 12 h)** – total waking time during the light phase as a percentage of 12 hours; **TST-light phase (% 12 h)** – total sleep time during the light phase as a percentage of 12 hours; **Tnon-REM-Light phase (% 12 h)** – total non-REM sleep time during the light phase as a percentage of 12 hours; **TREM-Light phase (% 12 h)** – total REM sleep time during the light phase as a percentage of 12 hours; **TWT-Dark phase (% 12 h)** – total waking time during the dark phase as a percentage of 12 hours; **TST-Dark phase (% 12 h)** – total sleep time during the dark phase as a percentage of 12 hours; **Tnon-REM-Dark phase (% 12 h)** – total non-REM sleep time during the dark phase as a percentage of 12 hours; **TREM-Dark phase (% 12 h)** – total REM sleep time during the dark phase as a percentage of 12 hours.

Animal ID	RR3	RR4	RR5	Weighted mean
Body mass (g)	235 g	210g	228g	224g
Sex	Male	Female	Male	
TWT (% 24 h)	90	93	89	91
TST (% 24 h)	10	7	11	9
Tnon-REM (% 24 h)	8	5	8	7
TREM (% 24 h)	2	2	3	2
TWT-Light phase (% 12 h)	87	92	89	89
TST-Light phase (% 12 h)	13	8	11	11
Tnon-REM-Light phase (% 12 h)	11	5	9	8
TREM-Light phase (% 12 h)	2	3	2	3
TWT-Dark phase (% 12 h)	93	94	90	93
TST-Dark phase (% 12 h)	7	6	10	7
Tnon-REM-Dark phase (% 12 h)	6	5	8	6
TREM-Dark phase (% 12 h)	1	1	2	1

Table 5.2: Summary of the data for the number of epoch, episodes and average duration of Wake (**W**), non-REM (**N**) and REM (**R**) on a daily basis for the three East Africa root rats studied. This shows the consistency of these parameters across days and across individuals.

Animal ID	RR3			RR4			RR5			Group average
	Day 1	Day 2	Day 3	Day 1	Day 2	Day 3	Day 1	Day 2	Day 3	
No. of epochs (W)	1307	1310	1273	1321	1350	1341	1274	1305	1289	1308
No. of epochs (N)	110	109	144	79	70	71	122	108	123	104
No. of epochs (R)	23	21	23	40	20	28	44	27	28	28
No. of episodes (W)	48	50	54	46	37	36	59	58	50	49
No. of episodes (N)	56	62	57	51	38	38	66	58	61	54
No. of episodes (R)	17	17	17	22	13	19	34	26	23	21
Avg. duration (W)	27.23	26.2	23.57	28.72	36.49	37.25	21.59	22.5	25.78	28
Avg. duration (N)	1.96	1.79	2.53	1.55	1.84	1.87	1.89	1.86	2.02	2
Avg. duration (R)	1.15	1.24	1.35	1.82	1.54	1.4	1.29	1.04	1.22	1

Figure 5.1: Polygraphic trace illustrating the changes in the EEG (electroencephalogram) and EMG (electromyogram) during the transition from non-REM sleep to Wake in the East African root rat. Wake was characterized by low-amplitude, high-frequency EEG and high amplitude EMG, while non-REM sleep was characterized by high-amplitude, low frequency EEG and low amplitude EMG.

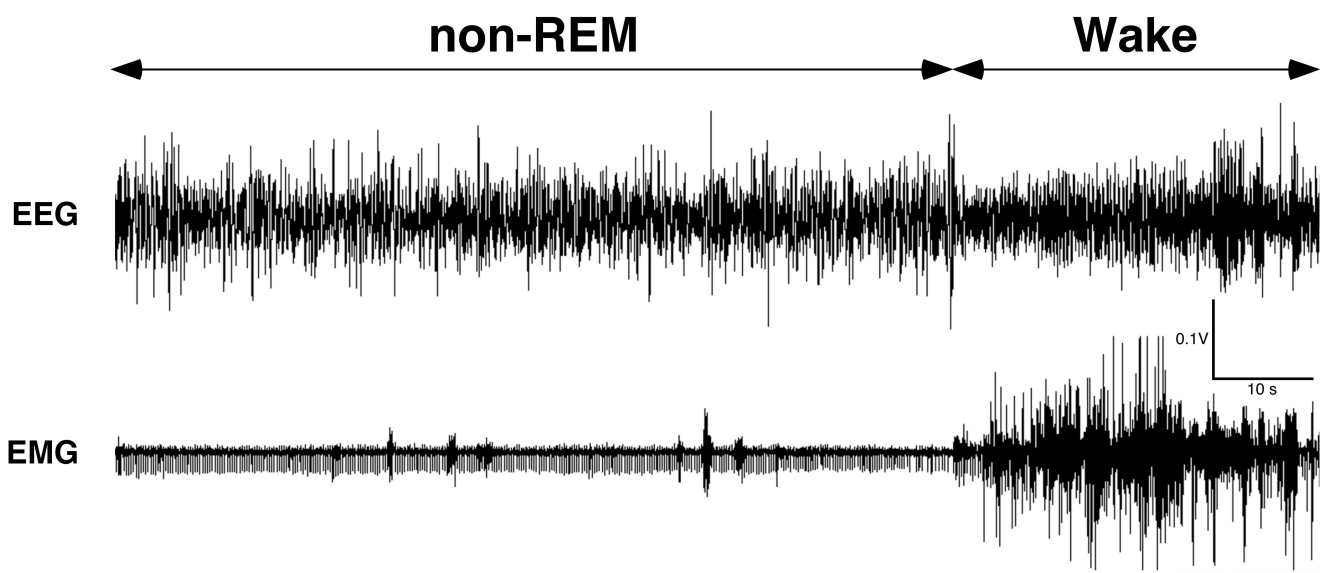


Figure 5.2: Polygraphic trace illustrating the changes in the EEG (electroencephalogram) and EMG (electromyogram) during the transition from Wake to non-REM sleep to REM sleep in the East African root rat. REM sleep was characterized by low-amplitude, high-frequency EEG (similar to that seen in Wake) and low-amplitude EMG.

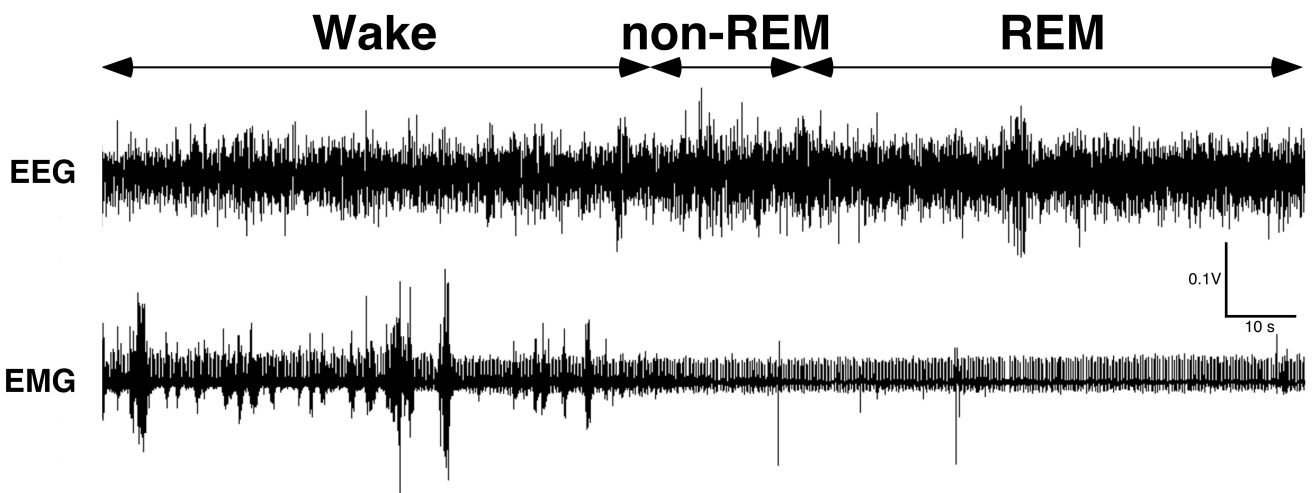
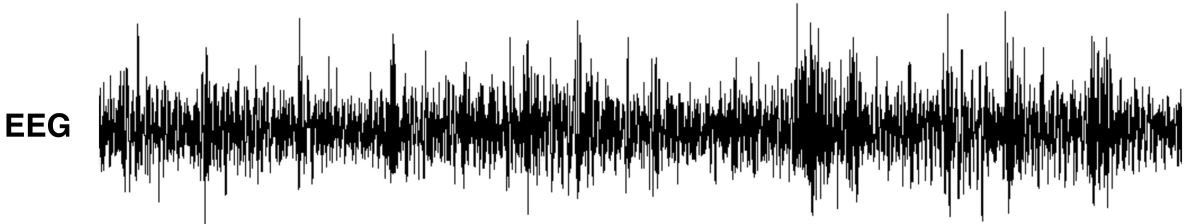


Figure 5.3: Polygraphic trace illustrating the EEG (electroencephalogram) and EMG (electromyogram) during non-REM sleep and REM sleep in the East African root rat. non-REM sleep was characterized by high-amplitude, low frequency EEG and low amplitude EMG, while REM sleep was characterized by low-amplitude, high-frequency EEG (similar to that seen in Wake) and low-amplitude EMG.

non-REM



REM

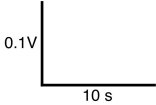
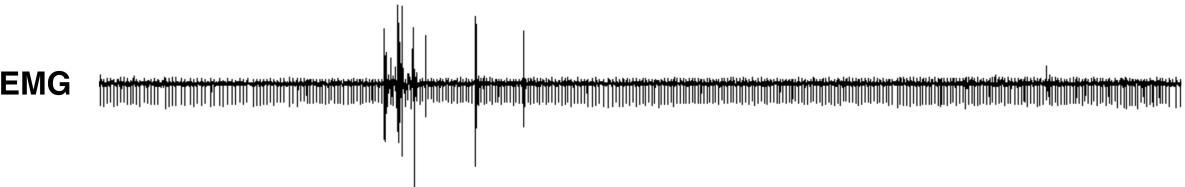


Figure 5.4: Graph indicating the spectral power range during Wake, non-REM and REM states for the East African root rat.

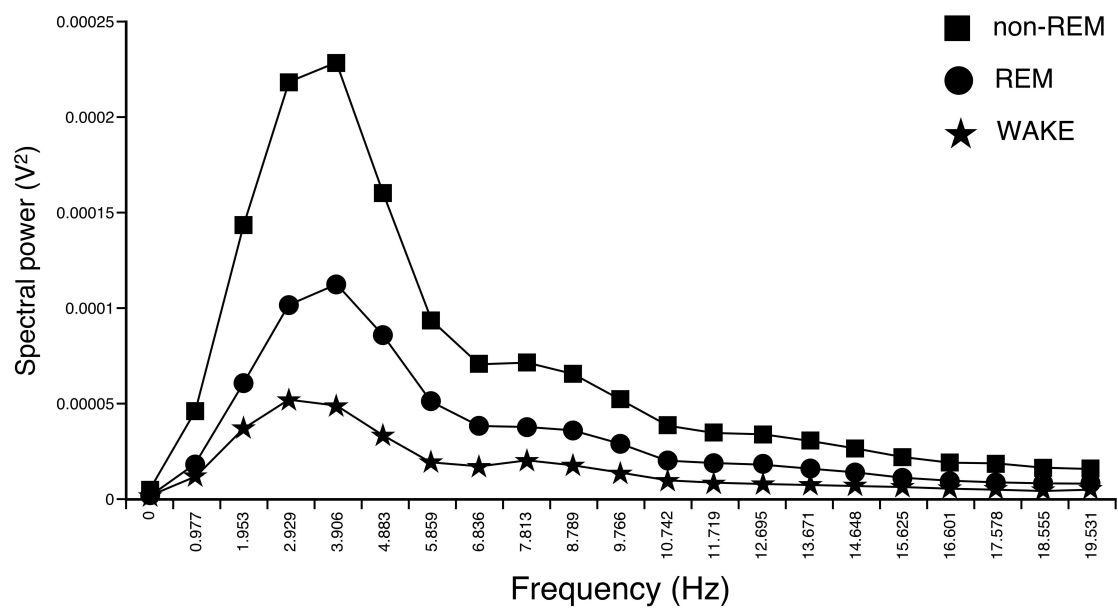


Figure 5.5: Graphs illustrating the physiological data for Wake, non-REM and REM during a 24-hour cycle, the 12 h light period and 12 h dark period in the East African root rat. **(A)** The percentage of time spent in Wake, non-REM and REM. **(B)** The number of 1 min episodes of Wake, non-REM and REM. **(C)** The average episode duration (in minutes) of Wake, non-REM and REM.

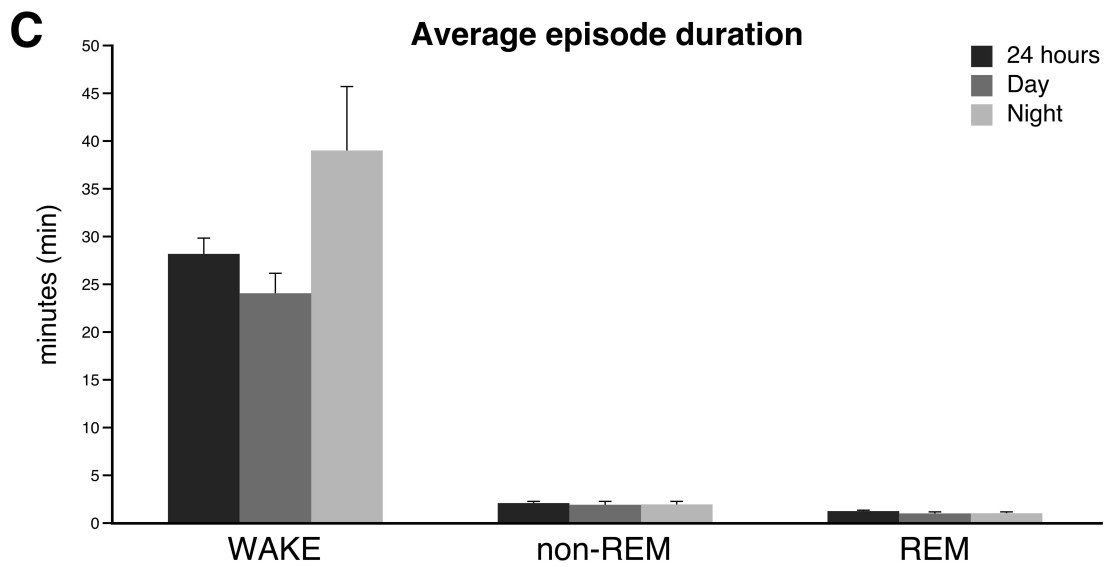
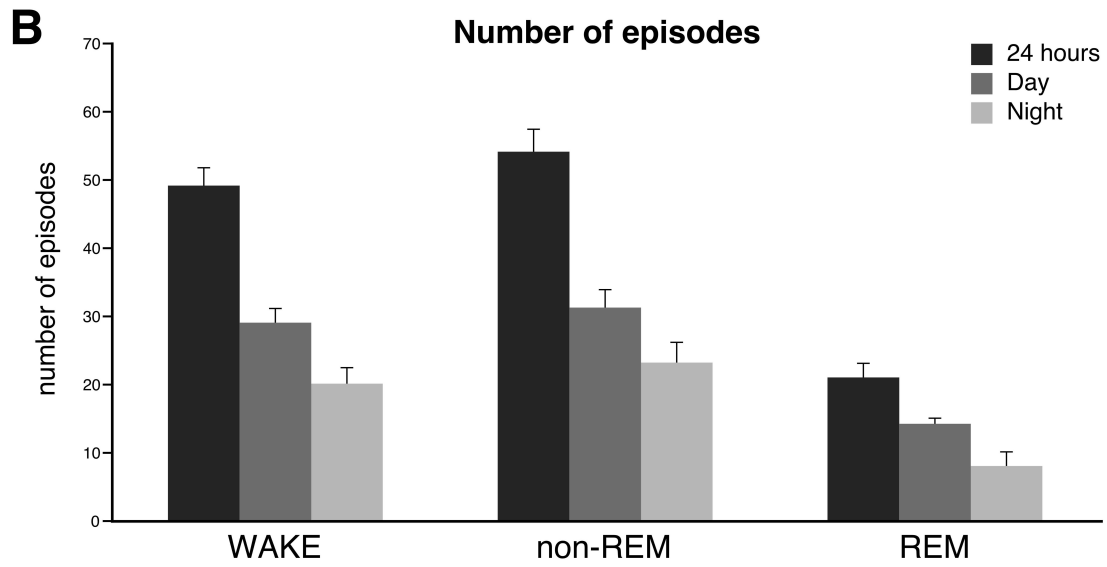
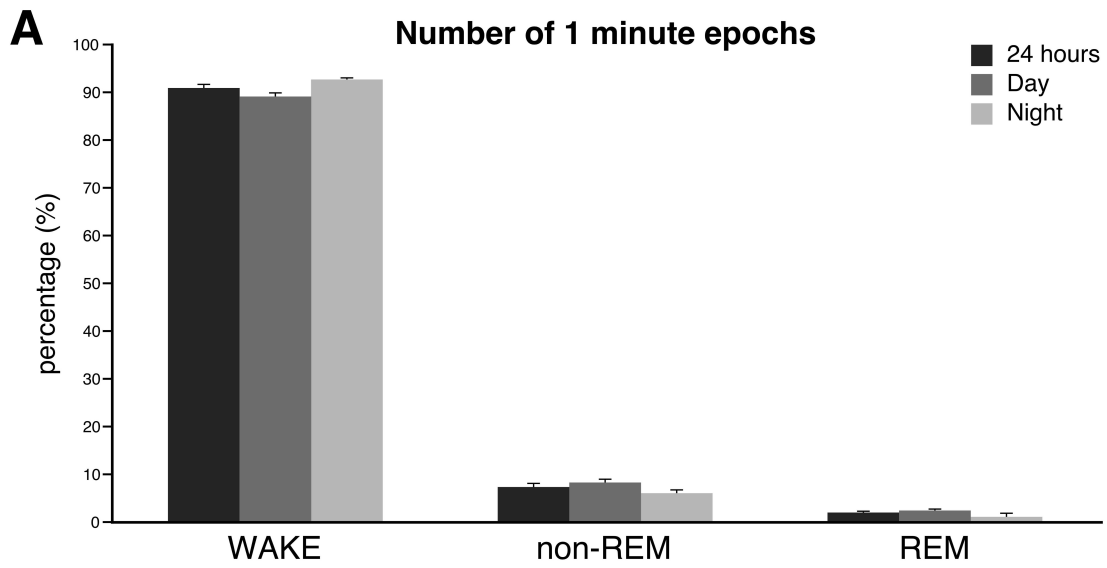


Figure 5.6: Graph representing the time lapse (5-min periods) between onsets of physiologically identified REM episodes (REM periodicity) for the East African root rats.

REM Periodicity

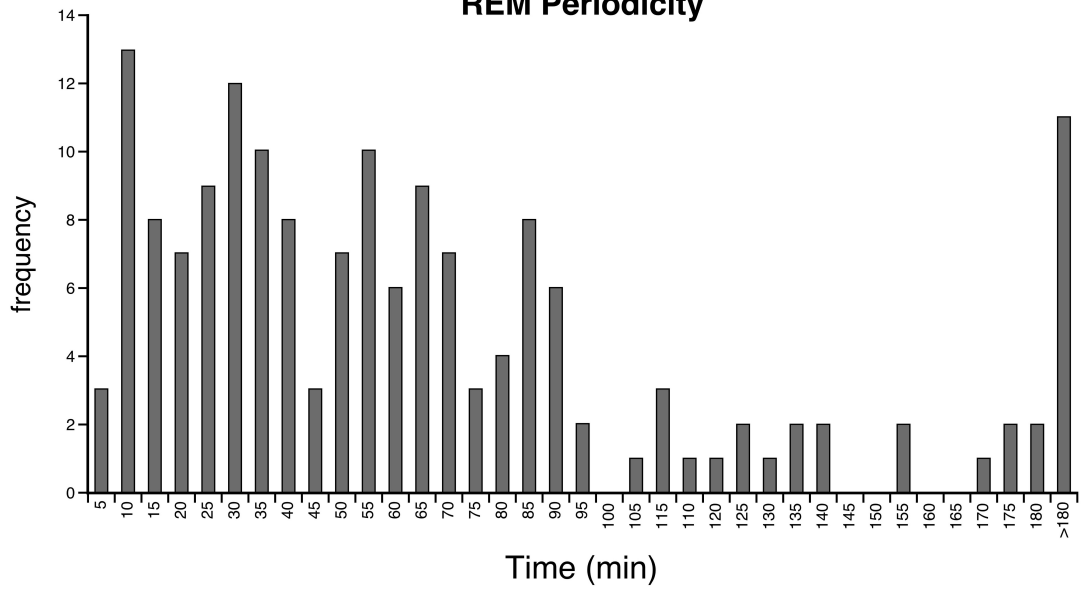
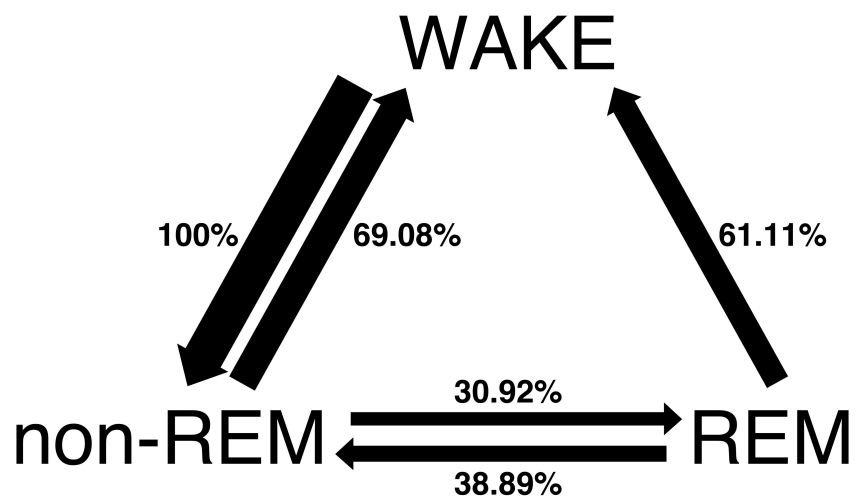


Figure 5.7: Flow diagram illustrating transitions (represented as a percentage) between Wake, non-REM and REM in the East African root rat. Note that Wake always transitions into non-REM sleep, and that both non-REM and REM transition to Wake more often than to each other.



5.4. Discussion

The present study examined sleep in the East African root rat to determine if any observed differences could be attributed to its subterranean lifestyle or regressed visual system. On average over a 24 hour period, these animals spent 21.8 h in wake, 1.73 h in non-REM sleep and 28 min in REM sleep, this being the least amount of sleep recorded in any rodent, or indeed any mammal, studied with electrophysiological methods to date (reviewed in Lesku et al., 2006). Our observations raise the question of whether the East African root rat is a nocturnal or diurnal species and whether this rodent is indeed the mammal with the shortest amount of sleep. These findings raise many important questions relating to the function and regulation of sleep.

5.4.1. Are East African root rats diurnal or nocturnal?

Field observations of the East African root rat conducted by Jarvis (1973), reported that these animals were diurnally active and were observed outside their burrows during the daylight period. In contrast, a laboratory study on the locomotor activity patterns of the East African root rat conducted by Katandukila et al. (2013) found that these animals had a distinctly nocturnal circadian rhythm in terms of locomotor activity. It has been shown previously that certain subterranean animals that are active during the day in the wild will adopt a nocturnal rhythm under laboratory conditions (e.g. Reig, 1970; Begall et al., 2002; Valentinuzzi et al., 2009; Tomatani et al., 2012), and this may explain the difference in circadian rhythmicity reported in the literature for this species.

In the present study, the number of non-REM and REM episodes increased in frequency during the light phase, but the average duration of each of these episodes was the same during the light phase and dark phase; however, it is clear that the animals slept more, and had more REM during the light phase than the dark phase. The number of waking episodes decreased slightly during the dark phase, but the average duration of these episodes increased, leading to a slight increase in time spent in Wake during the dark phase (11.1 h) compared to the light phase (10.7 h). In addition, the major sleep bout usually occurred at the end of the dark phase between 5 – 6 am, although occasionally it occurred in the late afternoon or early evening. The major sleep bout usually lasted 18 minutes and REM comprised 3 minutes of this sleep bout. From our findings, it would appear that the East African root rat has a tendency toward a nocturnal rhythm in the laboratory, but this is not a rule. Our video recording indicated that during the dark phase the root rats were highly active, being very mobile and showing a range of behaviours, and in the light phase they often adopted an activity pattern that could be described as quiet wake, where while not asleep, they did not move a great deal but were aware and vigilant of their surroundings. Given that the root rats examined in the current study had a total sleep time of only 2.2 h, it would appear that defining these animals as either nocturnal or diurnal is untenable. While they are definitely far more active during the dark period, with both our video observations and the circadian rhythm study of Katandukila et al. (2013) agreeing with this, the field observations of Jarvis (1973) are not contradicted by these findings as the animals did engage in quiet wake during the light period in the laboratory. We might conclude that while most active in the nocturnal period, the East African root rat can be active, or awake, at any time of the day.

5.4.2. Is the East African root rat the shortest sleeping mammal? Comparison to studies in other rodents and mammals

The most surprising finding of the current study on sleep in the East African root rat is the minimal amount of time it appears to sleep, only 2.2 h per day, which is significantly lower than any other rodent species previously studied (average TST is 13.58 h/day in rodents, with a standard deviation of 2.6 h, and range of 8.64 – 20.06 h), or indeed any other mammal previously studied (Campbell and Tobler, 1984; Lesku et al., 2006). Despite this, the root rat shows both non-REM and REM sleep states with physiological characteristics similar to that seen in other mammals. Moreover, the percentage of TST occupied by REM sleep in the root rat, at 21.2% is well within the range observed in other rodents, where on average REM occupies 17.41% of TST (s.d. 4.45%, range 9.58 – 24.71%) (Lesku et al., 2006). Thus, we can conclude that the East African root rat is the mammal with the shortest sleep studied to date, and that even though the amount of sleep in the root rat is far lower than that seen in other rodents, the physiology of this small amount of sleep does not differ.

One issue that needs to be raised is that the East African root rats studied here, while having been born and matured in the wild, were studied under laboratory conditions. In the wild, these animals normally sleep in an underground chamber, where they build a nest for sleeping (Jarvis and Sale, 1971). In the laboratory conditions used herein, the root rats were provided with enough bedding material to create a nest for sleeping, but the potential nest would have always been exposed to some degree of light

as there was no provision for them to build a nest either fully or partially shaded from the light source. This confounding factor may have led to the root rats becoming hypervigilant and thus reducing TST to the level observed in the present study. Despite this, before the commencement of the sleep recording, the animals were allowed to acclimatize to the new laboratory setting for a period of one month, and thus one might assume that their sleep patterns would have normalized during this period. Moreover, we would have expected to have seen a far greater variation in TST on a daily basis in these root rats, but this was not the case (Table 5.2). Our video recordings of these animals revealed that during the dark phase the animals were highly active (moving around the enclosure, digging, burrowing, making nesting material, eating and grooming); however, during the light phase the animals remained stationary in a curled up position, but were constantly repositioning and making small amplitude movements, which were scored as Wake periods based on the EEG and EMG polygraphic data. In addition, it was noted that during the dark period the animals would create a mound with the nesting material provided which could serve as a shelter during the light period, but the animals would consistently return to their customary sleeping location during the light period even though it was exposed. In order to remove this confound from the study, and to really determine whether sleep in the East African root rat is markedly shorter than that seen in other mammals, it would be advisable to perform further recordings with individuals where the possibility to avoid light during the light phase is made available.

Despite this potential methodological confound in the current study, the mole rats *Georhynchus capensis* (see preceding chapter) and *Fukomys mechowii* (Bhagwandin et al., 2011), which share a similar morphology and natural history to the root rats, that were

recorded in exactly the same experimental set up, exhibited TSTs that fell well within, or close to, the range of TST recorded in other rodent species previously studied (Lesku et al., 2006). Furthermore, earlier recordings of sleep in the blind mole rat, to which the root rats are closely related (Baskevich et al., 1993; Katandukila et al., 2013), had TSTs of 12.4 h (Tobler and Deboer, 2001). Lastly, it has been demonstrated that sloths sleeping under laboratory conditions, where food and water are provided *ad libitum*, and the risk of predation has been removed, the sloths sleep significantly more than when in the wild (Rattenborg et al., 2008). Thus, given the limits of the potential experimental confound and the circumstantial support from studies of animals in the same experimental set-up, closely related species and comparisons of captive vs wild sleep, support the conclusion that the East African root rat is truly the shortest sleeping mammal studied to date.

5.4.3. What is the cause of reduced sleep time in East African root rats?

The general biology and specific physiology of the East African root rat has not been intensively studied. It has been shown previously that genetics plays a significant role in sleep architecture (Lindowski et al., 1991; Tafti et al., 1997; Franken et al., 1998, 1999), and in particular there are certain chromosomes that result in a vigilant phenotype in mice (Tafti et al., 1997). It is therefore possible that further investigations may reveal that the East African root rat has genetic drivers for increased wakefulness and thus decreased sleep time. It has been noted that East African root rats are highly aggressive (Jarvis, 1973). In laboratory rats it has been found that increased testosterone levels lead to an increase in aggression in both male and female rats (Albert et al., 1992).

Furthermore, it has been seen in human subjects that an increase in testosterone leads to a decrease in TST (Liu et al., 2003). Therefore it would be useful to study the circulating levels of testosterone within these animals, as well as other hormones that may result in reduced TST. Unfortunately, as these aspects of the biology of the East African root rat have not been studied, the potential genetic or hormonal explanations of the decrease in TST in these species are purely speculative. Another potential explanation is that the root rats might be using local sleep (e.g. Huber et al., 2004; Murphy et al., 2011; Lesku et al., 2011) as a replacement for global sleep, thereby meeting the life-sustaining requirements of sleep without losing the potential to remain vigilant. Lastly, as stated above, it is possible that the laboratory environment is the cause of a reduced TST, but as argued, this appears unlikely. Clearly, understanding the short amount of sleep in the East African root rat will have major implications for our understanding of sleep as a general vertebrate phenomenon.

5.4.4. What can a short sleeper reveal about sleep and the function of sleep?

If, as argued above, the East African root rat is truly the shortest sleeping mammal, this species becomes a very interesting model species for the study of sleep function. It has been generally observed that larger mammals require less sleep than smaller mammals (Zepelin and Rechtschaffen, 1974; Lesku et al., 2006); however, it appears these correlations are not predictable (Siegel, 2013). The root rat, with a body mass of around 220 g, sleeps less than an Asian elephant does (Tobler, 1992). The root rat then may serve as an accessible model animal to determine what factors, genetic,

hormonal, environmental, local sleep processes, or other, determine total sleep time. It would appear to make sense that either biological or environmental factors control total sleep time and that the revelation of the processes that control total sleep time are likely to lead to the understanding of the precise function of sleep – an understanding that currently eludes scientists. Despite this, it would be prudent before taking this speculative path to remove the experimental confound that may affect the result to check that this species is truly a very short sleeping mammal. In addition, it would be worthwhile to study the other member of the same genus, the big-headed root rat *Tachyoryctes macrocephalus*, to evaluate whether this is a genus specific or species specific phenomenon. Given that the genus *Tachyoryctes* forms part of the subfamily *Spalacinae*, which also contains the blind mole rat which has a normal amount of sleep for a rodent (Tobler and Deboer, 2001), the comparison of molecular, hormonal and other aspects of the biology and natural history of *Tachyoryctes* species with *Spalax* species, may reveal significant insights regarding the control of, and ultimately the function of, sleep.

Chapter Six - Organization of sleep related nuclei and inhibitory neurons/terminal networks in five species of phenotypically and phylogenetically varied rodents

6.1. Introduction

The sleep/wake cycle is controlled and regulated through the complex interplay of several nuclei producing specific neurotransmitters located from the basal forebrain through to the pons (Siegel, 2004). The cholinergic nuclei of the basal forebrain and pons actively promote both wakefulness and rapid eye movement (REM) sleep (Bernston et al., 2002; Pace-Schott and Hobson, 2002; Jones, 2008; Platt and Riedel, 2011). The locus coeruleus complex located in the pons, containing noradrenergic neurons regulates sleep, wake and arousal states, including REM sleep (Jones, 1972, 2008; Monti, 1982; Pace-Schott and Hobson, 2002; Rasch et al., 2007). The serotonergic raphe nuclei of the hypothalamus promote cortical arousal, and function to inhibit REM sleep (Imeri et al., 1994; Portas et al., 2000; Pace-Schott and Hobson, 2002), while the orexinergic nuclei of the hypothalamus stabilise and regulate waking, thereby promoting a longer wake period (Kukkonen et al., 2002; Pace-Schott and Hobson, 2002; Ohno and Sakurai, 2008; Sakurai, 2007; Jones, 2008; Tsujino and Sakurai, 2009). γ -Aminobutyric acid (GABA) is the most abundant inhibitory neurotransmitter found in the brain and it plays a role in both the facilitation and inhibition of REM sleep through interactions with the cholinergic, catecholaminergic, serotonergic and orexinergic systems (Pace-Schott and Hobson, 2002). GABAergic neurons generally, but not always, contain the calcium

binding proteins parvalbumin (PV), calbindin (CB) and calretinin (CB) (Gritti et al., 2003). Due to the varied buffering effect that these calcium binding proteins have on the neurons in which they are found, they are of interest when investigating the neural basis of the control and regulation of the sleep/wake cycle (Baimbridge et al., 1992; Li et al., 1995).

While physiological sleep in rodents has been extensively studied, the vast majority of these studies have been limited to sleep in laboratory rodents with comparative analyses being often limited to single studies. The non-standard laboratory rodents where physiological sleep has been studied include the giant Zambian mole rat (Bhagwandin et al., 2011a), the middle east blind mole rat (Tobler and Deboer, 2001), the squirrel, (Folk, 1963; Chepkasov, 1980), the guinea pig (Tobler et al., 1993) and the hamster (Tobler and Jaggi, 1987; Deboer et al., 1994). The neural systems controlling and regulating the sleep/wake cycle have not been studied extensively across rodents, with mostly incidental non-targeted observations of these systems having been made in a range of rodent species (da Silva et al., 2006; Moon et al. 2007; Dwarika et al., 2008; Bhagwandin et al., 2008, 2011b; Limacher et al., 2008; Kruger et al., 2012); however, in the one specifically targeted study of the giant Zambian mole rat (Bhagwandin et al., 2013) found extensive similarities in the cholinergic, noradrenergic, serotonergic and orexinergic neurons with laboratory rodents, but noted specific differences in the expression levels of the neurons and terminal networks containing the calcium binding proteins that appeared to be related to differences in the expression of sleep in the mole rat compared to laboratory rodents. Due to the paucity in comparative data and the potential relationship between differences in the expression of these systems and sleep

physiology, the present study undertook a comparison of the sleep related neural systems in the brains of five species of phenotypically and phylogenetically varied rodents to determine what similarities or differences occurred in these areas between the species. The species studied were the African pygmy mouse (*Mus minutoides*), the greater cane rat (*Thryonomys swinderianus*), the agouti (*Dasyprocta agouti*), the East African root rat (*Tachyoryctes splendens*) and the Cape mole rat (*Georychus capensis*). These species show a large range in body mass (from 8 g to 3.9 kg), inhabit a variety of habitats including arid regions, grasslands, rainforest and subterranean tunnels, represent a range of life histories and are phylogenetically spread across the rodent order. These differences provide an opportunity to investigate the potential variation in the sleep/wake neural systems across rodents that would be predicted to sleep in quite different ways.

To investigate the sleep related neural systems, the brains of these species were immunohistochemically stained for choline acetyltransferase (ChAT), tyrosine hydroxylase (TH), serotonin (5HT), orexin (Orx), parvalbumin (PV), calbindin (CB) and calretinin (CR). A number of studies have found that there is predictability in the anatomical variance of the neural systems involved in the regulation and control of the sleep wake cycle (Manger, 2005; Maseko et al., 2007; Dell et al., 2010; Kruger et al., 2012), but a specifically targeted study within a single order has not yet been undertaken.

6.2. Materials and Methods

The brains from three adults of each species were used in this study: African pygmy mouse (average body mass = 8.8 g; average brain mass = 275 mg), East African

root rat (average body mass = 230 g; average brain mass = 2.6 g), Cape mole rat (average body mass = 200 g; average brain mass = 2.3 g), greater cane rat (average body mass = 2.7 kg, average brain mass = 13.8 g) and agouti (average body mass = 3.6 kg; average brain mass = 20.5 g). All animals were captured from a wild populations, with appropriate governmental approvals, and were treated and used according to the guidelines of the University of the Witwatersrand Animal Ethics Committee which parallel those of the NIH regarding the use and treatment of animals in scientific experiments. The animals were euthanased (Euthanase, 200 mg sodium pentobarbital/kg, i.p.) and upon cessation of respiration, perfused intracardially with an initial rinse of 0.9% saline solution at 4°C (1 ml/g of body mass), which was followed by a solution of 4% paraformaldehyde in 0.1M phosphate buffer (PB) (1 ml/g of body mass). After removal from the skull, each brain was post-fixed overnight in the paraformaldehyde solution and subsequently stored in anti-freeze at -20°C. Before sectioning, the brains were trimmed, leaving only the basal forebrain, diencephalon, midbrain and pontine regions as a single block, and allowed to equilibrate in 30% sucrose in 0.1 M PB at 4°C. These brain blocks were then frozen and sectioned into 50 µm thick serial coronal sections. A one in nine series of sections was used for Nissl, myelin, choline-acyltransferase (ChAT), tyrosine hydroxylase (TH), serotonin (5HT), orexin (hypocretin/OxA), parvalbumin (PV), calbindin (CB) and calretinin (CR). Sections for Nissl staining were mounted on 0.5% gelatine coated slides, cleared in a solution of 1:1 absolute alcohol and chloroform and then stained with 1% cresyl violet. The myelin series of sections were refrigerated for two weeks in 5% formalin then mounted on 1% gelatine coated slides and stained with a modified silver stain (Gallyas, 1979).

The sections for immunohistochemical staining were treated for 30 min in an endogenous peroxidase inhibitor (49.2% methanol: 49.2% 0.1M PB: 1.6% of 30% hydrogen peroxide) followed by three 10 min rinses in 0.1M PB. Sections were then preincubated for 2 h, at room temperature, in blocking buffer (3% normal goat serum, NGS, for TH, serotonin, orexin, PV, CB and CR sections; 3% normal rabbit serum, NRS, for ChAT sections, 2% bovine serum albumin for all sections and 0.25% Triton-X in 0.1M PB for all sections). Thereafter sections were incubated in the primary antibody solution in blocking buffer for 48 h at 4°C. Anti-cholineacetyltransferase (AB144P, Millipore, raised in goat) at a dilution of 1:3000 was used to reveal cholinergic neurons. Anti-tyrosine hydroxylase (AB151, Millipore, raised in rabbit) at a dilution of 1:7500 revealed the putative catecholaminergic neurons. Serotonergic neurons were revealed using anti-serotonin (AB938, Millipore, raised in rabbit) at a dilution of 1:7500. Orexinergic neurons were revealed using anti-OrexinA (AB3704, Millipore, raised in rabbit) at a dilution of 1:3000. To reveal parvalbumin, calbindin and calretinin neurons and terminal networks we used anti-parvalbumin (PV28, Swant, raised in rabbit), anti-calbindin (CB38a, Swant, raised in rabbit) and anti-calretinin (7699/3H, Swant, raised in rabbit), all at a dilution of 1:10 000. This incubation was followed by three 10 min rinses in 0.1M PB and the sections were then incubated in a secondary antibody solution (1:1000 dilution of biotinylated anti-rabbit IgG for TH, serotonin, orexin, PV, CB and CR sections, or a 1:1000 dilution of biotinylated anti-goat IgG for ChAT sections, in a blocking buffer containing 3% NGS/NRS and 2% BSA in 0.1M PB) for 2 h at room temperature. This was followed by three 10 min rinses in 0.1M PB, after which sections were incubated for 1 h in AB solution (Vector Labs), followed by three 10 min rinses in

0.1M PB. Sections were then placed in a solution of 0.05% diaminobenzidine (DAB) in 0.1M PB for 5 min, followed by the addition of 3 μ l of 3% hydrogen peroxide to each 1 ml of solution in which each section was immersed. Chromatic precipitation was visually monitored and verified under a low power stereomicroscope. Staining was allowed to continue until such time as the background stain was at a level that would assist reconstruction without obscuring the immunopositive structures. Precipitation was arrested by placing sections in 0.1M PB, followed by two more rinses in this solution. Sections were then mounted on 0.5% gelatine coated glass slides, dried overnight, dehydrated in a graded series of alcohols, cleared in xylene and coverslipped with Depex. The omission of the primary antibody and the omission of the secondary antibody in selected sections, for which no staining was evident, was used to test for non-specific staining of the immunohistochemical protocol.

Sections were examined under low power stereomicroscope and using a camera lucida, the architectonic borders of the sections were traced following the Nissl and myelin stained sections. Sections containing the immunopositive neurons were matched to the drawings and the neurons were marked. The immunopositive parvalbumin, calbindin and calretinin neurons and their extensive distribution of terminal networks were matched to these drawings using the microscope and the relative densities noted and photographed. All architectonic nomenclature was taken from the atlas of a rodent brain (Paxinos et al., 2009). All the nomenclature used was adopted from Bhagwandin et al. (2008, 2011b, 2013) and Kruger et al., (2012).

6.3. Results

In the present study several cholinergic, noradrenergic, serotonergic and orexinergic nuclei or clusters associated with the regulation and control of the sleep/wake cycle were observed in the rodents studied. Across the five rodent species, the parcellation of these clusters was, for the most part, identical; however, the noradrenergic locus coeruleus complex of *Mus minutoides* had a different appearance to the other species investigated. In contrast to this, the presence of neurons and terminal networks immunopositive for the calcium binding proteins parvalbumin, calbindin and calretinin, were more varied, with consistency in the density of neurons and terminal networks being found in some of the sleep associated nuclei, while in others the density of neurons and terminal networks varied significantly. In all species the thalamic reticular nucleus contained neurons and terminal networks consistently immunopositive for parvalbumin, but there was variance in the density of neurons and terminal networks immunopositive for calbindin and calretinin between species.

6.3.1. Cholinergic nuclei of the basal forebrain and pons

Within the basal forebrain, choline acetyltransferase immunopositive (ChAT+) neurons were identified in the medial septal nucleus, diagonal band of Broca, islands of Calleja and olfactory tubercle and nucleus basalis in three species studied (Fig. 6.1) (these regions of the brain were not available for analysis in *T. swinderianus* and *D. agouti*). Moreover, the location of each of these nuclei and the morphology and density of

the ChAT+ neurons within these nuclei was the same across the three species. The medial septal nucleus was found in the medioventral aspect of the septal nuclear complex, immediately adjacent to the midline. A moderate density of ChAT+ neurons was observed throughout this nucleus. The diagonal band of Broca was located at the ventromedial corner of the cerebral hemisphere, in a position ventral to the septal nuclear complex (Fig. 6.1A, 6.1E). A high density of ChAT+ neurons was observed in this nucleus and the neurons were larger than those in the medial septal nucleus. The olfactory tubercle, with the embedded islands of Calleja was found lateral to the diagonal band of Broca, on the ventral surface of the anterior portion of the cerebral hemisphere. The ChAT+ neurons within the olfactory tubercle were more sparsely distributed than those in the diagonal band of Broca, but regional higher densities within the olfactory tubercle represented the island of Calleja (Fig. 6.1E). The nucleus basalis was located caudal to the nucleus accumbens, dorsal to the olfactory tubercle, and medioventral to the globus pallidus. A moderate to high density of ChAT+ neurons were found within this nucleus.

Within the pontine region of all five species, choline acetyltransferase immunopositive (ChAT+) neurons were found to delineate the laterodorsal tegmental (LDT) and pedunculopontine (PPT) nuclei (Fig. 6.2A, 6.2E). The ChAT+ neurons forming the LDT were found as a distinct high density cluster within the ventrolateral periventricular gray matter, while the ChAT+ neurons forming the PPT nucleus were located ventrolaterally adjacent to the LDT, but lying within the dorsal pontine tegmentum. The density of ChAT+ neurons within the PPT was substantially lower than the LDT, but it appears that as the PPT covers a much greater expanse than the LDT, the

numbers of PPT neurons should be substantially higher than the number of LDT neurons. In all species the appearance of the LDT and PPT was very similar.

6.3.2. Catecholaminergic nuclei of the locus coeruleus complex

The neurons forming the locus coeruleus complex of the pons were identified using a tyrosine hydroxylase antibody. Within the locus coeruleus complex, we could identify five distinct nuclei in all species including two subdivisions of the subcoeruleus, the A7sc (subcoeruleus compact portion) and A7d (subcoeruleus diffuse portion), A6d (locus coeruleus diffuse portion, although in *M. minutoides* this is referred to as the A6c locus coeruleus compact portion, Kruger et al., 2012), the fifth arcuate nucleus (A5) and the dorsomedial division of the locus coeruleus (A4). As the A4 and A5 nuclei were composed of very few neurons they are not considered further here. Within the ventrolateral periaqueductal gray matter, adjacent to and partially mixing with the cholinergic neurons of the LDT nucleus, a cluster of moderately densely packed tyrosine hydroxylase immunopositive neurons (TH+) formed the diffuse portion of the locus coeruleus complex (A6d) (Fig. 6.3A, 6.3E) in all species studied except for *Mus minutoides*. As previously described (Kruger et al., 2012), the A6 region in *M. minutoides*, is evidenced as a highly compact cluster of TH+ neurons, and has been likened to the compact portion of the locus coeruleus of primates. This dense packing of the TH+ A6 neurons appears to be a feature specific to Murid rodents. In the pontine tegmentum adjacent to the A6 neurons but separated from them by the fifth mesencephalic tract, a tightly packed cluster of neurons formed the compact portion of the subcoeruleus (A7sc) (Fig. 6.3A). Radiating ventrally and laterally from the A7sc,

TH⁺ neurons formed the diffuse portion of the subcoeruleus (A7d) (Fig. 6.3E). In all species, apart from the A6 region in *M. minutoides*, the appearance and parcellation of the locus coeruleus was very similar.

6.3.3. Serotonergic nuclei of the dorsal raphe nuclear complex

Within the midbrain and rostral pons serotonergic immunoreactive neurons were observed in the dorsal raphe nuclear complex. In all species studied we could identify six distinct subdivisions of this nuclear complex, which included the interfascicular (DRif), ventral (DRv), dorsal (DRd), peripheral (DRp), lateral (DRl) and caudal (DRc) subdivisions. The neurons of the DRd, DRv and DRif formed a midline column within the central gray matter of the midbrain. The bipolar neurons within this cluster were tightly packed and numerous in all species (Fig. 6.4A). Lateral to the DRv, within the central gray matter anterior to the cholinergic LDT, a loosely packed cluster of multipolar serotonergic neurons formed the DRp subdivision. Some of the neurons of the DRp were also observed in the adjacent midbrain tegementum and are the only serotonergic neurons of the dorsal raphe complex found outside of the central gray matter (Fig. 6.4A).

Dorsolateral to the DRd, a loosely packed cluster of multipolar serotonergic neurons that formed an arc running parallel to the edges of the cerebral aqueduct were assigned to the DRl subdivision (Fig. 6.4A). As the DRl was followed caudally, where the neurons of the DRd disappeared at the midbrain-pontine junction where the cerebral aqueduct opened into the fourth ventricle, the DRl neurons formed a distinct arch of cells across the dorsal midline of the periventricular gray matter. At this point, the DRl has been termed the

DRc due to the absence of these neurons in some mammalian species. The multipolar serotonergic neurons of the DRc are more tightly clustered than those of the DRI and formed a distinct cluster of cells in all species examined (Fig. 6.4E).

6.3.4. Orexinergic neuronal clusters of the hypothalamus

Within the hypothalamus of all five rodent species studied, orexinergic immunoreactive neurons were observed in three distinct clusters: the main cluster (Mc), the zona incerta cluster (Zic) and the optic tract cluster (Otc). The vast majority of orexinergic neurons are found in the main cluster (Fig. 6.5A, 6.5E). These multipolar neurons are found in a moderate to high density surrounding the fornix, occupying the perifornical regions of the hypothalamus. From this main cluster, a distinct band of orexinergic neurons is seen to extend towards the dorsolateral edge of the hypothalamus near to the zona incerta (Fig. 6.5A, 6.5E). This cluster of neurons, termed the zona incerta cluster, has far fewer neurons than observed in the main cluster. Moreover, the neurons of the zona incerta cluster may sometimes be found outside of the hypothalamus intermingled with the zona incerta. The zona incerta neurons often have a mediolateral flattened appearance compared to the orexinergic neurons in the other clusters. Extending ventrally from the main cluster, a dispersed aggregation of orexinergic neurons in the ventrolateral hypothalamus, close to where the optic tract passes, have been termed the optic tract cluster (Fig. 6.5A, 6.5E). The orexinergic neurons in the optic tract cluster show a similar morphology to those observed in the main cluster.

6.3.5. Neurons and terminal networks containing calcium binding proteins

GABA is the predominant inhibitory neurotransmitter in the brain and plays a role in the transition between sleep states (e.g. Pace-Schott and Hobson, 2002). As a general rule the calcium binding proteins parvalbumin, calbindin and calretinin label different GABAergic neuronal populations throughout the brain; however, within the basal forebrain and brainstem this general rule does not always hold true as other neurons can contain these calcium binding proteins (Gritti et al., 2003). The calcium binding proteins have a marked effect on the physiology of the neurons in which they are found and will affect the action they exert on the neurons to which they project. Here we describe the relative densities of the parvalbumin (PV+), calbindin (CB+) and calretinin (CR+) immunopositive neurons and terminal networks within the sleep associated nuclei of the cholinergic, serotonergic, catecholaminergic and orexinergic systems described above, as well as the thalamic reticular nucleus (summarized in Tables 6.1, 6.2 and 6.3).

6.3.5.1. Neurons and terminal networks containing calcium binding proteins in the cholinergic nuclei of the basal forebrain and pons

Within the medial septal nucleus the density of PV+ neurons varied, with a moderate density population of neurons being observed in *M. minutoides*, while *G. capensis* exhibited a low density, and these neurons were absent in *T. splendens*. The density of PV+ terminal networks also varied, with *M. minutoides* having a moderately dense PV+ terminal network throughout the medial septal nucleus, but no PV+ terminal

networks could be found in either *G. capensis* or *T. splendens*. In all three species no CB+ neurons were observed in the medial septal nucleus, but all three species had CB+ terminal networks, but these varied from low to moderate to high in *M. minutoides*, *T. splendens* and *G. capensis*, respectively. The density of CR+ neurons in the three species studied varied from absent to low to moderate in *T. splendens*, *G. capensis* and *M. minutoides*, respectively, while the density of CR+ terminal networks also varied from absent to low to moderate in *G. capensis*, *T. splendens* and *M. minutoides*, respectively.

In the diagonal band of Broca, all three species showed low to moderate densities of PV+ neurons and terminal networks (Fig. 6.1B, 6.1F). CB+ neurons were absent in *M. minutoides*, but were present in a low density in both *T. splendens* and *G. capensis* (Fig. 6.1C, 6.1G). Similarly, the density of the CB+ terminal networks was low in *M. minutoides* and moderate in *T. splendens* and *G. capensis*. The density of CR+ neurons was low in both *M. minutoides* and *T. splendens* (Fig. 6.1D), but of a moderate density in *G. capensis* (Fig. 6.1H), while the density of CR+ terminal networks were moderate in both *M. minutoides* and *G. capensis* and low in *T. splendens*.

Within the olfactory tubercle and embedded islands of Calleja no PV+ neurons were observed in either *M. minutoides* or *G. capensis* (Fig. 6.1F), but the occasional PV+ neuron was observed in *T. splendens*. In both *T. splendens* and *G. capensis* no PV+ terminal networks were observed, but in *M. minutoides* a high density PV+ terminal network was present. A high density of CB+ neurons were observed in both *T. splendens* and *G. capensis* (Fig. 6.1G), but no CB+ neurons were present in *M. minutoides*. The density of CB+ terminal networks varied across species from absent to moderate to high in *M. minutoides*, *G. capensis* and *T. splendens*, respectively. CR+ neurons were absent

in *M. minutoides* and present in a low density in *T. splendens* and *G. capensis* (Fig. 6.1H), while the density of CR+ terminal networks varied from low to moderate to high in *T. splendens*, *G. capensis* and *M. minutoides*, respectively.

Within the region of cholinergic neurons defining the nucleus basalis the density of PV+ neurons were low in *M. minutoides*, but moderate in *T. splendens* and *G. capensis*. In contrast, *M. minutoides* showed a moderate density PV+ terminal network, while no PV+ terminal network was observed in *T. splendens* and a low terminal network density was observed in *G. capensis*. CB+ neurons were absent in *M. minutoides*, but of a moderate density in *T. splendens* and *G. capensis*, while the CB+ terminal network densities were low in *M. minutoides* and moderate in *T. splendens* and *G. capensis*. A moderate density of CR+ neurons were observed in *T. splendens* and *G. capensis*, but no CR+ neurons were present in *M. minutoides*. In all three species a moderately dense CR+ terminal network was present.

For all five species, a low density or absence of PV+ neurons and PV+ terminal networks was observed in both the LDT and the PPT (Fig. 6.2B, 6.2F). CB+ neurons ranged in density from low to high in both the LDT and PPT across species (Fig. 6.2C, 6.2G), with *T. splendens* showing the highest density of CB+ neurons. Only low to moderate densities of CB+ terminal networks were observed in all species in these nuclei. The densities of CR+ neurons varied across species (Fig. 6.2D, 6.2H), being absent in the PPT of *M. minutoides* and *D. agouti*, through to high density in the LDT of *T. swinderianus*, *T. splendens* and *G. capensis*. The densities of CR+ terminal networks also varied widely, being absent in the PPT of *D. agouti* and showing a high density in the LDT of *T. splendens*.

6.3.5.2. Neurons and terminal networks containing calcium binding proteins in the locus coeruleus complex

Within the compact portion of the subcoeruleus (A7sc) PV+ neurons were absent in *T. swinderianus*, *D. agouti* and *G. capensis* (Fig. 6.3B, 6.3F), and in moderate density in *M. minutoides* and *T. splendens*. PV+ terminal networks were absent in all species apart from *T. splendens* where a low density PV+ terminal network was observed. The density of CB+ neurons was low to moderate in all species, with a moderate to high density CB+ terminal network observed in all species (Fig. 6.3C, 6.3G). CR+ neurons were observed in a low to moderate density in the A7sc (Fig. 6.3D, 6.3H), while the CR+ terminal networks were of a moderate density in all species apart from *T. splendens*, where the CR+ terminal network density was high.

Within the diffuse portion of the subcoeruleus (A7d) a low density of PV+ neurons was observed, but no PV+ neurons were present in the A7d of *D. agouti*, *T. splendens* or *G. capensis* (Fig. 6.3B, 6.3F). No PV+ terminal networks were observed in three species, but a low and moderate density PV+ terminal network was observed in *D. agouti* and *M. minutoides*, respectively. The density of CB+ neurons ranged from absent in *T. splendens* through to moderate in *M. minutoides* (Fig. 6.3C, 6.3G), while four species showed a moderately dense CB+ terminal network except for *G. capensis*, where a low density CB+ terminal network was observed. CR+ neurons were observed in a low to moderate density in the A7d of all species (Fig. 6.3D, 6.3H), while the density of CR+ terminal networks ranged from low in *T. swinderianus* through to high in *T. splendens*.

While there is variation in the anatomy of the A6 region across rodents, with the Murid rodents having a different appearance to other rodents (Kruger et al., 2012), this does not appear to have impacted the neurons or terminal networks of the putative GABAergic neurons in a significant manner. Two species, *D. agouti* and *G. capensis* lacked any PV+ neurons or terminal networks in this nucleus (Fig. 6.3B, 6.3F), while the other three species presented with a low density of PV+ neurons and low density PV+ terminal networks in the A6 region. All species showed a moderate density of CB+ neurons and terminal networks in the A6 region (Fig. 6.3C, 6.3G), apart from *D. agouti* which evinced a high density of CB+ terminal networks in this nucleus. The density of CR+ neurons varied from low in *M. minutoides* through to high in *G. capensis* in the A6 nucleus, while the density of CR+ terminal networks was moderate in four species, but high in *G. capensis* (Fig. 6.3D, 6.3H).

6.3.5.3. Neurons and terminal networks containing calcium binding proteins in the serotonergic dorsal raphe nuclei

Within the dorsal raphe complex there appears to be two subsets of the six nuclear subdivisions based on both cell morphology and the presence of neurons and terminal networks containing the calcium binding proteins. The first of these subsets is the midline nuclei, the dorsal, ventral and interfascicular subdivisions, while the second one contains the more laterally placed nuclei including the lateral, peripheral and caudal subdivisions. Regarding the dorsal, ventral and interfascicular subdivisions, the PV+ neurons were either absent or in low density, but the densities were higher in both *D. agouti* and *T.*

splendens (Fig. 6.4B). Throughout all these three subdivisions, in all species, there were either no PV+ terminal networks, or the density was low. The density of CB+ neurons ranged from low in *D. agouti* and *T. splendens*, to high in *G. capensis* (Fig. 6.4C). In all species the density of CB+ terminal networks was either moderate or high. The density of CR+ neurons ranged from low in *M. minutoides* and *D. agouti* to high in the dorsal subdivision in *T. swinderianus* (Fig. 6.4D). The density of CR+ terminal networks was generally moderate to high in all three subdivisions in all species, although in *M. minutoides* (ventral and dorsal subdivisions) and *T. swinderianus* (interfascicular subdivision) the CR+ terminal network density was low.

In terms of the more laterally located subset of subdivisions, the lateral, peripheral and caudal subdivisions, that contain the larger multipolar serotonergic neurons, the density of PV+ neurons was generally low to moderate in these nuclei (Fig. 6.4F), apart from the caudal subdivision in *D. agouti* that presented with a high density of PV+ neurons. PV+ terminal networks were absent from most of these nuclei, with in the lateral and peripheral, and lateral and caudal, subdivisions of *M. minutoides* and *D. agouti*, respectively, a moderate density of PV+ terminal networks were observed. In all three subdivisions in all species a moderate to high density of CB+ neurons were observed (Fig. 6.4G), but no CB+ neurons could be observed in the lateral subdivision of *D. agouti*. A moderate to high density of CB+ terminal networks was observed in all three subdivisions in all species. The density of CR+ neurons varied from absent to high in the three subdivisions across species, with *M. minutoides* generally having less CR+ neurons, while *T. swinderianus* and *G. capensis* generally had higher densities of CR+ neurons (Fig. 6.4H). A similar situation was observed for the CR+ terminal networks, with *M.*

minutoides generally having low CR+ terminal network densities, while *T. swinderianus* and *G. capensis* generally had higher CR+ terminal network densities.

6.3.5.4. Neurons and terminal networks containing calcium binding proteins in the hypothalamic orexinergic nuclei

In the main orexinergic cluster, found in the perifornical region of the hypothalamus, the density of PV+ neurons and terminal networks was generally low across species (Fig. 6.5B, 6.5F), but no PV+ neurons or terminal networks were observed in *G. capensis*. In all species a moderate density of CB+ neurons was observed in the perifornical region of the hypothalamus (Fig. 6.5C, 6.5G), while the density of CB+ terminal networks ranged from low in *M. minutoides* to moderate or high in the other species. The density of CR+ neurons varied from low in *D. agouti* to high in *T. swinderianus* and *G. capensis* (Fig. 6.5D, 6.5H), but the density of CR+ terminal networks was moderate to high in all species.

The optic tract cluster, located in the ventrolateral hypothalamus, generally contained no PV+ neurons, but in both *T. swinderianus* and *G. capensis* a moderate density of PV+ neurons was observed (Fig. 6.5B, 6.5F). The density of PV+ terminal networks was also generally low, but in *T. swinderianus* a moderately dense PV+ terminal network was observed. The density of CB+ neurons ranged from low in *M. minutoides* to high in *T. swinderianus* (Fig. 6.5C, 6.5G), while the density of CB+ terminal networks was low in *M. minutoides*, but high in the remaining four species. The density of CR+ neurons ranged from low in *M. minutoides* and *D. agouti* to high in *G.*

capensis (Fig. 6.5D, 6.5H), while all species exhibited a moderate to high density CR+ terminal network.

Within the dorsolateral region of the hypothalamus, where the orexinergic neurons of the zona incerta cluster were located, there were either no, or a low density of, PV+ neurons (Fig. 6.5B, 6.5F). The density of PV+ terminal networks ranged from absent in *T. splendens* and *G. capensis* to high in *T. swinderianus*. The density of CB+ neurons ranged from low in *D. agouti* and *T. splendens* to high in *T. swinderianus* (Fig. 6.5C, 6.5G), while all species exhibited a moderate to high density of CB+ terminal networks. Similarly, the density of CR+ neurons ranged from low in *D. agouti* and *T. splendens* to high in *T. swinderianus* (Fig. 6.5D, 6.5H), while all species exhibited a moderate to high density of CR+ terminal networks.

6.3.5.5. Neurons and terminal networks containing calcium binding proteins in the thalamic reticular nucleus

The thalamic reticular nucleus was located surrounding the ventrolateral, medial and anterior aspects of the dorsal thalamus in all species studied (Fig. 6.6). PV+ neurons and terminal networks were observed in a moderate to high density across all species, this being a distinguishing feature of this nucleus in comparison to the surrounding parenchyma. CB+ neurons were absent and the CB+ terminal network density low in *M. minutoides*, *T. swinderanus* and *D. agouti*, but a low density of CB+ neurons and a moderate density CB+ terminal network was observed in both *T. splendens* and *G. capensis*, the two subterranean rodents. CR+ neurons were absent *D. agouti* and *T.*

splendens, but were found in a very low density in the thalamic reticular nucleus of the other species. A moderate density CR+ terminal network was observed throughout the thalamic reticular nucleus in all species, but in *T. swinderianus* and *D. agouti*, the two larger brained rodent species studied, the CR+ network was observed to form a distinct band along and within the upper perimeter of the thalamic reticular nucleus (Fig. 6.6L, 6.6O).

Table 6.1: Qualitative assessment of the relative density of parvalbumin immunopositive neurons and terminal networks in the various cholinergic, catecholaminergic, serotonergic and orexinergic sleep related nuclei, as well as the thalamic reticular nucleus. Cells highlighted in grey shading indicate those nuclei with relative consistency in the densities of immunopositive structures across the species, while those without shading indicate the nuclei with varying densities of immunopositive neurons and terminal networks.

Sleep Related Nuclei	Species	Parvalbumin immunopositive structures									
		Neurons					Terminal networks				
		<i>M.minutoides</i>	<i>T.swinderianus</i>	<i>D.agouti</i>	<i>T.splendens</i>	<i>G.capensis</i>	<i>M.minutoides</i>	<i>T.swinderianus</i>	<i>D.agouti</i>	<i>T.splendens</i>	<i>G.capensis</i>
Cholinergic nuclei											
Medial Septal nucleus		++	?	?	-	+	++	?	?	-	-
Diagonal Band of Broca		+	?	?	++	+	++	?	?	+	+
Is.Calleja/olfactory tub.		-	?	?	+	-	+++	?	?	-	-
Nucleus Basalis		-	?	?	++	++	++	?	?	-	+
Pedunculopontine teg.		-	+	-	-	+	+	-	-	-	+
Laterodorsal tegmental		-	+	-	-	+	+	+	-	+	-
Catecholaminergic nuclei											
A7 compact subcoeruleus		++	-	-	++	-	-	-	-	+	-
A7 diffuse subcoeruleus		+	+	-	-	-	++	-	+	-	-
A6 locus coeruleus		+	+	-	+	-	+	+	-	+	-
Dorsal Raphe serotonergic nuclei											
Interfascicular division		-	-	++	+	+	-	-	+	-	-
Ventral division		-	-	+++	+++	+	+	-	-	-	-
Dorsal division		+	-	+++	++	+	+	-	-	-	-
Lateral division		+	+	++	+	+	++	-	++	-	-
Peripheral division		+	+	++	+	+	++	-	-	-	-
Caudal division		++	+	+++	+	+	-	-	++	-	-
Orexinergic nuclei											
Main cluster		+	+	+	+	-	+	+	+	+	-
Optic tract cluster		-	++	-	-	++	+	++	-	+	+
Zona incerta cluster		+	-	-	-	+	++	+++	+	-	-
Thalamic Reticular nuc.		++	++	++	+++	+++	+++	++	++	+++	++

Table 6.2: Qualitative assessment of the relative density of calbindin immunopositive neurons and terminal networks in the various cholinergic, catecholaminergic, serotonergic and orexinergic sleep related nuclei, as well as the thalamic reticular nucleus. Cells highlighted in grey shading indicate those nuclei with relative consistency in the densities of immunopositive structures across the species, while those without shading indicate the nuclei with varying densities of immunopositive neurons and terminal networks.

Sleep Related Nuclei	Species	Calbindin immunopositive structures									
		Neurons					Terminal networks				
		<i>M.minutoides</i>	<i>T.swinderianus</i>	<i>D.agouti</i>	<i>T.splendens</i>	<i>G.capensis</i>	<i>M.minutoides</i>	<i>T.swinderianus</i>	<i>D.agouti</i>	<i>T.splendens</i>	<i>G.capensis</i>
Cholinergic nuclei											
Medial Septal nucleus		-	?	?	-	-	+	?	?	++	+++
Diagonal Band of Broca		-	?	?	+	+	+	?	?	++	++
Is.Calleja/olfactory tub.		-	?	?	+++	+++	-	?	?	+++	++
Nucleus Basalis		-	?	?	++	++	+	?	?	++	++
Pedunculopontine teg.		+	++	+	++	++	+	++	+	++	++
Laterodorsal tegmental		+	++	++	+++	++	+	++	++	++	++
Catecholaminergic nuclei											
A7 compact subcoeruleus		++	+	+	++	++	++	++	++	+++	++
A7 diffuse subcoeruleus		++	+	+	-	+	++	++	++	++	+
A6 locus coeruleus		++	++	++	++	++	++	++	+++	++	++
Dorsal Raphe serotonergic nuclei											
Interfascicular division		++	++	+	+	++	++	++	++	+++	++
Ventral division		++	++	+	+	+++	++	++	++	+++	++
Dorsal division		++	++	+	+	+++	++	+++	++	+++	++
Lateral division		+	+++	-	+	+++	++	+++	++	+++	++
Peripheral division		++	++	++	++	++	++	+++	++	+++	++
Caudal division		++	++	++	+++	++	++	+++	+++	+++	++
Orexinergic nuclei											
Main cluster		++	++	++	++	++	+	++	+++	+++	+++
Optic tract cluster		+	+++	++	++	++	+	+++	+++	+++	+++
Zona incerta cluster		++	+++	+	+	++	++	+++	++	+++	+++
Thalamic Reticular nuc.		-	-	-	+	+	+	+	+	++	++

Table 6.3: Qualitative assessment of the relative density of calretinin immunopositive neurons and terminal networks in the various cholinergic, catecholaminergic, serotonergic and orexinergic sleep related nuclei, as well as the thalamic reticular nucleus. Cells highlighted in grey shading indicate those nuclei with relative consistency in the densities of immunopositive structures across the species, while those without shading indicate the nuclei with varying densities of immunopositive neurons and terminal networks.

Sleep Related Nuclei	Species	Calretinin immunopositive structures									
		Neurons					Terminal networks				
		<i>M.minutoides</i>	<i>T.swinderianus</i>	<i>D.agouti</i>	<i>T.splendens</i>	<i>G.capensis</i>	<i>M.minutoides</i>	<i>T.swinderianus</i>	<i>D.agouti</i>	<i>T.splendens</i>	<i>G.capensis</i>
Cholinergic nuclei											
Medial Septal nucleus		++	?	?	-	+	++	?	?	+	-
Diagonal Band of Broca		+	?	?	+	++	++	?	?	+	++
Is.Calleja/olfactory tub.		-	?	?	+	+	+++	?	?	+	++
Nucleus Basalis		-	?	?	++	++	++	?	?	++	++
Pedunculopontine teg.		-	++	-	++	++	+	+	-	++	++
Laterodorsal tegmental		+	+++	+	+++	+++	+	++	+	+++	++
Catecholaminergic nuclei											
A7 compact subcoeruleus		++	+	+	++	++	++	++	++	+++	++
A7 diffuse subcoeruleus		++	+	+	+	+	++	+	++	+++	++
A6 locus coeruleus		+	++	++	++	+++	++	++	++	++	+++
Dorsal Raphe serotonergic nuclei											
Interfascicular division		+	+	+	++	++	++	+	++	+++	++
Ventral division		+	++	+	++	++	+	+++	++	+++	++
Dorsal division		+	+++	+	++	++	+	+++	+++	+++	++
Lateral division		+	++	++	+	+++	++	++	++	+++	++
Peripheral division		++	+++	++	++	++	++	++	+	+++	++
Caudal division		-	+++	++	+	++	-	+++	+++	+++	++
Orexinergic nuclei											
Main cluster		++	+++	+	++	+++	++	++	++	+++	+++
Optic tract cluster		+	++	+	++	+++	++	+++	++	+++	+++
Zona incerta cluster		++	+++	+	+	++	++	+++	++	+++	+++
Thalamic Reticular n.		+	+	-	-	+	++	++	++	++	++

Figure 6.1: Photomicrographs of representative cholinergic nuclei within the basal forebrain of *Tachyoryctes splendens* (**A – D**) and *Georhychus capensis* (**E – F**). These photomicrographs show adjacent sections stained for choline acetyltransferase (**A, E**), parvalbumin (**B, F**), calbindin (**C, G**) and calretinin (**D, H**). Note the higher density of choline acetyltransferase immunopositive neurons in the diagonal band of Broca (**Diag.B**) compared to the surrounding nuclei. In general, the densities of parvalbumin neurons and terminal networks is low in these nuclei, while those of calbindin and calretinin are moderate. Scale bar in **D** = 500 μm and applies to **A – D**. Scale bar in **H** = 1000 μm and applies to **E – H**. **ac** – anterior commissure, **C** – caudate nucleus, **N.Acc** – nucleus accumbens, **TOL** – olfactory tubercle.

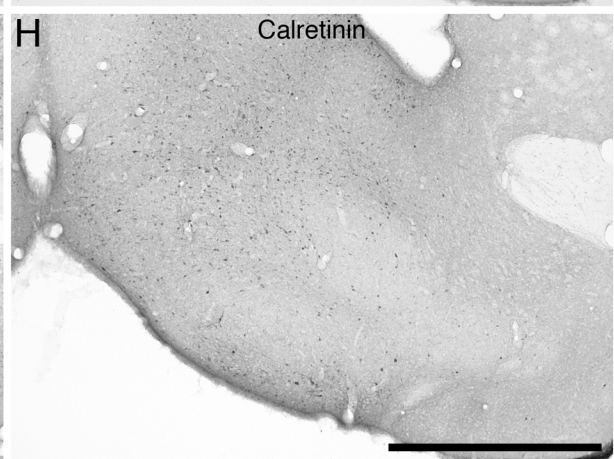
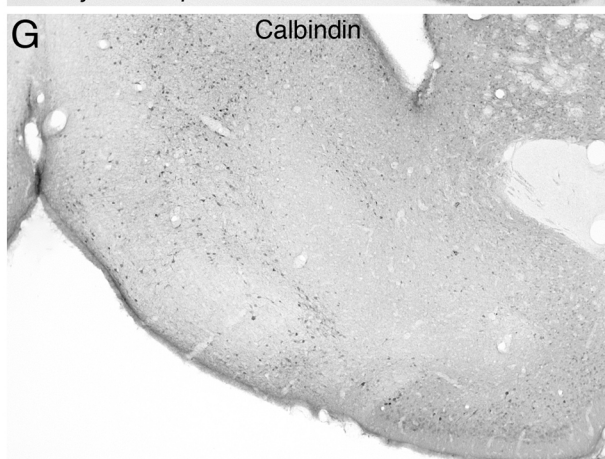
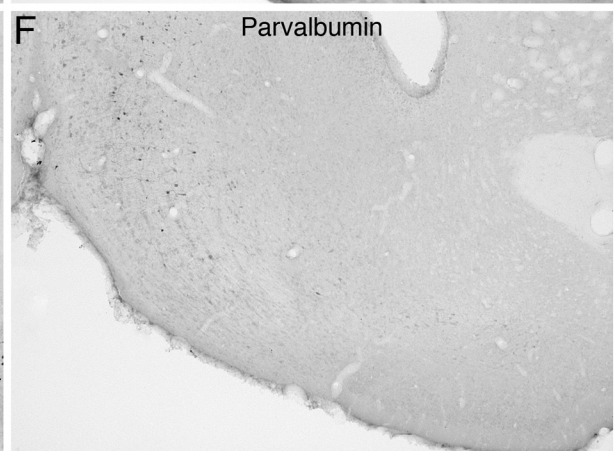
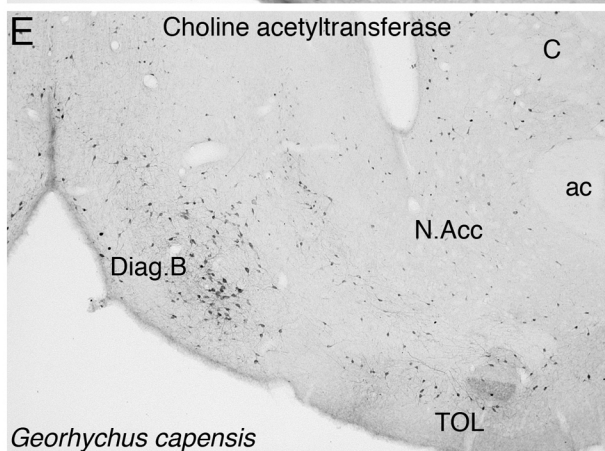
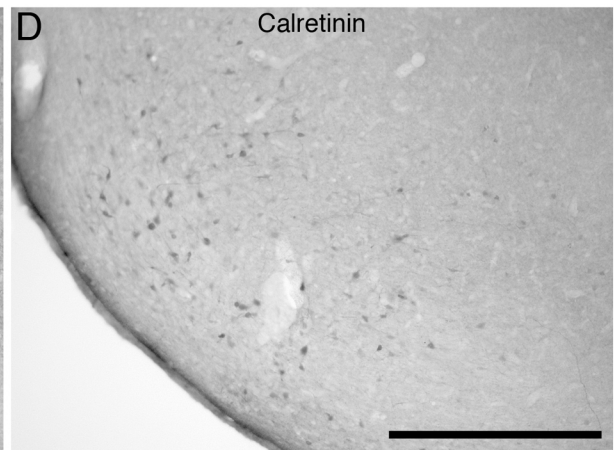
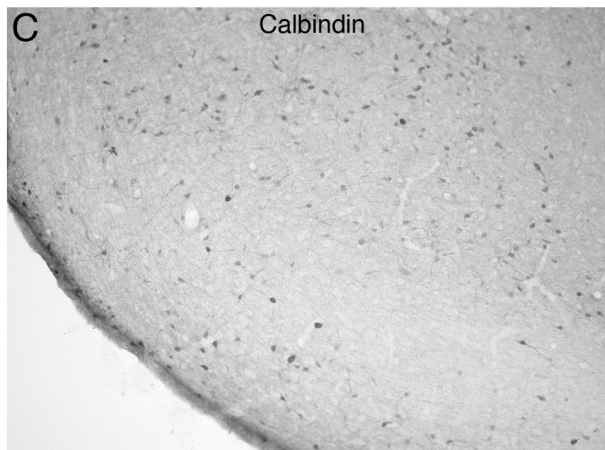
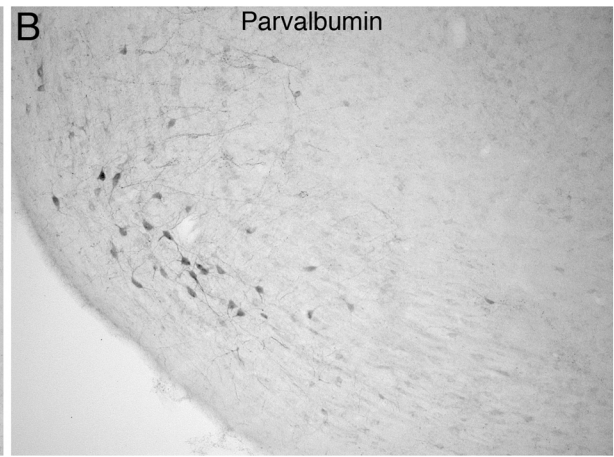
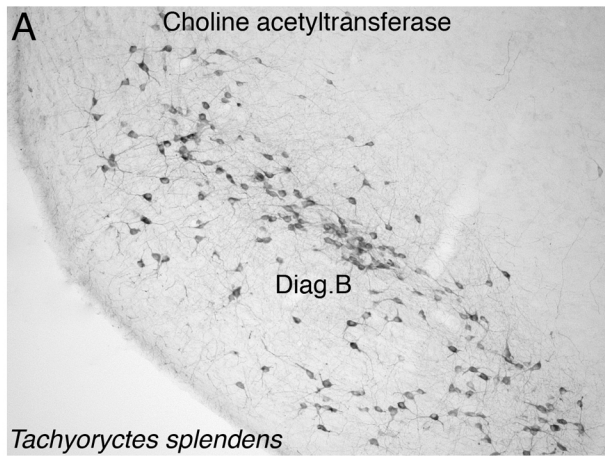
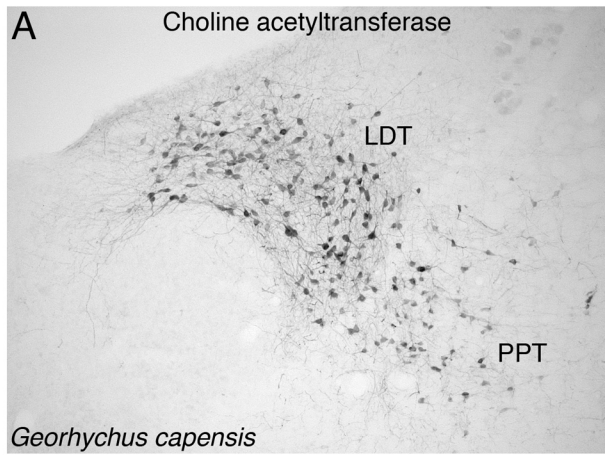
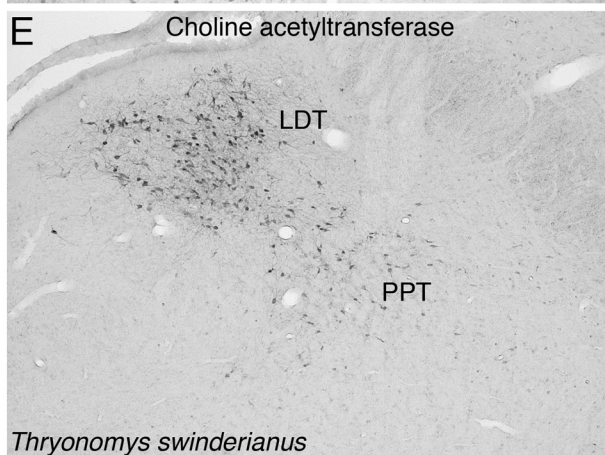
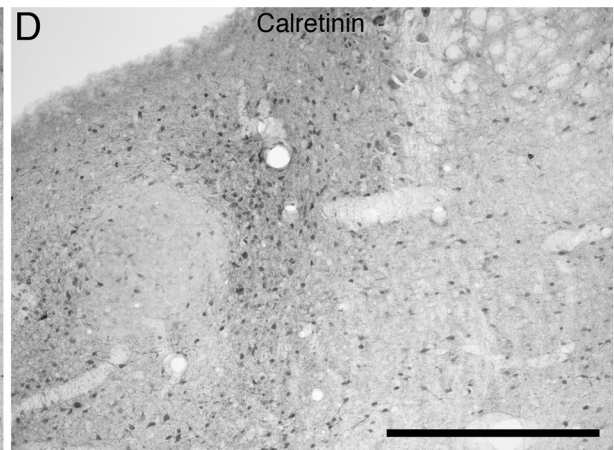
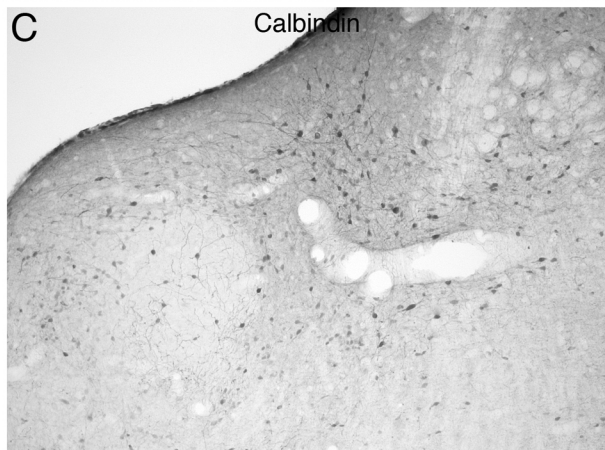
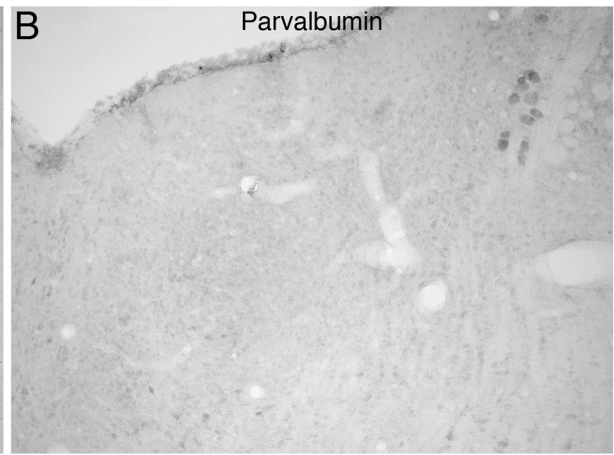


Figure 6.2: Photomicrographs of representative cholinergic nuclei within the pons of *Georhynchus capensis* (**A – D**) and *Thryonomys swinderianus* (**E – F**). These photomicrographs show adjacent sections stained for choline acetyltransferase (**A, E**), parvalbumin (**B, F**), calbindin (**C, G**) and calretinin (**D, H**). Note the distinct laterodorsal tegmental (**LDT**) and pedunculo pontine tegmental (**PPT**) cholinergic nuclei within and adjacent to the periventricular gray matter (**A, E**). In general, the densities of parvalbumin neurons and terminal networks is low in these nuclei, while those of calbindin and calretinin are moderate to high in density. Scale bar in **D** = 500 μm and applies to **A – D**. Scale bar in **H** = 1000 μm and applies to **E – H**.



Georhynchus capensis



Thryonomys swinderianus

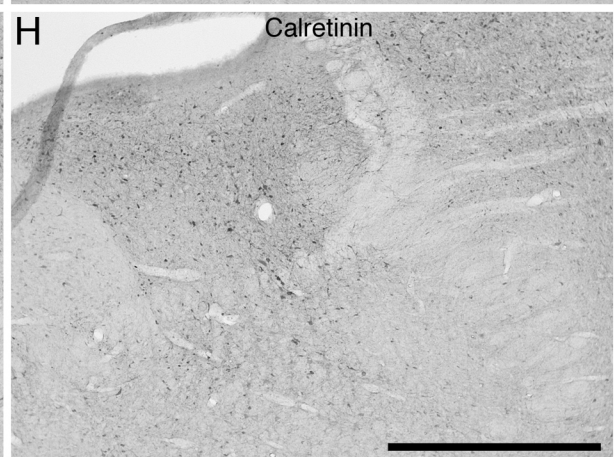
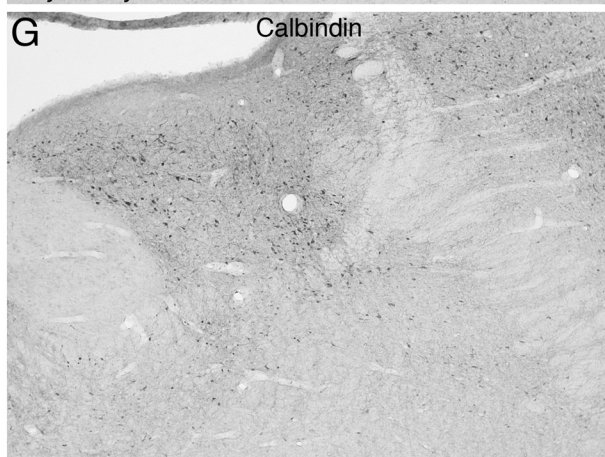


Figure 6.3: Photomicrographs of the locus coeruleus complex within the pons of *Georhynchus capensis* (**A – D**) and *Dasyprocta agouti* (**E – F**). These photomicrographs show adjacent sections stained for tyrosine hydroxylase (**A, E**), parvalbumin (**B, F**), calbindin (**C, G**) and calretinin (**D, H**). Note the distinct, but diffusely packed, locus coeruleus (**A6d**) within the periventricular gray matter, and the compact (**A7sc**) and diffuse (**A7d**) portions of the subcoeruleus in the adjacent pontine tegmentum. In general, the densities of parvalbumin neurons and terminal networks is low to absent in these nuclei, while those of calbindin and calretinin are moderate to high in density. Scale bar in **D** = 500 μm and applies to **A – D**. Scale bar in **H** = 1000 μm and applies to **E – H**.

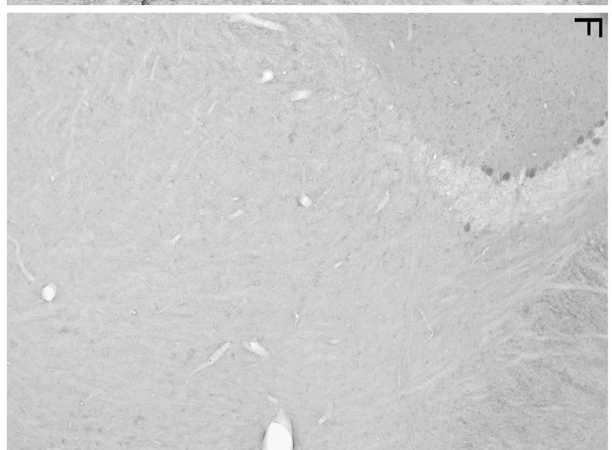
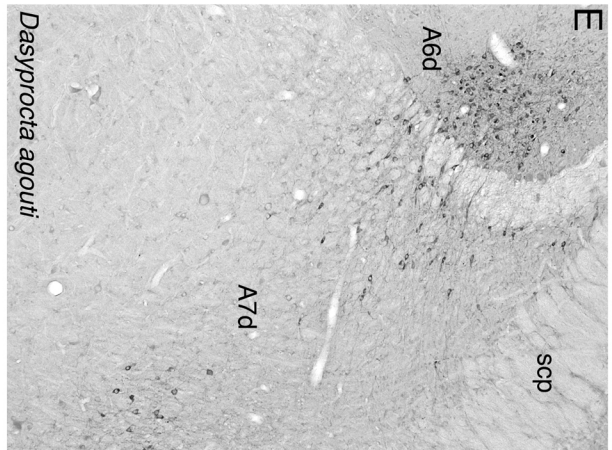
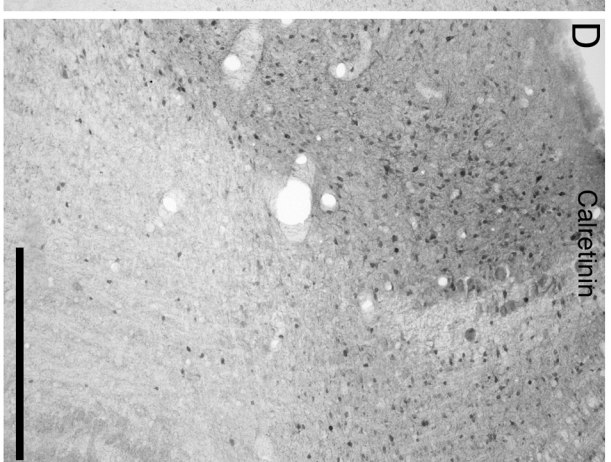
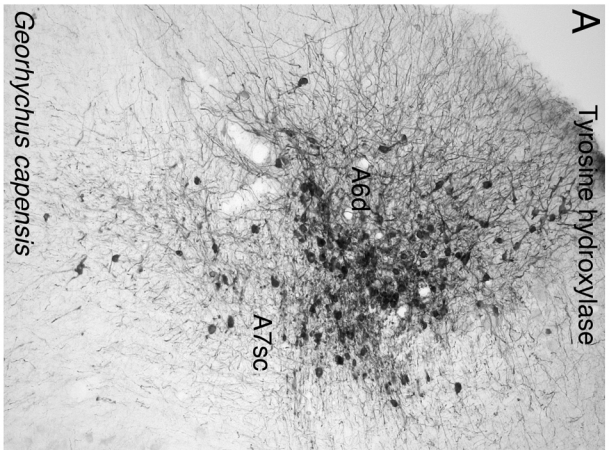


Figure 6.4: Photomicrographs of the dorsal raphe nuclear complex within the midbrain and pons of *Tachyoryctes splendens* (**A – D**) and *Thryonomys swinderianus* (**E – F**). These photomicrographs show adjacent sections stained for serotonin (**A, E**), parvalbumin (**B, F**), calbindin (**C, G**) and calretinin (**D, H**). Note the distinct clustering of the serotonergic immunopositive neurons into six specific divisions of the dorsal raphe complex including the lateral (**DRl**), peripheral (**DRp**), dorsal (**DRd**), ventral (**DRv**), interfascicular (**DRif**) and caudal (**DRc**) divisions. In general, the densities of parvalbumin neurons and terminal networks is low to absent in these nuclei, while those of calbindin and calretinin are moderate in density. Scale bar in **H** = 1000 μm and applies to all.

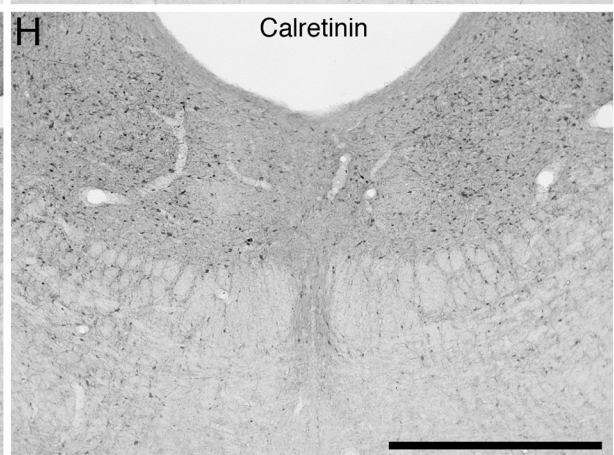
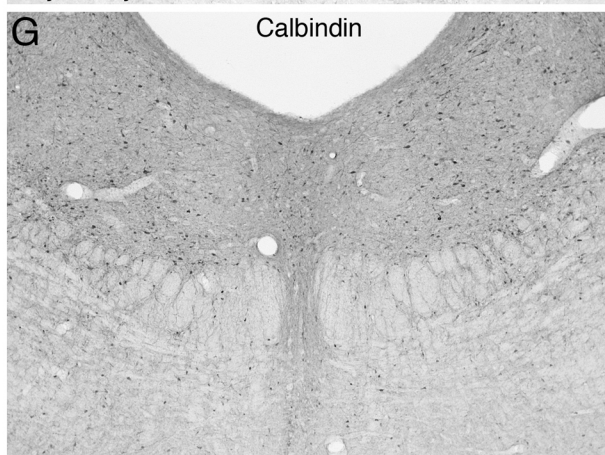
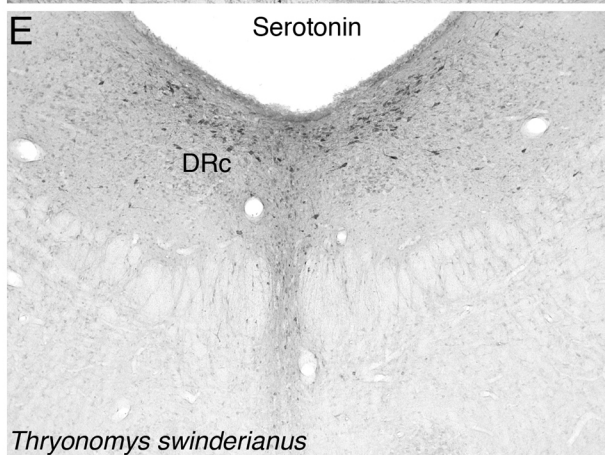
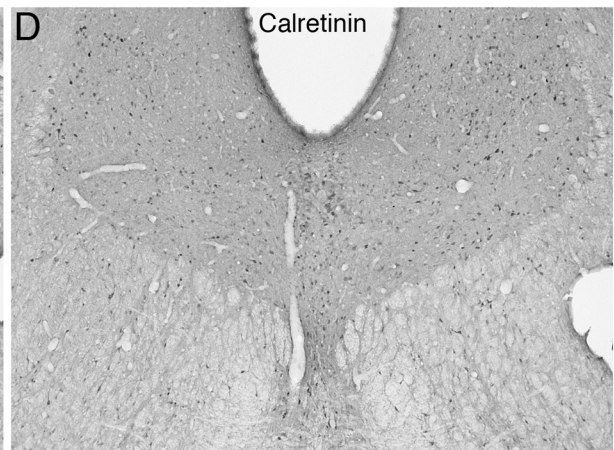
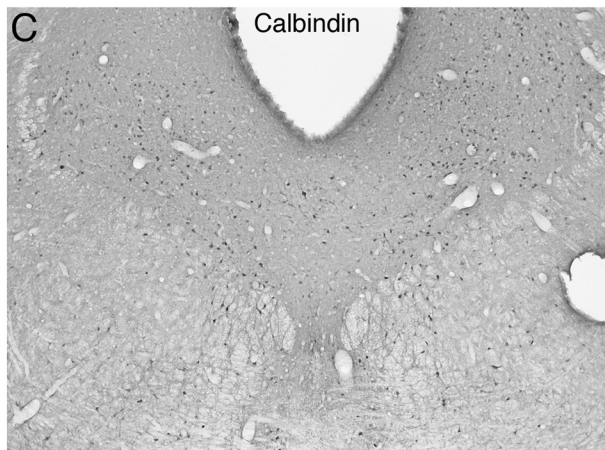
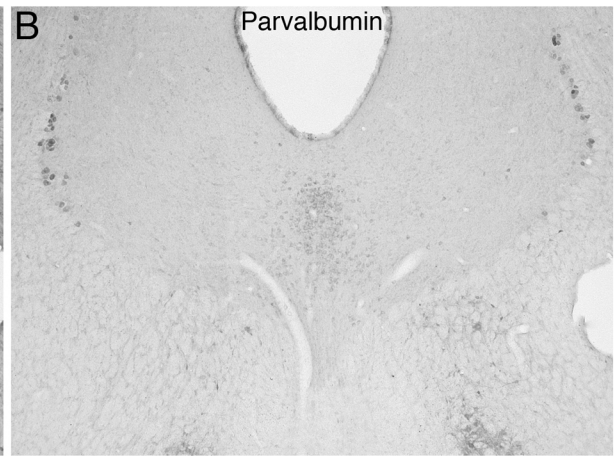
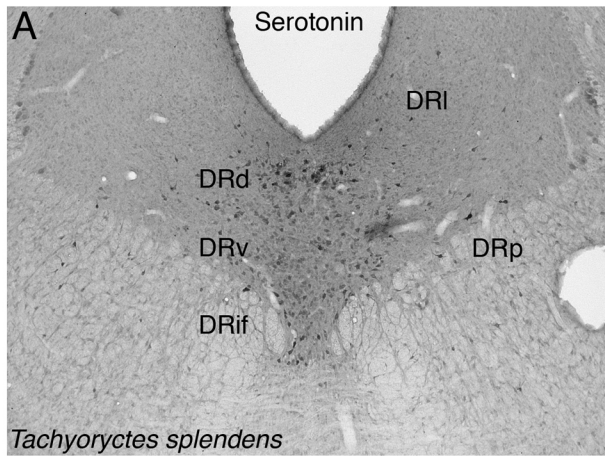


Figure 6.5: Photomicrographs of orexinergic immunopositive neurons within the hypothalamus of *Tachyoryctes splendens* (**A – D**) and *Dasyprocta agouti* (**E – F**). These photomicrographs show adjacent sections stained for orexin-A (**A, E**), parvalbumin (**B, F**), calbindin (**C, G**) and calretinin (**D, H**). Note the distinct aggregation of the orexinergic immunopositive neurons into three specific clusters including the main (**Mc**), zona incerta (**Zic**) and optic tract (**Otc**) clusters in the different regions of the hypothalamus. In general, the densities of parvalbumin neurons and terminal networks is low to absent in the hypothalamus, while those of calbindin and calretinin are moderate to high in density. Scale bar in **H** = 1000 μm and applies to all.

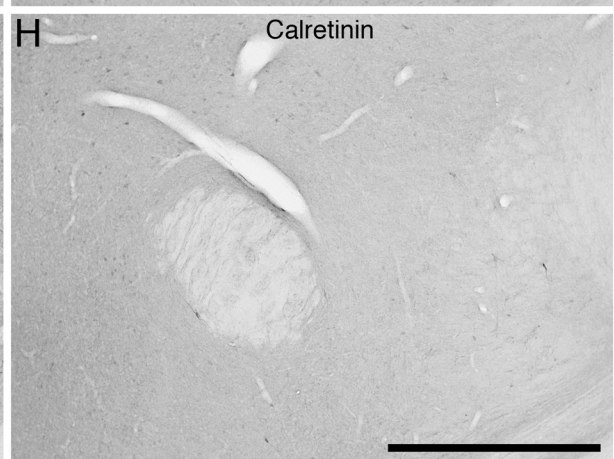
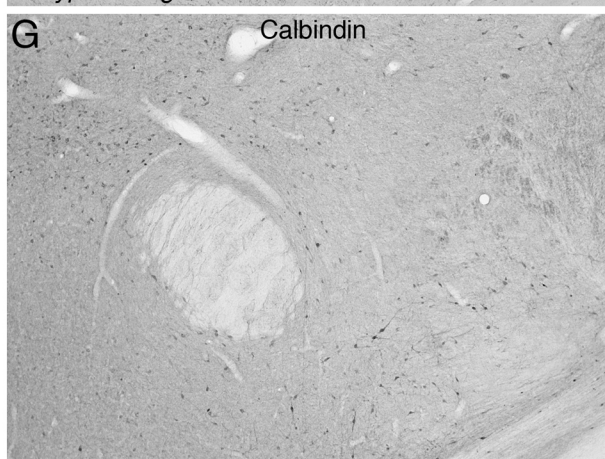
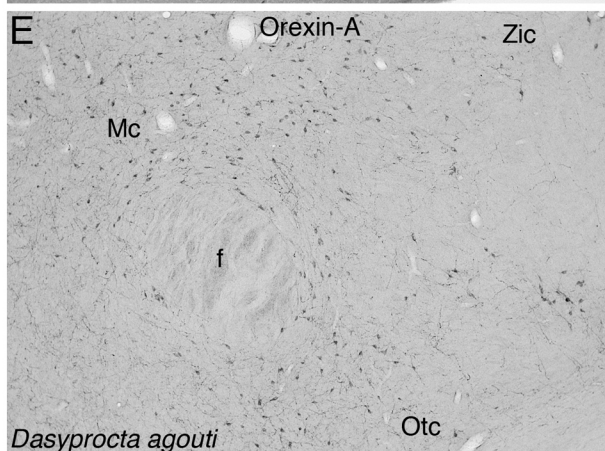
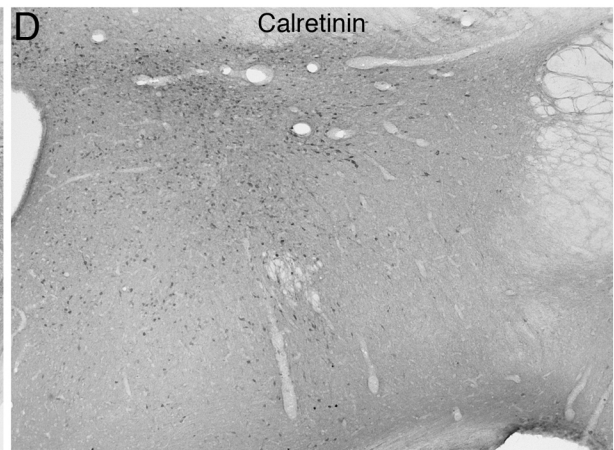
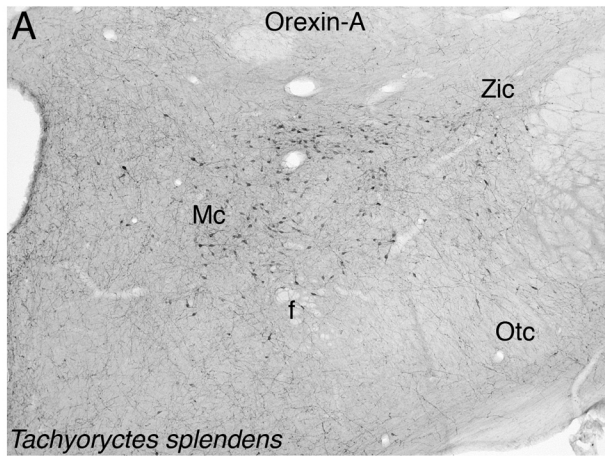
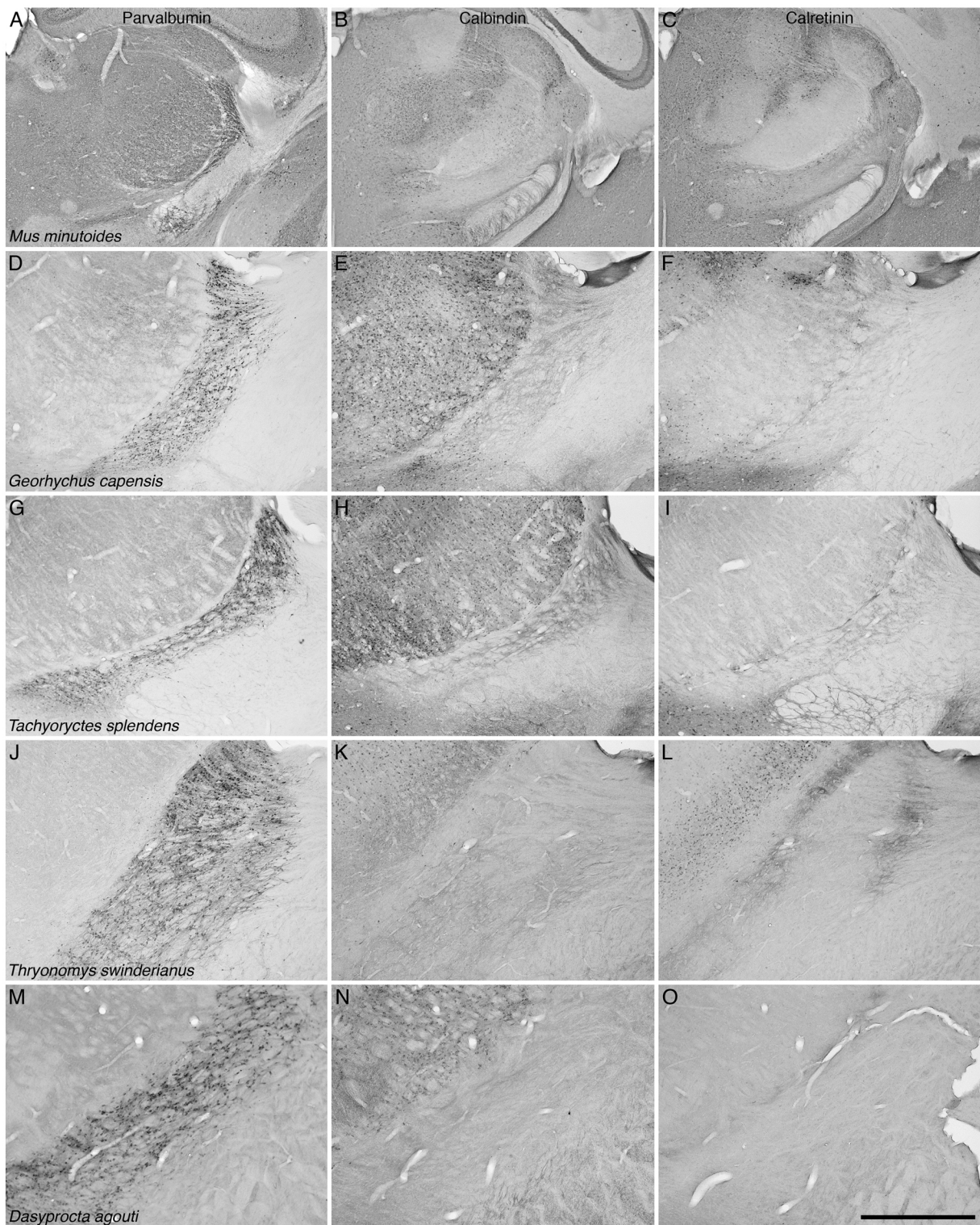


Figure 6.6: Photomicrographs of the thalamic reticular nucleus in *Mus minutoides* (**A – C**), *Georhynchus capensis* (**D – F**), *Tachyoryctes splendens* (**G – I**), *Thryonomys swinderianus* (**J – L**) and *Dasyprocta agouti* (**M – O**) following immunostaining for parvalbumin (**A, D, G, J, M**), calbindin (**B, E, H, K, N**) and calretinin (**C, F, I, L, O**). Note that in all species the neurons of the thalamic reticular nucleus are strongly immunopositive for parvalbumin. A low density of calbindin and calretinin immunopositive neurons and terminal networks are observed in all species. In both *T. swinderianus* and *D. agouti*, the larger brained species, a distinct band of calretinin terminal network staining can be seen within the dorsal aspect of the thalamic reticular nucleus (**L, O**) which is not clear in the smaller brained species. Scale bar in **O** = 1000 μm and applies to all.



6.4. Discussion

The present study undertook a comparison of the sleep related neural systems in the brains of five species of phenotypically and phylogenetically varied rodents to determine what similarities or differences occurred in these systems between the species and how these similarities or differences related to the sleep patterns seen in these rodents. Within all five species studied the cholinergic, catecholaminergic, serotonergic and orexinergic immunopositive neurons and nuclei were similar, with the exception of the noradrenergic locus coeruleus complex of *Mus minutoides*, which had a different appearance to the other species investigated. In terms of the neurons and terminal networks of the calcium-binding proteins parvalbumin, calbindin and calretinin, there was far more variation between the different species, although there was some consistency within certain sleep related nuclei. Differences were also noted between the species studied and the laboratory rat and the Zambian mole rat (Celio, 1990; Resibois and Rogers, 1992; Bhagwandin et al., 2013). All species had a positive expression of parvalbumin (neurons and terminal networks) in the thalamic reticular nucleus, although there was variation in the density of neurons and terminal networks immunopositive for calretinin and calbindin.

6.4.1. Similarities in the cholinergic, catecholaminergic, serotonergic and orexinergic sleep-related nuclei across the five rodent species

As previously stated, the complement and organization of the sleep-related nuclei of the cholinergic, catecholaminergic, serotonergic and orexinergic systems were similar

across all five rodent species, as well as across rodents in general, and as such indicates that there is an evolutionary constraint preventing changes in the organization of these systems despite phenotypic, phylogenetic and natural history differences (Manger, 2005). This can also be seen in the general sleep architecture of rodents, where Wake, non-REM and REM sleep are readily identified and found to be common to all rodents studied to date and no rodent species has exhibited any novel sleep states (van Twyver, 1969; Lesku et al., 2006; Bhagwandin et al., 2011a; see also the two preceding chapters of this thesis). Interestingly, across most Eutherian mammals studied to date, the cholinergic nuclei of the basal forebrain and pons, the locus coeruleus complex, the dorsal raphe complex and the orexinergic neurons in the hypothalamus are organized in a very similar way (e.g. Dell et al., 2010, 2013; Calvey et al., 2013). These sleep-associated nuclei, which are responsible for the generation and regulation of both wake and sleep states appear to be producing strong similarities in the neurophysiological expression of wake and sleep across mammals (Tobler, 1995). Indeed, where variations in the anatomical expression of these systems occur, for example in the cholinergic pontine nuclei of the rock hyrax (Gravett et al., 2009), differences in the neurophysiological expression of sleep states have been noted (Gravett et al., 2012).

What is specifically interesting in regards to these systems is the fact that while most mammals, with some exceptions as noted above, are producing the same two sleep states only (non-REM and REM), the amount of time spent in these states, both within the rodents and across mammals, can vary significantly. In the two preceding chapters of this thesis, this variation within rodents is demonstrated dramatically, with the East African root rat being the shortest sleeper of all mammals studied to date. Despite this

significant variation in total sleep time, the organization of the nuclei associated with sleep in the East African root rat does not differ in any dramatic way from the other rodents, or indeed many other mammals. Thus, we can conclude that the consistency in organization of the cholinergic nuclei of the basal forebrain and pons, the locus coeruleus complex, the dorsal raphe and the hypothalamic orexinergic neurons creates a consistency in the production of Wake, non-REM and REM states. Interestingly though, these nuclei do not appear to be involved in the regulation of the time spent in these states, and are presumably controlled by other factors that mediate the duration a particular animal spends asleep, or in a particular sleep state.

6.4.2. Similarities and variances in the locations of neurons and terminal networks containing the calcium binding proteins associated with inhibitory neurons

GABAergic neurons are known to play a central role in the promotion and regulation of the sleep-wake cycle by affecting the discharge rate of the cholinergic, noradrenergic, serotonergic and orexinergic neuronal populations (Siegel, 2004). For example, some GABAergic neurons are maximally active during non-REM but minimally active during REM and Wake (Szymusiak, 1995; Szymusiak et al., 2001), whereas others are more active during REM and Wake (Hassani et al., 2009). Moreover, the presence of the different calcium binding proteins in these GABAergic neurons will alter the way they depolarize and therefore the effect they exert over their target neurons. Parvalbumin acts as a slow buffer of calcium dynamics, calbindin is a faster buffer of calcium dynamics, while calretinin is a calcium modulator, showing dual kinetic

properties rather than acting only as a buffer (Billing-Marczal and Kuznicki, 1999; Schmidt et al., 2003; Barinka and Druga, 2010). Thus, the presence of these calcium binding proteins may alter the function of the GABAergic neurons – parvalbumin containing neurons are associated with fast spiking displaying tonic discharges with no accommodation, calbindin containing neurons are associated with regular spiking characterized by a marked accommodation, and calretinin containing neurons are associated with bursts of spiking at irregular frequencies (Cauli et al., 1997). Therefore the variation in the presence of these calcium binding proteins in the GABAergic neurons exerting an influence over the cholinergic, noradrenergic, serotonergic and orexinergic neurons, may alter the production and maintenance of sleep and wake states by these neurons.

Interestingly, across the five rodent species studied, there was a general global similarity in the presence/absence of neurons and terminal networks containing the calcium binding proteins in the regions of the sleep-associated cholinergic, noradrenergic, serotonergic and orexinergic nuclei (summarized in Tables 6.1, 6.2 and 6.3). The differences observed were not major and in the individual species were limited to one or two nuclei, rather than as broad changes between species (summarized in Tables 6.1, 6.2 and 6.3). Moreover, these variations did not indicate any specific phylogenetic signature. Thus, as with the organization of the sleep-associated cholinergic, noradrenergic, serotonergic and orexinergic nuclei, the GABAergic input to these nuclei, even when analyzed at the level of the calcium binding proteins dividing these neurons into three types, appear to maintain a substantial consistency across species. This then provides a potential anatomical basis for the global similarity in the production of sleep states (non-

REM and REM) across mammalian species (Tobler, 1995). Thus, due to the findings of the short sleep times in the East African root rat, the GABAergic neurons, as with the sleep-associated cholinergic, noradrenergic, serotonergic and orexinergic nuclei, do not appear to play a substantial role in the amount of time spent in a particular state, and appear to be more involved in the production and maintenance of a state than global amounts of time spent in a state.

6.4.3. So what controls the variation in sleep times across mammals?

The current study has shown that across rodent species, the sleep-associated cholinergic, noradrenergic, serotonergic and orexinergic nuclei, plus the GABAergic projections (including the subdivisions into the three types containing the different calcium binding proteins) are very similar. This similarity is in line with the similarity in the physiology of sleep and wake states in the rodents – all rodents studied to date show Wake, non-REM and REM with very similar physiological signatures (Tobler, 1995). Indeed, even in the very short sleeping East African root rat, the percentage of total sleep time occupied by REM is similar to other rodents (see preceding chapter). The only thing that appears to vary significantly across rodents is the total amount of time spent in sleep (both non-REM and REM) (see Lesku et al., 2006). The present study rules out the sleep associated cholinergic, noradrenergic, serotonergic and orexinergic nuclei, as well as the GABAergic projections to these nuclei, as the regulators of total sleep time in a particular species. While previous analyses have shown that larger mammals generally require less sleep than smaller mammals (Zepelin and Rechtschaffen, 1974; Lesku et al., 2006), these

correlations are not truly predictive (Siegel, 2013). Genetic studies have begun to identify specific mutations associated with short sleep in humans that similarly affect transgenic mice that carry the same mutation (He et al., 2009), but the mechanism of how the proteins built by these genes regulate total sleep time are not yet known. Additionally, repeat alleles of clock genes associated with the circadian rhythm have also been shown to affect total sleep time (Dijk and Archer, 2010), but again, the mechanism of how these different alleles affect total sleep time is unknown. Despite this, the mutations and repeat alleles in the genes associated with sleep and circadian rhythms provide a promising avenue towards understanding how total sleep time is regulated across species. Genetic studies of the East African root rat, seemingly the shortest sleeping mammal (see preceding chapter), may help to highlight the genes involved in the regulation of total sleep time. Understanding the control of total sleep time will be an important step towards understanding the function of sleep and why this physiological state, that leaves an animal unable to obtain nutrition, reproduce and increases their vulnerability to predation, has evolved.

CHAPTER SEVEN: General Discussion

7.1. Hypothesis 1 - The pygmy mouse, cane rat, agouti, root rat and mole rat will share the same complement of nuclear subdivisions within the hypnogenic system regardless of differences in brain size, phenotype or lifestyle.

Upon investigation of the cholinergic, catecholaminergic, serotonergic and orexinergic systems in all five species we found that there was no discernible difference in the complement and number of nuclei in these systems despite very large differences in brain size, phenotype and natural history. The only real difference seen was in the pygmy mouse, where cortical cholinergic neurons were present and the A6 locus coeruleus had a different appearance to that seen in non-Murid rodents. While it is unclear why these differences are only seen in the Murid rodents, it would seem that these differences are evolutionarily neutral. These sleep-associated nuclei, which are responsible for the generation and regulation of both wake and sleep states appear to be producing strong similarities in the neurophysiological expression of wake and sleep across mammals (Tobler, 1995). Our findings support Manger's proposal (2005) that changes in organisational complexity of these nuclei does not occur at the systems level within orders, but rather between orders.

Furthermore we investigated the calcium-binding proteins parvalbumin, calbindin and calretinin as a means to investigate the GABAergic system associated with the above mentioned sleep-related nuclei. Whilst there was far more variation in the density of neurons and terminal networks containing the calcium-binding proteins between the various species studied, there was still a global consistency. This then provides an anatomical basis for the global similarity in the production of sleep states (non-REM and

REM) across mammalian species (Tobler, 1995). Thus it does not appear that the GABAergic neurons play a substantial role in the amount of time spent in a particular state, and appear to be more involved in the production and maintenance of a state than global amounts of time spent in a state.

7.2. Hypothesis 2 - The sleep physiology should remain constant despite interspecies differences.

We investigated sleep physiology in two of the five species – the Cape mole rat and the East African root rat. Our findings were very different between the two species and as such each will be dealt with separately. The Cape mole rat showed both non-REM and REM sleep, which concurs with findings for other mole rat species studied, as well all rodents studied to date (Lesku et al., 2006), which indicates that sleep has a very similar physiological signature across rodents and in fact across mammals (Tobler, 1995). In the present study, we found that the Cape mole rat compared most favourably with the giant Zambian mole rat previously studied (Bhagwandin et al., 2011). These two species however varied somewhat from the blind mole rat which had a greater TST, as well as an increased duration of the non-REM sleep episode (Tobler and Deboer, 2001) compared to the two Bathyergid mole rats. Despite these differences, there were similarities seen in the percentage of TST occupied by REM across all three species, and indeed across rodents (Lesku et al., 2006), indicating that there is some baseline function for REM in the rodents that requires a certain amount of the TST to be REM, and that it is conserved across the rodent species. The differences in episode duration of non-REM and REM of the Cape mole rat and Zambian mole rat when compared to other rodents may be

attributable to their regressed visual system and their subterranean lifestyle, but it seems far more likely that there exists a complex interplay between phylogenetic history (genetics), environmental pressures (past and present) and natural history that will better explain the observed differences.

On average over a 24 hour period, the East African root rat spent only 2.2 h awake, this being the least amount of sleep recorded in any rodent, or indeed any mammal, studied with electrophysiological methods to date (reviewed in Lesku et al., 2006). This is a highly surprising finding, but it is imperative that further studies be conducted on this species as it is possible that this result is due to a methodological confound in the experimental setup. Nevertheless, if the East African root rat truly is the shortest sleeper of all mammals this rodent may serve as an accessible model animal to determine what factors - genetic, hormonal, environmental, local sleep processes, or other, determine total sleep time. It would appear to make sense that either biological or environmental factors control total sleep time and that the revelation of the processes that control total sleep time are likely to lead to the understanding of the precise function of sleep – an understanding that currently eludes scientists. Furthermore in the field these animals have been found to be diurnal but under laboratory conditions they show a nocturnal circadian rhythm. In our study there was no clear delineation between time awake or asleep between the dark and light phase and so the answer of the circadian rhythm in the East African root rat remains inconclusive (Jarvis, 1973; Katandukila et al., 2013).

7.3. Hypothesis 3 - The EEG and EMG recordings should show rodent specific features which correlate to brain and body size and which remain consistent between species of the same order.

Our studies of sleep in the Cape mole rat and East African root rat concur with all studies to date on the polygraphic aspects of sleep in rodents. All rodents show very clear stages of Wake, non-REM and REM sleep. Wake was characterised by a high-frequency, low-voltage EEG and a high-voltage EMG; non-REM sleep was characterised by a low-frequency, high-voltage EEG, and a low-voltage EMG; and REM sleep was characterised by an EEG that resembled wake but with an EMG that was low-voltage as seen in non-REM sleep or slightly lower. The only notable difference in the polygraphic data in the current studies was seen in the EMG recordings during REM sleep where the muscle tone did not decrease when compared to that of non-REM sleep.

7.4. Can the neuroanatomy lead to any predictability of sleep parameters within the rodent order?

It would appear that the neuroanatomy of the sleep-related nuclei of the cholinergic, catecholaminergic, serotonergic and orexinergic systems, in concert with the GABAergic system lead to the predictable sleep stages and architecture as seen across all rodent species; however, these systems do not shed any light on the changes in the sleep patterns that are seen between various rodent species such as changes in TST, non-REM episode duration. While certain changes in these systems may produce unusual sleep states, such as seen in the rock hyrax (Gravett et al., 2009, 2012), the lack of variation seen within a mammalian order, such as the rodents, suggests that the sleep patterns of

animals within an order should be very similar for all species of that order. This includes the states of sleep produced, such as non-REM, REM or something novel, and the percentage of TST occupied by REM sleep. Thus, the neuroanatomy studied to date has some predictive aspects to it, but the conservative nature of the neuroanatomy falls in line with the conservative nature of sleep physiology across species.

7.5. Future studies

The studies presented in this thesis have shown that a decrease in brain size does not lead to a decrease in organisational complexity, the pygmy mouse being the example used; however, to date no studies have been conducted at the other end of the scale within rodents. For example, does a rodent with a relative increase in brain size have any changes in organisational complexity in the brain? Combining studies of the neuroanatomy and sleep in species such as the scaly-tailed squirrels and the springhares would help to answer this question.

The Cape mole rat showed many similarities in its sleep structure to that of the giant Zambian mole rat, but both these species are highly aggressive solitary species. Given this it would be of great interest to conduct further studies on social and eusocial mole rat species to determine if the differences noted between the mole rat species already studied and other rodents are in fact Genus specific changes within the Bathyergids. As there are many Bathyergid species showing a range of body sizes and social environments, even with species splitting chores in the eusocial species, this Genus could provide interesting answers to specifically targeted questions regarding sleep physiology and function.

Lastly, and most interestingly, it was found that the East African root rat is potentially the shortest sleeper of all mammals studied to date. While there is the possibility of a methodological confound, it is important that further sleep recordings are undertaken with this species, to remove the possible confound found in the present study. If, after removal of this potential confound, the root rat still remains the shortest sleeping mammal, then a range of interesting possibilities arise. Initially it would be important to investigate sleep in the other species of the *Tachyoryctes* genus, the big-headed root rat, *T. macrocephalus*, to determine if this unusually short sleep is Genus specific or species-specific. Following on from this, it would be important to investigate if the root rat makes use of local sleep as a means to shorten the time spent in global sleep. The behavioural observations are particularly important here, as it was observed that during the dark phase the root rat was highly active, but that during the light phase it remained quite still, but alert to changes in its environment. The EEG and EMG recordings undertaken here suggested that the animal was awake during this period, in a state that could be described as quiet wake. Despite this, it is possible that the root rat, while being in quiet wake, could be undergoing local sleep in different regions of the brain. If the root rat is undergoing local sleep, this may obviate the need for longer periods of global sleep. In this sense the root rat would be an excellent model animal to study the physiology and function of local sleep, as it would have an exaggerated form of this type of sleep. If, however, the root rat was truly in quiet wake and did not show signs of local sleep, then it would become known as the shortest sleeping mammal studied to date. This again raises interesting possibilities, as determining why total sleep time is so short in this species would lead to interesting results regarding total sleep times across mammals, the

evolution of sleep and ultimately may aid in answering the elusive question of the function of sleep.

References

Albert, D.J., Jonik, R.H., Walsh, M.L., 1992. Hormone-dependent aggression in male and female rats: experiential, hormonal, and neural foundations. *Neurosci. Biobehav. Rev.* 16, 177-192.

Agnati, L.F., Franzen, O., Ferre, S., Leo, G., Franco, R., Fuxe, K., 2003. Possible role of intramembrane receptor-receptor interactions in memory and learning via formation of long-lived heteromeric complexes: focus on motor learning in the basal ganglia. *J. Neural. Transm. Suppl.* 65, 1-28.

Baimbridge, K.G., Celio, M.R., Rogers, J.H., 1992. Calcium-binding proteins in the nervous system. *Trends Neurosci.* 15, 303–308.

Baldo, B.A., Daniel, R.A., Berridge, C.W., Kelley, A.E., 2003. Overlapping distributions of orexin/hypocretin- and dopamine-beta-hydroxylase immunoreactive fibers in rat brain regions mediating arousal, motivation, and stress. *J. Comp. Neurol.* 464, 220-237.

Barinka, F., Druga, R., 2010. Calretinin expression in the mammalian neocortex: a review. *Physiol. Rev.* 59, 665-677.

Baskevich, M.I., Orlov, V.N., Bekele, A., Mebrate, A., 1993. Notes on the karyotype of *Tachyoryctes splendens* (Rüppell 1836) (Rodentia: Rhizomyidae) from Ethiopia. *Trop. Zool.* 6, 81-88.

Bayraktar, T., Staiger, J.F., Acsady, L., Cozzari, C., Freund, T.F., Zilles, K., 1997. Co-localization of vasoactive intestinal polypeptide, gamma-aminobutyric acid and choline acetyltransferase in the neocortical interneurons of the adult rat. *Brain Res.* 757, 209-217.

Begall, S., Daan, S., Burda, H., Overkamp, G.J.F., 2002. Activity patterns in a subterranean social rodent, *Spalacopus cyanus* (Octodontidae). *J. Mammol.* 83, 153-158.

Bennett, N. C., Jarvis, J. U. (1988). The social structure and reproductive biology of colonies of the mole-rat, *Cryptomys damarensis* (Rodentia, Bathyergidae). *J. Mammal.* 293-302.

Berntson, G. G., Shafi, R., Sarter, M., 2002. Specific contributions of the basal forebrain corticopetal cholinergic system to electroencephalographic activity and sleep/waking behaviour. *Eur. J. Neurosci.* 16, 2453-2461.

Bhagwandin, A., Fuxe, K., Manger, P.R., 2006. Choline acetyltransferase immunoreactive cortical interneurons do not occur in all rodents: a study of the phylogenetic occurrence of this neural characteristic. *J. Chem. Neuroanat.* 32, 208-216.

Bhagwandin, A., Fuxe, K., Bennett, N.C., Manger, P.R., 2008. Nuclear organization and morphology of cholinergic, putative catecholaminergic and serotonergic neurons in the brains of two species of African mole-rat. *J. Chem. Neuroanat.* 35, 371-387.

Bhagwandin, A., Fuxe, K., Bennett, N.C., Manger, P.R., 2011. Distribution of orexinergic neurons and their terminal networks in the brains of two species of African mole rats. *J. Chem. Neuroanat.* 41, 32-42.

Bhagwandin, A., Gravett, N., Lyamin, O.I., Oosthuizen, M., Bennett, N.C., Siegel, J.M., Manger, P.R., 2011. Sleep and wake in rhythmic vs arrhythmic chronotypes of a microphthalmic species of African mole rat (*Fukomys mechowii*). *Brain Behav. Evol.* 78, 162-183

Bhagwandin, A., Gravett, N., Bennett, N.C., Manger, P.R., 2013. Distribution of parvalbumin, calbindin and calretinin containing neurons and terminal networks in relation to sleep associated nuclei in the brain of the giant Zambian mole-rat (*Fukomys mechowii*). J. Chem. Neuroanat. 52, 69-79.

Billing-Marczak, K., Kuznicki, J., 1999. Calretinin – sensor or buffer – function still unclear. Pol. J. Pharmacol. 51, 173-178.

Björklund, A., Lindvall, O., 1984. Dopamine-containing systems in the CNS, in: Björklund, A., Hökfelt, T. (Eds.), Handbook of Chemical Neuroanatomy, vol. 2. Classical Neurotransmitters in the CNS, part 1. Elsevier, Amsterdam, pp. 55-122.

Blanga-Kanfi, S., Miranda, H., Penn, O., Pupko, T., DeBry, R.W., Huchon, D., 2009. Rodent phylogeny revised: analysis of six nuclear genes from all major rodent clades. BMC Evo. Biol. 9, 71.

Calvey, T., Patzke, N., Kaswera, C., Gilissen, E., Bennett, N.C., Manger, P.R., 2013. Nuclear organization of some immunohistochemically identifiable neural systems in three Afrotherians species – *Potomogale velox*, *Amblysomus hottentotus* and *Petrodromus tetradactylus*. J. Chem. Neuroanat. 50-51, 48-65.

Campbell, S.S., Tobler, I., 1984. Animal Sleep: A review of sleep duration across phylogeny. Neurosci. Biobehav. Rev. 8, 296-300.

Capellini, I., Barton, R.A., McNamara, P., Preston, B.T., Nunn, C.L., 2008. Phylogenetic analysis of the ecology and evolution of mammalian sleep. Evolution 62, 1764–1776.

Cauli, B., Audinat, E., Lambolez, B., Angulo, M.C., Ropert, N., Tsuzuki, K., Hestrin, S., Rossier, J., 1997. Molecular and Physiological Diversity of Cortical Nonpyramidal Cells. *J. Neurosci.* 17, 3894-3906.

Celio, M.R., 1990. Calbindin D-28k and parvalbumin in the rat nervous system. *Neuroscience* 35, 375– 475.

Chen, C.T., Dun, S.L., Kwok, E.H., Dun, N.J., Chang, J.K., 1999. Orexin A-like immunoreactivity in the rat brain. *Neurosci. Lett.* 260, 161-164.

Chepkasov, I. E., 1980. Daily rhythm of sleep and wakefulness in the arctic ground squirrel *Citellus parryi* during the summer season. *J. Evol. Biochem. Physiol.* 17, 77-80.

Clancy, J. J., Caldwell, D. F., Villeneuve, M. J., Sangiah, S., 1978. Daytime sleep-wake cycle in the rat. *Physiol. Behav.* 21, 457-459.

Cutler, D.J., Morris, R., Sheridhar, V., Wattam, T.A.K., Kolmes, S., Patel, S., Atch, J.R.S., Wilson, S., Buckingham, R.E., Evans, M.L., Leslie, R.A., Williams, G., 1999. Differential distribution of orexin-A and orexin-b immunoreactivity in the rat brain and spinal cord. *Peptides* 20, 1455-1470.

Czeisler, C.A., Weitzman, E.D., Moore-Ede, M.C., Zimmerman, J.C., Knauer, R.S., 1980. Human sleep: its duration and organization depend on its circadian phase. *Science* 210, 1264-1267.

Dahlström, A., Fuxe, K., 1964. Evidence for the existence of monoamine-containing neurons in the central nervous system. I. Demonstration of monoamine in the cell bodies of brainstem neurons. *Acta Physiol. Scand.* 62, 1-52.

- Da Silva, J.N., Fuxe, K., Manger, P.R., 2006. Nuclear parcellation of certain immunohistochemically identifiable neuronal systems in the midbrain and pons of the Highveld mole-rat (*Cryptomys hottentotus*). *J. Chem. Neuroanat.* 31, 37-50.
- Deboer, T., Franken, P., Tobler, L. (1994). Sleep and cortical temperature in the Djungarian hamster under baseline conditions and after sleep deprivation. *J. Comp. Physiol. A.* 174, 145-155.
- Dell, L.A., Kruger, J.L., Bhagwandin, A., Jillani, N.E., Pettigrew, J.D., Manger, P.R., 2010. Nuclear organization of cholinergic, putative catecholaminergic and serotonergic systems in the brains of two megachiropteran species. *J. Chem. Neuroanat.* 40, 177-195.
- Dell, L.A., Kruger, J.L., Pettigrew, J.D., Manger, P.R., 2013. Cellular location and major terminal networks of the orexinergic system in the brain of two megachiropterans. *J. Chem. Neuroanat.* 53, 64-71.
- Dijk, D.J., Archer, S.N., 2010. PERIOD3, circadian phenotypes, and sleep homeostasis. *Sleep Med. Rev.* 14, 151-160.
- Dijk, D.J., Daan, S., 1989. Sleep EEG spectral analysis in a diurnal rodent: *Eutamias sibiricus*. *J. Comp. Physiol.* 165, 205-215.
- Dijk D.J., Franken, P., 2005. Interaction of sleep homeostasis circadian rhythmicity: dependent or independent systems? In: Meir, H., Kryger, M.H., Rothm T., Dement, W. (eds.). *Principles and Practice of Sleep Medicine*. Saunders/Elsevier, Philadelphia. Pp. 418-434.

- Downs, C.T., Perrin, M.R., 1996. The thermal biology of southern Africa's smallest rodent, *Mus minutoides*. S. Afr. J. Sci. 92, 282-285.
- Dubost, G., 1988. Ecology and social life of the red acouchy, *Myoprocta exilis*; comparison with the orange-rumped agouti, *Dasyprocta leporina*. J. Zool. 214, 107-123.
- Du Toit, J.T., Jarvis, J.U.M., Louw, G.N., 1985. Nutrition and burrowing energetics of the Cape mole rat, *Georhynchus capensis*. Oecologia 66, 81-87.
- Dwarika, S., Maseko, B.C., Ihunwo, A.O., Fuxe, K., Manger, P.R., 2008. Distribution and morphology of putative catecholaminergic and serotonergic neurons in the brain of the greater canerat, *Thryonomys swinderianus*. J. Chem. Neuroanat. 35, 108-122.
- Ebbesson, S.O., 1980. The parcellation theory and its relation to interspecific variability in brain organization, evolutionary and ontogenetic development, and neuronal plasticity. Cell Tissue Res. 213, 179-212.
- Eckenstein, F., Baughman, R.W., 1984. Two types of cholinergic innervation in the cortex, one co-localised with vasoactive intestinal polypeptide. Nature 309, 153-155.
- Elgar, M.A., Pagel, M.D., Harvey, P.H., 1988. Sleep in mammals. Anim. Behav. 36, 1407-1419.
- Espana, R.A., Reis, K.M., Valentino, R.J., Berridge, C.W., 2005. Organization of hypocretin/orexin efferents to locus coeruleus and basal forebrain arousal-related structures. J. Comp. Neurol. 481, 160-178.
- Ewer, R. F. 1969. Form and function in the grass cutter, *Thryonomys swinderianus* Temm.(Rodentia, Thryonomyidae). Ghana J. Sci. 9, 131-141.

- Faulkes, C.G., Bennett, N.C., 2013. Plasticity and constraints on social evolution in African mole-rats: ultimate and proximate factors. *Philos. Trans. R. Soc. Lond. B. Biol. Sci.* 368, 201203467.
- Feldman, J.L., Ellenberger, H.H., 1988. Central coordination of respiratory and cardiovascular control in mammals. *Annu. Rev. Physiol.* 50, 593-606.
- Ferguson, A.V., Samson, W.K., 2003. The orexin/hypocretin system: a critical regulator of neuroendocrine and autonomic function. *Front. Neuroendocrin.* 24, 141-150.
- Ferreira, G., Meurisse, M., Tillet, Y., Levy, F., 2001. Distribution and co-localization of choline acetyltransferase and P75 neurotrophin receptors in the sheep basal forebrain: implications for the use of a specific cholinergic immunotoxin. *Neuroscience.* 104, 419-439.
- Folk, M. A. (1963). The daily distribution of sleep and wakefulness in the Arctic ground squirrel. *J. Mammal.*, 575-577.
- Franken, P., Malafosse, A., Tafti, M., 1998. Genetic variation in the EEG during sleep in inbred mice. *Am. J. Physiol.* 275, R1127-R1137.
- Franken, P., Malafosse, A., Tafti, M., 1998. Genetic determinants of sleep regulation in inbred mice. *Sleep* 22, 155-169.
- Fuxe, K., 1964. Cellular localization of monoamines in the median eminence and the infundibular stem of some mammals. *Zeitschrift für Zellforschung* 61, 710-724.

- Fuxe, K., Hökfelt, T., Ungerstedt, U., 1969. Distribution of monoamines in the mammalian central nervous system by histochemical studies, in: Hooper, G. (Ed.), *Metabolism of Amines in the Brain*. Macmillan, London, pp. 10–22.
- Fuxe, K., Hökfelt, T., Ungerstedt, U., 1970. Morphological and functional aspects of central monoamine neurons. *Int. Rev. Neurobiol.* 13, 93–126.
- Fuxe, K., Härfstrand, A., Agnati, L.F., Kalia, M., Fredholm, B., Svensson, T., Gustafsson, J.A., Lang, R., Ganten, D., 1987. Central catecholamine-neuropeptide Y interactions at the pre- and postsynaptic level in cardiovascular centers. *J. Cardiovasc. Pharmacol.* 10, Suppl 12, S1-13.
- Gallyas, F., 1979. Silver staining of myelin by means of physical development. *Neurolog. Res.* 1, 203–209.
- Gerashchenko, D., Wisor, J. P., Burns, D., Reh, R. K., Shiromani, P. J., Sakurai, T., Kilduff, T. S. 2008. Identification of a population of sleep-active cerebral cortex neurons. *Proc. Nat. Acad. Sci. U.S.A.* 105, 10227-10232.
- Ginovart, N., Marcel, D., Bezin, L., Garcia, C., Gagne, C., Pujol, J.F., Weissman, D., 1996. Tyrosine hydroxylase expression within Balb/C and C57Black6 mouse locus coeruleus. I. Topological organization and phenotypic plasticity of the enzyme-containing cell population. *Brain Res.* 721, 11-21.
- Gravett, N., Bhagwandin, A., Fuxe, K., Manger, P.R., 2009. Nuclear organization and morphology of cholinergic, putative catecholaminergic and serotonergic neurons in the brain of the rock hyrax, *Procavia capensis*. *J. Chem. Neuroanat.* 38, 57-74.

- Gravett, N., Bhagwandin, A., Fuxe, K., Manger, P.R., 2011. Distribution of orexin-A immunoreactive neurons and their terminal networks in the brain of the rock hyrax, *Procavia capensis*. *J. Chem. Neuroanat.* 41, 86-96.
- Gravett, N., Bhagwandin, A., Lyamin, O.I., Siegel, J.M., Manger, P.R., 2012. Sleep in the rock hyrax, *Procavia capensis*. *Brain Behav. Evol.* 79, 155-169.
- Gritti, I., Manns, I.D., Mainville, L., Jones, B.E., 2003. Parvalbumin, calbindin, or calretinin in cortically projecting and GABAergic, cholinergic, or glutaminergic basal forebrain neurons of the rat. *J. Comp. Neurol.* 458, 11-31.
- Hassani, O.K., Lee, M.G., Henny, P., Jones, B.E., 2009. Discharge profiles of identified GABAergic in comparison to cholinergic and putative glutamatergic basal forebrain neurons across the sleep-wake cycle. *J. Neurosci.* 29, 11828-11840.
- He, Y., Jones, C.R., Fujiki, N., Xu, Y., Guo, B., Holder, J.L., Rossner, M.L., Nishino, S., Fu, Y.H., 2009. The transcriptional repressor DEC2 regulates sleep length in mammals. *Science* 325, 866-870.
- Hickman, G. C., 1983. Burrows, surface movement, and swimming of *Tachyoryctes splendens* (Rodentia: Rhizomyidae) during flood conditions in Kenya. *J. Zool.* 200, 71-82.
- Hökfelt, T., Johansson, O., Fuxe, K., Goldstein, M., Park, D., 1976. Immunohistochemical studies on the localization and distribution of monoamine neuron systems in the rat brain. I. Tyrosine hydroxylase in the mes- and diencephalon. *Med. Biol.* 54, 427-53.

- Hökfelt, T., Martenson, R., Björklund, A., Kleinau, S., Goldstein, M., 1984. Distributional maps of tyrosine-hydroxylase-immunoreactive neurons in the rat brain, in: Björklund, A., Hökfelt, T. (Eds.), Handbook of Chemical Neuroanatomy, vol. 2. Classical Neurotransmitters in the CNS, part 1. Elsevier, Amsterdam, pp. 277–379.
- Huber, R., Ghilardi, M.F., Massimini, M., Tononi, G., 2004. Local sleep and learning. Nature 430, 78-81.
- Imeri, L., De Simoni, M. G., Giglio, R., Clavenna, A., Mancina, M., 1994. Changes in the serotonergic system during the sleep-wake cycle: simultaneous polygraphic and voltammetric recordings in hypothalamus using a telemetry system. Neuroscience 58, 353-358.
- Jacobs, B.L., Azmitia, E.C., 1992. Structure and function of the brain serotonin system. Physiol. Rev. 72, 165–229.
- Jansa, S.A., Weksler, M., 2004. Phylogeny of the murid rodents: relationships within and among major lineages as determined by IRBP gene sequences. Mol. Phylogenet. Evol. 31, 256–276.
- Jarvis, J.U.M., 1973. The structure of a population of mole-rats, *Tachyoryctes splendens*, (Rodentia: Rizomyidae). J. Zool. Lond. 171, 1-14.
- Jarvis, J.U.M., Sale, J.B., 1971. Burrowing and burrow patterns of East African mole-rats. J. Zool. Lond. 163, 451-479.

Jones, B. E., 1972. The respective involvement of noradrenaline and its deaminated metabolites in waking and paradoxical sleep: a neuropharmacological model. *Brain Res.* 39, 121-136.

Jones, B. E. , 2008. Modulation of cortical activation and behavioral arousal by cholinergic and orexinergic systems. *Ann. New York Acad. Sci.*, 1129, 26-34.

Jones, B.E., Cuello, A.C., 1989. Afferents to the basal forebrain cholinergic cell area from pontomesencephalic catecholamine, serotonin and acetylcholine neurons. *Neuroscience.* 31, 37-61.

Jori, F., Mensah, G. A., Adjanohoun, E., 1995. Grasscutter production: an example of rational exploitation of wildlife. *Biodiv. Conserv.* 4, 257-265.

Katandukila, J.V., Bennett, N.C., Chimimba, C.T., Faulkes, C.G., Oosthuizen, M.K., 2013. Locomotor activity patterns of captive East African root rats, *Tachyoryctes splendens* (Rodentia: Spalacidae) from Tanzania, East Africa. *J. Mammal.* 94, 1393-1400.

Kavanau, J.L., 2002. REM and NREM sleep as natural accompaniments of the evolution of warm-bloodedness. *Neurosci. Biobehav. Rev.* 26, 889-906.

Kerley, G.I.H., 1991. Seed removal by rodents, birds and ants in the semiarid Karoo, South Africa. *J. Arid. Environ.* 20, 63-69.

Khorooshi, R.M., Klingenspor, M., 2005. Neuronal distribution of melanin-concentrating hormone, cocaine- and amphetamine regulated transcript and orexin B in the brain of the Djungarian hamster (*Phodopus sungorus*). *J. Chem. Neuroanat.* 29, 137-148.

- Kitahama, K., Geffard, M., Okamura, H., Nagatsu, I., Mons, N., Jouvét, M., 1990. Dopamine- and dopa-immunoreactive neurons in the cat forebrain with reference to tyrosine hydroxylase-immunohistochemistry. *Brain Res.* 518, 83-94.
- Kitahama, K., Sakamoto, N., Jouvét, A., Nagatsu, I., Pearson, J., 1996. Dopamine-beta-hydroxylase and tyrosine hydroxylase immunoreactive neurons in the human brainstem. *J. Chem. Neuroanat.* 10, 137-146.
- Kirouac, G.J., Parson, M.P., Li, S., 2005. Orexin (hypocretin) innervation of the paraventricular nucleus of the thalamus. *Brain Res.* 1059, 179-188.
- Kruger, J-L., Dell, L-A., Pettigrew, J.D., Manger, P.R., 2010a. Cellular location and major terminal networks of the orexinergic system in the brains of five microchiropteran species. *J. Chem. Neuroanat.* 40, 256-262.
- Kruger, J-L., Dell, L-A., Bhagwandin, A., Jillani, N.E., Pettigrew, J.D., Manger, P.R., 2010b. Nuclear organization of cholinergic, putative catecholaminergic and serotonergic systems in the brains of five microchiropteran species. *J. Chem. Neuroanat.* 40, 210-222.
- Kruger, J.L., Patzke, N., Fuxe, K., Bennett, N.C., Manger, P.R., 2012. Nuclear organization of cholinergic, putative catecholaminergic, serotonergic and orexinergic systems in the brain of the African pygmy mouse (*Mus minutoides*): organizational complexity is preserved in small brains. *J. Chem. Neuroanat.* 44, 45-56
- Kukkonen, J. P., Holmqvist, T., Ammoun, S., Åkerman, K. E., 2002. Functions of the orexinergic/hypocretinergic system. *Am. J. Physiol. Cell Physiol.* 283, C1567-C1591.

Lesku, J.A., Roth, T.C., Amlaner, C.J., Lima, S.L., 2006. A phylogenetic analysis of sleep architecture in mammals: the integration of anatomy, physiology, and ecology. *Am. Nat.* 168, 441-453.

Lesku, J.A., Roth, T.C., Rattenborg, N.C., Amlaner, C.J., Lima, S.L., 2008. Phylogenetics and the correlates of mammalian sleep: a reappraisal. *Sleep Med. Rev.* 12, 229-244.

Lesku, J.A., Vyssotski, A.L., Martinez-Gonzalez, D., Wilzeck, C., Rattenborg, N.C., 2011. Local sleep homeostasis in the avian brain: convergence of sleep function in mammals and birds? *Proc. Biol. Sci.* 278, 2419-2428.

Leshin, L.S., Kraeling, R.R., Kineman, R.D., Barb, C.R., Rampacek, G.B., 1995. Immunocytochemical distribution of catecholamine-synthesizing neurons in the hypothalamus and pituitary gland of pigs: tyrosine hydroxylase and dopamine- β -hydroxylase. *J. Comp. Neurol.* 364, 151-168.

Li, Z., Decavel, C., Hatton, G.I., 1995. Calbindin-D28K: role in determining intrinsically generated firing patterns in rat supraoptic neurones. *J. Physiol.* 488, 601-608.

Limacher, A.M., Bhagwandin, A., Fuxe, K., Manger, P.R., 2008. Nuclear organization and morphology of cholinergic, putative catecholaminergic and serotonergic neurons in the brain of the Cape porcupine (*Hystrix africaeaustralis*): Increased brain size does not lead to increased organizational complexity. *J. Chem. Neuroanat.* 36, 33-52.

Lindowski, P., Kerkhofs, M., Hauspie, R., Mendlewicz, J., 1991. Genetic determinants of EEG sleep: A study in twins living apart. *Electroencephalogr. Clin. Neurophysiol.* 79, 114-118.

Liu, P.Y., Yee, B., Wishart, S.M., Jimenez, M., Jung, D.G., Grunstein, R.R., Handelsman, D.J., 2003. The short-term effects of high-dose testosterone on sleep, breathing, and function in older men. *J. Clin. Endocrin. Metabol.* 88, 3605-3613.

Liu, Z. W., Faraguna, U., Cirelli, C., Tononi, G., Gao, X. B. 2010. Direct evidence for wake-related increases and sleep-related decreases in synaptic strength in rodent cortex. *J. Neurosci.* 30, 8671-8675.

Lovegrove, B. G., Papenfus, M. E. 1995. Circadian activity rhythms in the solitary Cape molerat (*Georychus capensis*: Bathyergidae) with some evidence of splitting. *Physiol. Behav.* 58, 679-685.

Lyamin, O.I., Manger, P.R., Ridgway, S.H., Mukhametov, L.M., Siegel, J.M., 2008. Cetacean sleep: an unusual form of mammalian sleep. *Neurosci. Biobehav. Rev.* 32, 1451-1484.

Manger, P.R., 2005. Establishing order at the systems level in mammalian brain evolution. *Brain Res. Bull.* 66, 282-289.

Manger, P.R., Cort, J., Ebrahim, N., Goodman, A., Henning, J., Karolia, M., Rodrigues, S.L., Strkalj, G., 2008. Is 21st Century neuroscience too focussed on the rat/mouse model of brain function and dysfunction? *Front. Neuroanat.* 2, 5.

- Maseko, B.C., Bourne, J.A., Manger, P.R., 2007. Distribution and morphology of cholinergic, putative catecholaminergic and serotonergic neurons in the brain of the Egyptian Rousette flying fox, *Rousettus aegyptiacus*. *J. Chem. Neuroanat.* 34, 108-127.
- McGranaghan, P.A., Piggins, H.D., 2001. Orexin A-like immunoreactivity in the hypothalamus and thalamus of the Syrian hamster (*Mesocricetus auratus*) and Siberian hamster (*Phodopus sungorus*), with special reference to circadian structures. *Brain Res.* 904, 234-244.
- McNamara, P., Capellini, I., Harris, E., Nunn, C.L., Barton, R.A., Preston, B., 2008. The phylogeny of sleep database: a new resource for sleep scientists. *The Open Sleep J.* 1, 11-14.
- Meddis, R., 1983. The evolution of sleep. In: Mayes, A. (ed.). *Sleep Mechanisms and Functions*. Van Nostrand Reinhold, Berkshire. Pp. 57-95.
- Meester, J. A. J., IL Rautenbach, NJ Dippenaar, and CM Baker. 1986. Classification of southern African mammals. *Transvaal Museum Monograph*, 5, 1-359.
- Meister, B., Hökfelt, T., Steinbusch, H.W., Skagerberg, G., Lindvall, O., Geffard, M., Joh, T.H., Cuello, A.C., Goldstein, M., 1988. Do tyrosine hydroxylase-immunoreactive neurons in the ventrolateral arcuate nucleus produce dopamine or only L-dopa? *J. Chem. Neuroanat.* 1, 59-64.
- Mintz, E.M., van Den Pol, A.N., Casano, A.A., Albers, H.E., 2001. Distribution of hypocretin (orexin) immunoreactivity in the central nervous system of Syrian hamsters (*Mesocricetus auratus*). *J. Chem. Neuroanat.* 21, 225–238.

Monadjem, A., 1999. Populations dynamics of *Mus minutoides* and *Steatomys pratensis* (Muridae: Rodentia) in a subtropical grassland in Swaziland. *Afr. J. Ecol.* 37, 202-210.

Monti, J. M., 1982. Catecholamines and the sleep-wake cycle I. EEG and behavioral arousal. *Life Sci.* 30, 1145-1157.

Moon, D.J., Maseko, B.C., Ihunwo, A., Fuxe, K., Manger, P.R., 2007. Distribution and morphology of catecholaminergic and serotonergic neurons in the brain of the highveld gerbil, *Tatera brantsii*. *J. Chem. Neuroanat.* 34, 134-144.

Murphy, M., Huber, R., Esser, S., Riedner, B.A., Massimini, M., Ferrarelli, F., Ghilardi, M.F., Tononi, G., 2011. The cortical topography of local sleep. *Curr. Top. Med. Chem.* 11, 2438-2446.

Naylor, E., Buxton, O. M., Bergmann, B. M., Easton, A., Zee, P. C., Turek, F. W. 1998. Effects of aging on sleep in the golden hamster. *Sleep* 21, 687-694.

Nicolau, M.C., Akaârîr, M., Gamundí, A., Gonzáles, J., Rial, R.V., 2000. Why we sleep: the evolutionary pathway to the mammalian sleep. *Prog. Neurobiol.* 62, 379-406.

Nixon, J.P., Smale, L., 2007. A comparative analysis of the distribution of immunoreactive orexin A and B in the brain of nocturnal and diurnal rodents. *Behav. Brain Funct.* 3, 28.

Novak, C.M., Albers, H.E., 2002. Localization of hypocretin-like immunoreactivity in the brain of the diurnal rodent, *Arvicanthis niloticus*. *J. Chem. Neuroanat.* 23, 49-58.

Ohno, K., Sakurai, T., 2008. Orexin neuronal circuitry: role in the regulation of sleep and wakefulness. *Front. Neuroendocrin.* 29, 70-87.

- Olson, L., Fuxe, K., 1972. Further mapping out of the central noradrenaline neurons systems: projections of the “subcoeruleus” area. *Brain Res.* 43, 289-295.
- Oosthuizen, M.K., Cooper, H.M., Bennett, N.C., 2003. Circadian rhythms of locomotor activity in solitary and social species of African mole-rats (family: Bathyergidae). *J. Biol. Rhythms* 18, 481-490.
- Pace-Schott, E. F., Hobson, J. A., 2002. The neurobiology of sleep: genetics, cellular physiology and subcortical networks. *Nat. Rev. Neurosci.* 3, 591-605.
- Paxinos, G., Watson, C., 2009. *Chemoarchitectonic Atlas of the Mouse Brain*. Academic Press, New York.
- Peyron, C., Tighe, D.K., van den Pol, A.N., de Lecea, L., Heller, H.C., Sutcliffe, J.G., Kilduff, T.S., 1998. Neurons containing hypocretin (orexin) project to multiple neuronal systems. *J. Neurosci.* 18, 9996-10015.
- Phillips, A. J., Robinson, P. A., Kedziora, D. J., Abeyesuriya, R. G. (2010). Mammalian sleep dynamics: how diverse features arise from a common physiological framework. *PLoS Comp. Biol.* 6, e1000826.
- Platt, B., Riedel, G., 2011. The cholinergic system, EEG and sleep. *Behav. Brain Res.* 221, 499-504.
- Portas, C. M., Bjorvatn, B., Ursin, R., 2000. Serotonin and the sleep/wake cycle: special emphasis on microdialysis studies. *Prog. Neurobiol.* 60, 13-35.
- Previc, F.H., 1999. Dopamine and the origins of human intelligence. *Brain Cogn.* 41, 299-350.

Rasch, B., Dodt, C., Mölle, M., Born, J., 2007. Sleep-stage-specific regulation of plasma catecholamine concentration. *Psychoneuroendocrin.* 32, 884-891.

Rattenborg, N.C., Voirin, B., Vyssotski, A.L., Kays, R.W., Spoelstra, K., Kuemmeth, F., Heidrick, W., Wikelski, M., 2008. Sleeping outside the box: electroencephalographic measures of sleep in sloths inhabiting a rainforest. *Biol. Lett.* 4, 402-405.

Reig, O.A., 1970. Ecological notes on the fossorial octodont rodent *Spalacopus cyanus* (Molina). *J. Mammal.* 592-601.

Reiner, P.B., Fibiger, H.C., 1995. Functional heterogeneity of central cholinergic systems, in: Bloom, F.E., Kupfer, D.J. (Eds.), *Psychopharmacology: The Fourth Generation of Progress*. Raven, New York, pp 147-153.

Résibois A, Rogers JH (1992): Calretinin in rat brain: an immunohistochemical study. *Neuroscience* 46:101-134.

Richardson, G. S., Moore-Ede, M. C., Czeisler, C. A., Dement, W. C., 1985. Circadian rhythms of sleep and wakefulness in mice: analysis using long-term automated recording of sleep. *Am. J. Physiol.-Reg. Integrat. Comp. Physiol.* 248, R320-R330.

Rodrigues, S.L., Maseko, B.C., Ihunwo, A.O., Fuxe, K., Manger, P.R., 2008. Nuclear organization and morphology of serotonergic neurons in the brain of the Nile crocodile, *Crocodylus niloticus*. *J. Chem. Neuroanat.* 35, 133-145.

Rosenberg, R. S., Bergmann, B. M., Rechtschaffen, A., 1976. Variations in slow wave activity during sleep in the rat. *Physiol. Behav.* 17, 931-938.

- Ruggiero, D.A., Anwar, M., Gootman, P.M., 1992. Presumptive adrenergic neurons containing phenylethanolamine N-methyltransferase immunoreactivity in the medulla oblongata of neonatal swine. *Brain Res.* 583, 105-119.
- Sakurai, T., 2007. The neural circuit of orexin (hypocretin): maintaining sleep and wakefulness. *Nat. Rev. Neurosci.* 8, 171-181.
- Schmidt, H., Stiefel, K.M., Racay, P., Schwaller, B., Eilers, J., 2003. Mutational analysis of dendritic Ca²⁺ kinetics in rodent Purkinje cells: role of parvalbumin and calbindin D_{28k}. *J. Physiol.* 551, 13-32.
- Siegel, J. M. 2005. Clues to the functions of mammalian sleep. *Nature*, 437, 1264-1271.
- Siegel, J.M., 2006. The stuff dreams are made of: anatomical substrates of REM sleep. *Nat. Neurosci.* 9, 721-722.
- Siegel, J.M., 2004. The neurotransmitters of sleep. *J. Clin. Psychiat.* 65, 4-7.
- Siegel, J. M. 2005. Clues to the functions of mammalian sleep. *Nature*, 437, 1264-1271.
- Siegel, J.M., 2008. Do all animals sleep? *Trends Neurosci.* 31, 208-213.
- Siegel, J.M., 2013. Evolution of sleep (Sleep Phylogeny). In: Kushida, C. (ed.). *The Encyclopedia of Sleep*. Volume 1, pp. 38-42. Waltham, MA: Academic Press.
- Siegel, J.M., Manger, P.R., Nienhuis, R., Fahringer, H.M., Pettigrew, J.D., 1998. Monotremes and the evolution of rapid eye movement sleep. *Philos. Trans. R. Soc. Lond. B.* 353, 1147-1157.

Silvius, K. M., Fragoso, J., 2003. Red-rumped agouti (*Dasyprocta leporina*) home range use in an Amazonian forest: Implications for the aggregated distribution of forest trees. *Biotropica* 35, 74-83.

Sirota, A., Csicsvari, J., Buhl, D., Buzsáki, G. 2003. Communication between neocortex and hippocampus during sleep in rodents. *Proc. Nat. Acad. Sci. U.S.A.* 100, 2065-2069.

Skagerberg, G., Meister, B., Hökfelt, T., Lindvall, O., Goldstein, M., Joh, T., Cuello, A.C., 1988. Studies on dopamine-, tyrosine hydroxylase- and aromatic L-amino acid decarboxylase-containing cells in the rat diencephalon: comparison between formaldehyde-induced histofluorescence and immunofluorescence. *Neuroscience*. 24, 605-620.

Skinner, J. D., Chimimba, C. T. 2005. The mammals of the southern African sub-region. Cambridge University Press.

Smeets, W.J.A.J., González, A., 2000. Catecholamine systems in the brain of vertebrates: new perspectives through a comparative approach. *Brain Res. Rev.* 33, 308-379.

Steinbusch, H.W.M., 1981. Distribution of serotonin-immunoreactivity in the central nervous system of the rat – cell bodies and terminals. *Neuroscience*. 6, 557-618.

Stephan, H., Frahm, H., Baron, G., 1981. New and revised data on volumes of brain structures in insectivores and primates, *Folia Primatol.* 35, 1–29.

Szymusiak, R., 1995. Magnocellular nuclei of the basal forebrain: substrates of sleep and arousal regulation. *Sleep* 18, 478-500.

- Syzmusiak, R., Steininger, T., Alam, N., McGinty, D., 2001. Preoptic area sleep-regulating mechanisms. *Arch. Ital. Biol.* 139, 77-92.
- Tafti, M., Franken, P., Kitahama, K., Malafosse, A., Jouvet, M., Valtax, J.L., 1997. Localisation of candidate genomic regions influencing paradoxical sleep in mice. *NeuroReport* 8, 3755-3758.
- Takakusaki, K., Takahashi, K., Saitoh, K., Harada, H., Okumura, T., Kayama, Y., Koyama, Y., 2005. Orexinergic projections to the cat midbrain mediate alternation of emotional behavioural states from locomotion to cataplexy. *J. Physiol.* 568, 1003-1020.
- Tang, X., Sanford, L. D., 2002. Telemetric recording of sleep and home cage activity in mice. *Sleep* 25, 691-9.
- Tillet, Y., Kitahama, K., 1998. Distribution of central catecholaminergic neurons: a comparison between ungulates, humans and other species. *Histol. Histopathol.* 13, 1163-1177.
- Timo-Iaria, C., Negrão, N., Schmidek, W. R., Hoshino, K., de Menezes, C. E. L., Da Rocha, T. L., 1970. Phases and states of sleep in the rat. *Physiol. Behav.* 5, 1057-1062.
- Tobler, I., 1992. Behavioral sleep in the Asian elephant in captivity. *Sleep* 15, 1-12.
- Tobler, I., 1995. Is sleep fundamentally different between mammalian species? *Behav. Brain Res.* 69, 35-41.
- Tobler, I., Deboer, T., 2001. Sleep in the blind mole rat *Spalax ehrenbergi*. *Sleep* 24, 147-154.

- Tobler, I., Franken, P., Jaggi, K., 1993. Vigilance states, EEG spectra, and cortical temperature in the guinea pig. *Am. J. Physiol.* 264, R1125-R1132.
- Tobler, I., Jaggi, K., 1987. Sleep and EEG spectra in the Syrian hamster (*Mesocricetus auratus*) under baseline conditions and following sleep deprivation. *J. Comp. Physiol. A.* 161, 449-459.
- Tomotani, B.M., Flores, D.E., Tachinardi, P., Paliza, J.D., Oda, G.A., Valentinuzzi, V.S., 2012. Field and laboratory studies provide insights into the meaning of day-time activity in a subterranean rodent (*Ctenomys aff. knightii*), the tuco-tuco. *PLoS One* 7, e37918.
- Törk, I., 1990. Anatomy of the serotonergic system. *Ann. N.Y. Acad. Sci.* 600, 9–35.
- Tsujino, N., Sakurai, T., 2009. Orexin/hypocretin: a neuropeptide at the interface of sleep, energy homeostasis, and reward system. *Pharmacol. Rev.* 61, 162-176.
- Valentinuzzi, V.S., Oda, G.A., Araujo, J.F., Ralph, M.R. (2009). Circadian pattern of wheel-running activity of a South American subterranean rodent (*Ctenomys cf knightii*). *Chronobiol. Internat.* 26, 14-27.
- van Twyver, H., 1969. Sleep patterns of five rodent species. *Physiol. Behav.* 4, 901-905.
- Veyrunes, F., Catalan, J., Tatard, C., Cellier-Holzem, E., Watson, J., Chevret, P., Robinson, T.J., Britton-Davidian, J., 2010. Mitochondrial and chromosomal insights into karyotypic evolution of the pygmy mouse, *Mus minutoides*, in South Africa. *Chromosome Res.* 18, 563-574.

- Vidal, L., Blanchard, J., Morin, L.P., 2005. Hypothalamic and zona incerta neurons expressing hypocretin, but not melanin concentrating hormone, project to the hamster intergeniculate leaflet. *Neuroscience*. 134, 1081-1090.
- von Coelln, R., Thomas, B., Savitt, J.M., Lim, K.L., Sasaki, M., Hess, E.J., Dawson, V.L., Dawson, T.M., 2004. Loss of locus coeruleus neurons and reduced startle in parkin null mice. *Proc. Natl. Acad. Sci. U.S.A.* 101, 10744-10749.
- Wagner, D., Salin-Pascual, R., Greco, M.A., Shiromani, P.J., 2000. Distribution of hypocretin-containing neurons in the lateral hypothalamus and c-fos-immunoreactive neurons in the VLPO. *Sleep Res. Online* 3, 35-42.
- Webb, W. B., Friedman, J. 1971. Attempts to modify the sleep patterns of the rat. *Physiol. Behav.* 6, 459-460.
- Welsh, D. K., Richardson, G. S., Dement, W. C. 1986. Effect of age on the circadian pattern of sleep and wakefulness in the mouse. *J. Geront.* 41, 579-586.
- Wilson, D.E., Reeder, D.M., 2005. *Mammal Species of the World: A Taxonomic and Geographic Reference*. Johns Hopkins University Press, Baltimore, USA.
- Woolf, N.J., 1991. Cholinergic systems in mammalian brain and spinal cord. *Prog. Neurobiol.* 37, 475-524.
- Woolf, N.J., Hameroff, S.R., 2001. A quantum approach to visual consciousness. *Trends. Cogn. Sci.* 5, 472-748.
- Wright, S., 1945. Tempo and mode in evolution – a critical review. *Ecology* 26, 415-419.

Zeitzer, J.M., Buckmaster, C.L., Parker, K.J., Hauck, C.M., Lyons, D.M., Mignot, E., 2003. Circadian and homeostatic regulation of hypocretin in a primate model: implications for the consolidation of wakefulness. *J. Neurosci.* 23, 3555-3560.

Zepelin, H., Rechtschaffen, A., 1974. Mammalian sleep, longevity, and energy metabolism. *Brain Behav. Evol.* 10, 425-470.

Zulley, J., Wever, R., Aschoff, J., 1981. The dependence of onset and duration of sleep on the circadian rhythm of rectal temperature. *Pflügers Arch.* 391, 314-318.



STRICTLY CONFIDENTIAL

ANIMAL ETHICS SCREENING COMMITTEE (AESC)

CLEARANCE CERTIFICATE NO. 2012/51/05

APPLICANT: Ms. J L Kruger

DEPARTMENT: Anatomical Sciences

PROJECT TITLE: The anatomy and physiology of sleep in four rodent species of vastly different body sizes: *Mus minutoides*, *Xerus inauris*, *Tachyoryctes splendens* and *Thryonomys swinderianus*

Number and Species

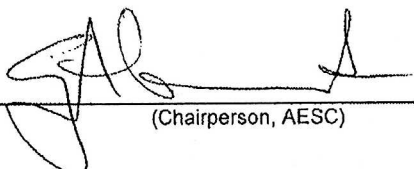
Approved (conditionally): 6 each of *Mus minutoides*, *Xerus inauris*, *Tachyoryctes splendens* and *Thryonomys swinderianus*

Approval was given for to the use of animals for the project described above at an AESC meeting held on **27 November 2012**. This approval remains valid until **30 November 2014**.

The use of these animals is subject to AESC guidelines for the use and care of animals, is limited to the procedures described in the application and to the following additional conditions:


Conditions:

- A score sheet must be used to monitor animal health. Details of this score sheet must be discussed with CAS staff.
- F10 instant sterilant, rather than Cidex, should be used to sterilise implants. In addition to F10 being less of an irritant than Cidex, it has a faster action, and implants need only be bathed for an hour before implantation.

Signed:  _____
(Chairperson, AESC)

Date: 5/12/12

I am satisfied that the persons listed in this application are competent to perform the procedures therein, in terms of Section 23 (1) (c) of the Veterinary and Para-Veterinary Professions Act (19 of 1982)

Signed:  _____
(Registered Veterinarian)

Date: 5/12/12

cc: Supervisor:
Director: CAS

Please note that only typewritten applications will be accepted. Should additional space be required for section "I" and/or "j", please use the back of this form.

ANIMAL ETHICS SCREENING COMMITTEE

MODIFICATIONS AND EXTENSIONS TO EXPERIMENTS

- a. Name: Jean-Leigh Kruger
- b. Department: Anatomical Sciences
- c. Experiment to be modified / extended

AESC NO:

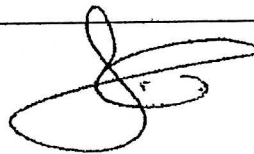
Original AESC number	2012	51	05
Other M&E's : each new species, or set of species requires a new M&E.			

- d. Project Title: The anatomy and physiology of sleep in four rodent species of vastly different body sizes: *Mus minutoides*, *Xerus inawris*, *Tachyoryctes splendens* and *Thryonomys swinderianus*

e. Number and species of animals originally approved:	24	4 species, see title above
f. Number of additional animals previously allocated on M&Es:	3	<i>Tachyoryctes splendens</i>
g. Total number of animals allocated to the experiment to date:	0	
h. Number of animals used to date:	9	All <i>Tachyoryctes splendens</i>
i. Specific modification / extension requested: I have been afforded the opportunity to obtain 6 <i>Georchychnus capensis</i> from Prof. Nigel Bennett (University of Pretoria) for which I would like to record sleep. These are animals that have been used in previous studies and thus instead of just euthanizing these animals, we felt it worthwhile to use them for sleep studies. Prof. Bennett obtained all the relevant permits and permissions for these animals. The housing and use of these animals (including anaesthesia) will be the same as that used for the <i>Tachyoryctes</i> . The use of these animals will contribute to my Doctoral studies and will likely replace the other species listed (i.e. it is unlikely that I will try to record sleep from <i>Xerus</i> , <i>Mus</i> and <i>Thryonomys</i> during my PhD, although I have examined aspects of the brain of these species). I trust all is in order with this request, but do let me know if you require any further information.		
j. Motivation for modification / extension: see above		

Date: 10, March, 2014

Signature:



RECOMMENDATIONS: APPROVED use of six *Georchychnus capensis* from University of Pretoria for sleep study in the CAS.

Date: 13 March 2014

Signature:



Chairman, AESC

Turnitin Originality Report

FullThesisexport.pdf

From Final written report

(sAwUZ4lbsKwwJ4371nt6i5GhQ7Fa4J4LYJOMuVY57aKaeMHNzX6pwdW1mSOov2fWcXETD8TK1y9183K9Bp9G62KJYeBP31mMrL)

- Processed on 12-Mar-2015 11:47 AM SAST
- ID: 515504654
- Word Count: 52558

Similarity Index

39%

Similarity by Source

Internet Sources:

25%

Publications:

28%

Student Papers:

19%

sources:

1 13% match (publications)

Calvey, Tanya, Nina Patzke, Consolate Kaswera, Emmanuel Gilissen, Nigel C. Bennett, and Paul R. Manger. "Nuclear organisation of some immunohistochemically identifiable neural systems in three Afrotherian species—Potomogale velox, Amblysomus hottentotus and Petrodromus tetradactylus". Journal of Chemical Neuroanatomy. 2013.

2 4% match (student papers from 13-Nov-2012)

Submitted to University of Witwatersrand on 2012-11-13

3 2% match (publications)

Limacher, A. "Nuclear organization and morphology of cholinergic, putative catecholaminergic and serotonergic neurons in the brain of the Cape porcupine (Hystrix africaeaustralis): Increased brain size does not lead to increased organizational complexity". Journal of Chemical Neuroanatomy. 200809

4 2% match (Internet from 04-Aug-2012)

<http://www.uq.edu.au/nuq/jack/MegabatBrainstem.pdf>

5 1% match (Internet from 13-Oct-2014)

http://www.sleep.ru/lib/bhagwandin_sleep_in_mole_rat.pdf

6 1% match (publications)

Kruger, J.L. "Nuclear organization of cholinergic, putative catecholaminergic and serotonergic systems in the brains of five microchiropteran species". Journal of Chemical Neuroanatomy. 201011

7 1% match (Internet from 27-Jan-2013)

<http://neuroscience.com/forums/neuropharmacology/nuclear-organization-cholinergic-putative-catecholaminergic-serotonergic>

8 1% match (publications)

Maseko, B.C. "Distribution and morphology of cholinergic, putative catecholaminergic and serotonergic neurons in the brain of the Egyptian rousette flying fox, Rousettus aegyptiacus". Journal of Chemical Neuroanatomy. 200711

9 1% match (Internet from 13-Oct-2014)

http://www.sleep.ru/lib/Gravett_Manger_Siegel.pdf

10 1% match (publications)

Bux, F. "Organization of cholinergic, putative catecholaminergic and serotonergic nuclei in the diencephalon, midbrain and pons of sub-adult male giraffes". Journal of Chemical Neuroanatomy. 201005

11 < 1% match (Internet from 04-Dec-2013)

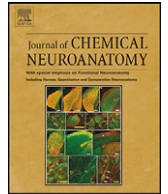
<http://www.science.gov/topicpages/c/calbindin+d-28k+cb.html>

12 < 1% match (Internet from 16-Aug-2014)

http://www.evolbiol.ru/large_files/sleep.pdf

13 < 1% match (Internet from 05-Jan-2014)

http://epublications.uef.fi/pub/urn_isbn_978-952-61-0436-2/urn_isbn_978-952-61-0436-2.pdf



Nuclear organization of cholinergic, putative catecholaminergic, serotonergic and orexinergic systems in the brain of the African pygmy mouse (*Mus minutoides*): Organizational complexity is preserved in small brains

Jean-Leigh Kruger^a, Nina Patzke^a, Kjell Fuxe^b, Nigel C. Bennett^c, Paul R. Manger^{a,*}

^aSchool of Anatomical Sciences, Faculty of Health Sciences, University of the Witwatersrand, 7 York Road, Parktown 2193, Johannesburg, South Africa

^bDepartment of Neuroscience, Karolinska Institutet, Retzius väg 8, S-171 77 Stockholm, Sweden

^cMammal Research Institute, Department of Zoology and Entomology, University of Pretoria, Pretoria 0002, South Africa

ARTICLE INFO

Article history:

Received 19 February 2012

Received in revised form 16 April 2012

Accepted 16 April 2012

Available online 22 April 2012

Keywords:

Choline acetyl transferase

Tyrosine hydroxylase

Serotonin

Hypocretin

Evolution

Mammal

Rodent

ABSTRACT

This study investigated the nuclear organization of four immunohistochemically identifiable neural systems (cholinergic, catecholaminergic, serotonergic and orexinergic) within the brain of the African pygmy mouse (*Mus minutoides*). The African pygmy mice studied had a brain mass of around 275 mg, making these the smallest rodent brains to date in which these neural systems have been investigated. In contrast to the assumption that in this small brain there would be fewer subdivisions of these neural systems, we found that all nuclei generally observed for these systems in other rodent brains were also present in the brain of the African pygmy mouse. As with other rodents previously studied in the subfamily Murinae, we observed the presence of cortical cholinergic neurons and a compactly organized locus coeruleus. These two features of these systems have not been observed in the non-Murinae rodents studied to date. Thus, the African pygmy mouse displays what might be considered a typical Murinae brain organization, and despite its small size, the brain does not appear to be any less complexly organized than other rodent brains, even those that are over 100 times larger such as the Cape porcupine brain. The results are consistent with the notion that changes in brain size do not affect the evolution of nuclear organization of complex neural systems. Thus, species belonging to the same order generally have the same number and complement of the subdivisions, or nuclei, of specific neural systems despite differences in brain size, phenotype or time since evolutionary divergence.

© 2012 Elsevier B.V. All rights reserved.

1. Introduction

The order Rodentia is comprised of over 2300 species in 34 families (Jansa and Weksler, 2004; Wilson and Reeder, 2005). Within the family Muridae are the true rats and mice, including the African pygmy mouse (*Mus minutoides*) (Wilson and Reeder, 2005). This omnivorous nocturnal mouse is one of the smallest extant African rodents with an average body mass of only 8 g and inhabits both arid areas and riverine forest (Kerley, 1991; Downs and Perrin, 1996; Monadjem, 1999). *M. minutoides* is an interesting species, not only because of its diminutive size, but also because this species exhibits an unusual form of sex determination. A large number (~75%) of fertile females of this species have been found with the XY chromosome pairing, which would typically be associated with a male genotype (Veyrunes et al., 2010).

The current study investigates several systems within the brain of *M. minutoides*, using immunohistochemical techniques

to reveal the cholinergic, putative catecholaminergic, serotonergic and orexinergic systems. The cholinergic system, which is found from the olfactory bulbs to the spinal cord, is involved in certain sleep stages and wakefulness (Jones and Cuello, 1989; Siegel, 2006), learning and memory (Reiner and Fibiger, 1995; Ferreira et al., 2001), the determination of EEG patterns such as during REM sleep (Siegel, 2006) and even in the generation of the conscious experience (Woolf and Hameroff, 2001). The catecholaminergic system is also widely distributed throughout the brain and has a variety of functions including cognitive (memory, abstract thinking and motor planning) (Previc, 1999; Agnati et al., 2003), neuroendocrine (including stress and growth functions) (Fuxe, 1964; Fuxe et al., 1970; Tillet and Kitahama, 1998; Leshin et al., 1995) and cardiorespiratory functions (Feldman and Ellenberger, 1988; Fuxe et al., 1987). The serotonergic system plays a role in mood, sleep and pain regulation (Törk, 1990; Jacobs and Azmitia, 1992), and orexin (hypocretin) is a hypothalamic neuromodulatory peptide produced by neurons in the perifornical and lateral hypothalamus that has been shown to have a role in the control of feeding and arousal (Mintz et al., 2001; Ferguson and Samson, 2003;

* Corresponding author. Tel.: +27 11 717 2497; fax: +27 11 717 2422.

E-mail address: Paul.Manger@wits.ac.za (P.R. Manger).

Zeitzer et al., 2003; Kirouac et al., 2005; Takakusaki et al., 2005).

If we consider the pygmy mouse's life history, phenotype, sex determination, body size and most importantly its tiny absolute brain mass (~275 mg), this species is uniquely placed to shed further light on rodent brain evolution and more generally on patterns of brain evolution across mammals. Studies of the cholinergic, catecholaminergic, serotonergic and orexinergic systems in a range of rodent species including the greater canerant (*Dwarika et al., 2008*), the highveld gerbil (*Moon et al., 2007*), the African molerats (*Da Silva et al., 2006; Bhagwandin et al., 2006, 2008, 2011*), the Cape porcupine (*Limacher et al., 2008*), the Syrian hamster (*McGranaghan and Piggins, 2001; Mintz et al., 2001*), the Siberian hamster (*McGranaghan and Piggins, 2001*) and the unstriped Nile grass rat (*Novak and Albers, 2002*) complement the wealth of published information on typical laboratory rodents (*Dahlström and Fuxe, 1964; Fuxe, 1964; Fuxe et al., 1969, 1970; Hökfelt et al., 1976, 1984; Steinbusch, 1981; Skagerberg et al., 1988; Jones and Cuello, 1989; Peyron et al., 1998; Chen et al., 1999; Cutler et al., 1999; Wagner et al., 2000; Baldo et al., 2003; Espana et al., 2005; Khorrooshi and Klingenspor, 2005; Kirouac et al., 2005; Vidal et al., 2005; Nixon and Smale, 2007*). Thus, to date, a range of rodent species with varying life histories (schedule and duration of key life events), phenotypes (including a range of brain and body sizes) and from a range of rodent families have been investigated; however, a rodent species with a very small brain has yet to be examined. Apart from the demonstration of the variation found in the species belonging to the family Muridae (*Dahlström and Fuxe, 1964; Björklund and Lindvall, 1984; Limacher et al., 2008* – locus coeruleus proper different in Murids compared to other rodents; *Bhagwandin et al., 2006* – cortical cholinergic neurons only found in Murid rodents, but not other species) all species within this order have the same nuclear organization of these systems regardless of the variation in phenotype, life history, or evolutionary temporal distance (*Manger, 2005*). Thus, the present study poses the question of whether, in a very small brain, the nuclear organization of the systems under investigation are less complexly organized, as might be proposed from theories and observations across mammalian orders (*Ebbesson, 1980; Stephan et al., 1981*), or whether, despite the small brain, does *M. minutoides* display a typically rodent-like organization of these system (*Manger, 2005*).

2. Materials and methods

The brains from three adult male African pygmy mice were used in this study (average body mass = 8.8 g; average brain mass = 275 mg). All the mice were captured from a wild population in the Eastern Cape of South Africa and were treated and used according to the guidelines of the University of the Witwatersrand Animal Ethics Committee. The animals were euthanized (Euthanase, 200 mg sodium pentobarbital/kg, i.p.) and, upon cessation of respiration, perfused intracardially with an initial rinse of 0.9% saline solution at 4 °C (10 ml), which was followed by a solution of 4% paraformaldehyde in 0.1 M phosphate buffer (PB) (10 ml). After removal from the skull, each brain was post-fixed overnight in the paraformaldehyde solution and subsequently stored in anti-freeze at –20 °C. Before sectioning, the brains were allowed to equilibrate in 30% sucrose in 0.1 M PB at 4 °C. Each brain was then frozen and sectioned into 50 µm thick serial coronal sections. A one in six series of sections was used for Nissl, myelin, choline-acyltransferase (ChAT), tyrosine hydroxylase (TH), serotonin (5HT) and orexin (hypocretin/OxA). Sections for Nissl staining were first mounted on 0.5% gelatine coated slides, cleared in a solution of 1:1 absolute alcohol and chloroform and then stained with 1% cresyl violet. The myelin series sections were refrigerated for two weeks in 5% formalin then mounted on 1% gelatine coated slides and stained with a modified silver stain (*Gallyas, 1979*).

The sections for immunohistochemical staining were treated for 30 min in an endogenous peroxidase inhibitor (49.2% methanol:49.2% 0.1 M PB:1.6% of 30% hydrogen peroxide) followed by three 10 min rinses in 0.1 M PB. Sections were then preincubated for 2 h, at room temperature, in blocking buffer (3% normal goat serum, NGS, for TH, serotonin and orexin sections; 3% normal rabbit serum, NRS, for ChAT sections, 2% bovine serum albumin for all sections and 0.25% Triton-X in 0.1 M PB for all sections). Thereafter sections were incubated in the primary antibody solution in blocking buffer for 48 h at 4 °C. Anti-cholineacetyltransferase (AB144P, Millipore, raised in goat) at a dilution of 1:3000 was used to reveal cholinergic

neurons. Anti-tyrosine hydroxylase (AB151, Millipore, raised in rabbit) at a dilution of 1:7500 revealed the putative catecholaminergic neurons. Serotonergic neurons were revealed using anti-serotonin (AB938, Millipore, raised in rabbit) at a dilution of 1:10000. Orexinergic neurons were revealed using anti-OrexinA (AB3704, Millipore, raised in rabbit) at a dilution of 1:3000. This incubation was followed by three 10 min rinses in 0.1 M PB and the sections were then incubated in a secondary antibody solution (1:1000 dilution of biotinylated anti-rabbit IgG for TH, serotonin and orexin sections, or a 1:1000 dilution of biotinylated anti-goat IgG for ChAT sections, in a blocking buffer containing 3% NGS/NRS and 2% BSA in 0.1 M PB) for 2 h at room temperature. This was followed by three 10 min rinses in 0.1 M PB, after which sections were incubated for 1 h in Avidin-Biotin solution (Vector Labs), followed by three 10 min rinses in 0.1 M PB. Sections were then placed in a 0.05% diaminobenzidine (DAB) in 0.1 M PB solution for 5 min, followed by the addition of 3 µl of 3% hydrogen peroxide to each 1 ml of solution in which each section was immersed. Chromatic precipitation was visually monitored and verified under a low power stereomicroscope. Staining continued until such time as the background stain was at a level that would assist reconstruction without obscuring the immunopositive neurons. Precipitation was arrested by placing sections in 0.1 M PB, followed by two more rinses in this solution. Sections were then mounted on 0.5% gelatine coated glass slides, dried overnight, dehydrated in a graded series of alcohols, cleared in xylene and coverslipped with Depex. The controls employed in this experiment included the omission of the primary antibody and the omission of the secondary antibody in selected sections for which no staining was evident.

Sections were examined under a low power stereomicroscope and using a camera lucida, the architectonic borders of the sections were traced following the Nissl and myelin stained sections. Sections containing the immunopositive neurons were matched to the drawings and the neurons were marked. All drawings were then scanned and redrawn using the Canvas 8 drawing program. All architectonic nomenclature was taken from the atlas of a rodent brain (*Paxinos and Watson, 2009*). The nomenclature used for the cholinergic system was adopted from *Woolf (1991)*, *Limacher et al. (2008)* and *Bhagwandin et al. (2008)*, the catecholaminergic from *Hökfelt et al. (1984)*, *Smeets and González (2000)*, *Limacher et al. (2008)* and *Bhagwandin et al. (2008)*, the serotonergic from *Törk (1990)*, *Limacher et al. (2008)* and *Bhagwandin et al. (2008)* and the orexinergic from *Kruger et al. (2010a)*, *Bhagwandin et al. (2011)* and *Gravett et al. (2011)*. While we use the standard nomenclature for the catecholaminergic system in this paper, we realise that the neuronal groups we revealed with tyrosine hydroxylase immunohistochemistry may not directly correspond with these nuclei as has been described in previous studies by *Dahlström and Fuxe (1964)*, *Hökfelt et al. (1976)*, *Meister et al. (1988)*, *Kitahama et al. (1990, 1996)*, and *Ruggiero et al. (1992)*. However, given the striking similarity of the results of the tyrosine hydroxylase immunohistochemistry to that seen in other mammals, we feel this terminology is appropriate. Clearly further studies in the pygmy mouse used with a wider range of antibodies, such as those to phenylethanolamine-N-methyltransferase (PNMT), dopamine-β-hydroxylase (DBH) and aromatic L-amino acid decarboxylase (AADC) would be required to fully determine the implied homologies ascribed in this study (e.g. *Weihe et al., 2006*). We address this potential problem with the caveat of putative catecholaminergic neurons where appropriate in the text.

Abbreviations of anatomical structures

- III – oculomotor nucleus
- IV – trochlear nucleus
- Vmot – motor division of trigeminal nerve nucleus
- Vsens – sensory division of trigeminal nerve nucleus
- VI – abducens nucleus
- VIII – dorsal division of facial nerve nucleus
- VIIv – ventral division of facial nerve nucleus
- X – dorsal motor vagus nucleus
- XII – hypoglossal nucleus
- 3V – third ventricle
- 4V – fourth ventricle
- 7n – facial nerve
- A1 – caudal ventrolateral medullary tegmental nucleus
- A2 – caudal dorsomedial medullary nucleus
- A4 – dorsolateral division of locus coeruleus
- A5 – fifth arcuate nucleus
- A6c – compact portion of locus coeruleus
- A7d – nucleus subcoeruleus, diffuse portion
- A7sc – nucleus subcoeruleus, compact portion
- A8 – retrorubral nucleus
- A9l – substantia nigra, lateral
- A9m – substantia nigra, medial
- A9pc – substantia nigra, pars compacta
- A9v – substantia nigra, ventral, pars reticulata
- A10 – ventral tegmental area
- A10c – ventral tegmental area, central
- A10d – ventral tegmental area, dorsal
- A10dc – ventral tegmental area, dorsal caudal
- A11 – caudal diencephalic group

A12 – tuberal cell group
 A13 – zona incerta cell group
 A14 – rostral periventricular nucleus
 A15d – anterior hypothalamic group, dorsal division
 A15v – anterior hypothalamic group, ventral division
 A16 – catecholaminergic neuros of the olfactory bulb
 ac – anterior commissure
 Amyg – amygdala
 AP – area postrema
 ARC – arcuate nucleus of the hypothalamus
 B9 – suprallemniscal serotonergic nucleus
 C1 – rostral ventrolateral medullary tegmental group
 C2 – rostral dorsomedial medullary nucleus
 C3 – rostral dorsal midline medullary nucleus
 C – caudate nucleus
 ca – cerebral aqueduct
 cc – corpus callosum
 Cer – cerebellum
 CLi – caudal linear nucleus
 CN – deep cerebellar nucleus
 CVL – caudal ventrolateral serotonergic group
 Diag.B – diagonal band of Broca
 DRc – dorsal raphe, caudal division
 DRd – dorsal raphe, dorsal division
 DRif – dorsal raphe, interfascicular division
 DRI – dorsal raphe, lateral division
 DRp – dorsal raphe, peripheral division
 DRv – dorsal raphe, ventral division
 DT – dorsal thalamus
 EW – Edinger-Westphal nucleus
 f – fornix
 fr – fasciculus retroflexus
 GC – central grey matter

GCL – granular cell layer of olfactory bulb
 GP – globus pallidus
 Hbl – lateral habenular nucleus
 Hbm – medial habenular nucleus
 HIP – hippocampus
 Hyp – hypothalamus
 Hyp.d – dorsal hypothalamic cholinergic nucleus
 Hyp.l – lateral hypothalamic cholinergic nucleus
 Hyp.v – ventral hypothalamic cholinergic nucleus
 IC – inferior colliculus
 ic – internal capsule
 io – inferior olive
 IP – interpeduncular nucleus
 Is.Call/TOL – islands of Calleja/olfactory tubercle
 LDT – laterodorsal tegmental nucleus
 LGv – ventral lateral geniculate nucleus
 LOT – lateral olfactory tract
 LV – lateral ventricle
 Mc – orexinergic main cluster
 mcp – middle cerebellar peduncle
 MnR – median raphe nucleus
 mtf – medullary tegmental field
 N.Acc – nucleus accumbens
 N.Amb – nucleus ambiguus
 N.Bas – nucleus basalis
 Neo – neocortex
 OB – olfactory bulb
 OC – optic chiasm
 OT – optic tract
 Otc – orexinergic optic tract cluster
 P – putamen nucleus
 PB – parabrachial nucleus
 PBg – parabigeminal nucleus

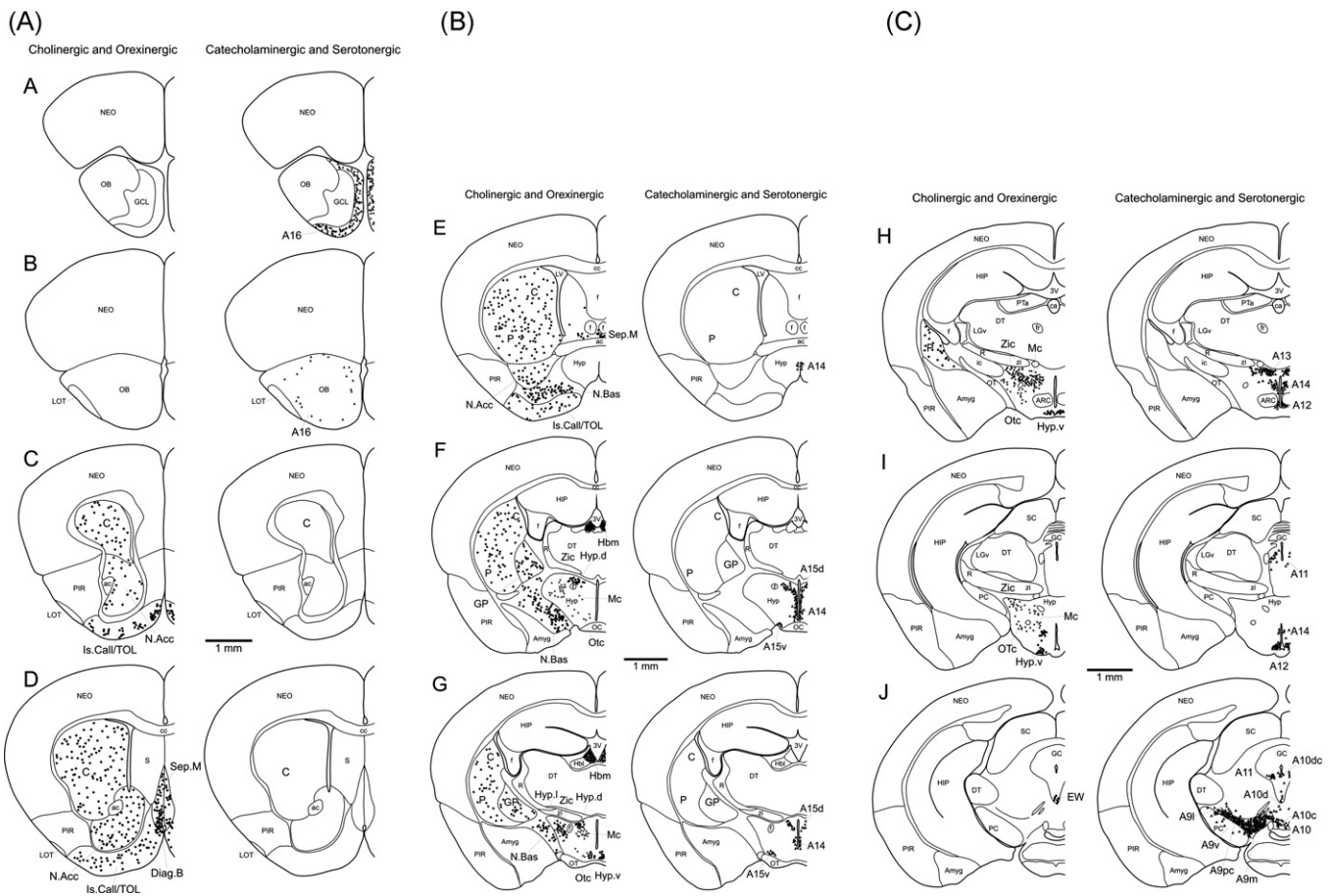


Fig. 1. (A–E) Serial drawings of coronal sections through one half of the African pygmy mouse brain from the olfactory bulb through to the spinomedullary junction. A is the most rostral section, R the most caudal. The outlines of the architectonic regions were drawn using Nissl and myelin stains and immunoreactive cells marked on the drawings. Solid black circles depict cholinergic neurons, solid triangles depict catecholaminergic neurons (those immunoreactive for tyrosine hydroxylase), open squares depict serotonergic neurons and closed stars represent orexinergic neurons. Each circle, triangle, square or star represents an individual neuron. The figures are approximately 600 μm apart. See list for abbreviations.

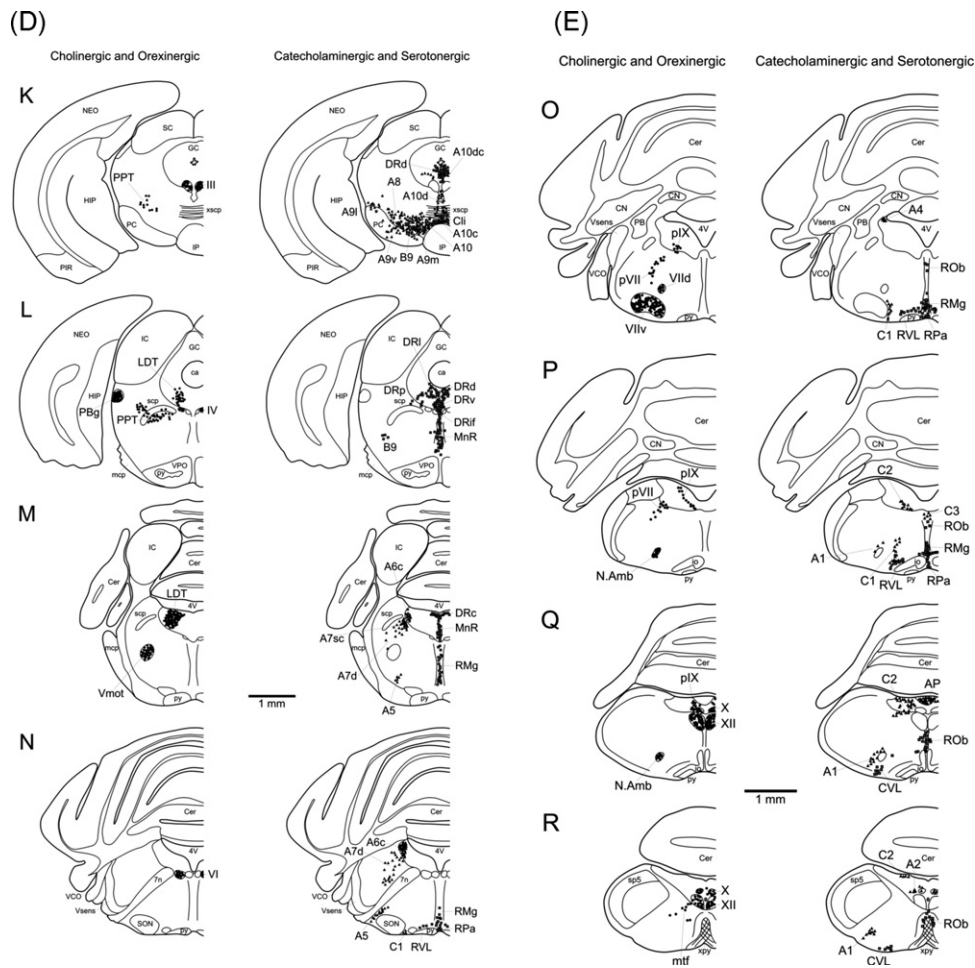


Fig. 1. (Continued).

PC – cerebral peduncle
 PIR – piriform cortex
 PPT – pedunculopontine nucleus
 Pta – pretectal area
 py – pyramidal tract
 pVII – preganglionic motor neurons of the superior salivatory nucleus or facial nerve
 pIX – preganglionic motor neurons of the inferior salivatory nucleus
 R – reticular nucleus of the thalamus
 RMg – raphe magnus nucleus
 ROb – raphe obscurus nucleus
 RPa – raphe pallidus nucleus
 RVL – rostral ventrolateral serotonergic group
 S – septal nuclear complex
 SC – superior colliculus
 scp – superior cerebellar peduncle
 Sep.M – medial septal nucleus
 SON – superior olivary nucleus
 sp5 – spinal trigeminal tract
 VCO – ventral cochlear nucleus
 VPO – ventral pontine nucleus
 xpy – decussation of the pyramidal tract
 xscp – decussation of the superior cerebellar peduncle
 zi – zona incerta
 Zic – orexinergic zona incerta cluster

3. Results

The current study delineates the nuclear organization of the cholinergic, putative catecholaminergic, serotonergic and orexinergic neural systems of the African pygmy mouse (Fig. 1). The three pygmy mice used in this study had an average body mass of 8.8 g and an average brain mass of 275 mg, making the African

pygmy mouse brain the smallest of any rodent species studied to date; however, this diminutively sized brain (in comparison to the mass of previously studied rodent brains) has not led to any reduction in the number of complement of nuclei present. In fact, the overall complexity of neural systems investigated within the pygmy mouse brain showed all the typical subdivisions across all of the regions that would be expected in a rodent brain (e.g. Bhagwandin et al., 2008, 2011; Limacher et al., 2008).

3.1. Cholinergic nuclei

The cholinergic system can be subdivided into the cortical interneurons, the striatal, basal forebrain, diencephalic, pontomesencephalic and the cranial motor nerve nuclei (Woolf, 1991), each subdivision containing a cluster of distinct nuclei (Figs. 1 and 2). Cholineacetyltransferase immunoreactive neurons (ChAT+) were identified in all these subdivisions, including the cortical cholinergic interneurons, which have a variable occurrence across rodent species studied to date (e.g. Bhagwandin et al., 2006).

3.1.1. Cortical cholinergic neurons

In a previous study (Bhagwandin et al., 2006) it was demonstrated that the appearance of cholinergic interneurons within the cerebral cortex of rodents appears to be limited to the members of the Murid family. The African pygmy mouse (*M. minutoides*) is a member of this family, and in the current study we observed cortical neurons immunoreactive to the ChAT antibody through all regions of the cortex (Fig. 2B). The majority of these neurons were found in the supragranular cortical layers, but were

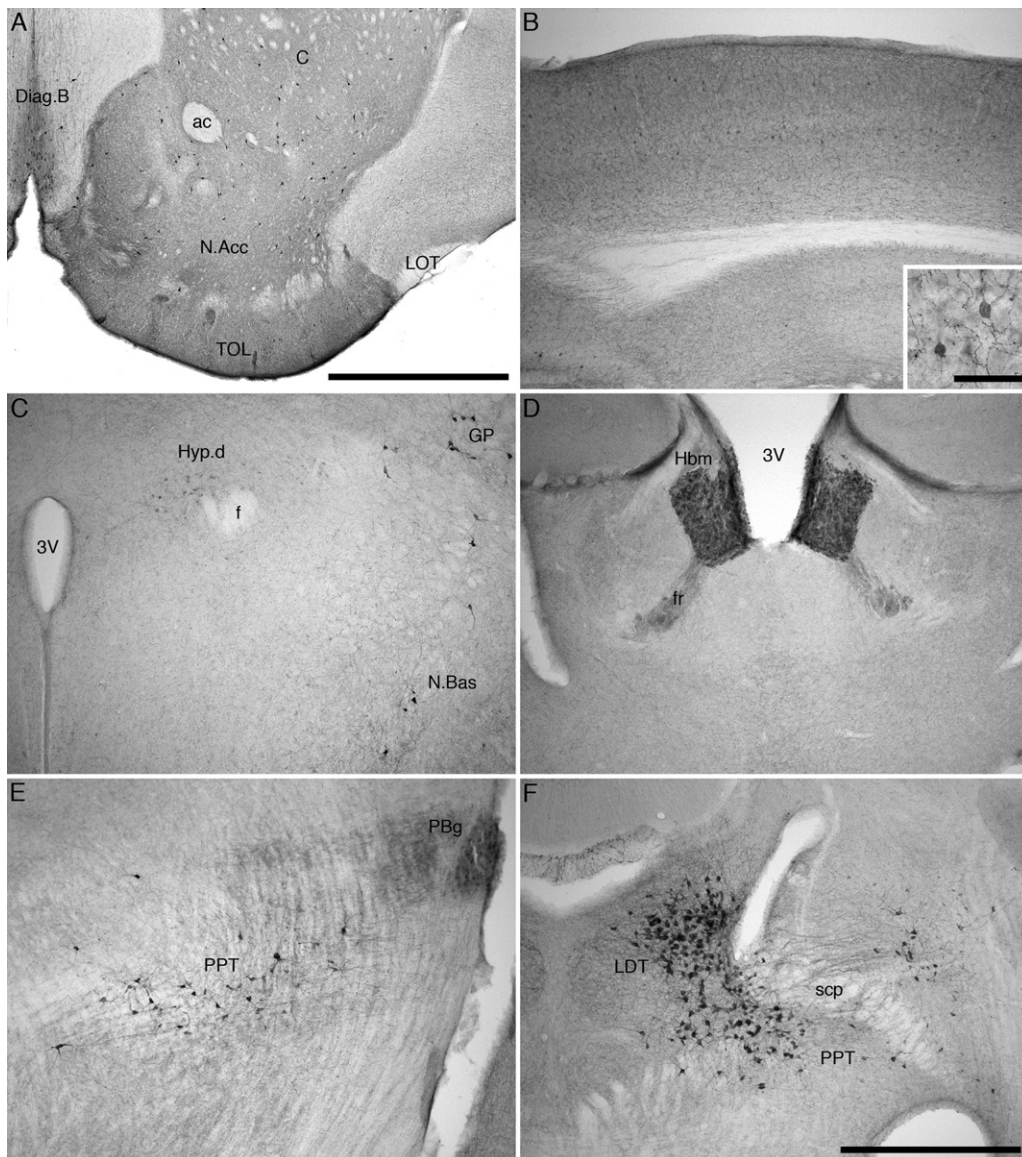


Fig. 2. Photomicrographs showing neuronal groups immunoreactive for choline acetyltransferase in the brain of the African pygmy mouse. (A) Basal forebrain region showing the diagonal band of Broca (Diag.B), the caudate nucleus (C), nucleus accumbens (N.Acc) and the olfactory tubercle (TOL). Scale bar in A = 1 mm. ac – anterior commissure; LOT – lateral olfactory tract. (B) Cerebral cortex showing the widespread distribution of cortical cholinergic neurons. Inset: high power photomicrograph of the cell bodies of cortical cholinergic neurons. Scale bar of inset = 50 μ m. (C) The dorsal hypothalamic cholinergic nucleus (Hyp.d) lying between and just dorsal to the third ventricle (3V) and the fornix (f). GP – globus pallidus; N.Bas – nucleus basalis. (D) The medial habenular nucleus (Hbm) and fasciculus retroflexus (fr). (E) The pedunculopontine (PPT) and parabigeminal (PBg) nuclei found in the pontine region. (F) The laterodorsal tegmental nucleus (LDT) and the pedunculopontine nucleus (PPT) lying immediately beneath the superior cerebellar peduncle (scp). In all images, except (D) which is at the midline, medial is to the left, and dorsal to the top. Scale bar in (F) = 500 μ m, and applies to (B)–(F), except for the inset in (B).

observed to occur in all cortical layers except layer one. The ChAT+ neurons were bipolar in nature with the majority being vertically oriented within the cortical mantle.

3.1.2. Striatal cholinergic interneurons

ChAT+ neurons were found in the caudate/putamen complex, the globus pallidus, the nucleus accumbens, the Islands of Calleja and the olfactory tubercle (Fig. 1C–H). A moderate density of ChAT+ neurons were found within the caudate/putamen and throughout the globus pallidus, but most densely at its borders with the putamen and nucleus basalis (Fig. 2A and C). Through the nucleus accumbens a moderate density of ChAT+ neurons was observed, and at the ventral border of this nucleus, they appear to intermingle with the most dorsal cholinergic neurons of the olfactory tubercle (Fig. 2A). The ChAT+ neurons within the olfactory tubercle and Islands of Calleja were found in the most

ventral portion of the anterior telencephalon (Fig. 2A). Throughout the olfactory tubercle a moderate density of ChAT+ neurons were observed, and within the most ventral portion of this region clusters of ChAT+ neurons were observed to form the Islands of Calleja.

3.1.3. Cholinergic nuclei of the basal forebrain

Cholinergic nuclei that could be identified within the basal forebrain of the African pygmy mouse included the medial septal nucleus, the Diagonal band of Broca and the nucleus basalis (Fig. 1D–G). The medial septal nucleus exhibited a moderate to high density of ChAT+ neurons and was located within the rostral half of the medial wall of the septal nuclear complex immediately below the rostrum of the corpus callosum. The ChAT+ neurons forming the diagonal band of Broca were evidenced as a high density of neurons located in the ventromedial corner of the

cerebral hemisphere anterior to the hypothalamus (Fig. 2A). It was possible to divide this nucleus into both horizontal and vertical limbs, but this was not deemed necessary since it would not add any value to the description. A cluster of moderate to high-density ChAT+ neurons located anterior and ventral to the globus pallidus and caudal to the olfactory tubercle were assigned to the nucleus basalis (Fig. 2C). At the posterior portion of this nucleus, the neurons appear to be continuous with those of the globus pallidus.

3.1.4. Diencephalic cholinergic nuclei

ChAT+ neurons were found in the medial habenular nucleus, as well as the dorsal, lateral and ventral hypothalamic clusters (Fig. 1F–I). The medial habenular nucleus was located in the dorsomedial aspect of the diencephalon adjacent to the third ventricle. The ChAT+ neurons within this nucleus were very densely packed (Fig. 2D). The three clusters of ChAT+ neurons within the hypothalamus all showed moderate to weak immunoreactivity, but were clearly observed. The dorsal cluster was found in the dorsomedial aspect of the hypothalamus between the third ventricle and fornix (Fig. 2C), the lateral cluster was found in the dorsolateral aspect of the hypothalamus, lateral to the fornix, while the ventral cluster was located in the ventral medial portion of the hypothalamus adjacent to the neurons of the A12 nucleus (see below).

3.1.5. Pontomesencephalic cholinergic nuclei

ChAT+ immunoreactive neurons were used to delineate the parabigeminal nucleus, as well as the pedunculopontine (PPT) and the laterodorsal (LDT) nuclei (Fig. 1K–M). The parabigeminal nucleus was located at the very lateral margin of the pontine tegmentum in a location ventral to the inferior colliculus. Within

this nucleus the ChAT+ neurons were moderately densely packed (Fig. 1E). The ChAT+ neurons forming the PPT were located within the dorsal aspect of the pontine tegmentum surrounding the superior cerebellar peduncle. A moderate to high density of ChAT+ neurons were observed in this region (Fig. 2E and F). Within the periventricular grey matter, caudal to the oculomotor nucleus, a moderate to high density of ChAT+ neurons were designated as those forming the LDT nucleus (Fig. 2F). The ventrolateral border of the PPT nucleus was contiguous with the dorsomedial border of the LDT nucleus, the only reason to separate these two nuclei being the transition from the periventricular grey matter to the pontine tegmentum.

3.1.6. Cholinergic cranial nerve motor nuclei

These nuclei were found in positions typical of all mammals (Woolf, 1991; Manger et al., 2002a; Maseko et al., 2007). The ChAT+ nuclei identified in the African pygmy mouse include: the oculomotor (III), trochlear (IV), motor division of the trigeminal (Vmot), abducens (VI), dorsal and ventral subdivisions of the facial (VII_d and VII_v), nucleus ambiguus, dorsal motor vagus (X), hypoglossal (XII), Edinger–Westphal (EW), medullary tegmental field (mtf) and the preganglionic motor neurons of the salivatory (pVII) and the glossopharyngeal (pIX) nerves (Fig. 1J and R).

3.2. Putative catecholaminergic nuclei

Tyrosine hydroxylase (TH) immunoreactivity was used to reveal the putatively catecholaminergic neurons (see above) in the African pygmy mouse brain. The nuclei formed by these neurons were arranged in a number of identifiable nuclear complexes that extended from the olfactory bulb through to the

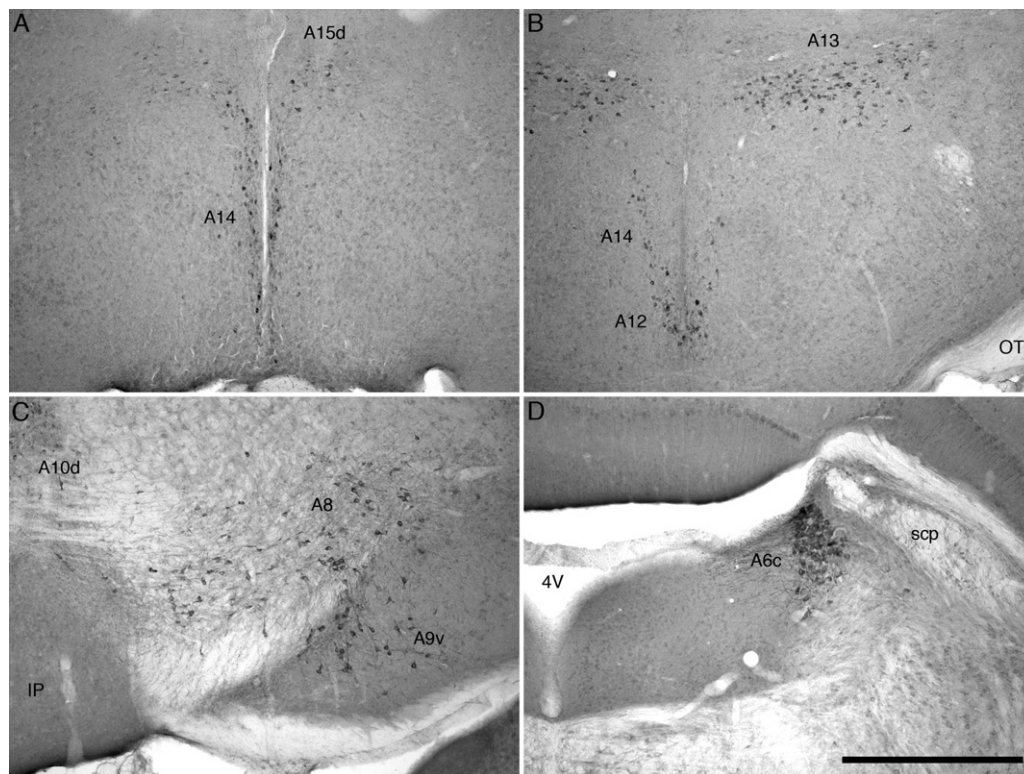


Fig. 3. Photomicrographs showing neuronal groups that are immunopositive for tyrosine hydroxylase in the brain of the African pygmy mouse. (A) In the rostral hypothalamus the dorsal division of the anterior hypothalamic group (A15d) and the rostral periventricular nucleus (A14) were observed. (B) In the caudal hypothalamus, the rostral periventricular nucleus (A14), zona incerta cell group (A13) and the tuberal cell group (A12) were observed. OT – optic tract. (C) In the ventral midbrain, the dorsal division of the ventral tegmental area (A10d), the retrorubral nucleus (A8) and the pars reticulata of the substantia nigra (A9v) nuclei were seen. IP – interpeduncular nucleus. (D) The compact nature of the locus coeruleus (A6c) in the African pygmy mouse is typical of Murid rodents. 4V – fourth ventricle; scp – superior cerebellar peduncle. In all images, except (A) which is at the midline, medial is to the left, and dorsal to the top. Scale bar in (D) = 500 μ m, and applies to all.

spinomedullary junction (Fig. 1). These complexes correspond to that seen in other rodents and could be divided into the olfactory bulb, diencephalic, midbrain, pontine and medullary nuclear clusters. For simplicity, in the current description, the nuclei are referred to using the nomenclature of Dahlström and Fuxe (1964) and Hökfelt et al. (1984). No putatively catecholaminergic nuclei outside the classically defined nuclei (e.g. Smeets and González, 2000) were observed.

3.2.1. Olfactory bulb (A16)

A high density of TH+ neurons was found in and around the stratum granulosum of the olfactory bulb. These neurons probably represent the periglomerular dopaminergic interneurons, were small in size, and were found in equal density surrounding the entire glomeruli (Fig. 1A and B).

3.2.2. Diencephalic nuclei (A15–A11)

Six clusters of TH+ neurons, forming distinct nuclei, were observed within the hypothalamus, these being: the anterior hypothalamic group, dorsal division (A15d); the anterior hypothalamic group, ventral division (A15v); the rostral periventricular cell group (A14); the zona incerta (A13); the tuberal cell group (A12); and the caudal diencephalic group (A11) (Fig. 1E–J). Within the dorsal anterior portion of the hypothalamus, between the third ventricle and the fornix, a moderate density of TH+ neurons was designated as the A15d nucleus (Fig. 3A). The TH+ neurons forming the A15v nucleus were located in the ventrolateral portion of the hypothalamus in a moderate density close to the floor of the brain. A low to moderate density of TH+ neurons within the hypothalamus and preoptic area, forming two columns adjacent to the lateral walls of the third ventricle, were assigned as the A14 nucleus (Fig. 3A and B). Within the dorsolateral aspect of the hypothalamus, lateral to the fornix and intermingling with the neurons forming the zona incerta of the ventral thalamus, was a low to moderate density of TH+ neurons belonging to the A13 nucleus (Fig. 3B). TH+ neurons assigned to the A12 nucleus were located in the ventromedial portion of the hypothalamus, surrounding and below the floor of the third ventricle in the arcuate nucleus and the immediate vicinity (Fig. 3B). Lastly, within the hypothalamic grey matter adjacent to the posterior pole of the third ventricle, a moderate density of TH+ neurons formed the A11 nucleus.

3.2.3. Midbrain nuclei (A10–A8)

Within the midbrain, the TH+ neurons were found within the ventral tegmental area (the A10 complex, including the A10, A10c, A10d, A10dc nuclei), the substantia nigra (the A9 complex, including the A9pc, A9l, A9v, A9m nuclei) and the retrorubral nucleus (A8) within the midbrain tegmentum (Fig. 1J and K). The nuclei of the A10 complex extended from within the periaqueductal grey matter around the base of the aqueduct, into the tegmentum below the periaqueductal grey matter around the midline, through to and around the interpeduncular nucleus. A high density of TH+ neurons, found dorsal and dorsolateral to the interpeduncular nucleus, between this nucleus and the root of the oculomotor nerve (III_n), was assigned to the A10 nucleus. Immediately dorsal to the interpeduncular nucleus, in a location just anterior to the decussation of the superior cerebellar peduncle, was a dense cluster of TH+ neurons forming the A10c nucleus. Immediately dorsal to A10c, between it and the oculomotor nucleus, was a dense bilateral parasagittal cluster of TH+ neurons that formed the A10d nucleus (Fig. 3C). The TH+ neurons assigned to the A10dc nuclear complex were found within the periaqueductal grey matter adjacent to and surrounding the ventral half of the cerebral aqueduct.

The substantia nigra nuclear complex was located in the ventral and lateral portions of the midbrain tegmentum, lying just dorsal

to the cerebral peduncles. Evidence for four distinct nuclei namely, the substantia nigra, pars compacta (A9pc), substantia nigra, ventral or pars reticulata (A9v), substantia nigra, pars lateralis (A9l) and substantia nigra, pars medialis (A9m), were found within the A9 complex. A9pc was seen to be a dense band of TH+ neurons that ran from medial to lateral immediately ventral to the medial lemniscus. Throughout the grey matter (pars reticulata of the substantia nigra) ventral to A9pc, several scattered TH+ neurons were assigned to the A9v nucleus (Fig. 3C). At the lateral edge of A9pc, a moderate density and loose aggregation of TH+ neurons formed the A9l nucleus. Medial to A9pc and lateral to the root of the oculomotor nerve (III_n), a dense cluster of TH+ neurons formed the A9m nucleus. Scattered throughout the midbrain tegmentum, in a position caudal to the magnocellular division of the red nucleus and dorsal to the A9 complex, was a sparsely packed but relatively numerous, cluster of TH+ neurons that formed the A8 nucleus (Fig. 3C).

3.2.4. Rostral rhombencephalon – the locus coeruleus complex, A7–A4

Within the pontine region a large number of TH+ neurons forming the locus coeruleus complex were readily observed (Fig. 1M–O). The locus coeruleus complex could be readily subdivided into five nuclei, these being: the subcoeruleus compact portion (A7sc), subcoeruleus diffuse portion (A7d), locus coeruleus compact portion (A6c), fifth arcuate nucleus (A5), and the dorsolateral division of locus coeruleus (A4). Within the dorsal portion of the pontine tegmentum adjacent to the ventrolateral region of the periaqueductal grey matter, a tightly packed cluster of TH+ neurons represented the A7 compact portion of the LC. This division is the same as what was previously described as the subcoeruleus (Dahlström and Fuxe, 1964; Olson and Fuxe, 1972). Ventral and lateral to the A7sc, a diffusely organized aggregation of TH+ neurons formed the A7d nuclear complex. These neurons are located both medially and laterally around the trigeminal motor nucleus (V_{mot}). Within the lateral portion of the periventricular grey matter a tightly packed, moderate to high density of TH+ neurons were assigned to the A6c nucleus (Fig. 3D). The neurons of this group were found adjacent to the wall of the fourth ventricle, stretching across the periventricular grey matter to its lateral edge as seen in the laboratory rat (Dahlström and Fuxe, 1964), and were not seen as a loosely packed cluster of neurons located in the ventrolateral half of the periventricular grey matter as seen in other non-Murid rodent species (Moon et al., 2007; Dwarika et al., 2008; Bhagwandin et al., 2008; Limacher et al., 2008). In the ventrolateral pontine tegmentum lateral to the superior olivary nucleus and lateral to V_{mot} and A7d, a small cluster of TH+ neurons formed the A5 nucleus. These neurons formed a rough meshlike dendritic network around the ascending fascicles located within the ventrolateral pontine tegmentum. Immediately adjacent to the wall of the fourth ventricle, in the dorsolateral portion of the periaqueductal grey matter, a very dense, but small cluster of TH+ neurons represent the A4 nucleus.

3.2.5. Medullary nuclei (C1, C2, C3, A1, A2, area postrema)

Within the medulla of the African pygmy mouse we found evidence for six putative catecholaminergic nuclei these being: rostral ventrolateral tegmental group (C1), rostral dorsomedial group (C2), rostral dorsal midline group (C3), caudal ventrolateral tegmental group (A1), caudal dorsomedial group (A2) and area postrema (AP) (Fig. 1N–R). A low density of TH+ neurons forming the C1 nucleus were found in the ventrolateral medulla from the level of the facial nerve nucleus to the mid-level of nucleus ambiguus. Continuing in the ventrolateral medulla, a column of TH+ neurons located laterally to the posterior most part of the C1 nucleus and extending to the spinomedullary junction was designated as the A1 nucleus. The A1 column was distinguished

from the ventrolateral C1 column by occupying a position lateral to the lateral reticular nucleus and nucleus ambiguus, whereas C1 was located medial to these structures. In the dorsal part of the medulla, in the region of the anterior part of the dorsal and medial border of the nucleus tractus solitarius, a distinct cluster of numerous TH+ neurons was designated as the C2 nucleus. Within this nucleus there was a clear region close to the floor of the fourth ventricle termed the dorsal strip and a continuation of this cluster into the region of the tractus solitarius termed the rostral subdivision of the C2 nucleus. Within the dorsal medial medullary tegmentum at the midline, dorsal to the raphe obscurus and close to the floor of the fourth ventricle, a very few TH+ neurons representing the C3 nucleus were found. Between the caudal portions of the dorsal motor vagus and hypoglossal cranial nerve nuclei, a small number of TH+ neurons represented the A2 nucleus. Some of these A2 neurons were located a small distance into the dorsal caudal medullary tegmentum. Straddling the midline, dorsal to the central canal and the dorsal motor vagus nucleus, and between the most caudal region of the bilateral C2 nucleus, was a single large, densely packed, cluster of intensely stained TH+ neurons, the area postrema.

3.3. Serotonergic nuclei

The serotonergic (5HT+) nuclei identified in the African pygmy mouse were the same as those previously identified in all rodents and other eutherian mammals studied to date (Steinbusch, 1981; Maseko et al., 2007; Dell et al., 2010). The serotonergic nuclei were all located within the brainstem and can be divided into a rostral and a caudal cluster. Both of these clusters contained a number of distinct nuclei that are found throughout the brainstem from the

level of the decussation of the superior cerebellar peduncle through to the spinomedullary junction (Fig. 1K–R).

3.3.1. Rostral cluster

Within the rostral cluster we found evidence for the caudal linear nucleus (CLi), the supralemniscal nucleus (B9), the median raphe nucleus (MnR) and the dorsal raphe complex formed of six distinct nuclei (Fig. 1K–M). The CLi nucleus was the most rostral of the serotonergic nuclei found and the 5HT+ neurons formed a moderate density cluster around the midline immediately dorsal to the interpeduncular nucleus in a location just anterior to the decussation of the superior cerebellar peduncle (Fig. 4A). The neurons forming the B9 nucleus appeared to be a lateral extension of the neuronal cluster comprising the most ventral portion of CLi. The 5HT+ B9 neurons were found in a low to moderate density immediately caudal to the A9pc (see above) within and above the medial lemniscus and extended as an arc of neurons into the lateral and ventrolateral portion of the midbrain tegmentum (Fig. 4A). The median raphe nucleus (MnR) was characterised by two distinct, densely packed 5HT+ neuronal columns on either side of the midline in a para-raphe position (Fig. 4B and C). The rostral border of this nucleus was coincident with the level of the decussation of the superior cerebellar peduncle and the caudal border of this nucleus was found at the level of the trigeminal motor nucleus.

Within the 5HT+ neuronal region designated as the dorsal raphe nuclear complex there were six distinct nuclei, these being: the dorsal raphe interfascicular (DRif) nucleus, dorsal raphe ventral (DRv) nucleus, dorsal raphe dorsal (DRd) nucleus, dorsal raphe lateral (DRI) nucleus, dorsal raphe peripheral (DRp) nucleus and the dorsal raphe caudal (DRc) nucleus (Figs. 1K–M, 4B, 4C). These six nuclei were found, for the most part, within the periaqueductal

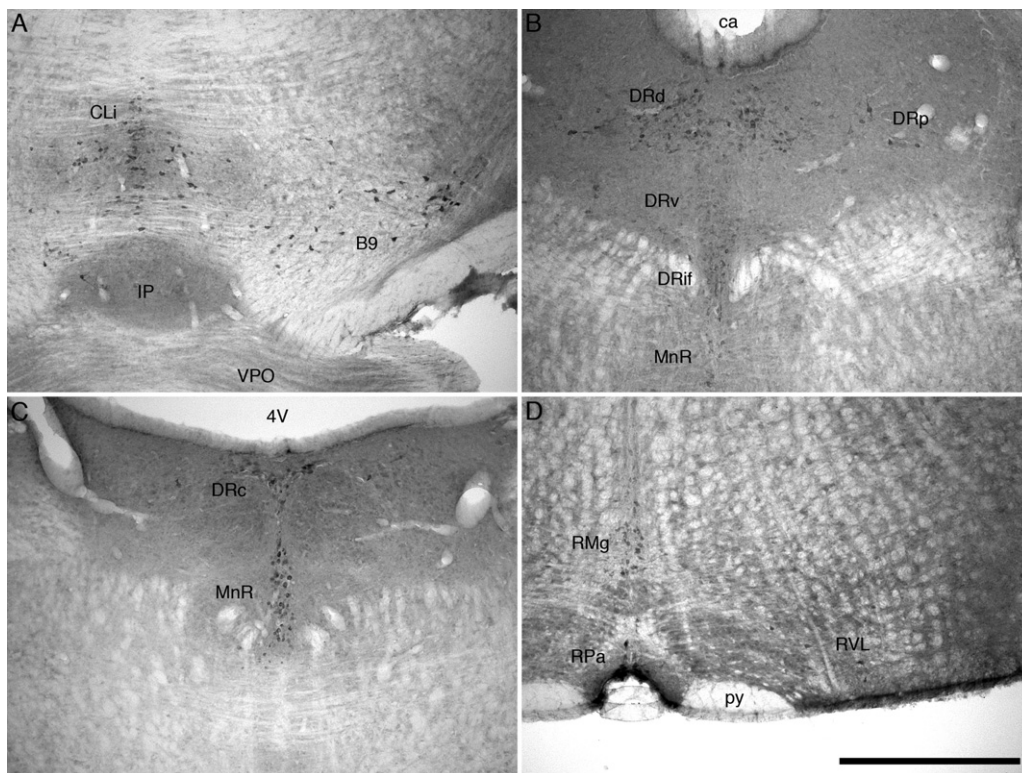


Fig. 4. Photomicrographs showing neuronal groups that are immunopositive for serotonin in the brain of the African pygmy mouse. (A) In the ventral portion of the rostral midbrain, the most rostral serotonergic nuclei, the caudal linear nucleus (CLi) and the supralemniscal serotonergic nucleus (B9) were observed dorsal and lateral to the interpeduncular nucleus (IP), respectively. VPO – ventral pontine nucleus. (B) In the central grey matter of the midbrain the dorsal (DRd), ventral (DRv), interfascicular (DRif) and peripheral (DRp) subdivisions of the dorsal raphe were observed. ca – cerebral aqueduct. (C) In the caudal most portion of the dorsal midbrain where the cerebral aqueduct opens in the fourth ventricle (4V) the caudal division of the dorsal raphe (DRc) and the median raphe nucleus (MnR) were observed. (D) In the ventral portions of the rostral medulla, the raphe magnus (RMg), raphe pallidus (RPa) and rostral ventrolateral serotonergic group (RVL) were observed close to the pyramidal tract (py). In all images, except (C) which is at the midline, medial is to the left, and dorsal to the top. Scale bar in (D) = 500 μ m, and applies to all.

and periventricular grey matter from the level of the oculomotor nucleus to the trigeminal motor nucleus. The DRif was located between the two medial longitudinal fasciculi and exhibited a high density of 5HT+ neurons. The DRv was found immediately dorsal to the DRif between and just caudal to the oculomotor nuclei. The DRv exhibited a high density of 5HT+ neurons. Immediately dorsal to DRv and ventral to the inferior border of the cerebral aqueduct a high-density cluster of 5HT+ neurons was designated as the DRd nucleus. A moderate density of 5HT+ neurons representing the DRp, were located in the ventrolateral portion of the periaqueductal grey matter lateral to the DRd and DRv. Some neurons of the DRp were found in the adjacent tegmentum and are the only ones found outside the periaqueductal grey matter. The 5HT+ neurons of the DRI were located dorsolateral to the DRd and adjacent to the ventrolateral edges of the cerebral aqueduct in a low to moderate density. The neurons of this nucleus were readily distinguishable from the remainder of the dorsal raphe nuclei since they were substantially larger. As we followed the DRI caudally, where the cerebral aqueduct opened into the fourth ventricle and the DRd, DRv and DRif disappeared, the neurons of the DRI formed an arc across the midline of the dorsal portion of the periventricular grey matter. This caudal arc of the DRI was classified as the DRc nucleus. We classified this as an independent nucleus due to the lack of 5HT+ neurons in this region in the brain of monotremes (Manger et al., 2002b; Maseko et al., 2007; Dell et al., 2010).

3.3.2. Caudal cluster

Within the caudal cluster we found evidence for the raphe magnus (RMg), rostral and caudal ventrolateral (RVL and CVL), raphe pallidus (RPa) and raphe obscurus (ROb) nuclei (Figs. 1M–R, 4D). This RMg was seen to be two columns of loosely aggregated moderate to large 5HT+ neurons located on either side of the midline from the level of the caudal pole of the trigeminal motor nucleus to the anterior pole of nucleus ambiguus. Within the left and right ventrolateral medullary tegmentum a distinct anteroposterior column of 5HT+ neurons extending from the level of the facial nucleus to the spinomedullary junction were observed. These have previously been termed the rostral and caudal ventrolateral serotonergic columns (e.g. Maseko et al., 2007; Moon et al., 2007; Dwarika et al., 2008). The RVL began as a lateroventral continuation of 5HT+ neurons from the lower portion of the RMg extending over the pyramidal tracts and consolidating as a distinct column lateral to the inferior olives. The inferior olive topologically distinguishes left and right RVL, and at the level of nucleus ambiguus the RVL becomes the CVL. The CVL continues in the caudal ventrolateral medullary tegmentum until the spinomedullary junction is reached. The number of neurons within this RVL/CVL column steadily decreases from rostral to caudal. Although the RVL and CVL are continuous in the African pygmy mice studied, and indeed several other eutherian mammals previously studied (e.g. Maseko et al., 2007; Moon et al., 2007; Dwarika et al., 2008), we make the distinction of two components of these ventrolateral columns, as the caudal portions have not been reported in the opossum or the monotremes (Crutcher and Humbertson, 1978; Manger et al., 2002b). The 5HT+ neurons forming the RPa nucleus were found in the ventral midline of the medulla associated with the pyramidal tracts. These neurons were for the most part located between the two pyramidal tracts, but some neurons belonging to this nucleus (based on neuronal morphology) were identified dorsal to the pyramidal tract, between it and the inferior olive. Two loosely arranged bilateral columns of 5HT+ neurons located either side of the midline from the level of nucleus ambiguus to the spinomedullary junction were classified as the ROb. Occasional 5HT+ neurons associated with this nucleus were identified within a short distance (less than 200 mm) lateral to the central columns.

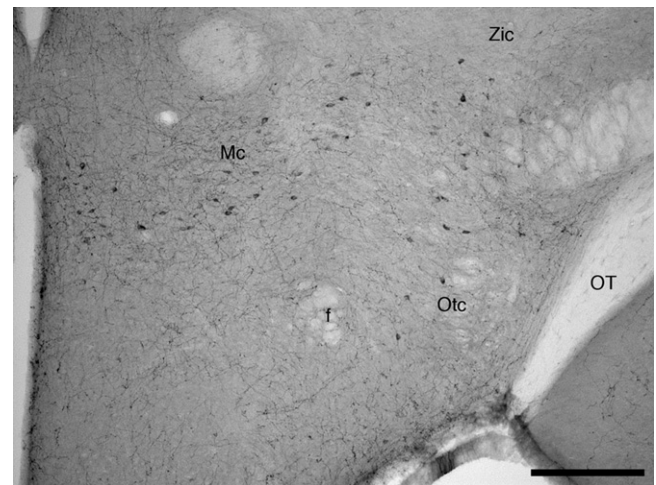


Fig. 5. Photomicrograph showing hypothalamic neuronal groups that are immunoreactive for orexin-A in the brain of the African pygmy mouse. f – fornix; Mc – main orexinergic cluster; OT – optic tract; Otc – optic tract orexinergic cluster; Zic – zona incerta orexinergic cluster. Dorsal is to the top and the midline is to the left. Scale bar = 250 μ m.

3.4. Orexinergic (hypocretineric) nuclei

The vast majority of orexin-A immunopositive neurons (OrX+) identified in the brain of the African pygmy mouse were localised in the hypothalamus (Fig. 1F–I). Within this aggregation of OrX+ cells we could identify three distinct clusters – a main cluster (Mc), a zona incerta cluster (Zic) and an optic tract cluster (Otc) (Fig. 5). The main cluster (Mc) was identified as a large group of densely packed OrX+ neuronal cell bodies located lateral to the third ventricle in the perifornical region, with a moderate number of neuronal cell bodies extending medially from this area into the dorsomedial hypothalamus and a larger number extending into the lateral hypothalamic areas. From the main cluster a group of OrX+ neuronal cell bodies extended laterally into the region of the zona incerta (Zic). This cluster had a very low density of OrX+ neurons that were mixed with neurons of the lateral hypothalamic cholinergic nucleus and the A13 nucleus of the catecholaminergic system (see above). The third cluster, the optic tract cluster (Otc) extended ventrolaterally from the main cluster to the ventrolateral region of the hypothalamus adjacent to the optic tract. This cluster exhibited a moderate density of OrX+ neuronal cell bodies.

4. Discussion

The African pygmy mouse, with its diminutive body mass (~8 g) and more importantly its small absolute brain mass (~275 mg), can shed much light on the suggestion that changes in brain size leads to increased or decreased differentiation within neural systems (Ebbesson, 1980; Stephan et al., 1981). The current study highlights that within the cholinergic, catecholaminergic, and serotonergic systems there is no difference in the number and complement of nuclei when compared with previous findings for the Cape porcupine (Limacher et al., 2008), which has a brain mass of approximately 37 g, or around 135 times larger than that of the pygmy mouse. Furthermore, the current findings underscore that even following major changes in phenotype, such as that observed in the microphthalmic African mole rats (Bhagwandin et al., 2008, 2011), or in the current study the small body mass of the African pygmy mouse, no changes in the complement or number of nuclei are apparent as long as the comparison is limited to rodent species. Thirdly, the range of rodent species in which these systems have now been investigated (e.g. Dahlström and Fuxe, 1964; Hökfelt

et al., 1976; Steinbusch, 1981; Jones and Cuello, 1989; Peyron et al., 1998; Chen et al., 1999; Wagner et al., 2000; McGranaghan and Piggins, 2001; Mintz et al., 2001; Novak and Albers, 2002; Da Silva et al., 2006; Bhagwandin et al., 2006, 2008, 2011; Nixon and Smale, 2007; Moon et al., 2007; Dwarika et al., 2008; Limacher et al., 2008) also indicates that, for the most part, it does not appear to matter how long a species has been separated from another of the same order (the time since they last shared a common ancestor), they will in all likelihood show the same complement and number of any given neural system (Manger, 2005). This finding appears not only to be relevant to the rodents, but also to be more generally relevant to all mammalian orders (e.g. Maseko et al., 2007; Dell et al., 2010) and perhaps even to other vertebrate classes (Rodrigues et al., 2008). Despite this general applicability of the conserved nature of systems level brain evolution, the current study highlighted two features of interest in the brain of the African pygmy mouse regarding intraordinal brain evolution and phylogeny, these being: (1) the presence of cortical cholinergic neurons; and (2) the anatomical appearance of the locus coeruleus (A6c); both features appearing to be found only within the subfamily Murinae from the range of rodent species studied to date.

4.1. Cortical cholinergic neurons

Cholinergic, or ChAT immunoreactive neurons have been observed in the brains of all species of the subfamily Murinae that have been examined (including *M. minutoides* – this study, *Rhabdomys pumilio*, *Rattus norvegicus* and *Mus musculus* – Bhagwandin et al., 2006); but have not been observed within the cerebral cortex of all other rodent species that have been examined with the AB144P Chemon/Millipore antibody to choline acetyltransferase (including *Tatera brantsii*, *Cryptomys hottentotus natalensis*, *Thryonomys swinderianus* – Bhagwandin et al., 2006; *Hystrix africaeaeaustralis* – Limacher et al., 2008; *Bathergus suillus*, *Cryptomys hottentotus pretoriae* – Bhagwandin et al., 2008). In studies on the occurrence of cholinergic neurons in the cerebral cortex of *R. norvegicus*, it was observed that up to 80% of these cortical cholinergic neurons were also immunoreactive for vasoactive intestinal polypeptide (VIP) (Eckenstein and Baughman, 1984), and that virtually all of these VIP neurons co-contain gamma-aminobutyric acid (GABA), with 88% of cortical cholinergic neurons co-containing GABA (Bayraktar et al., 1997). Interestingly, no cortical cholinergic neurons were immunoreactive for vesicular acetylcholine transporter (VChAT) (Bhagwandin et al., 2006), indicating that they do not form part of the traditionally defined cholinergic system (Woolf, 1991). The production of acetylcholine by cortical inhibitory interneurons appears to be limited to the rodent subfamily Murinae, and this may be related to increased functional demands on these cortical neurons allowing them to play a modulatory role in cortical microcirculation (Bhagwandin et al., 2006). As to exactly why this would appear only within the subfamily Murinae (cortical cholinergic neurons are not found in the closely related gerbil *T. brantsii*) is unclear at present; however, what is clear is that the Murinae are perhaps the most diverse and speciose (over 500 species) of the rodent subfamilies (Jansa and Weksler, 2004), indicating that either potentially some survival advantage is provided by this feature, or that this feature is evolutionarily neutral in terms of survival.

4.2. The appearance of the locus coeruleus (A6) across rodent species

The second feature observed in the current study that seems to be limited in its phylogenetic occurrence to the subfamily Murinae, is the appearance of the locus coeruleus, or A6, cluster of noradrenergic neurons. This cluster of neurons, first described

by Dahlström and Fuxe (1964) in *R. norvegicus*, was described as a tightly packed cluster of neurons stretching the majority of the way across the periventricular grey matter from the pontine tegmental border to the floor of the fourth ventricle (Dahlström and Fuxe, 1964; Hökfelt et al., 1976, 1984; Björklund and Lindvall, 1984). Similar descriptions have been furnished for *M. musculus* (Ginovart et al., 1996; von Coelln et al., 2004) and in the current study for *M. minutoides*. Interestingly, this compact appearance of the neurons forming the locus coeruleus does not occur in the closely related *T. brantsii* (Moon et al., 2007), or the more distantly related *T. swinderianus* (Dwarika et al., 2008), *H. africaeaeaustralis* (Limacher et al., 2008) or *B. suillus* and *C. hottentotus* (Bhagwandin et al., 2008). In these other rodent species a far less compact packing of the noradrenergic neurons forming the locus coeruleus is observed, and in general they do not approach the floor of the fourth ventricle as closely as they do in the Murinae. Again, it is unclear whether any advantage is to be gained by such a change to the structure of the locus coeruleus in the Murinae rodents, but as indicated above, the speciose nature of this subfamily does indicate that if anything, the genetic changes associated with this different adult phenotype are certainly not disadvantageous.

4.3. Systems level brain evolution

Manger (2005) proposed that all species within an order will have the same organization of nuclear systems regardless of life history, adult phenotypic variation (including variance in brain size) and time since evolutionary divergence. This concept is supported by the current findings for the African pygmy mouse, which, despite its very small absolute brain mass (~275 mg), shares the same number and complement of nuclei in the cholinergic, catecholaminergic, serotonergic and orexinergic systems as all other rodent species in which these systems have been studied to date. We can therefore conclude that decreases in absolute brain mass do not necessarily lead to a decrease in the nuclear differentiation of the systems investigated in species belonging to the same order, a finding that has been confirmed across several mammalian orders (Kruger et al., 2010b; Dell et al., 2010). Thus, in the Rodentia, species covering a range of brain masses, phylogenetic relatedness and phenotypes have been examined. The only potential variance regarding brain evolution that has yet to be explored is to examine rodents with a relatively large brain. Two closely related families of rodents, the scaly-tailed squirrels (Anomaluridae) and Springhares (Pedetidae) (Blanga-Kanfi et al., 2009), have relatively large brain sizes and thus would be of interest to examine to evaluate whether organizational complexity is altered with an increase in relative brain size. If, as seems likely, there is no change in organizational complexity at the systems level, these series of studies will have important ramifications for our understanding of systems level brain evolution.

Despite this well-supported generality regarding systems level complexity and evolution in mammalian brains, there are two specific examples that appear to not be entirely consistent with this generality. As outlined above, the Murinae rodents appears to have two features that distinguish them from the remainder of the Rodentia, the second example being that two species of microchiropterans (*Cardioderma cor* and *Coleura afra*) have three features (presence of a parabigeminal nucleus and the dorsal caudal nucleus of the ventral tegmental area, A10dc, and the poor expression of the ventral division of the hypothalamic group, A15v) that distinguish them from the remainder of microchiropterans that have been studied (Kruger et al., 2010b). The microchiroptera and the Rodentia, especially the Muroidea, are two extremely speciose mammalian groupings with long evolutionary histories. Due to this, and the diversity of the species within

these groupings, it is perhaps not surprising that some lineages within these groups have evolved specific apomorphies (derived features of the group) not represented in the remaining species of the order to which they belong (are they on an evolutionary trajectory that may lead to the establishment of a new mammalian order?). As noted above, the genetic alterations related to the appearance of these specific traits may be neutral in nature (unlike in experimentally manipulated mice, von Coelln et al., 2004), or they may indeed have some role that proves to be advantageous to the lineage in which they have appeared; however, the fact that these apomorphies do appear is of great interest. The laboratory rat and mouse (*R. norvegicus* and *M. musculus*) are known to be the two species most widely used in the neurosciences (Manger et al., 2008) and both have the Murinae apomorphies. Based on the range of rodents studied to date, this independent evolution of the cortical cholinergic neurons and the compact appearing locus coeruleus in the Murinae is cause for some concern, as it is highly likely that observations regarding these portions of the cholinergic and catecholaminergic systems will be difficult to translate to other species, especially humans that may have independently evolved similar apomorphies. It might also be true that these apomorphies in the different lineages (Murinae and Homo) are analogous, which would also be of great interest. Clearly, further comparative observational and functional assessments are required to determine whether any potential advantages or disadvantages to the extensive use of rats and mice as experimental animal models are apparent.

Acknowledgments

This work was supported by funding from the South African National Research Foundation (PRM, NCB), SIDA (KF) and by a fellowship within the Postdoc-Programme of the German Academic Exchange Service, DAAD (NP). We thank Prof. Neville Pillay of the University of the Witwatersrand for his kind assistance with obtaining some of the specimens used in this study.

References

- Agnati, L.F., Franzen, O., Ferre, S., Leo, G., Franco, R., Fuxe, K., 2003. Possible role of intramembrane receptor–receptor interactions in memory and learning via formation of long-lived heteromeric complexes: focus on motor learning in the basal ganglia. *Journal of Neural Transmission Supplementum* 65, 1–28.
- Baldo, B.A., Daniel, R.A., Berridge, C.W., Kelley, A.E., 2003. Overlapping distributions of orexin/hypocretin- and dopamine-beta-hydroxylase immunoreactive fibers in rat brain regions mediating arousal, motivation, and stress. *Journal of Comparative Neurology* 464, 220–237.
- Bayraktar, T., Staiger, J.F., Acsady, L., Cozzari, C., Freund, T.F., Zilles, K., 1997. Colocalization of vasoactive intestinal polypeptide, gamma-aminobutyric acid and choline acetyltransferase in the neocortical interneurons of the adult rat. *Brain Research* 757, 209–217.
- Bhagwandin, A., Fuxe, K., Manger, P.R., 2006. Choline acetyltransferase immunoreactive cortical interneurons do not occur in all rodents: a study of the phylogenetic occurrence of this neural characteristic. *Journal of Chemical Neuroanatomy* 32, 208–216.
- Bhagwandin, A., Fuxe, K., Bennett, N.C., Manger, P.R., 2008. Nuclear organization and morphology of cholinergic, putative catecholaminergic and serotonergic neurons in the brains of two species of African mole-rat. *Journal of Chemical Neuroanatomy* 35, 371–387.
- Bhagwandin, A., Fuxe, K., Bennett, N.C., Manger, P.R., 2011. Distribution of orexinergic neurons and their terminal networks in the brains of two species of African mole rats. *Journal of Chemical Neuroanatomy* 41, 32–42.
- Björklund, A., Lindvall, O., 1984. Dopamine-containing systems in the CNS. In: Björklund, A., Hökfelt, T. (Eds.), *Handbook of Chemical Neuroanatomy*, Vol. 2. Classical Neurotransmitters in the CNS, Part 1. Elsevier, Amsterdam, pp. 55–122.
- Blanga-Kanfi, S., Miranda, H., Penn, O., Pupko, T., DeBry, R.W., Huchon, D., 2009. Rodent phylogeny revisited: analysis of six nuclear genes from all major rodent clades. *BMC Evolutionary Biology* 9, 71.
- Chen, C.T., Dun, S.L., Kwok, E.H., Dun, N.J., Chang, J.K., 1999. Orexin A-like immunoreactivity in the rat brain. *Neuroscience Letters* 260, 161–164.
- Crutcher, K.A., Humbertson, A.O., 1978. The organization of monoamine neurons within the brainstem of the North American opossum (*Didelphis virginiana*). *J. Comp. Neurol.* 179, 195–222.
- Cutler, D.J., Morris, R., Sheridhar, V., Wattam, T.A.K., Kolmes, S., Patel, S., Atch, J.R.S., Wilson, S., Buckingham, R.E., Evans, M.L., Leslie, R.A., Williams, G., 1999. Differential distribution of orexin-A and orexin-B immunoreactivity in the rat brain and spinal cord. *Peptides* 20, 1455–1470.
- Da Silva, J.N., Fuxe, K., Manger, P.R., 2006. Nuclear parcellation of certain immunohistochemically identifiable neuronal systems in the midbrain and pons of the Highveld mole-rat (*Cryptomys hottentotus*). *Journal of Chemical Neuroanatomy* 31, 37–50.
- Dahlström, A., Fuxe, K., 1964. Evidence for the existence of monoamine-containing neurons in the central nervous system. I. Demonstration of monoamine in the cell bodies of brainstem neurons. *Acta Physiologica Scandinavica* 62, 1–52.
- Dell, L.-A., Kruger, J.-L., Bhagwandin, A., Jillani, N.E., Pettigrew, J.D., Manger, P.R., 2010. Nuclear organization of cholinergic, putative catecholaminergic and serotonergic systems in the brains of two megachiropteran species. *Journal of Chemical Neuroanatomy* 40, 177–195.
- Downs, C.T., Perrin, M.R., 1996. The thermal biology of southern Africa's smallest rodent, *Mus minutoides*. *South African Journal of Science* 92, 282–285.
- Dwarika, S., Maseko, B.C., Ihunwo, A.O., Fuxe, K., Manger, P.R., 2008. Distribution and morphology of putative catecholaminergic and serotonergic neurons in the brain of the greater canerat, *Thryonomys swinderianus*. *Journal of Chemical Neuroanatomy* 35, 108–122.
- Ebbesson, S.O., 1980. The parcellation theory and its relation to interspecific variability in brain organization, evolutionary and ontogenetic development, and neuronal plasticity. *Cell and Tissue Research* 213, 179–212.
- Eckenstein, F., Baughman, R.W., 1984. Two types of cholinergic innervation in the cortex, one co-localised with vasoactive intestinal polypeptide. *Nature* 309, 153–155.
- Espana, R.A., Reis, K.M., Valentino, R.J., Berridge, C.W., 2005. Organization of hypocretin/orexin efferents to locus coeruleus and basal forebrain arousal-related structures. *Journal of Comparative Neurology* 481, 160–178.
- Feldman, J.L., Ellenberger, H.H., 1988. Central coordination of respiratory and cardiovascular control in mammals. *Annual Review of Physiology* 50, 593–606.
- Ferguson, A.V., Samson, W.K., 2003. The orexin/hypocretin system: a critical regulator of neuroendocrine and autonomic function. *Frontiers in Neuroendocrinology* 24, 141–150.
- Ferreira, G., Meurisse, M., Tillet, Y., Levy, F., 2001. Distribution and co-localization of choline acetyltransferase and P75 neurotrophin receptors in the sheep basal forebrain: implications for the use of a specific cholinergic immunotoxin. *Neuroscience* 104, 419–439.
- Fuxe, K., 1964. Cellular localization of monoamines in the median eminence and the infundibular stem of some mammals. *Zeitschrift für Zellforschung* 61, 710–724.
- Fuxe, K., Hökfelt, T., Ungerstedt, U., 1969. Distribution of monoamines in the mammalian central nervous system by histochemical studies. In: Hooper, G. (Ed.), *Metabolism of Amines in the Brain*. Macmillan, London, pp. 10–22.
- Fuxe, K., Hökfelt, T., Ungerstedt, U., 1970. Morphological and functional aspects of central monoamine neurons. *International Review of Neurobiology* 13, 93–126.
- Fuxe, K., Härfstrand, A., Agnati, L.F., Kalia, M., Fredholm, B., Svensson, T., Gustafsson, J.A., Lang, R., Ganten, D., 1987. Central catecholamine-neuropeptide Y interactions at the pre- and postsynaptic level in cardiovascular centers. *Journal of Cardiovascular Pharmacology* 10 (Suppl. 12), S1–S13.
- Gallyas, F., 1979. Silver staining of myelin by means of physical development. *Neurological Research* 1, 203–209.
- Ginovart, N., Marcel, D., Bezin, L., Garcia, C., Gagne, C., Pujol, J.F., Weissman, D., 1996. Tyrosine hydroxylase expression within Balb/c and C57Black6 mouse locus coeruleus. I. Topological organization and phenotypic plasticity of the enzyme-containing cell population. *Brain Research* 721, 11–21.
- Gravett, N., Bhagwandin, A., Fuxe, K., Manger, P.R., 2011. Distribution of orexin-A immunoreactive neurons and their terminal networks in the brain of the rock hyrax, *Procavia capensis*. *Journal of Chemical Neuroanatomy* 41, 86–96.
- Hökfelt, T., Johansson, O., Fuxe, K., Goldstein, M., Park, D., 1976. Immunohistochemical studies on the localization and distribution of monoamine neuron systems in the rat brain. I. Tyrosine hydroxylase in the mes- and diencephalon. *Medical Biology* 54, 427–453.
- Hökfelt, T., Martenson, R., Björklund, A., Kleinau, S., Goldstein, M., 1984. Distributional maps of tyrosine-hydroxylase-immunoreactive neurons in the rat brain. In: Björklund, A., Hökfelt, T. (Eds.), *Handbook of Chemical Neuroanatomy*, Vol. 2. Classical Neurotransmitters in the CNS, Part 1. Elsevier, Amsterdam, pp. 277–379.
- Jacobs, B.L., Azmitia, E.C., 1992. Structure and function of the brain serotonin system. *Physiological Reviews* 72, 165–229.
- Jansa, S.A., Weksler, M., 2004. Phylogeny of the murid rodents: relationships within and among major lineages as determined by IRBP gene sequences. *Molecular Phylogenetics and Evolution* 31, 256–276.
- Jones, B.E., Cuello, A.C., 1989. Afferents to the basal forebrain cholinergic cell area from pontomesencephalic catecholamine, serotonin and acetylcholine neurons. *Neuroscience* 31, 37–61.
- Kerley, G.I.H., 1991. Seed removal by rodents, birds and ants in the semiarid Karoo, South Africa. *Journal of Arid Environment* 20, 63–69.
- Khoroshii, R.M., Klingenspor, M., 2005. Neuronal distribution of melanin-concentrating hormone, cocaine- and amphetamine regulated transcript and orexin B in the brain of the Djungarian hamster (*Phodopus sungorus*). *Journal of Chemical Neuroanatomy* 29, 137–148.
- Kirouac, G.J., Parson, M.P., Li, S., 2005. Orexin (hypocretin) innervation of the paraventricular nucleus of the thalamus. *Brain Research* 1059, 179–188.
- Kitahama, K., Geffard, M., Okamura, H., Nagatsu, I., Mons, N., Jouvét, M., 1990. Dopamine- and dopa-immunoreactive neurons in the cat forebrain with

- reference to tyrosine hydroxylase-immunohistochemistry. *Brain Research* 518, 83–94.
- Kitahama, K., Sakamoto, N., Jouvét, A., Nagatsu, I., Pearson, J., 1996. Dopamine-beta-hydroxylase and tyrosine hydroxylase immunoreactive neurons in the human brainstem. *Journal of Chemical Neuroanatomy* 10, 137–146.
- Kruger, J.-L., Dell, L.-A., Pettigrew, J.D., Manger, P.R., 2010a. Cellular location and major terminal networks of the orexinergic system in the brains of five microchiropteran species. *Journal of Chemical Neuroanatomy* 40, 256–262.
- Kruger, J.-L., Dell, L.-A., Bhagwandin, A., Jillani, N.E., Pettigrew, J.D., Manger, P.R., 2010b. Nuclear organization of cholinergic, putative catecholaminergic and serotonergic systems in the brains of five microchiropteran species. *Journal of Chemical Neuroanatomy* 40, 210–222.
- Leshin, L.S., Kraeling, R.R., Kineman, R.D., Barb, C.R., Rampacek, G.B., 1995. Immunocytochemical distribution of catecholamine-synthesizing neurons in the hypothalamus and pituitary gland of pigs: tyrosine hydroxylase and dopamine-beta-hydroxylase. *Journal of Comparative Neurology* 364, 151–168.
- Limacher, A.M., Bhagwandin, A., Fuxe, K., Manger, P.R., 2008. Nuclear organization and morphology of cholinergic, putative catecholaminergic and serotonergic neurons in the brain of the Cape porcupine (*Hystrix africaeaustralis*): increased brain size does not lead to increased organizational complexity. *Journal of Chemical Neuroanatomy* 36, 33–52.
- Manger, P.R., 2005. Establishing order at the systems level in mammalian brain evolution. *Brain Research Bulletin* 66, 282–289.
- Manger, P.R., Fahringer, H.M., Pettigrew, J.D., Siegel, J.M., 2002a. Distribution and morphology of cholinergic neurons in the brain of the monotremes as revealed by ChAT immunohistochemistry. *Brain Behav. Evol.* 60, 275–297.
- Manger, P.R., Fahringer, H.M., Pettigrew, J.D., Siegel, J.M., 2002b. Distribution and morphology of serotonergic neurons in the brain of the monotremes. *Brain Behav. Evol.* 60, 315–332.
- Manger, P.R., Cort, J., Ebrahim, N., Goodman, A., Henning, J., Karolia, M., Rodrigues, S.L., Strkalj, G., 2008. Is 21st century neuroscience too focussed on the rat/mouse model of brain function and dysfunction? *Frontiers in Neuroanatomy* 2, 5.
- Maseko, B.C., Bourne, J.A., Manger, P.R., 2007. Distribution and morphology of cholinergic, putative catecholaminergic and serotonergic neurons in the brain of the Egyptian Roussette flying fox, *Rousettus aegyptiacus*. *Journal of Chemical Neuroanatomy* 34, 108–127.
- McGranaghan, P.A., Piggins, H.D., 2001. Orexin A-like immunoreactivity in the hypothalamus and thalamus of the Syrian hamster (*Mesocricetus auratus*) and Siberian hamster (*Phodopus sungorus*), with special reference to circadian structures. *Brain Research* 904, 234–244.
- Meister, B., Hökfelt, T., Steinbusch, H.W., Skagerberg, G., Lindvall, O., Geffard, M., Joh, T.H., Cuello, A.C., Goldstein, M., 1988. Do tyrosine hydroxylase-immunoreactive neurons in the ventrolateral arcuate nucleus produce dopamine or only L-dopa? *Journal of Chemical Neuroanatomy* 1, 59–64.
- Mintz, E.M., van Den Pol, A.N., Casano, A.A., Albers, H.E., 2001. Distribution of hypocretin (orexin) immunoreactivity in the central nervous system of Syrian hamsters (*Mesocricetus auratus*). *Journal of Chemical Neuroanatomy* 21, 225–238.
- Monadjem, A., 1999. Populations dynamics of *Mus minutoides* and *Steatomys pratensis* (Muridae: Rodentia) in a subtropical grassland in Swaziland. *African Journal of Ecology* 37, 202–210.
- Moon, D.J., Maseko, B.C., Ihunwo, A., Fuxe, K., Manger, P.R., 2007. Distribution and morphology of catecholaminergic and serotonergic neurons in the brain of the highveld gerbil, *Tatera brantsii*. *Journal of Chemical Neuroanatomy* 34, 134–144.
- Nixon, J.P., Smale, L., 2007. A comparative analysis of the distribution of immunoreactive orexin A and B in the brain of nocturnal and diurnal rodents. *Behavioral and Brain Functions* 3, 28.
- Novak, C.M., Albers, H.E., 2002. Localization of hypocretin-like immunoreactivity in the brain of the diurnal rodent, *Arvicanthis niloticus*. *Journal of Chemical Neuroanatomy* 23, 49–58.
- Olson, L., Fuxe, K., 1972. Further mapping out of the central noradrenergic neurons systems: projections of the subcoeruleus area. *Brain Research* 43, 289–295.
- Paxinos, G., Watson, C., 2009. *Chemoarchitectonic Atlas of the Mouse Brain*. Academic Press, New York.
- Peyron, C., Tighe, D.K., van den Pol, A.N., de Lecea, L., Heller, H.C., Sutcliffe, J.G., Kilduff, T.S., 1998. Neurons containing hypocretin (orexin) project to multiple neuronal systems. *Journal of Neuroscience* 18, 9996–10015.
- Previc, F.H., 1999. Dopamine and the origins of human intelligence. *Brain and Cognition* 41, 299–350.
- Reiner, P.B., Fibiger, H.C., 1995. Functional heterogeneity of central cholinergic systems. In: Bloom, F.E., Kupfer, D.J. (Eds.), *Psychopharmacology: The Fourth Generation of Progress*. Raven, New York, pp. 147–153.
- Rodrigues, S.L., Maseko, B.C., Ihunwo, A.O., Fuxe, K., Manger, P.R., 2008. Nuclear organization and morphology of serotonergic neurons in the brain of the Nile crocodile, *Crocodylus niloticus*. *Journal of Chemical Neuroanatomy* 35, 133–145.
- Ruggiero, D.A., Anwar, M., Gootman, P.M., 1992. Presumptive adrenergic neurons containing phenylethanolamine N-methyltransferase immunoreactivity in the medulla oblongata of neonatal swine. *Brain Research* 583, 105–119.
- Siegel, J.M., 2006. The stuff dreams are made of: anatomical substrates of REM sleep. *Nature Neuroscience* 9, 721–722.
- Skagerberg, G., Meister, B., Hökfelt, T., Lindvall, O., Goldstein, M., Joh, T., Cuello, A.C., 1988. Studies on dopamine-, tyrosine hydroxylase- and aromatic L-amino acid decarboxylase-containing cells in the rat diencephalon: comparison between formaldehyde-induced histofluorescence and immunofluorescence. *Neuroscience* 24, 605–620.
- Smeets, W.J.A.J., González, A., 2000. Catecholamine systems in the brain of vertebrates: new perspectives through a comparative approach. *Brain Research Reviews* 33, 308–379.
- Steinbusch, H.W.M., 1981. Distribution of serotonin-immunoreactivity in the central nervous system of the rat – cell bodies and terminals. *Neuroscience* 6, 557–618.
- Stephan, H., Frahm, H., Baron, G., 1981. New and revised data on volumes of brain structures in insectivores and primates. *Folia Primatologica* 35, 1–29.
- Takakusaki, K., Takahashi, K., Saitoh, K., Harada, H., Okumura, T., Kayama, Y., Koyama, Y., 2005. Orexinergic projections to the cat midbrain mediate alternation of emotional behavioural states from locomotion to cataplexy. *Journal of Physiology* 568, 1003–1020.
- Tillet, Y., Kitahama, K., 1998. Distribution of central catecholaminergic neurons: a comparison between ungulates, humans and other species. *Histology and Histopathology* 13, 1163–1177.
- Törk, I., 1990. Anatomy of the serotonergic system. *Annals of the New York Academy of Sciences* 600, 9–35.
- Veyrunes, F., Catalan, J., Tatard, C., Cellier-Holzem, E., Watson, J., Chevret, P., Robinson, T.J., Britton-Davidian, J., 2010. Mitochondrial and chromosomal insights into karyotypic evolution of the pygmy mouse, *Mus minutoides*, in South Africa. *Chromosome Research* 18, 563–574.
- Vidal, L., Blanchard, J., Morin, L.P., 2005. Hypothalamic and zona incerta neurons expressing hypocretin, but not melanin concentrating hormone, project to the hamster intergeniculate leaflet. *Neuroscience* 134, 1081–1090.
- von Coelln, R., Thomas, B., Savitt, J.M., Lim, K.L., Sasaki, M., Hess, E.J., Dawson, V.L., Dawson, T.M., 2004. Loss of locus coeruleus neurons and reduced startle in parkin null mice. *Proceedings of the National Academy of Sciences of United States of America* 101, 10744–10749.
- Wagner, D., Salin-Pascual, R., Greco, M.A., Shiromani, P.J., 2000. Distribution of hypocretin-containing neurons in the lateral hypothalamus and c-fos-immunoreactive neurons in the VLPO. *Sleep Research Online* 3, 35–42.
- Weihe, E., Depboylu, C., Schultz, B., Schafer, M.K.H., Edien, L.E., 2006. Three types of tyrosine hydroxylase-positive CNS neurons distinguished by Dopa decarboxylase and VMAT2 co-expression. *Cellular and Molecular Neurobiology* 26, 659–678.
- Wilson, D.E., Reeder, D.M., 2005. *Mammal Species of the World: A Taxonomic and Geographic Reference*. Johns Hopkins University Press, Baltimore, USA.
- Wolf, N.J., 1991. Cholinergic systems in mammalian brain and spinal cord. *Progress in Neurobiology* 37, 475–524.
- Wolf, N.J., Hameroff, S.R., 2001. A quantum approach to visual consciousness. *Trends in Cognitive Sciences* 5, 472–748.
- Zeitzer, J.M., Buckmaster, C.L., Parker, K.J., Hauck, C.M., Lyons, D.M., Mignot, E., 2003. Circadian and homeostatic regulation of hypocretin in a primate model: implications for the consolidation of wakefulness. *Journal of Neuroscience* 23, 3555–3560.